

Electronic Thesis and Dissertation Repository

6-25-2020 2:15 PM

Functional and Structural Brain Reorganization After Unilateral Prefrontal Cortex Lesions In Macaques

Ramina Adam, *The University of Western Ontario*

Supervisor: Everling, Stefan, *The University of Western Ontario*

A thesis submitted in partial fulfillment of the requirements for the Doctor of Philosophy degree in Neuroscience

© Ramina Adam 2020

Follow this and additional works at: <https://ir.lib.uwo.ca/etd>



Part of the [Systems Neuroscience Commons](#)

Recommended Citation

Adam, Ramina, "Functional and Structural Brain Reorganization After Unilateral Prefrontal Cortex Lesions In Macaques" (2020). *Electronic Thesis and Dissertation Repository*. 7059.
<https://ir.lib.uwo.ca/etd/7059>

This Dissertation/Thesis is brought to you for free and open access by Scholarship@Western. It has been accepted for inclusion in Electronic Thesis and Dissertation Repository by an authorized administrator of Scholarship@Western. For more information, please contact wlsadmin@uwo.ca.

ABSTRACT

Visually exploring the surrounding environment relies on attentional selection of behaviourally relevant stimuli for further processing. The prefrontal cortex contributes to target selection as part of a frontoparietal network that controls shifts of gaze and attention towards relevant stimuli. Evidence from stroke patients and nonhuman primate lesion studies have shown that unilateral damage to the prefrontal cortex commonly impairs the ability to allocate attention toward stimuli in the contralesional visual hemifield. Although these impairments often exhibit a gradual improvement over time, the neural plasticity that underlies recovery of function remains poorly understood. The main objective of this dissertation was to study the relationship between large-scale network reorganization and the recovery of lateralized target selection deficits. To that aim, endothelin-1 was used to produce unilateral ischemic lesions in the caudal lateral prefrontal cortex of four rhesus macaques. Longitudinal behavioural and neuroimaging data were collected before and after the lesions, including eye-tracking while monkeys performed free-choice and visually guided saccades, resting-state fMRI, and diffusion-weighted imaging. Chapter 2 investigated the effects of unilateral prefrontal cortex lesions on saccade target selection and oculomotor parameters to disentangle attentional and motor impairments in the lasting contralesional target selection deficit. Chapter 3 examined the resting-state functional reorganization in a frontoparietal network during recovery of contralesional target selection. Finally, Chapter 4 investigated microstructural changes in cortical white matter tracts from diffusion-weighted imaging after behavioural recovery compared to pre-lesion. In general, spatiotemporal patterns of functional and structural network reorganization differed based on the extent of prefrontal damage. Altogether, these studies characterized the recovery of lateralized target selection deficits in a macaque model of focal cerebral ischemia and demonstrated involvement of both contralesional and ipsilesional networks throughout behavioural recovery. The broad implication of this research is that a network perspective is fundamental to understanding compensatory mechanisms of brain reorganization underlying recovery of function.

Keywords

frontal eye field, dorsolateral prefrontal cortex, target selection, saccade, visual attention, frontoparietal, endothelin-1, focal cerebral ischemia, neuroimaging, functional MRI, diffusion MRI, functional connectivity, fractional anisotropy

SUMMARY FOR LAY AUDIENCE

Exploring our surrounding environment involves continuous internal decisions about where to look. This ability to choose specific locations to look at out of many other options relies on a network of brain areas in the frontal and parietal cortex. Injury to one side of the brain that affects frontal-parietal areas usually impairs the ability to pay attention to and look toward the opposite side of space. For example, patients with a right-sided stroke may fail to apply make-up or shave the left half of their face, leave uneaten food on the left side of their plates, or frequently bump into objects on their left side. Fortunately, many patients show gradual improvement over time due to the brain's ability to repair itself and reorganize connections to compensate for lost function.

However, the extent of recovery varies across cases and many patients are left with long-term disability. The main goal of this research was to study the brain changes that underlie recovery of attention and gaze toward the ignored side of space. Eye-tracking and brain imaging data were collected before and after a right-sided lesion to part of the frontal cortex in nonhuman primates. Eye movements were recorded to monitor the frequency of looking toward the left versus right visual hemifield, while MRI scans were used to measure the corresponding changes in brain connections during recovery over time. Chapter 2 focused on studying the degree that a lack of left-sided awareness resulted from deficits in attention and/or eye movements. Brain imaging studies in Chapters 3 and 4 demonstrated changes in brain function and structure across frontal-parietal networks in both sides of the brain. We found that patterns of brain reorganization differed based on lesion size and that involvement of brain areas located far from the site of damage was associated with behavioural recovery. This work importantly contributes to the understanding of brain reorganization in visual attention networks and may have implications for treatment and rehabilitation strategies to optimize recovery after brain injury.

CO-AUTHORSHIP STATEMENT

Chapter 2

List of authors: Ramina Adam, Kevin Johnston, and Stefan Everling.

This paper has been published in the *Journal of Neurophysiology*. I performed the experiments, analyzed the data, created the figures, and wrote the manuscript. Dr. Johnston and Dr. Everling performed the surgical procedures and I provided assistance. All authors contributed to the research design, interpretation of results, and manuscript edits and revisions prior to publication.

Chapter 3

List of authors: Ramina Adam, Kevin Johnston, Ravi S. Menon, and Stefan Everling.

This paper has been published in the journal *NeuroImage*. I preprocessed and analyzed the resting-state functional MRI data, created the figures, and wrote the manuscript. All authors contributed to the research design, interpretation of results, and manuscript edits and revisions prior to publication.

Chapter 4

List of authors: Ramina Adam, David J. Schaeffer, Kevin Johnston, Ravi S. Menon, and Stefan Everling.

This manuscript has been posted as a preprint on *bioRxiv* and has been submitted to a journal for peer-review. I preprocessed and analyzed the diffusion-weighted MRI data, prepared the figures, and wrote the manuscript. Dr. Schaeffer provided technical guidance in preprocessing and analysis of the diffusion imaging data. All authors contributed to the research design, interpretation of results, and editing the manuscript.

ACKNOWLEDGEMENTS

I would like to express my most sincere appreciation to my supervisor, Dr. Stefan Everling, who made this work possible and has provided unwavering guidance throughout the years. I am immensely grateful to have had the privilege of being supervised by someone who not only strives for scientific excellence and innovation, but who is kind, supportive, patient, and has a great sense of humour. His endless curiosity and enthusiasm for discovery (and new technology) have always made the lab a refreshing and joyful place to be. I am thankful for the confidence he has instilled in me as a scientist – I truly could not have asked for a better advisor.

Dr. Kevin Johnston has been an invaluable part of my research and personal development, from the fine details of running experiments and analyzing data to discussions about art films and classic literature. His appreciation of the arts and encouragement of a holistic approach to scientific growth was a constant source of inspiration. I thank him for being a wonderful mentor and making my time in the lab a genuinely enjoyable experience.

I would also like to express my gratitude to Dr. Brian Corneil, Dr. Ravi Menon, Dr. Ingrid Johnsrude, Dr. Marco Prado, Dr. Susanne Schmid, Dr. Arthur Brown, Dr. Elizabeth Finger, Dr. Derek Mitchell, Dr. Jessica Grahn, Dr. Lisa Saksida, Dr. Jody Culham, and Dr. Savita Dhanvantari for their formal or informal mentorship over the years – from serving on my advisory committee or as mentors for my comprehensive exam and encouraging me to pursue a doctoral degree, to providing opportunities for teaching and leadership and empowering me to become a better science communicator and advocate. I feel incredibly fortunate to have been surrounded by such brilliant, inspiring, and compassionate leaders.

I am endlessly thankful to our outstanding animal care staff, Nicole Hague, Ashley Kirley, Darren Pitre, and Katherine Faubert, and to Joseph Gati and Trevor Szekeres for help with collecting MRI data. Without them, this research would not have been possible.

I would also like to give my warmest thanks to Sue Bedford for making CFMM at Robarts feel like a family and to Susan Simpson and Janelle Pritchard for their continuous support and guidance within the Neuroscience program and Schulich Graduate Studies. Special thanks to all past and present lab mates and friends in neighbouring labs, Dr. Alex Major, Dr. Sebastian Lehmann, Dr. Jason Chan, Dr. Liya Ma, Dr. Susheel Vijayraghavan, Dr. Maryam Ghahremani, Lauren Schaeffer, Dr. David Schaeffer, Janahan Selvanayagam, Raymond Wong, Dr. Justine Cléry, Dr. Yuki Hori, Andree Chartrand, Brandon Belbeck, Dr. Sahand Babapoor-Farrokhan, and Nikoo Hashemi – I feel lucky to have spent these years with such a fantastic and intelligent group of people. I also wish to thank my close friends who have been patient, understanding, and the best listeners throughout this entire process.

Finally, I would like to thank my family. Thanks to my brother, Ramsin Adam, whose curiosity and dedication to pursuing in-depth knowledge on specific subject matter has always inspired me. My parents, Adam and Mariam Adam, and grandmother, Mina Khochaba, have been an incredible source of inspiration throughout my life. They have taught me to be resilient when things get tough and, above all else, to remain optimistic and hopeful for the future. I will always remember the sacrifices they have made along the way that have been instrumental to my success – I would not be where I am today without their unconditional love and support. Thank you to Connie, Brian, and Brittney Hillman for all the moral support throughout the years – and a special shout out to Connie who could (accurately) explain my thesis topic to others in one sentence. To my wonderful husband and love of my life, Dr. Chris Hillman, thank you for your love and moral support, for being my sounding board when I needed it most, for bringing joy and laughter when times were tough, and for making sure I stayed human and socialized with friends when I would attempt staying home on Friday nights to analyze data. You have kept me sane throughout this process and for that I will always be grateful.

TABLE OF CONTENTS

Abstract.....	ii
Summary for Lay Audience.....	iv
Co-Authorship Statement.....	v
Acknowledgements.....	vi
Table of contents.....	viii
List of Tables.....	x
List of Figures.....	xi
List of Abbreviations.....	xiii
Chapter 1.....	1
1. General Introduction.....	1
1.1. Neural basis of visuospatial attention and saccadic eye movements.....	2
1.2. Visuospatial neglect and extinction after unilateral damage to the frontoparietal network.....	17
1.3. Unilateral lesions in nonhuman primate frontoparietal cortex.....	32
1.4. Large-scale network alterations during recovery from focal brain damage.....	46
1.5. Objectives.....	61
1.6. References.....	64
Chapter 2.....	90
2. Recovery of contralesional saccade choice and reaction time deficits after a unilateral lesion in the macaque prefrontal cortex.....	90
2.1. Introduction.....	90
2.2. Methods.....	93
2.3. Results.....	103
2.4. Discussion.....	130
2.5. Supplemental Material.....	141
2.6. References.....	152
Chapter 3.....	158
3. Functional reorganization during the recovery of contralesional target selection deficits after prefrontal cortex lesions in macaque monkeys.....	158
3.1. Introduction.....	158
3.2. Methods.....	162
3.3. Results.....	178
3.4. Discussion.....	196
3.5. References.....	208
Chapter 4.....	220
4. Structural alterations in cortical white matter tracts after recovery from prefrontal cortex lesions in macaques.....	220
4.1. Introduction.....	220
4.2. Methods.....	223
4.3. Results.....	242

4.4. Discussion	250
4.5. References	259
Chapter 5	269
5. General discussion	269
5.1. Summary of main findings.....	269
5.2. Caveats and Limitations.....	278
5.3. Future directions	281
5.4. Concluding Remarks.....	283
5.5. References.....	284
Appendix A: Ethics Approval.....	291
Curriculum Vitae	292

LIST OF TABLES

Table 2.1. Point of equal selection on the free-choice saccade task.	111
Table 2.2. The proportion of saccades made to the contralesional stimulus during simultaneous presentation of both stimuli.	112
Table 2.3. Saccadic reaction times to a single contralesional and ipsilesional stimulus.	119
Table 2.4. Saccadic duration to a single contralesional and ipsilesional stimulus.	120
Table 2.5. Saccadic peak velocity to a single contralesional and ipsilesional stimulus.	121
Table 3.1. List of the cortical structures included as regions of interest in the frontoparietal network.....	174
Table 4.1. Average streamline probability of the suprathreshold voxels in the reconstructed white matter fiber tracts.....	239
Table 4.2. Changes in resting-state FC between frontoparietal areas of interest.....	248

LIST OF FIGURES

Figure 1.1. Schematic of the prefrontal and posterior parietal cortex in a human and macaque brain.	6
Figure 1.2. Behavioural tasks.....	11
Figure 1.3. A common network for attention and saccades.....	15
Figure 1.4. Scan paths of patients with visual neglect.....	19
Figure 1.5. Self-portraits by the German artist Anton Räderscheidt before and after a right hemispheric stroke in the parietal lobe.	20
Figure 1.7. Superior longitudinal fasciculus in macaque monkeys and humans.	26
Figure 1.6. Summary of the maladaptive and adaptive network-wide changes following focal brain damage.....	49
Figure 2.1. Free-choice saccade task.	96
Figure 2.2. Lesion maps superimposed on the macaque F99 template brain.	105
Figure 2.3. Performance on the free-choice saccade task.	109
Figure 2.4. Saccade performance on single stimulus trials.....	115
Figure 2.5. Effects of a right PFC lesion on saccade metrics to single targets.	118
Figure 2.6. Point of equal selection on the free-choice task and the mean reaction time difference towards a contralesional vs ipsilesional stimulus.	124
Figure 2.7. Observed versus simulated contralesional saccade choice on the free-choice saccade task.....	127
Figure 2.8. Saccadic reaction times to the selected contralesional or ipsilesional stimulus at each SOA condition on paired trials.	129
Figure 2.S1. Cumulative reaction time distributions for Monkey L.....	141
Figure 2.S2. Cumulative reaction time distributions for Monkey S.	142
Figure 2.S3. Cumulative reaction time distributions for Monkey B.....	143
Figure 2.S4. Cumulative reaction time distributions for Monkey F.	144
Figure 2.S5. Correlations between lesion volumes and the duration and severity of contralesional target selection deficits in each monkey.....	145
Figure 2.S6. The LATER model and longitudinal reciprobbit plots of contralesional reaction time distributions.	147
Figure 2.S7. Data points for the reciprobbit plots of the contralesional reaction time distributions for Monkey L.	148

Figure 2.S8. Data points for the reciprobbit plots of the contralesional reaction time distributions for Monkey S.	149
Figure 2.S9. Data points for the reciprobbit plots of the contralesional reaction time distributions for Monkey B.	150
Figure 2.S10. Data points for the reciprobbit plots of the contralesional reaction time distributions for Monkey F.	151
Figure 3.1. Temporal SNR maps for each resting-state fMRI session.	170
Figure 3.2. Reconstructed lesions superimposed on the macaque F99 template brain... ..	179
Figure 3.3. Contralesional saccade choice deficit and gradual recovery on the free-choice saccade task.....	182
Figure 3.4. Pairwise functional connectivity changes of the frontoparietal network across time.	187
Figure 3.5. Functional connections that correlated with the recovery of contralesional saccade choice following a right caudal PFC lesion.....	190
Figure 3.6. Degree centrality for contralesional dorsolateral PFC.	193
Figure 3.7. Changes in the whole-brain functional connectivity with contralesional dorsolateral PFC from pre-lesion to post-lesion.	195
Figure 4.1. Lesion masks projected onto the macaque F99 template brain.....	225
Figure 4.2. Behavioural task.	228
Figure 4.3. Saccade target selection deficits and compensation from pre-lesion to early and late post-lesion.	229
Figure 4.4. Seed masks to reconstruct fiber tracts of interest using probabilistic tractography.	235
Figure 4.5. Representative white matter tracts reconstructed with probabilistic tractography.	238
Figure 4.6. Changes in the average tract-wise DTI parameters over time.....	244
Figure 4.7. Changes in segment-wise FA from pre-lesion to late post-lesion.....	246
Figure 4.8. Schematic summary of the changes in tract-specific FA and rsFC.....	249

LIST OF ABBREVIATIONS

ANOVA	Analysis of variance
BOLD	Blood-oxygen level-dependent
CSF	Cerebrospinal fluid
DLPFC	Dorsolateral prefrontal cortex
DTI	Diffusion tensor imaging
DWI	Diffusion-weighted imaging
ET-1	Endothelin-1
FA	Fractional anisotropy
FC	Functional connectivity
FDR	False discovery rate
FEF	Frontal eye field
fMRI	Functional magnetic resonance imaging
FSL	FMRIB Software Library
LATER	Linear approach to threshold with ergodic rate
LIP	Lateral intraparietal area
MCA	Middle cerebral artery
MRI	Magnetic resonance imaging
PES	Point of equal selection
PFC	Prefrontal cortex
PPC	Posterior parietal cortex
ROI	Region of interest
rsFC	Resting-state functional connectivity
SEM	Standard error of the mean
SLF	Superior longitudinal fasciculus
SNR	Signal to noise ratio
SOA	Stimulus onset asynchrony
SRT	Saccadic reaction time
TOJ	Temporal-order judgement

CHAPTER 1

1. General Introduction

Naturally exploring our surrounding visual world requires selective processing of relevant visual stimuli among many others that compete for our attention. Since our visual world is full of many more stimuli than our sensory system can successfully process at a time, selection mechanisms are necessary for our ability to attend or respond to those that are behaviourally relevant. Visuospatial attention is one type of attentional selection mechanism that selects a visual stimulus for further processing based on where it is located in space (Petersen and Posner, 2012; Posner, 1980). Relevant stimuli may be selected and processed by a covert shift in attention (without overtly directing the eyes to the visual stimulus) or by additionally directing an overt eye movement toward the stimulus (Desimone and Duncan, 1995). Saccades are the rapid eye movements that shift gaze to a new location of interest and are followed by a period of fixation, which is when the eyes are stationary and focused on the new stimulus, before the next location is selected for a saccade target (Liversedge et al., 2012). Saccades are used to align a location of interest with the fovea for high acuity visual processing during fixation. Thus, when exploring a visual scene, we are continuously making decisions about where to look in space through covert selective attention and overt orienting to that selected location by generating an appropriate saccade. This interactive relationship between covert shifts in visual attention to select the next saccade target and overt saccadic eye movements requires the coordination of several brain areas in largely overlapping networks. Unilateral damage to those brain areas commonly results in visual neglect and/or extinction, two related disorders of visuospatial attention that impair the ability to

attend to stimuli in the contralesional visual field (i.e., the visual field opposite to the lesion; e.g., right hemisphere damage impairs visuospatial attention in the left visual hemifield) and may spontaneously recover over a period of weeks to months. Visual neglect and extinction are thought to reflect the breakdown of visual attention to contralesional space which recovers gradually over time. Thus, these disorders are potentially valuable models for studying the brain networks that control overt shifts of visuospatial attention and how those networks reorganize to compensate for loss of function. In this introductory chapter, I will review (1) the brain areas involved in covert visual attention and overt saccadic eye movements, (2) clinical and experimental evidence for visual extinction and neglect, and (3) how the relevant brain network changes functionally and structurally after focal damage to support the recovery of visuospatial attention deficits.

1.1. Neural basis of visuospatial attention and saccadic eye movements

Although visual attention may be allocated to a location in space without a saccade directed to that location (covert visual attention), a saccadic eye movement relies on a shift in visual attention towards the upcoming saccade target prior to executing the saccade to that location of interest. In other words, overt shifts of visuospatial attention rely on both covert visual attention to select the next saccade target and an overt saccadic eye movement to foveate the location of interest. This behavioural link between visuospatial attention and saccadic eye movements has been demonstrated by psychophysical evidence that visual stimulus detection and discrimination accuracy was highest for the stimulus located at a pre-determined saccade endpoint, indicating that attention was allocated to the saccade target location prior to saccade execution (Deubel and Schneider, 1996; Hoffman and Subramaniam, 1995; Kowler et al., 1995). Evidence

for this close association between attention and saccades is also found at the neurophysiological level, where some researchers have proposed that covert visuospatial attention and saccades are part of the same neural process (Rizzolatti et al., 1987). In this ‘premotor theory of attention’, Rizzolatti and colleagues postulate that covert shifts of spatial attention to a visual stimulus merely arises from the saccade preparation commands within oculomotor structures even when an overt saccadic response is not made (Rizzolatti et al., 1987). Although this theory has garnered support over the years from studies showing a common cortical brain network for both attention and saccades, there is convincing evidence that these two mechanisms are served by separate neuronal populations within an individual oculomotor area that is part of that common network (Juan et al., 2004; Pouget et al., 2009; Sato and Schall, 2003; Thompson et al., 2005). These findings better account for the phenomenon of covertly attending to a peripheral location in space without looking towards it while still in support of attentional selection functions by a cortical oculomotor network.

Much of our current understanding of primate oculomotor function has been gleaned from studies in nonhuman primates, mostly macaque monkeys. Not only do human and nonhuman primates share comparable eye movements (Fuchs, 1967) and visual search strategies for saccade targets (Berg et al., 2009; Ramkumar et al., 2015; Segraves et al., 2017), but the oculomotor systems that form the neural basis for eye movement control are also highly conserved across species in terms of their cytoarchitecture (Fig. 1.1) (Amiez and Petrides, 2009; Petrides and Pandya, 2002, 1999), anatomical connectivity (Croxson et al., 2005; Thiebaut de Schotten et al., 2012), and functional organization (Hutchison et al., 2012; Hutchison and Everling, 2012; Koyama et al., 2004). As I will describe in this section, a common network of frontal and parietal brain regions is involved in the covert shifts of visuospatial attention and saccadic eye movements in

humans and nonhuman primates. This section will review studies of healthy brain function from (1) electrophysiological and microstimulation studies of the frontal and parietal oculomotor areas in nonhuman primates and their role in saccade target selection and (2) functional neuroimaging studies that reveal the homologues of those cortical areas in humans. Evidence from lesion and inactivation studies will be reviewed in Section 1.2.

1.1.1. Nonhuman primate neurophysiology

Experimental evidence from monkey electrophysiological and microstimulation studies over the past several decades have established that areas of the caudal prefrontal cortex (PFC) and posterior parietal cortex (PPC) are the main cortical areas that modulate shifts of visuospatial attention and saccadic eye movements (Bisley and Goldberg, 2003; Buschman and Miller, 2007; Colby et al., 1996; Desimone and Duncan, 1995; Everling et al., 2002; Moore and Fallah, 2001; Saalman et al., 2007; Schall et al., 1995).

Specifically, these cortical areas include the frontal eye field (FEF) and dorsolateral PFC (DLPFC) located in the caudal PFC and the lateral intraparietal area (LIP) in the PPC (See Fig. 1.1A). Although this review will focus on cortical control of visuospatial attention, it is worth mentioning that recent studies have also demonstrated a role for the subcortical superior colliculus in selecting targets for saccades (Krauzlis, 2014; Krauzlis et al., 2013; McPeck and Keller, 2004; Müller et al., 2005).

Lateral areas of the primate PFC have been classically defined based on cytoarchitecture by the presence of a granular layer IV (Brodmann, 1913; Petrides and Pandya, 1999) and input from the mediodorsal nucleus of the thalamus (Akert, 1964; Fuster, 2008).

Anatomically located within the caudolateral PFC, the macaque FEF corresponds to the cytoarchitecturally defined area 8A and is located along the anterior bank of arcuate

sulcus, while the DLPFC corresponds to area 9/46D and is located posterior third of the dorsal bank of the principal sulcus, just anterior to the FEF (Fig. 1.1A) (Petrides and Pandya, 1999). Both regions exert their roles in target selection and saccades through shared extensive reciprocal connections with ipsilateral cortical oculomotor structures, including the LIP, other higher order visual areas, and with nearby and contralateral PFC areas (Barbas et al., 2005; Barbas and Mesulam, 1985; Borra et al., 2019; Kunzle and Akert, 1977; Maioli et al., 1983; Petrides and Pandya, 1999, 1984; Stanton et al., 1993). FEF and DLPFC also send projections to subcortical oculomotor areas, including the superior colliculus (Fries, 1984; Goldman and Nauta, 1976; Stanton et al., 1988a), caudate and putamen (Stanton et al., 1988b; Yeterian and Pandya, 1991), and pontine nuclei (Kunzle and Akert, 1977; Schmammann and Pandya, 1997; Stanton et al., 1988b), and in turn receive subcortical input via the mediodorsal thalamus (Goldman-Rakic and Porrino, 1985; Tian and Lynch, 1997). While some descriptions of DLPFC also include the FEF due to variations in nomenclature, here I will describe the FEF separately from the DLPFC based on its distinct characteristics including a high concentration of large pyramidal neurons in layer V (Stanton et al., 1989) and that microstimulation at low currents ($< 50 \mu\text{A}$) elicits saccadic eye movements (Bruce and Goldberg, 1985a).

It is well established that the FEF plays a critical role in the control of saccadic eye movements and target selection (Johnston and Everling, 2012; Schall, 2002; Schall and Thompson, 1999). Early microstimulation studies demonstrated that applying low currents ($< 50 \mu\text{A}$) to the FEF can evoke saccades to the contralateral visual field with a fixed vector and amplitude that varies depending on stimulation site (Bruce and Goldberg, 1985a; Robinson and Fuchs, 1969). Single neuron recordings in the macaque FEF during various oculomotor tasks (e.g., visual search, visually-guided saccade, memory-guided saccade; Fig 1.2) revealed pre-saccadic activity related to visual stimuli, movement, and anticipation of a predicted future saccade (Bruce and Goldberg, 1985b; Schall, 1991). This work supported a role for FEF neurons in saccade generation and visual processing.

Recently, several studies have demonstrated that the FEF is important in the spatial selection of visual targets (i.e., covert visuospatial attention) for a saccade (Murthy et al., 2009; Sato et al., 2001; Schall, 2004; Schall et al., 1995; Schall and Hanes, 1993; Thompson et al., 1997). During a visual search task (see Fig 1.2), visually responsive neurons in FEF signal the location of an oddball target stimulus among non-target distractors such that FEF activity is increased when the target is in the response field and is suppressed when the non-target is in the response field (Thompson et al., 2001). This selective process by FEF neurons took longer when distractors were similar to the target (Sato et al., 2001) and this spatial selectivity signal appeared even in the absence of an overt saccadic response (Thompson et al., 2005, 1997) or in the absence of a visual stimulus in the attended location (Zhou and Thompson, 2009). Monosov et al. (2008) provided evidence that the FEF locally computes the spatial selection of a relevant target, rather than receiving spatial selectivity signals from other sources. Local field potentials (LFPs) are thought to reflect the summed synaptic input activity whereas spiking activity

are the action potentials reflecting neural output (Logothetis, 2002). The authors recorded LFPs and spiking activity in the FEF of monkeys performing a covert visual search task where they had to identify the location of a target by turning a lever in the same direction but in the absence of eye movements. The spatial selectivity that signaled the target location appeared in the spiking activity before the LFP response, suggesting that FEF neurons are locally coding a spatial representation of the behaviourally relevant targets necessary for guiding visual attention and saccades. Thompson and Bichot (2005) reviewed several experiments which demonstrate that the FEF identifies locations of interest by combining bottom-up/stimulus-driven and top-down/goal-oriented influences for target selection in a topographic visual salience map – providing further support that the FEF is important for covert visuospatial attention in addition to generating overt gaze shifts (Thompson and Bichot, 2005). A causal link between FEF activation and covert visual attention was shown in a microstimulation study by Moore and Fallah (2001). In their experiments, subthreshold microstimulation (i.e., less than that needed to evoke a saccade) was delivered to the FEF while monkeys indicated with a blink when a peripheral visual target dimmed in the presence of flashing distractor stimuli. The authors found that FEF microstimulation improved performance for targets in the response field, indicating that FEF can directly enhance visuospatial attention to a target without a saccadic eye movement. It was later suggested that FEF likely modulates attention in the visual cortex via feedback signals to higher order visual area V4 (Armstrong et al., 2006; Ekstrom et al., 2008; Moore and Armstrong, 2003; Premereur et al., 2012). Altogether, extensive evidence accumulated over the last several decades establish the involvement of FEF in the covert visuospatial attention processes necessary for target selection and saccadic eye movements.

The DLPFC (area 9/46D) lies dorsal to the principal sulcus and just anterior to the FEF with a connectivity pattern that makes this area well suited for regulating visual target selection for saccades. As described earlier, the DLPFC is densely and reciprocally connected with the ipsilateral FEF, LIP, and higher order visual areas in the cortex and sends projections to subcortical oculomotor structures, including the superior colliculus. It is thought that the DLPFC computes flexible associations between stimulus input and goal-oriented behavioural output and modulates activity in connected brain areas by sending biased signals in favour of a behaviourally relevant response (Miller and Cohen, 2001). Seminal electrophysiological studies of the DLPFC in monkeys showed activity related to the onset of visual stimuli and saccadic eye movements and persistent activity during the delay period after a peripheral visual cue was presented to signal the location of an upcoming visual saccade target (Funahashi et al., 1991, 1990, 1989). This persistent delay-period activity in DLPFC neurons can represent spatial information about the target location and the saccade direction (Funahashi et al., 1991, 1990, 1989), maintain task rules (Asaad et al., 2000; White and Wise, 1999), and can modulate visual attention by selecting and maintaining behaviourally relevant targets (Everling et al., 2006, 2002; Hasegawa et al., 2000; Iba and Sawaguchi, 2003; Rainer et al., 1998).

Although decades of research have attributed DLPFC activity to working memory representations, several lines of evidence suggest that DLPFC activity also represents covert visuospatial attention as demonstrated by its ability to bias saccade target selection (Buschman and Miller, 2007; Everling et al., 2002; Johnston and Everling, 2006; Kaping et al., 2011; Lebedev et al., 2004; Opris et al., 2005). Everling et al. (2002) recorded single neuron activity in the DLPFC during a task in which monkeys maintained central fixation while covertly attending to a cued peripheral location until a visual target appeared which required a saccade to the target. The authors found that DLPFC activity

discriminated between targets and non-targets in the attended location before saccade onset, with enhanced activity for targets and suppressed activity for non-targets (Everling et al., 2002). Further support for the involvement of DLPFC in saccade target selection was demonstrated after microstimulation of DLPFC neurons during the delay period on a delayed match-to-sample saccade task biased saccade target selection in a manner that was related to the neuron's response field (Opris et al., 2005). Johnston and Everling (2006) later found direct evidence that the DLPFC exerts its influence on target selectivity by directly sending signals to the superior colliculus to bias the upcoming saccadic eye movement (Johnston and Everling, 2006). While the DLPFC likely does not signal oculomotor commands for saccade generation, it is clear that the DLPFC plays a role in allocating visuospatial attention by regulating target selection and saccadic eye movements.

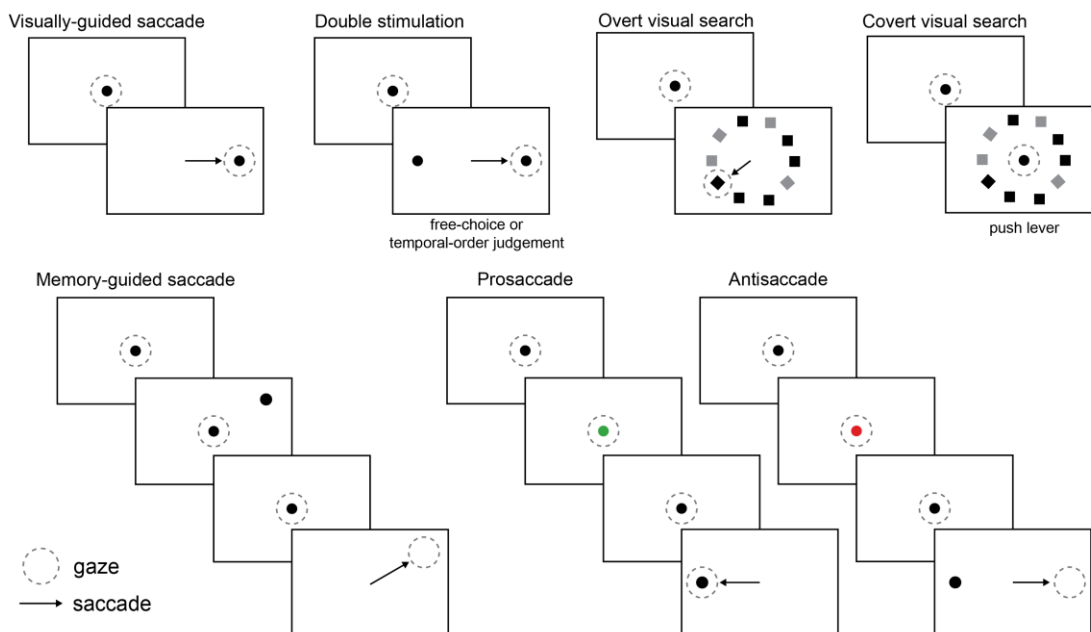


Figure 1.2. Behavioural tasks.

These tasks are mentioned throughout Chapter 1. In visually-guided saccade tasks, monkeys are required to fixate a central stimulus until a peripheral target appears, at which point the monkey must saccade towards the target. In a double stimulus task, two targets appear after fixation either simultaneously or with presentation of either target before the other by a stimulus onset asynchrony (e.g., left stimulus presented before the right stimulus by 150 ms). In free-choice double stimulus tasks, the monkey can saccade to either target for a reward, whereas in temporal-order judgement tasks, the saccade must be directed toward the first-appearing stimulus in the asynchronous trials. In visual search tasks, monkeys must identify an oddball stimulus by either directing a saccade towards the target (overt task) or pushing a lever to indicate its presence (covert). In memory-guided saccade tasks, a peripheral visual target is briefly flashed while the monkey maintains central fixation and must saccade towards the remembered target location after the central fixation point has disappeared. Pro- or antisaccade trials are indicated by a flashed green or red visual cue, respectively. For prosaccades, the monkey must direct a saccade toward the peripheral target, whereas antisaccade trials require the monkey to saccade away from the target.

Another important cortical area for visual attention and gaze shifts is the LIP in the posterior parietal cortex (Gottlieb, 2007). LIP is located in the lateral wall of the intraparietal sulcus and is also highly connected to brain areas mediating saccadic eye movements, including reciprocal connections with the caudal PFC, including FEF and DLPFC (Barbas and Mesulam, 1985; Blatt et al., 1990; Borra et al., 2019; Lewis and Van Essen, 2000; Petrides and Pandya, 1984), and with the superior colliculus (Andersen et al., 1990; Lynch et al., 1985), and receives input from several higher order visual areas, including areas PO, V3, V4, TEO, MT, and MST (Blatt et al., 1990; Lewis and Van Essen, 2000). Similar to the DLPFC, the LIP is not directly involved in saccade generation, but contributes to attentional selection for eye movements. It is thought that the LIP represents a ‘priority map’ (Fecteau and Munoz, 2006) that combines visual stimulus saliency and top-down goal-oriented information into a spatial map of behaviourally relevant target locations to guide saccade target selection (Bisley and Goldberg, 2010; Paré and Dorris, 2012). Single neuron recordings in the LIP showed that activity was modulated by the saliency of the visual stimulus in their response fields, such that activity was enhanced for visual stimuli that were behaviourally relevant and suitable candidates for saccade targets (Bushnell et al., 1981; Gottlieb et al., 1998; Robinson et al., 1978). Early work reported that this enhanced LIP activity did not predict whether a saccade would be initiated or to which location the saccade would be directed (Gottlieb and Goldberg, 1999; Powell and Goldberg, 2000). This suggested that LIP does not necessarily represent the final decision for a saccade target, but instead reflects the covert shift in visual attention towards a salient stimulus (Robinson et al., 1995; Yantis et al., 2002), reinforces the attentional priority of that stimulus (Bisley and Goldberg, 2003), and serves to provide that information about stimulus priority to connected oculomotor areas more directly involved in saccade target selection (Gottlieb et al., 2005). However, evidence for a more direct role for LIP in saccade target selection was reported during

more naturalistic task conditions than previous studies (Ipata et al., 2006). Ipata et al. (2006) recorded from LIP neurons during a free-viewing visual search task and reported that LIP activity was enhanced when the target was in the neuron's response field which correlated with the selection of the saccade target and with saccadic reaction time. Nonetheless, it is clear that LIP has an important part in selecting relevant visual targets for overt shifts in visuospatial attention with saccadic eye movements.

1.1.2. Functional neuroimaging evidence of a frontoparietal network for attention and saccades

As outlined above, a cortical network of prefrontal and parietal areas are thought to be the major source of top-down biasing signals to resolve attentional competition between stimuli by overt shifts of visuospatial attention with saccadic eye movements (Corbetta and Shulman, 2002; Kastner and Ungerleider, 2000). While the functions of FEF/DLPFC and LIP were described above from nonhuman primate studies, here I will highlight their human homologs and describe findings from functional imaging studies in both humans and monkeys that reveal this frontoparietal network subserving visual attention and saccades.

In humans, the likely FEF homologue is thought to be located in the caudal portion of the middle frontal gyrus, immediately anterior to the precentral sulcus and ventral to the superior frontal gyrus, roughly corresponding to Brodmann areas 8A and 6 (Fig. 1.1B) (Blanke et al., 2000; Paus, 1996; Tehovnik et al., 2000). Human DLPFC generally corresponds to area 9 and 46 and lies in the middle third portions of the middle frontal gyrus and superior frontal gyrus (Hagler and Sereno, 2006; Rajkowska and Goldman-Rakic, 1995). While the exact location for the putative LIP homologue in humans is still debated, many suggest it is likely situated within the dorsomedial wall of the intraparietal

sulcus, in the ventral part of the superior parietal lobule (de Haan et al., 2015; Grefkes and Fink, 2005; Koyama et al., 2004).

Functional neuroimaging techniques offer the advantage of noninvasively measuring whole brain activation to identify areas associated with the cognitive functions necessary for task performance. Several task-based functional imaging studies have established that covert shifts of visuospatial attention and saccadic eye movements recruit a highly overlapping frontoparietal network (Fig 1.3), including the FEF, DLPFC, and LIP, both in monkeys (Wardak et al., 2011) and in humans (Corbetta, 1998; Grosbras et al., 2005). The evidence for an overlapping network in monkeys comes from separate functional MRI (fMRI) studies showing activation during either saccade tasks (Baker et al., 2006; Koyama et al., 2004) or covert visuospatial attention (Bogadhi et al., 2018; Caspari et al., 2015; Wardak et al., 2010).

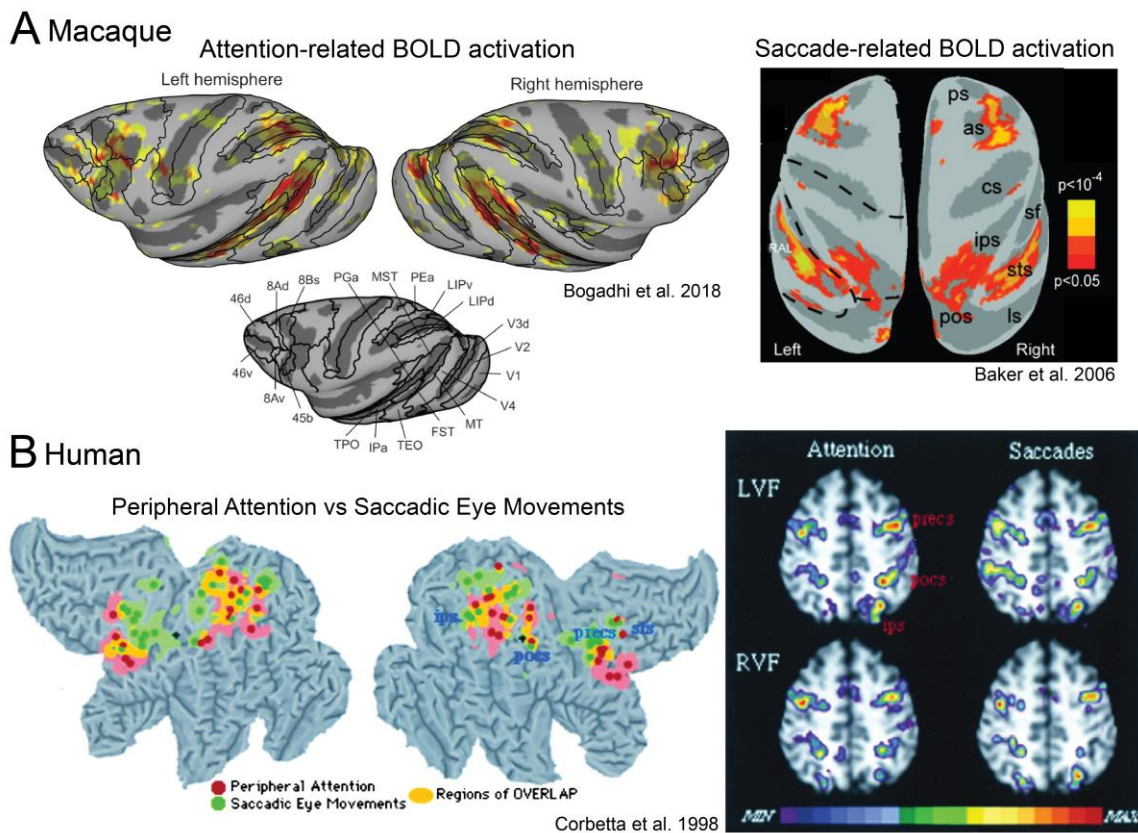


Figure 1.3. A common network for attention and saccades.

BOLD activation maps from functional MRI during attention and saccade tasks in (A) macaque monkeys and (B) humans. In macaques, covert visual attention (left) activates prefrontal, posterior parietal, and superior temporal areas; modified with permission from: Bogadhi et al. (2018) Brain regions modulated during covert visual attention in the macaque. *Scientific Reports*, 8:15237. Saccadic eye movements in monkeys (right) activate similar areas around the arcuate sulcus (as), principal sulcus (ps), intraparietal sulcus (ips), and superior temporal sulcus (sts); modified with permission from: Baker et al. (2006) Distribution of activity across the cerebral cortical surface, thalamus and midbrain during rapid, visually guided saccades. *Cerebral Cortex*, 16:447-459. Similar overlapping networks are seen in humans; modified with permission from Corbetta et al. (1998) Frontoparietal cortical networks for directing attention and the eye to visual locations: Identical, independent, or overlapping neural systems? *Cerebral Cortex*, 95: 831-838.

Monkey fMRI studies revealed saccade-related activation in bilateral FEF, DLPFC, LIP, and superior temporal sulcus (Baker et al., 2006; Koyama et al., 2004). In another fMRI study, covert shifts of spatial attention to a peripheral visual stimulus recruited caudal portions of area 46 corresponding to the DLPFC, areas in the posterior parietal cortex including LIP and superior parietal lobule/area PE, and higher order visual area V6/V6a (Caspari et al., 2015). Wardak et al. (2010) additionally showed that covert target selection during a visual search task mostly recruited bilateral FEF and LIP. Altogether, evidence from fMRI studies in monkeys shows that the areas recruited by both saccades and covert visuospatial attention include the FEF, DLPFC, and LIP, confirming results from the electrophysiological and microstimulation studies reviewed above.

In humans, early evidence from a study using position emission tomography (PET) showed that areas in the superior frontal gyrus, corresponding to FEF, and superior parietal lobule, corresponding to LIP, were more active during covert shifts of visuospatial attention than maintaining attention at central gaze fixation (Corbetta et al., 1993). Mounting evidence from fMRI studies later demonstrated that those regions involved in covert attention shifts were also activated during overt shifts of visuospatial attention via saccadic eye movements (Beauchamp et al., 2001; Corbetta et al., 1998; de Haan et al., 2008; Nobre et al., 2000; Perry and Zeki, 2000). While this frontoparietal network was bilaterally activated during attention and saccade tasks, there is clear evidence for hemispheric asymmetry during covert shifts of visuospatial attention such that activation was stronger in the right hemisphere compared to the left (Corbetta et al., 1998, 1993; de Haan et al., 2008; Szczepanski et al., 2010). This concept of right hemisphere dominance for visuospatial attention will become relevant in the following section when discussing the functional neuroanatomy for disorders of visuospatial attention.

1.2. Visuospatial neglect and extinction after unilateral damage to the frontoparietal network

Historically, the dominant view in neuroscience was that cognitive functions arise from the localized activity of discrete brain regions. This ‘modular’ view of the brain was largely reinforced by early clinical lesion case studies that ascribed the cognitive or behavioural functions that were impaired to the lesioned brain area (Broca, 1861; Harlow, 1848; Scoville and Milner, 1957). While this perspective led to significant advancements in our understanding of brain function and specialization, it had also hindered our appreciation of the brain as a complex network capable of processing information across distributed and interconnected areas (Fornito et al., 2015; McIntosh, 1999). As reviewed in earlier sections, covert visuospatial attention and saccadic eye movements are mediated by the distributed frontoparietal network, rather than a single brain area. This is supported by insights from the brain lesions causing visual neglect and/or extinction – disorders of visuospatial attention that are better accounted for by unilateral damage to the frontoparietal network, rather than to a single brain area alone (Bartolomeo et al., 2012, 2007; Corbetta and Shulman, 2011). Unilateral damage to frontoparietal areas commonly leads to impaired allocation of spatial attention to the visual hemifield that is contralateral to the side of the lesion – herein termed *contralesional*.

Visual neglect and extinction are two related neuropsychological disorders which reflect the disruption of visuospatial attention toward the *contralesional* hemifield. Patients with visual neglect are unable to allocate attention toward the *contralesional* hemifield (Heilman et al., 1984; Li and Malhotra, 2015; Vallar, 1998), while those with extinction are only unable to attend to a *contralesional* stimulus in the presence of a competing *ipsilesional* stimulus (Baylis et al., 1993; Bender and Furlow, 1945; Critchley, 1949; Di

Pellegrino and De Renzi, 1995). Eye tracking in patients with neglect shows the decreased visual exploration with saccadic eye movements in the contralesional hemifield and the resting fixation bias toward the ipsilesional hemifield (Fig. 1.4). Lateralized effects of visual neglect have also been demonstrated in the case of German artist Anton Räderscheidt who suffered a right hemispheric stroke in the parietal cortex and continued to paint self-portraits (Fig 1.5). Many patients show gradual recovery over several months following brain damage (Fig. 1.4–1.5), although the extent of recovery varies across cases and many are left with lasting impairment (Li and Malhotra, 2015). Visual extinction has also been observed when both stimuli are on the ipsilesional side with impaired detection of the stimulus closest to the contralesional hemifield (Rapcsak et al., 1987), indicating that visuospatial impairments appear along a gradient. Whether visual extinction is a mild form of neglect or a distinct phenomenon altogether is still a topic of debate (Driver and Vuilleumier, 2001; Geeraerts et al., 2005; Milner and McIntosh, 2005). Visual neglect is distinct from hemianopia, which is a loss of vision arising from damage to the primary visual areas or pathways (Vallar et al., 1991). In contrast, patients with visual neglect and/or extinction are able to ‘see’ but are unable to direct their attention to and process the visual information from the contralesional hemifield. While visual neglect and hemianopia represent distinct syndromes, they may occur together.

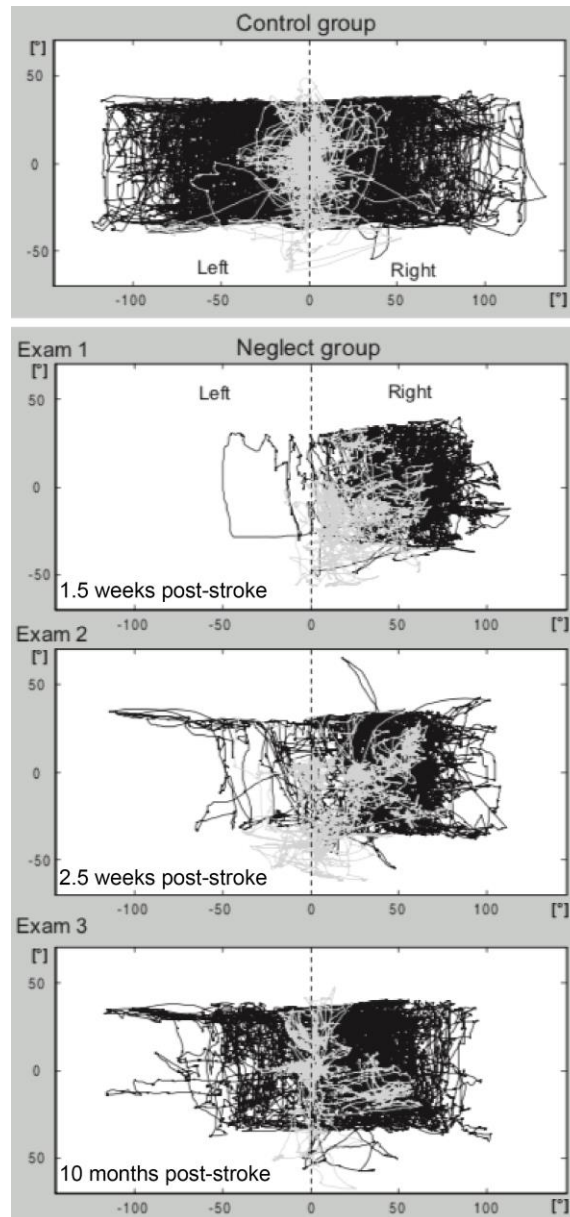


Figure 1.4. Scan paths of patients with visual neglect.

Eye tracking shows the path of gaze during active visual search (black lines) and at rest (grey lines). Top panel shows the eye movement behaviour of a control group without neglect; note the symmetrical search patterns in both hemifields. Second and third panels shows the pattern of gaze in patients with neglect at the acute stage and the bottom panel shows recovered behaviour in the chronic stage. Reprinted with permission from: Fruhmann Berger, Johannsen, and Karnath (2008) Time course of eye and head deviation in spatial neglect. *Neuropsychology*, 22(6), 697–702.



Figure 1.5. Self-portraits by the German artist Anton Räderscheidt before and after a right hemispheric stroke in the parietal lobe.

This series of paintings reveal the gradual recovery from neglect of the contralesional (left) side of space over several months post-stroke. Sources: Andersen, 1987; Berti, Cappa, and Folegatti, 2007; Petcu et al., 2016.

On a broader scale, neglect is a heterogenous disorder and can occur across modalities (visual, auditory, somatosensory, motor), locations in space (personal space, extrapersonal space, internal/representational space), and within different reference frames (egocentric/body-centered or allocentric/object-centered), all of which are not mutually exclusive and may manifest alone or in combination (Mattingley et al., 1997; Rode et al., 2017). In this thesis, the subtype of neglect that I focus is visual neglect with inattention to extrapersonal space manifesting with an egocentric reference frame, which reflects impaired attention to the contralesional hemifield in reference to the viewer's body/head orientation and is associated with lesions of parietal cortex or white matter pathways connecting frontal and parietal cortex (Rode et al., 2017). In contrast, allocentric visual neglect refers to neglecting the contralesional side of individual objects regardless of their location in space with respect to the patient, and is typically associated with temporal cortex lesions (Rode et al., 2017).

1.2.1. Historical review of neglect and extinction from early case studies

Clinical descriptions of neglect and extinction were first documented more than a century ago. The method of simultaneous double stimulation, which is typically used to reveal extinction deficits, was first introduced by Jacques Loeb in 1885 in animals with unilateral lesions where he notes that stimuli in the contralesional visual field are less salient than those on the ipsilesional side. German neurologist Hermann Oppenheim was the first to use Loeb's "double stimulation" task in a clinical setting to assess a patient with paralysis on the right side of the body (Oppenheim, 1885). Oppenheim noted that the patient showed no sign of sensory loss, but when pricked with a pin simultaneously in both arms, the patient only reported feeling the pinprick on the left side. In 1917, Walther Poppelreuter used the method of double stimulation for clinical assessments, but this time

in the visual domain, and found a similar extinction phenomenon which he termed “visual inattention” (Poppelreuter, 1917). Poppelreuter reported that the patient was able to detect an object presented alone in either peripheral visual hemifield but was unable to detect an object in one hemifield when objects were presented simultaneously in both visual fields. Another early case of visual extinction was documented by Holmes (1918) during his time as a neurologist in the First World War in which he described the case of a soldier with a gunshot wound in the right parietal lobe (Holmes, 1918). Holmes noted that the man had normal vision in both visual fields and could identify finger movement when presented to him in either hemifield alone, but that the man only reported movement on the right side when fingers on hands in both hemifields moved at once. However, the term “extinction” was only later introduced by neurologist Morris Bender in his description of a patient who reported that a visual stimulus in the affected hemifield was “extinguished” by the presentation of a stimulus in the opposite visual field (Bender, 1952).

As for case reports of neglect, English neurologist John Hughlings Jackson (1876) documented one of the earliest case reports that described a patient who showed signs of visual “imperception” of the left side of space (Jackson, 1876). Jackson asked the patient to read the Snellen visual acuity chart and noted that the patient started reading from an area on the right side of the chart, which was unusual since native English speakers read from left to right. This patient presented with a myriad of other neurological deficits and so the symptoms of visual neglect were only considered minor and were not the main focus at the time. Several decades later, Zingerle (1913) appears to have described another case of neglect in patients with right hemisphere lesions who had lost the ability to perceive the left side of their personal and extrapersonal space, including the visual domain (Benke et al., 2004). The term ‘neglect’ was first used in 1931 by Pineas in his

description of a 60 year old patient with a right hemisphere lesion showing “neglect” of her left side without any visual or motor deficits (Halligan and Marshall, 1993; Pinéas, 1931). He suggested that the patient likely lost the representation of the left side of her body and extrapersonal space. Later reports of patients with visual neglect described methods to measure the neurological condition, including qualitative bedside tests where patients were asked to eat from a plate of food and it was noted that they would frequently leave the left half uneaten (Mcfie et al., 1950; Paterson and Zangwill, 1944) and more quantitative paper-and-pencil tests where patients were asked to copy simple line drawings (Critchley, 1953) or cross out lines spanning a sheet of paper (Albert, 1973) and in most cases they tend to omit the left side.

Despite several accounts of the attentional impairments towards one side of space, Halligan and Marshall (1993) give credit to British neurologist Russell Brain for being the first to characterize visual neglect as a distinct syndrome (Brain, 1941). In Brain’s (1941) seminal paper, he described three patients that presented with impaired perception of the left side of space without visual deficits and concluded that the main features of visual neglect were: (1) the involvement of posterior lesions in the right hemisphere, (2) that it could not be explained by a sensory visual deficit or memory loss, and (3) that it was distinct from a general visual agnosia and left-right discrimination impairments. Since his influential report, not only has research on visual neglect grown rapidly, but the insights gleaned from neglect have been fundamental to the fields of clinical neurology and neuropsychology in understanding mechanisms of attention and visual processing.

1.2.2. Etiology and theoretical accounts of visual neglect and extinction

Visual neglect and extinction of the contralesional hemifield are most commonly observed after damage to the right hemisphere , usually as a result of unilateral ischemic

stroke (Buxbaum et al., 2004; Stone et al., 1993). Less often, damage to the left hemisphere may cause neglect and extinction though deficits are typically object-centered, less severe, and recover more rapidly (Beis et al., 2004; Kleinman et al., 2007). Ischemic strokes most often affect the middle cerebral artery, which is the largest branch of the internal carotid artery and the main source of blood supply to lateral areas of the frontal, parietal, and superior temporal cortex (Teasell et al., 2016). Final lesion outcome after a middle cerebral artery occlusion is highly variable in terms of its size and location and will differ based on the original site of occlusion.

The heterogeneity of middle cerebral artery strokes has indeed made the localization for precise lesion correlates for visual neglect and extinction difficult. Patients that present with visual neglect also present with a multitude of other neurological deficits at the same time, which further complicates the understanding of underlying anatomy and mechanisms specific to visual neglect (Bartolomeo, 2007). Although lesions in patients with spatial neglect often overlap with the temporo-parietal junction (Corbetta et al., 2005; Karnath et al., 2001, 2011, 2004), which is the zone between the inferior parietal lobule and superior temporal gyrus, the role of superior temporal gyrus in the pathophysiology for contralateral visual neglect, specifically, has been questioned (Bartolomeo, 2007). Areas of the superior temporal cortex are in the middle cerebral artery territory and thus commonly affected by stroke, however their dysfunction relates more closely to object-centered neglect (Chechlacz et al., 2010) and non-lateralized impairments in visual search (Ellison et al., 2004; Gharabaghi et al., 2006) rather than to the specific lateralized deficits of visual neglect (Friedrich et al., 1998).

I will focus on neglect and extinction in the visual domain as it relates to the impaired contralesional shifts in visuospatial attention and saccade target selection. As reviewed earlier, those attentional abilities require the normal functioning of the frontoparietal

network. Visual neglect and/or extinction have been classically associated with right hemisphere lesions in the posterior parietal cortex (Brain, 1941; Critchley, 1953; B. de Haan et al., 2012; Di Pellegrino et al., 1997; Mcfie et al., 1950; Mort et al., 2003; Rorden et al., 2009, 1997), though more recent evidence has shown that right frontal cortex lesions also cause visual neglect or extinction (Committeri et al., 2007; Heilman and Valenstein, 1972; Husain and Kennard, 1996; Mesulam, 1999; Rengachary et al., 2011; Vallar, 2001). More recent work has also shown that damage to the frontoparietal white matter pathways in the right hemisphere also results in neglect/extinction and relates with the severity of deficits (Bartolomeo, 2007; Bartolomeo et al., 2012, 2007; Lunven and Bartolomeo, 2017). Bartolomeo et al. (2007) describe visual neglect as a “disconnection syndrome” and review the evidence linking the pathophysiology of neglect to damage of the superior longitudinal fasciculus (see Fig. 1.7), the major white matter tract connecting frontal and parietal areas within hemisphere (Bartolomeo et al., 2012; Corbetta et al., 2005; Doricchi et al., 2008; Doricchi and Tomaiuolo, 2003; Gaffan and Hornak, 1997; Thiebaut de Schotten et al., 2005).

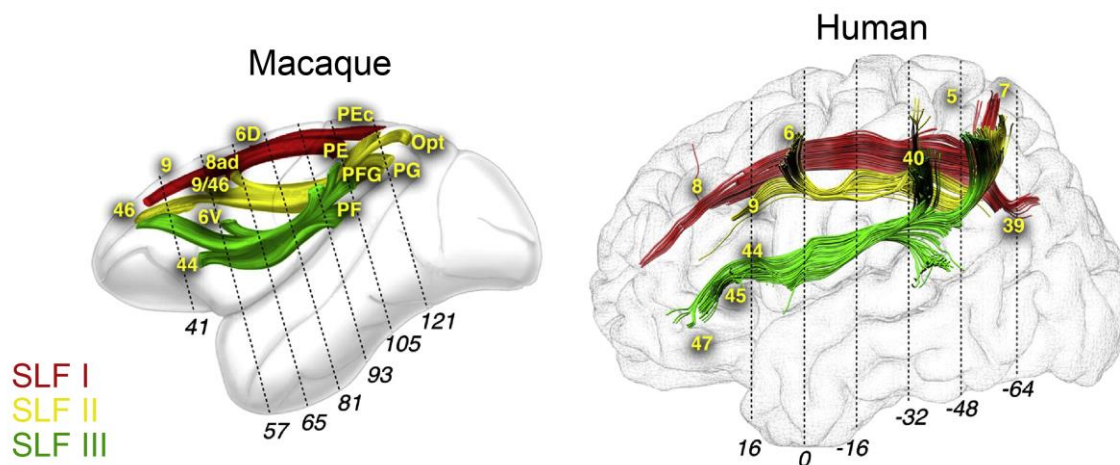


Figure 1.7. Superior longitudinal fasciculus in macaque monkeys and humans.

Three branches of the superior longitudinal fasciculus (SLF) are shown from *ex vivo* axonal tracing data in a macaque and from diffusion-weighted MRI tractography in a human. Modified with permission from: Thiebaut de Schotten et al. (2012) Monkey to human comparative anatomy of the frontal lobe association tracts. *Cortex*, 48: 82–96.

As mentioned above, neglect is more severe and more frequently observed after damage to the right hemisphere, which results in neglect of the left visual hemifield with attention and eye movements biased towards the right hemifield (Heilman and Van Den Abell, 1980; Kinsbourne, 1970; Mesulam, 1981). Several theories of spatial attention have attempted to explain the mechanism of neglect at the acute stage and the phenomenon of right hemisphere dominance for visual attention. According to Kinsbourne's theory of interhemispheric rivalry, each hemisphere directs attention to the contralateral side of space and will inhibit the other hemisphere during shifts of attention (Kinsbourne, 1970). This theory posits that damage to one hemisphere impairs its contralateral direction vector and releases inhibition of the other hemisphere's direction vector, causing it to become hyperactive and bias attention to the contralateral/ipsilesional hemifield, which appears as neglect of the contralesional hemifield. Kinsbourne (1987) attempted to explain the phenomenon that right hemisphere lesions more commonly result in neglect by suggesting that the contralateral direction vector is weaker in the right hemisphere than the left, such that damage to the left hemisphere would not result in as strong of a contralateral bias from the right hemisphere towards the left visual field (Kinsbourne, 1987).

Heilman and Watson (1977) supported this idea of an ipsilesional bias to explain neglect but suggested that the bias manifested because the damaged hemisphere was hypoactive, not because the intact hemisphere was hyperactive (Heilman and Watson, 1977). In support of this model, Heilman and Van Den Abell (1980) provided evidence from neurologically healthy participants that accounted for the right hemisphere dominance. They found parietal activation in the right hemisphere for both left and right visual stimuli, whereas the left parietal cortex was only activated by right stimuli (Heilman and Van Den Abell, 1980). Heilman and Van Den Abell (1980) proposed that the right

parietal cortex controls shifts of attention towards both hemifields whereas the left parietal cortex only controls attention to the contralateral (right) hemifield. In this case, left parietal damage is less likely to result in contralesional neglect since the right parietal cortex can compensate for attending to the contralesional hemifield.

Mesulam (1981) supported Heilman's theory of right hemisphere dominance for visuospatial attention, but expanded the parietal-centric model to highlight the role of a widespread cortical network in directing attention and underlying neglect that included areas of the frontal cortex. Corbetta et al. (1993) provided evidence in support of Mesulam's theory; using positron emission tomography (PET) in neurologically-healthy participants, the authors showed increased activity in the right superior frontal cortex (near FEF) and posterior parietal cortex during shifts of attention compared to fixation, further supporting a role for the frontoparietal network, and that the right parietal lobe showed similar activation levels for both left and right shifts of attention, supporting the right hemisphere dominance component (Corbetta et al., 1993).

These two major theories by Kinsbourne (1970) and Mesulam (1981) also differ in their assumptions about the role of the intact left hemisphere and the phenomenon of visual extinction. Kinsbourne's model of interhemispheric rivalry posits that the left-right parietal imbalance is more severe in neglect than in extinction without neglect, suggesting that left hemisphere activation is causative for neglect. However, Umarova et al. (2011) found evidence against Kinsbourne's theory of neglect; the degree of left hemisphere activation was unrelated to the severity of neglect at the acute stage and was instead an epiphenomenon of all right hemisphere lesions that was also observed in stroke patients with extinction or with normal visuospatial processing (Umarova et al., 2011). Activity in the left hemisphere is even considered beneficial in Mesulam's theory as it may reflect the emergence of a dormant representation of the ipsilateral hemifield to

compensate for the attentional bias. In this case, neglect is assumed to result from less compensatory activation from the left hemisphere whereas extinction without neglect occurs from greater compensation by the left hemisphere. Empirical support for this theory comes from an fMRI study showing that acute patients with neglect and those with extinction alone both showed a correlation between increased activation of the left prefrontal and parietal cortex and detection of left (contralesional) visual stimuli, indicating a beneficial role of the left hemisphere (Umarova et al., 2011). In addition, patients with extinction differed from those with neglect in that they showed an overall increased level of activation in the left middle frontal gyrus/DLPFC and right FEF across target detection for both hemifields.

1.2.3. Clinical assessments of visual neglect and extinction: severity of deficits and timecourse of recovery

Target detection tasks are commonly used to investigate the severity and subsequent recovery of visual neglect and extinction. Visual neglect can be determined from single stimulation paradigms in which one visual stimulus is presented in either hemifield at a time and patients are asked to report or attend to the stimulus (Walker and Findlay, 1996). Poor detection performance for contralesional stimuli compared to ipsilesional stimuli is an indicator of neglect and the severity of deficits may be assessed from reaction times and percent correct detection. Normal performance upon single stimulation may exclude neglect but does not rule out the possibility of visual extinction, which is better detected with double stimulation. Double stimulation paradigms involve the presentation and interaction of stimuli in both hemifields simultaneously or in rapid succession.

The Posner cueing task includes the presentation of a visual cue in one hemifield followed by the subsequent presentation of a visual target in either hemifield; a ‘validly cued’ trial is when the target was presented in the cued hemifield and an ‘invalidly cued’ trial is when the target was presented in the hemifield opposite to the visual cue (Posner and Cohen, 1984). Onset time between cue and target may vary from 0 to 1000 ms; shorter cue-target onset differences may serve as double stimulation trials (to detect extinction deficits) whereas longer differences are effectively single stimulation trials (to detect neglect deficits). Patients with visual neglect or extinction (classified as mild neglect) were drastically slower to respond to contralesional targets that appeared on invalidly cued trials with an ipsilesional cue, compared to all other trial conditions (Posner et al., 1984; Posner and Petersen, 1990). Temporal-order judgement (TOJ) tasks are another behavioural paradigm used to assess neglect or extinction deficits. In TOJ tasks, two stimuli are presented simultaneously or in rapid succession in either hemifield and with a variable delay between stimulus onsets (see ‘double stimulus task’ in Fig 1.2). Participants then report which stimulus was presented first using a verbal response (Baylis, 2002; Di Pellegrino et al., 1997; Rorden et al., 2009, 1997) or saccade response (Ro et al., 2001; Walker and Findlay, 1996). In this case, patients with extinction show maximal deficits when the ipsilesional stimulus is presented slightly before or after the contralesional stimulus, but minimal impairments with a longer time delay between stimulus onsets (Di Pellegrino et al., 1997). Patients with neglect show poor performance in reporting contralesional targets across all trial conditions compared to ipsilesional targets (Van der Stigchel and Nijboer, 2018). A longitudinal study of stroke patients with neglect found that patients showed a severe ipsilesional bias for visual stimuli when measured at 2 weeks post-stroke, with gradual improvements over the first 3 months (Ramsey et al., 2016). They reported that recovery plateaued after 3 months without completely reaching baseline performance and without further improvement when tested

one year later (Ramsey et al., 2016). Similarly, Farne et al. (2004) measured neglect and extinction deficits in stroke patients using a battery of paper-and-pencil tests and also reported severe visuospatial deficits for the contralesional side of space at the initial subacute stage, but that deficits partially recovered over 2 months post-stroke (Farne, 2004).

Most recovery of neglect occurs within the first 6 months post-injury, with later improvements being much less common (Hier et al., 1983; Kwasnica, 2002). At this later stage, patients may show milder neglect but with a lasting visual extinction deficit (Hier et al., 1983; Li and Malhotra, 2015). These attentional disorders represent valuable models for studying brain networks that control shifts of gaze and attention for target selection and how those networks reorganize to compensate for loss of function. Studying mechanisms of attention in patient populations is limited by the lack of pre-injury data and the heterogenous nature of the stroke etiology that leads to visual neglect and extinction. Animal models using experimental lesion methods are important for furthering our understanding of the mechanisms underlying recovery from visuospatial target selection deficits. It is important to mention that the discussion of visual neglect and extinction syndromes are herein used as models to study brain mechanisms of visual attention and saccade target selection. In the following section, animal models of focal brain damage will be discussed in terms of lateralized impairments in visual attention and/or saccade target selection, rather than as animal models of visual neglect or extinction.

1.3. Unilateral lesions in nonhuman primate frontoparietal cortex

More than a century ago, Bianchi (1895) reported that monkeys with large PFC lesions would frequently rotate their body towards the ipsilesional side and did not respond to food presented to them in the contralesional side of space, which he described as similar to a contralateral hemianopia (Bianchi, 1895). In the late 1930s, neurologist Margaret A. Kennard extended Bianchi's experiments by systematically lesioning small areas of the PFC to identify the region responsible for producing the contralateral visual impairments (Kennard, 1939a). In her experiments, before the time of head fixing animals to perform controlled oculomotor tasks, Kennard (1939) developed a chamber that monkeys entered and eventually reached a narrow passage (to limit movements) where they were presented with small pieces of food arranged across a wide area covering both visual hemifields. She reported that monkeys with unilateral lesions in area 8, an area that is now referred to as the FEF, did not respond to food located in the far-contralesional side of their visual field. In addition, Kennard (1939) differentiated these deficits from a hemianopia by showing that monkeys with known hemianopia after an occipital lesion were able to compensate for their deficits by reaching out to explore both sides of space, even in the absence of vision. Monkeys with area 8 lesions did not actively explore the contralesional side of space (Kennard, 1939a), indicating deficits in visuospatial attention that resemble visual neglect in humans. These early observations of neglect-like behaviour toward contralateral space after unilateral FEF lesions in monkeys were supported by other groups (Clark and Lashley, 1947; Welch and Stuteville, 1958).

Similar findings of a contralesional visuospatial impairment were reported after unilateral PPC lesions in monkeys, albeit with some inconsistencies across studies. Denny-Brown and Chambers (1958) reported that monkeys with PPC lesions failed to grasp objects that

were brought towards them from the contralesional side of space and were unaware of their deficits (Denny-Brown and Chambers, 1958). Yet other groups did not find these neglect-like behaviours after PPC lesions in monkeys (Ettlinger and Kalsbeck, 1962; Heilman et al., 1970; Lamotte and Acuña, 1978). When Heilman et al. (1970) presented visual stimuli to monkeys in one hemifield at a time, the monkey's responded to both visual fields normally. However, they reported that monkeys responded less to the contralesional hemifield when tested with bilateral visual stimuli simultaneously in both hemifields, analogous to extinction-like behaviour (Heilman et al., 1970). Deuel and Regan (1985) subsequently showed signs of both neglect- and extinction-like behaviours while observing monkeys reaching to visual stimuli presented either unilaterally or bilaterally and simultaneously (Deuel and Regan, 1985).

While early studies were largely observational, later lesion studies, that will be described in this section, used more controlled experimental conditions and systematic measures of behaviour that provide more information about the lateralized impairment in monkeys. Experimental lesions in animal models have been created using unilateral reversible inactivation methods, in which brain areas are inactivated only temporarily, or with permanent unilateral lesion techniques more representative of the clinical etiology of focal cerebral ischemia which allow for longitudinal assessment. In this section, I will review findings from nonhuman primate studies that demonstrate lateralized visuospatial impairments after reversible inactivation or lesions in the caudal PFC and PPC.

1.3.1. Reversible inactivation techniques

Reversible inactivation allows for the investigation of a specific brain region on behaviour by 'silencing' the area and immediately observing the behavioural consequences without compensation from other regions and without causing damage to

neural tissue (Bell and Bultitude, 2018). Some of the commonly used reversible inactivation techniques that will be described in the studies below include the use of pharmacological injections (e.g., muscimol, lidocaine) or cryogenic loops.

Reversible inactivation of the posterior parietal cortex

Wardak et al. (2002) used muscimol to reversibly inactivate area LIP while monkeys performed various saccade tasks. Muscimol is a GABA_A receptor agonist which inhibits synaptic transmission within about 60 minutes, lasts for several hours (Hikosaka and Wurtz, 1985; Schiller et al., 1987) and does not affect fibers of passage since GABA receptors are not found along axons (Majchrzak and Di Scala, 2000). Wardak and colleagues found that unilateral LIP inactivation had no effect on the contralateral saccades to single targets on the visually- or memory-guided saccade tasks, but drastically reduced the overall proportion of contralateral saccades on the two-choice saccade task with intermixed single target trials for trials with bilateral or single stimulus presentation (Wardak et al., 2002). The authors speculated that the two-choice task created a “virtual competition” environment between the two sides of space, even for the single target trials, which is more representative of a naturalistic environment with constant visual information on both sides. No effects were found on the single target tasks or two-choice task when a nearby area in the posterior parietal cortex was inactivated (ventral intraparietal area).

To dissociate whether those deficits were oculomotor in nature or attention-based, this group later tested LIP inactivation on a covert visual search task in which monkeys had to detect the presence of a visual target amongst distractor stimuli without directing a saccade to the target but by pressing a manual lever (Wardak et al., 2004). They found that unilateral LIP inactivation also resulted in slower detection time for contralateral

targets during covert visual search. These findings of contralateral deficits after muscimol-induced LIP inactivation were later replicated and supported by other groups (Balan and Gottlieb, 2009; Christopoulos et al., 2018; Kubanek et al., 2015; Liu et al., 2010; Wilke et al., 2012).

Wilke and colleagues (2012) investigated the cortical reorganization after unilateral LIP inactivation using event-related fMRI in monkeys performing memory-guided saccades to single targets or on two-choice trials. While behavioural findings showed an overall reduction in contralesional saccade choices on the two-choice trials, fMRI results additionally revealed that whenever a contralesional choice was made, it was accompanied by increased activity in frontal and parietal areas in both hemispheres, including bilateral FEF and contralateral LIP (Wilke et al., 2012). This finding further supports the idea that a cortical network plays a role in allocating visuospatial attention. In addition, Wilke et al. did not find overactivation in the intact hemisphere for ipsilesional saccade choices. Altogether, their findings suggest that activity in the intact hemisphere is not disadvantageous after unilateral inactivation, refuting Kinsbourne's theory of interhemispheric rivalry (Kinsbourne, 1987), but may instead play a compensatory role to maintain contralateral visuospatial attention.

Reversible inactivation of the caudal prefrontal cortex

Similar reversible inactivation studies in the caudal PFC, including the FEF and DLPFC, reveal strong visuospatial deficits of the contralesional hemifield. Keating and Gooley (1988) used a reversible cooling technique with cryogenic loops to unilaterally inactivate the FEF during a visually-guided saccade task. Cryogenic loops are small metal loops that are surgically implanted along the cortical surface and controlled by a cooling pump that regulates the flow of chilled methanol through the loops (Lomber et al., 1999).

Cryogenic loop temperatures of 1–5°C will lower surrounding tissue temperatures below 20°C which will temporarily inactivate postsynaptic activity of neurons up to ~2 mm away, without affecting fibers of passage (Lomber et al., 1999; Lomber and Payne, 2000). Keating and Gooley found that cooling the FEF mainly resulted in an absence of response to contralateral visual targets, which was alleviated by increasing the cryoloop temperature.

Sommer and Tehovnik (1997) investigated the effects of lidocaine injections in the FEF. Lidocaine binds to and blocks voltage-gated sodium ion channels, located along axons and axon terminals, which inactivates neural activity within minutes and lasts for about one hour (Sommer and Tehovnik, 1997). They found that FEF inactivation impaired monkeys' ability to direct saccades to single contralateral targets on the memory-guided and single-step saccade tasks. The authors reported less saccades to contralateral targets and increased reaction times and targeting errors for contralateral saccades. Several others have reported lateralized impairments to single contralateral visual targets after unilateral FEF inactivation using muscimol (Dias and Segraves, 1999; Monosov and Thompson, 2009; Wardak et al., 2006) and cryogenic loops (Peel et al., 2014) in monkeys.

Wardak and colleagues (2006) tested whether contralateral deficits after FEF inactivation were mainly a result of deficits in saccade generation or whether covert visuospatial attention was also impaired. They injected muscimol during a covert visual search task that required monkeys to maintain central fixation while attending to peripheral stimuli and respond only when a visual target was presented in the array. To dissociate overt saccadic deficits from covert attentional ones, responses were made by pressing a manual lever when the target was detected, in the absence of a saccadic eye movement. Wardak et al. reported that FEF inactivation increased reaction times for contralateral targets, but

that error rates were not spatially selective; they speculate that the lack of contralateral-specific errors may have been due to long response times permitted in their task which favoured accuracy over speed (Wardak et al., 2006). Monosov and Thompson (2009) also measured monkey's performance on a covert visual search task during FEF inactivation, but expanded on the study from Wardak et al. (2006) by requiring target identification in addition to detection (Monosov and Thompson, 2009). Here, monkeys detected and identified targets by moving a manual lever in the same orientation as the visual target. In addition to increased reaction times, Monosov and Thompson (2009) also reported decreased performance for contralateral target identification on the covert search task, similar to visual extinction amongst competing stimuli. Both Wardak et al. (2006) and Monosov and Thompson (2009) also measured saccade performance to single contralateral targets and reported almost no saccades to single contralateral targets.

Schiller and Tehovnik (2003) tested for visual extinction using a free-choice saccade task, in which two visual stimuli are presented in either hemifield with a variable delay between their onset (0 – 50 ms) and the monkey could freely choose either stimulus as a saccade target. They found that FEF inactivation induced a contralateral extinction, such that it drastically reduced the proportion of saccades made to the contralateral target, even when it was presented earlier than the ipsilateral target (Schiller and Tehovnik, 2003).

Reversible inactivation of the DLPFC did not affect saccades to single targets on a visually-guided saccade task, but resulted in impaired target selection on a visual search task (Iba and Sawaguchi, 2003). Using cryogenic inactivation, Johnston et al. (2016) extended this work by testing the effects of DLPFC inactivation on the free-choice saccade task, where two visual stimuli compete for becoming the target of an upcoming saccade. The authors reported an overall decrease in the proportion of contralateral saccade choices during bilateral target presentation, representative of contralateral

extinction deficits (Johnston et al., 2016). In addition to the reported extinction deficits after DLPFC inactivation, Koval et al. (2014) found that cooling the DLPFC also impaired saccadic performance to contralateral targets on pro- and anti-saccade tasks. Anti-saccade trials require the animal to direct a saccade away from a visual stimulus, to the opposite side of space (Munoz and Everling, 2004). They reported decreased performance and increased reaction times for contralateral saccades and increased performance for ipsilateral saccades, suggestive of an ipsilateral visuospatial bias (Koval et al., 2014). These deficits were not observed during cooling of the anterior cingulate cortex in this study (Koval et al., 2014). Inactivation studies in another frontal area, the dorsomedial frontal cortex, has also not produced these lateralized deficits for single saccades, but instead revealed deficits for generating saccade sequences on a double-step saccade task (Sommer and Tehovnik, 1999).

Reversible inactivation techniques are important for exploring which brain areas are critical for a specific function without having to permanently damage the neural tissue. Permanent lesions cause altered activity in connected areas (termed ‘diaschisis’, discussed in later sections) and tests of function are typically performed at least one day later allowing more time for neural reorganization to take place, making it difficult to identify whether deficits result from the lesioned site or a connected area. However, since the effects of reversible inactivation can be observed within minutes and during task performance, researchers are better able to identify the immediate consequences of silencing that region on a given task. Additionally, the short duration of inactivation periods reduces the likelihood for compensatory processes (Carrera and Tononi, 2014; Payne et al., 1996; Wilke et al., 2012). However, in the interest of investigating the long-term recovery processes of the lateralized visuospatial impairments following unilateral

brain damage, the use of permanent lesions becomes a more ideal model since it allows for assessment of longitudinal behavioural recovery and brain reorganization.

1.3.2. Permanent lesion techniques

Animal models using permanent lesion methods allow for longitudinal investigations of the recovery process and may better represent the pathophysiology of ischemic stroke, which is the most common clinical etiology of neglect and extinction in humans. Common experimental lesion techniques include surgical aspiration or excision, injection of neurotoxins (e.g., ibotenic acid), and blood vessel occlusion via vasoconstrictive agents or microvascular clips. Longitudinal studies after permanent lesions are especially crucial for investigating the behavioural and neural compensation processes during recovery.

Lesions in the posterior parietal cortex

Experimental lesions created by aspiration is one of the oldest documented methods of creating permanent lesions, starting around the early 1800s (Bell and Bultitude, 2018). Aspiration lesions involve the removal of brain tissue by excision or cautery and suction and allow for complete removal of an area with discrete borders by visual guidance during surgery. Early PPC lesion studies described above relied on observations to examine the effects of a lesion on behaviour (Denny-Brown and Chambers, 1958; Deuel and Regan, 1985; Ettliger and Kalsbeck, 1962; Heilman et al., 1970; Lamotte and Acuña, 1978), which may explain the contradictory results between studies with some reports of mild to no lateralized visuospatial impairment after PPC lesions.

Lynch and McLaren (1989) created unilateral aspiration lesions in the inferior parietal lobule part of the PPC and tested monkeys' ability to detect dimming of visual stimuli using electrooculographic recordings to measure eye movements. The authors found that when tested one week post-lesion, monkeys were still able to saccade towards and detect the dimming of contralesional visual stimuli when it occurred alone, albeit with slightly increased saccade reaction times compared to ipsilesional stimuli. However, when visual stimuli dimmed simultaneously in both hemifields, the monkeys almost completely ignored the contralesional stimulus and responded to the ipsilesional stimulus (Lynch and McLaren, 1989). While monkeys did not show neglect-like behaviour, they clearly demonstrated extinction-like deficits during bilateral presentation which did not improve over the 2 weeks that the data was shown.

In contrast, other studies found evidence of behaviours more closely resembling neglect of contralesional stimuli after unilateral PPC lesions (Crowne and Mah, 1998; Deuel and Farrar, 1993). Deuel and Farrar (1993) reported that monkeys showed decreased responses to unilateral presentations of food bait in the contralesional hemifield, from ~80% response rate before the lesion down to ~40% response rate for single contralesional presentations. They also reported almost a complete absence of response to contralesional food bait during bilateral simultaneous presentations in both hemifields (Deuel and Farrar, 1993). Similarly, Crowne and Mah (1998) reported increased reaction times for single contralesional visual stimuli that was not observed for ipsilesional stimuli and which took about 2 months to recover. They suggested that the discrepancies between studies in monkeys with PPC lesions may stem from whether LIP (area POa) was damaged or not. Lynch and McLaren's lesions mostly spared area POa/LIP, and instead damaged areas PF and PG located ventrally which may explain the lack of impairment in attending to contralesional stimuli.

Many studies directly compared lesions of the PPC and caudal PFC/FEF in the same experiments (Crowne and Mah, 1998; Deuel and Farrar, 1993; Lynch and McLaren, 1989) and while deficits are of a similar nature (contralesional visuospatial impairments), the deficits after FEF lesions are more severe and took longer to recover, more representative of the gaze behaviour in neglect.

Lesions in the caudal prefrontal cortex

Early PFC lesion experiments in monkeys reported deficits based on observing responses to food or frightening visual stimuli that were brought towards the monkey from its contralesional side (Bianchi, 1895; Clark and Lashley, 1947; Ferrier, 1886; Jacobsen and Nissen, 1937; Kennard, 1938; Kennard and Ectors, 1938; Welch and Stuteville, 1958). Like the PPC lesion studies, these early experiments also varied in precise lesion location and the degree of visuospatial bias severity, potentially due to task differences in the horizontal eccentricity of visual stimulus presentation. In the 1970s, Alan Cowey and Richard Latto conducted the first experiments in which eye movements were systematically photographed in monkeys with unilateral FEF lesions while they performed an oculomotor task (Latto and Cowey, 1971a, 1971b). In the task, a flashing visual stimulus appeared in either hemifield and the monkeys had to direct their gaze towards the stimulus. Latto and Cowey (1971) found that the animals ignored the contralesional visual stimulus to an increasing degree the farther into the periphery it appeared. They reported that the deficit could not be simply attributed to an ipsilesional deviation of gaze fixation and that the deficit recovered within 2-4 weeks, and in one case recovery took 12 weeks.

After small unilateral lesions restricted to the FEF, Rizzolatti et al. (1983) presented food bait either unilaterally, with one piece of food in either hemifield separately, or

bilaterally, with two pieces of food presented simultaneously in both hemifields. They found that monkeys did not orient towards a single food item presented in the contralesional hemifield (i.e., no shift in gaze or reach towards the food) and only oriented towards the ipsilesional food item on bilateral presentations. Neglect-like behaviour to unilateral stimuli recovered within 2 weeks, but the extinction-like deficit to bilateral stimuli lasted until 8 weeks post-lesion. Other research groups have also lesioned the caudal PFC, including both FEF and DLPFC, using aspiration and reported similar results by showing a combination of increased reaction times, increased errors, decreased gaze shifts, and/or reaching movements towards contralesional visual stimuli (Crowne et al., 1981; Crowne and Mah, 1998; Deuel and Collins, 1984; Deuel and Farrar, 1993). Recovery of contralesional impairment to unilateral stimuli was reported usually within 2 to 3 weeks and during bilateral stimuli presentation within 4 to 10 weeks post-lesion (Bianchi, 1895; Crowne et al., 1981; Crowne and Mah, 1998; Deuel and Collins, 1983; Kennard, 1939b; Rizzolatti et al., 1983). However, these studies did not use methods to restrain monkey's heads from moving during task performance; head reorientations may have shifted the location of a visual stimulus from the assumed contralesional location more towards the vertical midline, which would make the monkey more likely to notice the stimulus.

In another lesion study of the caudal PFC, including both FEF and the caudal portions of principal sulcus (DLPFC), Schiller and Chou (1998) showed substantial and long-lasting contralesional impairments on a visually guided saccade task with both single and paired visual stimuli. These impairments were not observed for lesions of the supplementary eye field in the dorsomedial frontal cortex (Schiller and Chou, 1998). During the task, monkeys had their heads restrained and eye movements were recorded using an implanted scleral search coil. Trials with a single visual target in either the contralesional

or ipsilesional hemifield rewarded the monkeys for directing a saccade towards the target. Prior to the lesion, average saccadic reaction times to single left or right targets only differed by 3 ms. At 3 weeks post-lesion, the difference between average reaction times for ipsilesional and contralesional saccades increased to 54 ms, resulting from increased saccadic reaction times for contralesional targets (+45 ms) and decreased reaction times for ipsilesional targets (-13 ms). Slower reaction times for single contralesional targets persisted up to four months post-lesion. Recovery of contralesional impairment in this model is remarkably similar to that observed in humans, with gradual recovery over 4 months and then performance plateaus without further improvements even one year later (Schiller and Chou, 1998). Deficits in orienting to contralesional visual targets after lesions or inactivation of the FEF/caudal PFC have not been associated with changes in contrast sensitivity, which rules out sensory deficits as the underlying cause (Schiller and Chou, 2000; Wardak et al., 2006). For paired stimulus trials, visual stimuli were presented in both hemifields with a variable stimulus onset asynchrony, which is the time difference between the onset of the first and second visual stimulus. Under normal conditions, monkeys directed an equal proportion of saccades to the left or right target when they were presented simultaneously (0 ms onset asynchrony) and directed more saccades to the first-appearing target (left or right) with an increasing proportion as the lead stimulus onset asynchrony value increased. Two weeks after a unilateral lesion was made in the FEF/DLPFC, no saccades were made to the contralesional stimulus when it was presented up to ~50 ms before the ipsilesional stimulus and an equal probability of saccades were made to either stimulus only when the contralesional stimulus was leading by ~120 ms. This contralesional extinction (i.e., decreased contralesional saccade choice) gradually improved over 4 months, yet recovery was only partial with lasting impairments; even 4 months later, a stimulus onset asynchrony of 54 ms with the contralesional target appearing first was needed to achieve an equal probability of

contralesional or ipsilesional saccades (Schiller and Chou, 1998). On the paired stimulus trials, monkeys were rewarded for directing a saccade towards either the first- or second-appearing target. This ‘free-choice’ model for the paired stimulus trials better represents the true bias in saccade choice since it does not over-train the animals to compensate for their deficits in order to complete the task. In addition, measuring saccade choice with a range of stimulus onset asynchronies, varying from 0 ms (simultaneous presentation) to ~220 ms (left or right first), is more sensitive to the degree of visual extinction throughout the recovery period as deficits get smaller but may still be significant. This task design may explain why Schiller and Chou (1998) are the first to show such severe and long-lasting contralesional impairments after caudal PFC lesions. The study described in **Chapter 2** addresses the question of whether contralesional extinction deficits after damage to the caudal PFC are due to impairments in generating saccades or an impaired ability to allocate attention towards the contralesional visual hemifield.

Although aspiration lesions and reversible inactivation techniques have been critical in the understanding of brain-behaviour relationships, they do not mimic the cellular processes that occur following ischemic injury which is most often the cause of neglect and extinction in humans. Animal models of ischemic injury traditionally occluded the MCA after exposing it with a parietal craniotomy or a transorbital approach (Fan et al., 2017; Jones et al., 1981; West et al., 2009). While these approaches may be well-suited for studying the post-injury cellular and vascular mechanisms or motor dysfunction (Fukuda and del Zoppo, 2003), they have several limitations. MCA occlusion models of ischemic injury produce highly variable and unpredictable lesion sizes and usually lead to severe motor deficits which cause suffering to the animal. The surgical techniques themselves may confound studies of oculomotor behaviour; the transorbital approach to the MCA requires enucleation of the eyeball which is impractical for eye movement studies

and the parietal craniotomy method would put the animal at higher risk for post-operative infection and may create MRI artifacts over critical dorsal parietal areas. Instead, focal ischemic lesions can be induced using injections of the vasoconstrictor endothelin-1 directly into the area of interest, which produces relatively confined lesions compared to MCA occlusions. Endothelin-1 is a 21-amino acid peptide that is naturally produced by vascular endothelial cells. Yanagisawa et al. (1988) was the first to isolate endothelin-1 and reveal its potent and long-acting vasoconstrictive properties (Yanagisawa et al., 1988). Endothelin-1 acts by inducing a focal occlusion with subsequent reperfusion (~4 hours later) and has been used to induce focal cerebral ischemia in rats (Fuxe et al., 1997; Macrae et al., 1993; Sharkey et al., 1993) and more recently in the visual cortex of marmoset monkeys (Teo and Bourne, 2014) and the motor cortex of macaque monkeys (Dai et al., 2017; Herbert et al., 2015; Murata and Higo, 2016). Thus, using endothelin-1 to create monkey models of focal cerebral ischemia is advantageous since it can mimic the cerebrovascular pathophysiology in humans after ischemic strokes (Fukuda and del Zoppo, 2003) while still inducing relatively confined lesions for precise experiments of the specific behavioural domain of interest. In the following section, I will describe how focal damage can alter brain activity across the widespread network of interconnected brain areas and how this process may contribute to the behavioural compensation (e.g., recovery of contralesional visuospatial impairment) observed in the months following unilateral brain damage.

1.4. Large-scale network alterations during recovery from focal brain damage

After Schiller and Chou (1998) observed gradual recovery of the saccade choice deficit in monkeys with aspiration lesions that included area 8A (FEF) and area 9/46 (caudal DLPFC), they speculated that a posterior region involved in the control of visually guided saccades compensated for the loss of function. This points to area LIP in the posterior parietal cortex (PPC), given that it is part of the cortical network for covert visuospatial attention and saccadic eye movements. In addition to the extensive literature supporting a role for both the caudal PFC and PPC in allocating visuospatial attention within a frontoparietal cortical network, there is also some evidence for the idea that damage to the one network node (e.g., PPC) is compensated for by areas in the other network nodes (e.g., PFC). Lynch and McLaren (1989) created sequential lesions within one monkey and reported the behavioural changes following each lesion on an oculomotor task with single or double simultaneous trials. They found that a right PPC lesion induced extinction-like behaviour for visual targets in the contralesional (left) hemifield on bilateral trials, but no impairment to single left targets. Following a subsequent lesion to the homologous PPC in the opposite (left) hemisphere, the authors reported a reversal of extinction-like deficits such that the monkey was now ignoring targets in the right visual hemifield on bilateral trials, but was still not ignoring single right targets. When a third lesion was made in the right caudal PFC (area 8AD of the FEF and area 9/46D of the DLPFC), the animal now completely ignored stimuli in the left visual hemifield, even when presented alone. The monkey did not direct any saccades to single targets in the left hemifield for one week post-lesion, after which the monkey began to make saccades to left targets during single target trials but not bilateral simultaneous trials, suggesting a lasting target selection deficit (Lynch and McLaren, 1989). They did not report details of

the performance on the single target trials about the recovery following the third lesion in the PFC. These findings demonstrate that damage to both parts of the frontoparietal network (PFC and PPC) produces more severe deficits than damage to only one part of the network within the same hemisphere. Connected areas within a network may compensate for the loss of one region to minimize the impairments.

The concepts put forward by Lynch and McLaren (1989) and Schiller and Chou (1998) highlight the importance of neuroplasticity and network reorganization in the recovery of function after brain injury. In this section, I will review the mechanisms and theories of post-lesion neural and behavioural compensation and how modern neuroimaging techniques can shed light on the changes in functional and structural brain networks that underlie recovery. The study in Chapter 3 focuses on functional network changes using resting-state fMRI and the last study in Chapter 4 shows changes in the structural network using diffusion-weighted imaging after caudal PFC lesions in monkeys recovering from contralesional target selection deficits.

1.4.1. Mechanisms of neuroplasticity and network reorganization after focal ischemic injury

Ischemic stroke initiates a cascade of cellular and molecular events in both perilesional and eventually in brain areas remote from the site of the lesion. In the early/acute stage (~1-4 weeks), focal ischemia triggers neuronal depolarization and excess glutamate release, which leads to disinhibition and hyperexcitability of connected widespread networks in both ipsilesional and contralesional hemispheres, until local cell death occurs resulting in a focal lesion (Buchkremer-Ratzmann and Witte, 1997; Carmichael, 2012, 2010; Fornito et al., 2015; Liepert et al., 2000). Large-scale hyperexcitability may initiate axonal sprouting, dendritic spine elongation, and synaptogenesis in local and remote

areas (Buchkremer-Ratzmann et al., 1996; Carmichael and Chesselet, 2002; Lee and van Donkelaar, 1995; Murphy and Corbett, 2009; Napieralski et al., 1996). However, persistent hyperactivation may lead to remote degeneration across connected areas due to excitotoxicity and excessive metabolic stress (Buchkremer-Ratzmann and Witte, 1997; W. de Haan et al., 2012; Fornito et al., 2015; Ross and Ebner, 1990; Saxena and Caroni, 2011). In the chronic stage after cell death, neural repair and reorganization take place to promote recovery, which involves an interplay between synaptogenesis and dendritic/axonal pruning and sprouting to selectively strengthen certain neural pathways while weakening others to refine the newly formed neuronal circuitry (Carmichael, 2012; Jones and Schallert, 1992; Murphy and Corbett, 2009; Stroemer et al., 1995). The brain undergoes maladaptive changes associated with the loss of function and adaptive changes for the subsequent compensation of lost function during recovery (Fig. 1.6).

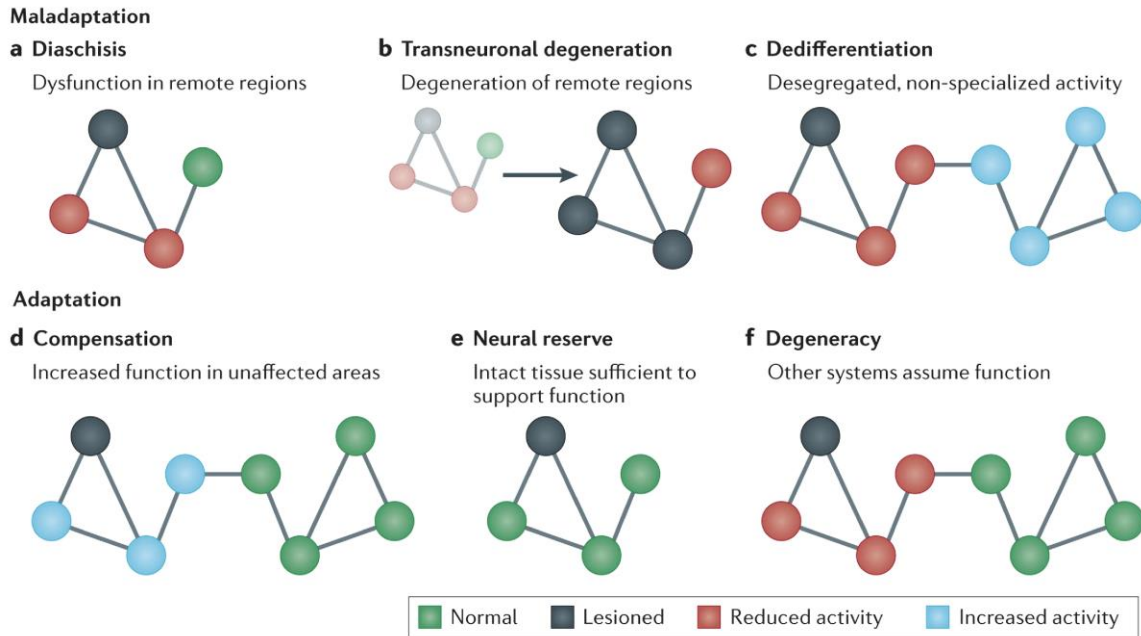


Figure 1.6. Summary of the maladaptive and adaptive network-wide changes following focal brain damage.

Possible outcomes are represented in a simple example network with four nodes (i.e., brain areas) that is specialized to carry out a specific behavioural function. Each panel illustrates a potential change in the network after damage to a network node (shown in black). Maladaptive responses to focal injury include (A) diaschisis, which is the functional disruption of remote network areas, (B) transneuronal degeneration, which represented the structural degradation of remote network areas, and (C) dedifferentiation, which is the suboptimal recruitment of areas in another network that is not specialized for the specific behavioural function. Adaptive responses include (D) compensation from increased activity in undamaged remote network areas, (E) sufficient neural reserve in undamaged remote network areas to continue carrying out normal behaviour, and (D) utilizing the neural reserve in a related network that can support normal behaviour without altering its activity. Modified with permission from: Fornito, Zalesky, and Breakspear (2015) The connectomics of brain disorders. *Nature Reviews Neuroscience*, 16(3): 159-172.

In terms of the maladaptive changes following focal damage, early 19th century pioneers of neuroscience speculated that large-scale brain networks were affected through a process called ‘diaschisis’ that describes remote dysfunction of connected areas (Monakow, 1914, 1897) or by disconnection of white matter pathways (Thiebaut De Schotten et al., 2015; Wernicke, 1874). Indeed, the previously described molecular processes following cerebral ischemia can lead to detrimental changes in areas remote to the lesion that contribute to loss of function (Fig. 1.6A–C), including diaschisis (functional disruption), transneuronal degeneration (structural degradation), and dedifferentiation (suboptimal recruitment of non-specialized areas for task performance).

Diaschisis is a phenomenon typically described as a consequence of stroke and is thought to result from a loss of excitatory input to remote areas connected to the lesion (Carrera and Tononi, 2014; Feeney and Baron, 1986). These widespread changes affect areas connected to the lesion either directly through a monosynaptic connection or indirectly via polysynaptic connections as part of a shared functional network (Fornito et al., 2015; Nomura et al., 2010).

Transneuronal degeneration differs from diaschisis in that it refers to the *structural* deterioration of areas distant from the lesion. Initially, structural degeneration occurs in areas surrounding the lesion, particularly in perilesional tissue and along axons that innervate the lesioned site via anterograde (i.e., Wallerian) or retrograde axonal degeneration (Beaulieu, 2002; Pierpaoli et al., 2001; Thomalla et al., 2004; Werring et al., 2000). After the initial deterioration period, white matter atrophy may occur in axons *remote* to the lesion by either anterograde transneuronal degeneration, from loss of excitatory input, or retrograde transneuronal degeneration, from loss of trophic support (Baron et al., 2014; Fornito et al., 2015; Grayson et al., 2017; Zhang et al., 2012).

Dedifferentiation involves the diffuse recruitment of non-specialized areas to perform the affected behaviour or cognitive process normally controlled by the damaged regions. It is thought to result from a lesion-induced imbalance between excitatory and inhibitory activity within a neural circuit that is remote from the lesion site, which disrupts the normally segregated processing within that neural circuit (Fornito et al., 2015). For example, in the case of subcortical stroke that results in motor impairments, maladaptive overactivation of the motor cortex in the contralesional hemisphere has been associated with poor outcomes and is thought to be caused by an imbalance in activity between the left and right primary motor cortices (Rehme et al., 2011).

The brain's adaptive response to focal damage is necessary to maintain normal function or to restore lost function (Fig. 1.6D–F). This process may utilize the *neural reserve* in nearby or remote intact areas to maintain sufficient task performance or may rely on *compensation* from those intact areas of the affected network whereby increased activity is required to support the recovery of lost function (Fornito et al., 2015). In some cases, the neural reserve for performance of a given task may be highly distributed across areas within a shared functional network. After focal damage to that network, normal activity levels in the spared regions may be sufficient to continue carrying out the task without any deficits manifesting (i.e., *degeneracy*; Fig. 1.6F).

However, in many cases focal damage impairs the normal function subserved by the large-scale network which can manifest as cognitive or behavioural deficits. Here, recovery of impaired function may rely on the compensatory recruitment (i.e., increased activation) of those remote and intact areas of the shared network to take over the function normally carried out by the damaged area. Structural plasticity after an ischemic lesion is critical for functional compensation to take place and may be induced by the initial hyperexcitability of nerve fibers across both hemispheres connected to the lesioned

site (Carmichael and Chesselet, 2002; Fornito et al., 2015; Gonzalez and Kolb, 2003; Jones and Schallert, 1992; Lin et al., 2015). It is thought that the formation of new connections to compensate for lost function may depend on the favourable environment created by these structural changes (e.g., axonal and dendritic growth of undamaged fibers, myelin remodeling, synaptogenesis). Neural compensation following brain damage can appear as increased activity within an area or increased structural/functional connectivity between areas of the network that are associated with improved cognitive or behavioural function.

1.4.2. Functional network reorganization during the recovery of lateralized visuospatial impairments

Neuroimaging techniques offer a large-scale view of the brain and permits the study of the post-lesion neural compensation that occurs across widespread functional and structural networks (Carter et al., 2012; Fornito et al., 2015; Grefkes and Fink, 2014). In this section, I will review the neuroimaging studies of visual neglect and extinction in stroke patients and in animal models of lateralized visuospatial impairments and describe the network consequences of focal damage and the compensation associated with recovery of function.

Functional MRI (fMRI) is a non-invasive functional imaging technique that can provide an indirect measure of whole brain activity *in vivo* by detecting changes in blood oxygenation. In the early 1990s, Seiji Ogawa and colleagues showed that the magnetic resonance signal is sensitive to changes in deoxyhemoglobin concentration and that this blood-oxygen level-dependent (BOLD) signal could be used to infer brain activity (Ogawa et al., 1992, 1990). When neurons become active, local blood flow increases to replace the deoxygenated blood with oxygenated blood, and this decreased ratio of

deoxyhemoglobin/oxyhemoglobin appears as an increased BOLD signal. When fMRI is combined with sensory stimulation or cognitive tasks, the measured BOLD signal can be used to reveal the brain activation related to the stimuli/task and how activation patterns might change in a disease state.

Post-lesion changes in brain activation have been investigated using fMRI during a task or stimulation that probes the impaired function in human studies (Calautti and Baron, 2003; Grefkes and Fink, 2011; Rehme and Grefkes, 2013) or animal models (Dijkhuizen et al., 2012; Weber et al., 2008). Most studies have investigated the reorganization of the motor network following stroke that affected motor function. In the case of post-stroke motor recovery, task- or stimulation-related fMRI experiments have generally shown a pattern of decreased activation in the ipsilesional hemisphere and increased contralesional activation in the acute stage when deficits are most severe, followed by a normalization of activity between hemispheres in the chronic stage in those with optimal recovery of motor function (Calautti and Baron, 2003; Dijkhuizen et al., 2003, 2001; Rehme et al., 2011; Ward et al., 2003). Patients with larger lesions or severe and longer lasting motor impairments in the chronic stage typically show greater BOLD-related activation in the contralesional hemisphere during task performance (Rehme and Grefkes, 2013; Ward et al., 2007; Ward and Cohen, 2004).

In the case of neglect, a task-related fMRI study in patients with right frontoparietal stroke supported the theory that sustained activity in the intact hemisphere at the chronic stage was detrimental to the recovery of function (Corbetta et al., 2005). Corbetta et al. (2005) showed that reduced detection of visual targets in the contralesional hemifield at the acute stage (~ 4 weeks post-stroke) correlated with a relative hyperactivation of the posterior parietal cortex in the intact hemisphere compared to the lesioned hemisphere.

At the chronic stage, recovery of deficits corresponded with a normalization of the left and right parietal activity imbalance.

However, a later study by Umarova and colleagues showed that all patients with right hemisphere strokes exhibited an imbalance in functional activation between hemispheres at the acute stage whether they had neglect, extinction only, or no visuospatial deficits at all (Umarova et al., 2011). Moreover, they found that detection of contralesional visual targets in patients with neglect and extinction correlated with increased BOLD signal activation in the prefrontal and parietal cortex of the intact hemisphere. This suggested that hyperactivation of the intact hemisphere does not necessarily cause neglect, but instead reflects an epiphenomenon of right hemisphere lesions and may play a compensatory role for contralesional visuospatial attention in the acute stage. In support of a compensatory role for the intact hemisphere, Wilke et al. (2012) showed that monkeys with unilateral LIP inactivation selected contralesional visual targets less often than ipsilesional targets, but that the occasional selection of contralesional targets was accompanied by increased task-related BOLD activity in frontoparietal areas in both hemispheres. The authors also reported that ipsilesional target selection correlated with decreased activity in the inactivated hemisphere, but not with hyperactivation of the intact hemisphere.

Longitudinal task-related fMRI studies of neglect are necessary for insights into the functional reorganization that supports recovery, however these types of studies have been limited in number. In one such study, Thimm et al. (2008) found that patients with neglect showed better detection of contralesional visual targets at the chronic (~ 4 months post-stroke) compared to the acute stage (~ 3 weeks post-stroke), which was associated with increased task-related BOLD activation in bilateral frontoparietal areas. In another longitudinal fMRI study, Umarova et al. (2016) found that patients with better recovery

of neglect/extinction showed increased activation in the contralesional/intact prefrontal cortex and ipsilesional parietal cortex. Although these few studies have shown that recovery from neglect/extinction is associated with large-scale functional network reorganization, a potential confound of task-based fMRI is that it infers brain activation during a task that patients have difficulty performing and are likely using different behavioural strategies to compensate, which further complicates interpretation.

In contrast, resting-state fMRI measures the spontaneous low frequency (0.01 – 0.1 Hz) fluctuations in the BOLD signal across the brain in the absence of a task while the subject is at rest. Seminal work from Biswal and colleagues (1995) showed that these BOLD signal fluctuations are highly correlated among areas involved in motor function in both hemispheres (Biswal et al., 1995). These correlations are thought to reflect a hemodynamic manifestation of the functional connectivity between resting neural activity across regions with shared functions (Biswal et al., 1995; Fox and Raichle, 2007).

Resting-state BOLD functional connectivity is thought to reflect the temporal correlation between brain areas that are either directly connected through a monosynaptic pathway or indirectly connected via polysynaptic pathways (Fox and Raichle, 2007; Greicius et al., 2009; Honey et al., 2009; Hori et al., 2020). Areas that are activated together as a task-related functional network are also highly correlated at rest and are preserved between wake and sedation or anesthesia in humans, monkeys, and rats (Biswal et al., 1995; Greicius et al., 2008, 2003; Hutchison et al., 2014, 2010; Vincent et al., 2007). Resting-state functional networks show strong spatiotemporal homology between humans and nonhuman primates and have been characterized for cognitive, sensory, and motor systems, including the frontoparietal network for oculomotor control and visuospatial attention (Hutchison et al., 2012, 2011; Vincent et al., 2007).

Resting-state fMRI has emerged as a valuable technique to study changes in functional connectivity due to lesions across large-scale networks in patients or animal models with severe deficits (Carter et al., 2012; Dijkhuizen et al., 2012; Grefkes and Fink, 2014). Following focal lesions, the changes in functional connectivity across relevant networks in both hemispheres from resting-state fMRI have been shown to correlate with the degree of behavioural impairment in human stroke patients (Baldassarre et al., 2014; Carter et al., 2010; He et al., 2007; Park et al., 2011; Ramsey et al., 2016; Wang et al., 2010) and experimental stroke models in rats (van Meer et al., 2012, 2010b, 2010a) and nonhuman primates (Ainsworth et al., 2018; Hernandez-Castillo et al., 2017; Meng et al., 2016).

While the majority of resting-state fMRI studies in stroke patients and animal lesion models focus on behaviour and functional connectivity in the sensorimotor domain, a few studies in stroke patients have examined neglect at the acute stage (Baldassarre et al., 2014; Carter et al., 2010; He et al., 2007) and one study reported the longitudinal changes associated with recovery of neglect (Ramsey et al., 2016). In stroke patients with right frontoparietal lesions, He et al. (2007) demonstrated that the severity of neglect deficits two weeks post-stroke correlated with decreased functional connectivity between the left and right posterior parietal cortex (He et al., 2007). Similarly, Carter et al. (2010) also found that the impaired detection of contralesional visual targets in stroke patients was strongly correlated with disruptions of interhemispheric functional connectivity within a cortical attention network (bilateral FEF, posterior parietal cortex, and middle temporal area), but that recovery did not correlate with intrahemispheric functional connectivity between those areas. In a study of stroke patients with large and heterogenous lesions that resulted in contralesional deficits of visuospatial attention and motor actions, Baldassarre et al. (2014) showed that neglect deficits were associated with the breakdown of

interhemispheric functional connectivity in both attention and somatomotor networks. In a longitudinal study of recovery from neglect, Ramsey et al. (2016) reported that impairments were largely recovered by 3 months post-stroke and plateaued up to 1 year later and also correlated with restoration of interhemispheric functional connectivity across attention and motor networks.

Overall, resting-state fMRI studies in human stroke patients demonstrate that changes in functional connectivity are behaviourally relevant in the recovery of lateralized visuospatial deficits. However, these studies have several limitations inherent to stroke populations: no pre-lesion baseline measures of functional connectivity and lesions were highly variable and spanned several distinct brain networks. These limitations may confound interpretations of the reported functional network reorganization and the degree of relevance to the recovery of visuospatial function. Thus, patient studies alone are insufficient for understanding the specific compensatory mechanisms that underlie attentional recovery following focal damage to one distinct region of the frontoparietal network.

As described earlier, focal unilateral aspiration of the caudal PFC in macaque monkeys resulted in severe impairments in directing attention to the contralesional visual hemifield, especially in the presence of a competing stimulus in the ipsilesional hemifield. These deficits gradually recovered along a similar timecourse as stroke patients with neglect. A better understanding of the compensatory mechanisms underlying recovery of neglect/extinction necessitates the examination of how discrete and focal lesions affect the distributed cortical network and how these changes relate to visuospatial attention. Experimental lesions in macaque monkeys have shown that resting-state functional connectivity correlates with recovery of motor function (Hernandez-Castillo et al., 2017) or visuospatial working memory (Ainsworth et al.,

2018; Meng et al., 2016). The study in **Chapter 3** investigates the changes in functional connectivity using longitudinal resting-state fMRI before and after unilateral endothelin-1-induced lesions in the caudal PFC of four macaque monkeys. Imaging data is reported alongside performance on a visually guided saccade task (single ipsilesional or contralesional visual stimulus) or on a free-choice saccade task (bilateral visual stimulus presentation with varying stimulus onset asynchronies) to measure the extent and recovery of contralesional target selection deficits.

1.4.3. Structural alterations in white matter pathways during the recovery of lateralized visuospatial impairments

The last section reviewed how the recovery of function after a focal lesion may be supported by network-wide changes in brain activity as shown using fMRI techniques. Alterations in functional network organization usually correspond to structural changes of the related neural components in brain tissue (e.g., axonal loss or sprouting, demyelination or remyelination) that can be imaged using an *in vivo* diffusion-weighted MRI technique to characterize axonal organization (Mori and Zhang, 2006). Diffusion-weighted MRI has emerged as a non-invasive whole brain imaging method that can be used *in vivo* to infer the structural properties of white matter pathways connecting areas within and between networks. Diffusion-weighted MRI is sensitive to the rate of water diffusion in biological tissue and can be used to characterize the microstructure and orientation of axonal tracts (Beaulieu, 2002). Since white matter is arranged in bundles of highly organized axonal tracts, the rate of water diffusion is higher in the direction parallel to the white matter fiber orientation and lower for the perpendicular direction (Beaulieu, 2002; Chenevert et al., 1990). Thus, water diffusion in white matter tissue is

considered highly anisotropic since it flows faster in one direction rather than equally in all directions (isotropic diffusion).

Diffusion tensor imaging (DTI) is one method of analyzing diffusion-weighted MR images in which a three-dimensional diffusion tensor is fit at each voxel to describe the local orientation and diffusivity (Basser et al., 1994a, 1994b). DTI can be used to visualize white matter tracts using tractography and the structural network connectivity can be described by calculating tract-specific diffusion properties of those pathways. Structural connectivity between two areas is generally reported using a measure of the degree of anisotropy within a white matter fiber tract. Fractional anisotropy is an estimate of the degree of anisotropy from DTI and is thought to reflect structural properties of white matter tissue, including axonal fiber density, myelination, and pathology (Basser and Pierpaoli, 1996; Beaulieu, 2002; Mori and Zhang, 2006; Song et al., 2005; Sotak, 2002).

Lesion-induced structural modifications of axonal fiber tracts may be reflected in the local fractional anisotropy throughout the various stages of post-lesion recovery (Sotak, 2002). For instance, in the acute post-lesion stage, anterograde and retrograde axonal degeneration may cause decreased fractional anisotropy in the surrounding perilesional tissue and along fibers that directly innervate the lesion (Pierpaoli et al., 2001; Sotak, 2002; Thomalla et al., 2004; van der Zijden et al., 2008; Werring et al., 2000). At the chronic stage, axonal regeneration or remyelination in perilesional or transneuronal white matter fibers may appear as increased fractional anisotropy on DTI (Dijkhuizen et al., 2012; Grayson et al., 2017; Sotak, 2002; Zhang et al., 2012). Several DTI studies have reported the behavioural relevance of network-wide alterations in fractional anisotropy following focal lesions in the degree of acute impairment and during recovery in brain injured patients (Byblow et al., 2015; Chen and Schlaug, 2013; Crofts et al., 2011;

Dacosta-Aguayo et al., 2014; Lin et al., 2015; Lindenberg et al., 2012, 2010; Liu et al., 2015; Ramsey et al., 2017; Schaechter et al., 2009; Umarova et al., 2017; Wang et al., 2006) and animal models (Harris et al., 2016; Liu et al., 2007; van der Zijden et al., 2008; van Meer et al., 2012). Evidence from rodent and nonhuman primate models of stroke have demonstrated that white matter structural alterations in the ipsilesional and contralesional hemispheres corresponded with improved motor function (Brus-Ramer et al., 2007; Carmichael and Chesselet, 2002; Dancause et al., 2005; Liu et al., 2008; Stroemer et al., 1995). Likewise, DTI studies in stroke patients with motor impairments have shown that increased fractional anisotropy in white matter tracts in the contralesional hemisphere were strongly correlated with better motor function (Liu et al., 2015; Schaechter et al., 2009). Longitudinal DTI studies in neurologically-healthy participants have demonstrated supporting evidence for behaviourally relevant changes in white matter that occur within weeks to months (Keller and Just, 2009; Scholz et al., 2009).

Recent evidence from DTI in acute or subacute stroke patients has shown that neglect was strongly associated with decreased fractional anisotropy in the right superior longitudinal fasciculus, an association fiber tract providing intrahemispheric communication between frontal and parietal areas (Hattori et al., 2018; Lunven et al., 2015; Thiebaut De Schotten et al., 2014; Urbanski et al., 2011). Moreover, decreased fractional anisotropy was also observed in the frontoparietal network of the unaffected contralesional hemisphere and was associated with the severity or persistence of neglect (Lunven et al., 2015; Umarova et al., 2014). Lunven et al. (2015) additionally found that the severity of neglect correlated with white matter changes in the splenium of the corpus callosum, which connects bilateral parietal areas. In one longitudinal DTI study, Umarova and colleagues (2017) reported that white matter degeneration in contralesional

frontoparietal connections correlated strongly with the degree of unrecovered neglect (Umarova et al., 2017). Overall, it appears that the recovery of function following focal damage is associated with compensatory structural changes across the distributed network which may relate with alterations in functional brain activity. The study in **Chapter 4** examines the structural changes in the white matter pathways connecting the bilateral frontoparietal network using longitudinal diffusion-weighted imaging before PFC lesions in macaque monkeys and after recovery from target selection deficits.

1.5. Objectives

Covert shifts in visuospatial attention and overt saccadic eye movements in primates rely on coordinated activity of the frontoparietal brain network. The major cortical nodes of the frontoparietal network include areas in the caudal prefrontal cortex (FEF, DLPFC) and the posterior parietal cortex (LIP), which are largely connected within hemisphere by the superior longitudinal fasciculus (SLF) and between hemisphere through the genu or isthmus of the corpus callosum. Unilateral damage to any region of the frontoparietal network typically results in impaired allocation of visual attention to the contralesional side of space, as shown in stroke patients (Corbetta and Shulman, 2011; B. de Haan et al., 2012; Li and Malhotra, 2015) and after experimental lesions or inactivation in nonhuman primates (Deuel and Farrar, 1993; Johnston et al., 2016; Lynch and McLaren, 1989; Schiller and Chou, 1998; Wardak et al., 2006, 2004, 2002). These lateralized visuospatial deficits typically manifest as reduced detection, discrimination, or selection of visual stimuli in the contralesional hemifield, especially in the presence of a competing stimulus in ipsilesional hemifield. Although these contralesional visuospatial deficits gradually improve over 2 to 4 months post-lesion, the degree of recovery varies across subjects and the compensatory neural mechanisms are not well understood. Longitudinal resting-state

fMRI and DTI offer *in vivo* and non-invasive measures of the functional and structural changes across large-scale networks after focal brain lesions and have been associated with behavioural outcome (Cappa and Perani, 2010; Dijkhuizen et al., 2012; Rehme and Grefkes, 2013). The broad objective of this thesis was to investigate the functional and structural changes in the frontoparietal network after a unilateral caudal PFC lesion and how those changes relate with behavioural recovery. To that aim, we made endothelin-1-induced lesions in the right caudal PFC of four macaque monkeys and obtained longitudinal pre- and post-lesion measures of (1) behavioural performance on a saccade task, (2) functional connectivity using resting-state fMRI, and (3) structural changes in white matter tracts using DTI.

In **Chapter 2**, we examined the effects of an endothelin-1-induced lesion in the right caudal PFC on saccade target selection of visual stimuli presented in the contralesional and ipsilesional hemifield on a free-choice saccade task. We also tested whether the reduction in saccade choice for contralesional stimuli was a result of impaired oculomotor processing. Behaviour was tested before and after the lesion until performance plateaued without further improvements. We found a reduction in saccades to contralesional stimuli that varied in severity and time to recovery based on lesion size and location, though deficits largely recovered over 2 to 4 months. Contralesional reaction times returned to baseline before the saccade choice bias had recovered and could not account for the severity of the choice bias throughout recovery. These findings demonstrate that the saccade choice bias was not exclusively due to oculomotor deficits alone but may instead reflect a combination of impaired motor and attentional processing.

The aim of **Chapter 3** was to investigate the functional reorganization of the frontoparietal network throughout the recovery of a saccade choice bias after unilateral caudal PFC lesions. The goal was to examine the pattern of functional connectivity

changes that was associated with better recovery. Functional imaging data was collected using resting-state fMRI at 7T before the lesion and at weeks 1, 4, and 8 or 16 post-lesion to correspond with the time course of behavioural recovery. We found that the pattern of functional reorganization associated with the recovery of contralesional saccade choice differed based on lesion size; functional connectivity normalized after smaller lesions and increased after larger lesions throughout recovery. We also found that the functional connectivity between contralesional DLPFC and ipsilesional posterior parietal cortex correlated with behavioural performance and that the contralesional DLPFC also showed increasing connectivity with the other frontoparietal network areas. The broad implication of the findings in this study is that both the contralesional and ipsilesional frontoparietal networks support the recovery of contralesional target selection. Importantly, our findings provide evidence for greater recruitment of the bilateral frontoparietal network during recovery from larger lesions, while recovery after smaller lesions was optimally supported by a normalization of the functional network.

In **Chapter 4**, the aim was to determine whether the temporal changes in resting-state BOLD activity synchronization of areas in the frontoparietal network was associated with structural alterations in the white matter fiber tracts that connect the network. DTI data was collected before the lesion and at a chronic post-lesion stage when behaviour had recovered. Probabilistic tractography and tensor-derived diffusion parameters were used to investigate the microstructural changes of four major fiber tracts connecting the frontoparietal network within and between hemispheres. The fiber tracts of interest included two lesion-affected white matter tracts, the ipsilesional SLF and transcallosal PFC tract, and two remote fiber tracts, contralesional SLF and transcallosal posterior parietal cortex tract. We found that the diffusion parameters for the remote white matter pathways, contralesional SLF and transcallosal PPC tracts, were differentially altered

based on lesion size. We suggest that these remote tracts may be involved in supporting neural compensation after small caudal PFC lesions and conversely that larger PFC lesions may recruit alternative pathways for neural and/or behavioural compensation beyond the cortical frontoparietal network.

1.6. References

- Ainsworth, M., Browncross, H., Mitchell, D.J., Mitchell, A.S., Passingham, R.E., Buckley, M.J., Duncan, J., Bell, A.H., 2018. Functional reorganisation and recovery following cortical lesions: A preliminary study in macaque monkeys. *Neuropsychologia* 119, 382–391.
- Akert, K., 1964. Comparative anatomy of frontal cortex and thalamofrontal connections, in: Warren, J.M., Akert, K. (Eds.), *The Frontal Granular Cortex and Behavior*. McGraw-Hill, New York, pp. 372–396.
- Albert, M.L., 1973. A simple test of visual neglect. *Neurology* 23, 658–664.
- Amiez, C., Petrides, M., 2009. Anatomical organization of the eye fields in the human and non-human primate frontal cortex. *Prog. Neurobiol.* 89, 220–230.
- Andersen, R.A., 2011. Inferior Parietal Lobule Function in Spatial Perception and Visuomotor Integration. *Compr. Physiol.*
- Andersen, R.A., Asanuma, C., Essick, G., Siegel, R.M., 1990. Corticocortical connections of anatomically and physiologically defined subdivisions within the inferior parietal lobule. *J. Comp. Neurol.* 296, 65–113.
- Armstrong, K.M., Fitzgerald, J.K., Moore, T., 2006. Changes in Visual Receptive Fields with Microstimulation of Frontal Cortex. *Neuron* 50, 791–798.
- Asaad, W.F., Rainer, G., Miller, E.K., 2000. Task-specific neural activity in the primate prefrontal cortex. *J. Neurophysiol.* 84, 451–459.
- Baker, J.T., Patel, G.H., Corbetta, M., Snyder, L.H., 2006. Distribution of activity across the monkey cerebral cortical surface, thalamus and midbrain during rapid, visually guided saccades. *Cereb. Cortex* 16, 447–459.
- Balan, P.F., Gottlieb, J., 2009. Functional significance of nonspatial information in monkey lateral intraparietal area. *J Neurosci* 29, 8166–8176.
- Baldassarre, A., Ramsey, L.E., Hacker, C.L., Callejas, A., Astafiev, S. V., Metcalf, N. V., Zinn, K., Rengachary, J., Snyder, A.Z., Carter, A.R., Shulman, G.L., Corbetta, M., Zinn, K., Siegel, J.S., Metcalf, N. V., M., S., Snyder, A.Z., Corbetta, M., 2014. Large-scale changes in network interactions as a physiological signature of spatial neglect. *Brain* 137, 3267–3283.

- Barbas, H., Medalla, M., Alade, O., Suski, J., Zikopoulos, B., Lera, P., 2005. Relationship of prefrontal connections to inhibitory systems in superior temporal areas in the rhesus monkey. *Cereb. Cortex* 15, 1356–1370.
- Barbas, H., Mesulam, M.-M., 1985. Cortical afferent input to the principals region of the rhesus monkey. *Neuroscience* 15, 619–637.
- Baron, J.C., Yamauchi, H., Fujioka, M., Endres, M., 2014. Selective neuronal loss in ischemic stroke and cerebrovascular disease. *J. Cereb. Blood Flow Metab.* 34, 2–18.
- Bartolomeo, P., 2007. Visual neglect. *Curr. Opin. Neurol.* 20, 381–386.
- Bartolomeo, P., Thiebaut de Schotten, M., Chica, A.B., 2012. Brain networks of visuospatial attention and their disruption in visual neglect. *Front. Hum. Neurosci.* 6, 1–10.
- Bartolomeo, P., Thiebaut De Schotten, M., Doricchi, F., 2007. Left unilateral neglect as a disconnection syndrome. *Cereb. Cortex* 17, 2479–2490.
- Basser, P., Mattiello, J., LeBihan, D., 1994a. MR diffusion tensor spectroscopy and imaging. *Biophys. J.* 66, 259–267.
- Basser, P., Mattiello, J., LeBihan, D., 1994b. Estimation of the effective self-diffusion tensor from the NMR spin echo. *J. Magn. Reson.* 103, 247–254.
- Basser, P., Pierpaoli, C., 1996. Microstructural and physiological features of tissues elucidated by quantitative-diffusion-tensor MRI. *J. Magn. Reson.* 111, 209–219.
- Baylis, G., 2002. Visual extinction with double simultaneous stimulation: what is simultaneous? *Neuropsychologia* 40, 1027–1034.
- Baylis, G.C., Driver, J., Rafal, R.D., 1993. Visual extinction and stimulus repetition. *J. Cogn. Neurosci.* 5, 453–466.
- Beauchamp, M.S., Petit, L., Ellmore, T.M., Ingelholm, J., Haxby, J. V., 2001. A parametric fMRI study of overt and covert shifts of visuospatial attention. *Neuroimage* 14, 310–321.
- Beaulieu, C., 2002. The basis of anisotropic water diffusion in the nervous system - A technical review. *NMR Biomed.*
- Beis, J.-M., Keller, C., Morin, N., Bartolomeo, P., Bernati, T., Chokron, S., Leclercq, M., Louis-Dreyfus, A., Marchal, F., Martin, Y., Perennou, D., Pradat-Diehl, P., Prairial, C., Rode, G., Rousseaux, M., Samuel, C., Sieroff, E., Wiart, L., Azouvi, P., 2004. Right spatial neglect after left hemisphere stroke. *Neurology* 63, 1600 LP – 1605.
- Bell, A.H., Bultitude, J.H., 2018. Methods matter: A primer on permanent and reversible interference techniques in animals for investigators of human neuropsychology. *Neuropsychologia* 115, 211–219.
- Bender, M.B., 1952. Disorders in perception. Springfield.
- Bender, M.B., Furlow, L.T., 1945. Phenomenon of visual extinction in homonymous

- fields and psychologic principles involved. *Arch. Neurol. Psychiatry* 53, 29–33.
- Benke, T., Luzzatti, C., Vallar, G., 2004. Hermann Zingerle's "Impaired perception of the own body due to organic brain disorders" An introductory comment, and an abridged translation. *Cortex* 40, 265–274.
- Berg, D.J., Boehnke, S.E., Marino, R.A., Munoz, D.P., Itti, L., 2009. Free viewing of dynamic stimuli by humans and monkeys. *J. Vis.* 9, 1–15.
- Berti, A., Cappa, S.F., Folegatti, A., 2007. Spatial representations, distortions and alterations in the graphic and artistic production of brain-damaged patients and of famous artists. *Funct. Neurol.* 22, 243–256.
- Bianchi, L., 1895. The functions of the frontal lobes. *Brain* 18, 497–522.
- Bisley, J., Goldberg, M., 2003. Neuronal Activity in the Lateral Intraparietal Area and Spatial Attention. *Science* (80-.). 299, 81–86.
- Bisley, J.W., Goldberg, M.E., 2010. Attention, Intention, and Priority in the Parietal Lobe. *Annu. Rev. Neurosci.* 33, 1–21.
- Biswal, B., Yetkin, F.Z., Haughton, V.M., Hyde, J.S., 1995. Functional connectivity in the motor cortex of resting human brain using echo-planar MRI. *Magn Reson Med* 34, 537–541.
- Blanke, O., Spinelli, L., Thut, G., Michel, C.M., Perrig, S., Landis, T., Seeck, M., 2000. Location of the human frontal eye field as defined by electrical cortical stimulation: Anatomical, functional and electrophysiological characteristics. *Neuroreport* 11, 1907–1913.
- Blatt, G.J., Andersen, R.A., Stoner, G.R., 1990. Visual receptive field organization and cortico-cortical connections of the lateral intraparietal area (area LIP) in the macaque. *J. Comp. Neurol.* 299, 421–445.
- Bogadhi, A.R., Bollimunta, A., Leopold, D.A., Krauzlis, R.J., 2018. Brain regions modulated during covert visual attention in the macaque. *Sci. Rep.* 8, 1–15.
- Borra, E., Ferroni, C.G., Gerbella, M., Giorgetti, V., Mangiaracina, C., Rozzi, S., Luppino, G., 2019. Rostro-caudal Connectional Heterogeneity of the Dorsal Part of the Macaque Prefrontal Area 46. *Cereb. Cortex* 29, 485–504.
- Brain, W.R., 1941. Visual disorientation with special reference to lesions of the right cerebral hemisphere. *Brain* 64, 244–272.
- Broca, P.P., 1861. Perte de la parole: ramollissement chronique et destruction partielle du lobe antérieur gauche du cerveau. *Bull. la Soc. d'anthropologie* 2, 235–238.
- Brodmann, K., 1913. Neuere Forschungsergebnisse der Großhirnrinden-anatomie mit besonderer Berücksichtigung anthropologischer Fragen. *Naturwissenschaften*.
- Bruce, C., Goldberg, M., 1985a. Primate frontal eye fields. II. Physiological and anatomical correlates of electrically evoked eye movements. *J. Neurophysiol.* 54, 714–734.

- Bruce, C., Goldberg, M., 1985b. Primate frontal eye fields. I. Single neurons discharging before saccades. *J. Neurophysiol.* 53, 603–635.
- Brus-Ramer, M., Carmel, J.B., Chakrabarty, S., Martin, J.H., 2007. Electrical stimulation of spared corticospinal axons augments connections with ipsilateral spinal motor circuits after injury. *J. Neurosci.*
- Buchkremer-Ratzmann, I., August, M., Hagemann, G., Witte, O.W., 1996. Electrophysiological transcortical diaschisis after cortical photothrombosis in rat brain. *Stroke* 27, 1105–1111.
- Buchkremer-Ratzmann, I., Witte, O.W., 1997. Extended brain disinhibition following small photothrombotic lesions in rat frontal cortex. *Neuroreport* 8, 519–522.
- Buschman, T.J., Miller, E.K., 2007. Top-down versus bottom-up control of attention in the prefrontal and posterior parietal cortices. *Science* (80-.). 315, 1860–1864.
- Bushnell, M.C., Goldberg, M.E., Robinson, D.L., 1981. Behavioral enhancement of visual responses in monkey cerebral cortex. I. Modulation in posterior parietal cortex related to selective visual attention. *J. Neurophysiol.* 46, 755–772.
- Buxbaum, L.J., Ferraro, M.K., Veramonti, T., Farne, A., Whyte, J., Ladavas, E., Frassinetti, F., Coslett, H.B., 2004. Hemispatial neglect: Subtypes, neuroanatomy, and disability. *Neurology* 62, 749–756.
- Byblow, W.D., Stinear, C.M., Barber, P.A., Petoe, M.A., Ackerley, S.J., 2015. Proportional recovery after stroke depends on corticomotor integrity. *Ann. Neurol.* 78, 848–859.
- Calautti, C., Baron, J.C., 2003. Functional neuroimaging studies of motor recovery after stroke in adults: A review. *Stroke.*
- Cappa, S.F., Perani, D., 2010. Imaging studies of recovery from unilateral neglect. *Exp. Brain Res.* 206, 237–241.
- Carmichael, S.T., 2012. Brain excitability in stroke: The yin and yang of stroke progression. *Arch. Neurol.* 69, 161–167.
- Carmichael, S.T., 2010. Molecular mechanisms of neural repair after stroke, in: Nudo, R.J., Cramer, S.C. (Eds.), *Brain Repair After Stroke*. Cambridge University Press, Cambridge, pp. 11–22.
- Carmichael, S.T., Chesselet, M.F., 2002. Synchronous neuronal activity is a signal for axonal sprouting after cortical lesions in the adult. *J. Neurosci.* 22, 6062–6070.
- Carrera, E., Tononi, G., 2014. Diaschisis: Past, present, future. *Brain* 137, 2408–2422.
- Carter, A.R., Astafiev, S. V., Lang, C.E., Connor, L.T., Rengachary, J., Strube, M.J., Pope, D.L.W., Shulman, G.L., Corbetta, M., 2010. Resting interhemispheric functional magnetic resonance imaging connectivity predicts performance after stroke. *Ann. Neurol.* 67, 365–375.
- Carter, A.R., Shulman, G.L., Corbetta, M., 2012. Why use a connectivity-based approach

- to study stroke and recovery of function? *Neuroimage* 62, 2271–2280.
- Caspari, N., Janssens, T., Mantini, D., Vandenberghe, R., Vanduffel, W., 2015. Covert shifts of spatial attention in the macaque monkey. *J. Neurosci.* 35, 7695–7714.
- Chechlacz, M., Rotshtein, P., Bickerton, W.L., Hansen, P.C., Deb, S., Humphreys, G.W., 2010. Separating neural correlates of allocentric and egocentric neglect: Distinct cortical sites and common white matter disconnections. *Cogn. Neuropsychol.* 27, 277–303.
- Chen, J.L., Schlaug, G., 2013. Resting state interhemispheric motor connectivity and white matter integrity correlate with motor impairment in chronic stroke. *Front. Neurol.* 4 NOV, 1–7.
- Chenevert, T.L., Brunberg, J.A., Pipe, J.G., 1990. Anisotropic diffusion in human white matter: Demonstration with MR techniques in vivo. *Radiology* 177, 401–405.
- Christopoulos, V.N., Kagan, I., Andersen, R.A., 2018. Lateral intraparietal area (LIP) is largely effector-specific in freechoice decisions. *Sci. Rep.* 8, 1–13.
- Clark, G., Lashley, K.S., 1947. Visual disturbances following frontal ablations in the monkey. *Anat. Rec.* 97, 326.
- Colby, C.L., Duhamel, J.R., Goldberg, M.E., 1996. Visual, presaccadic, and cognitive activation of single neurons in monkey lateral intraparietal area. *J. Neurophysiol.* 76, 2841–2852.
- Committeri, G., Pitzalis, S., Galati, G., Patria, F., Pelle, G., Sabatini, U., Castriota-Scanderbeg, A., Piccardi, L., Guariglia, C., Pizzamiglio, L., 2007. Neural bases of personal and extrapersonal neglect in humans. *Brain* 130, 431–441.
- Corbetta, M., 1998. Frontoparietal cortical networks for directing attention and the eye to visual locations: Identical, independent, or overlapping neural systems? *Proc. Natl. Acad. Sci. U. S. A.* 95, 831–838.
- Corbetta, M., Akbudak, E., Conturo, T.E., Snyder, A.Z., Ollinger, J.M., Drury, H. a., Linenweber, M.R., Petersen, S.E., Raichle, M.E., Van Essen, D.C., Shulman, G.L., 1998. A common network of functional areas for attention and eye movements. *Neuron* 21, 761–773.
- Corbetta, M., Kincade, M.J., Lewis, C., Snyder, A.Z., Sapir, A., 2005. Neural basis and recovery of spatial attention deficits in spatial neglect. *Nat. Neurosci.* 8, 1603–10.
- Corbetta, M., Miezin, F.M., Shulman, G.L., Petersen, S.E., 1993. A PET study of visuospatial attention. *J. Neurosci.* 13, 1202–1226.
- Corbetta, M., Shulman, G.L., 2011. Spatial Neglect and Attention Networks. *Annu. Rev. Neurosci.* 34, 569–599.
- Corbetta, M., Shulman, G.L., 2002. Control of goal-directed and stimulus-driven attention in the brain. *Nat. Rev. Neurosci.* 3, 201–15.
- Critchley, M., 1953. *The parietal lobes.*, The parietal lobes. Williams and Wilkins,

Oxford, England.

- Critchley, M., 1949. The phenomenon of tactile inattention with special reference to parietal lesions. *Brain* 72, 538–561.
- Crofts, J.J., Higham, D.J., Bosnell, R., Jbabdi, S., Matthews, P.M., Behrens, T.E.J., Johansen-Berg, H., 2011. Network analysis detects changes in the contralesional hemisphere following stroke. *Neuroimage* 54, 161–169.
- Crowne, D.P., Mah, L.W., 1998. A comparison of hemispatial neglect from posterior parietal and periarculate lesions in the monkey. *Psychobiology* 26, 103–108.
- Crowne, D.P., Yeo, C.H., Russell, I.S., 1981. The effects of unilateral frontal eye field lesions in the monkey: visual-motor guidance and avoidance behaviour. *Behav. Brain Res.* 2, 165–187.
- Crosson, P.L., Johansen-Berg, H., Behrens, T.E.J., Robson, M.D., Pinski, M.A., Gross, C.G., Richter, W., Richter, M.C., Kastner, S., Rushworth, M.F.S., 2005. Quantitative investigation of connections of the prefrontal cortex in the human and macaque using probabilistic diffusion tractography. *J. Neurosci.* 25, 8854–8866.
- Dacosta-Aguayo, R., Graña, M., Fernández-Andújar, M., López-Cancio, E., Cáceres, C., Bargalló, N., Barrios, M., Clemente, I., Monserrat, P.T., Sas, M.A., Dávalos, A., Auer, T., Mataró, M., 2014. Structural integrity of the contralesional hemisphere predicts cognitive impairment in ischemic stroke at three months. *PLoS One* 9, 1–11.
- Dai, P., Huang, H., Zhang, L., He, J., Zhao, X., Yang, F., Zhao, N., Yang, J., Ge, L., Lin, Y., Yu, H., Wang, J., 2017. A pilot study on transient ischemic stroke induced with endothelin-1 in the rhesus monkeys. *Sci. Rep.* 7, 45097.
- Dancause, N., Barbay, S., Frost, S.B., Plautz, E.J., Chen, D., Zoubina, E. V., Stowe, A.M., Nudo, R.J., 2005. Extensive Cortical Rewiring after Brain Injury. *J. Neurosci.* 25, 10167–10179.
- de Haan, B., Bither, M., Brauer, A., Karnath, H.O., 2015. Neural Correlates of Spatial Attention and Target Detection in a Multi-Target Environment. *Cereb. Cortex* 25, 2321–2331.
- de Haan, B., Karnath, H.O., Driver, J., 2012. Mechanisms and anatomy of unilateral extinction after brain injury. *Neuropsychologia* 50, 1045–1053.
- de Haan, B., Morgan, P.S., Rorden, C., 2008. Covert orienting of attention and overt eye movements activate identical brain regions. *Brain Res.* 1204, 102–111.
- de Haan, W., Mott, K., van Straaten, E.C.W., Scheltens, P., Stam, C.J., 2012. Activity Dependent Degeneration Explains Hub Vulnerability in Alzheimer’s Disease. *PLoS Comput. Biol.* 8.
- Denny-Brown, D., Chambers, R.A., 1958. The parietal lobe and behavior. *Res. Publ. Assoc. Res. Nerv. Ment. Dis.*

- Desimone, R., Duncan, J., 1995. Neural Mechanisms of Selective Visual Attention. *Annu. Rev. Neurosci.* 18, 193–222.
- Deubel, H., Schneider, W.X., 1996. Saccade target selection and object recognition: Evidence for a common attentional mechanism. *Vision Res.* 36, 1827–1837.
- Deuel, R., Collins, R., 1983. Recovery from unilateral neglect. *Exp. Neurol.* 81, 733–748.
- Deuel, R.K., Collins, R.C., 1984. The functional anatomy of frontal lobe neglect in the monkey: behavioral and quantitative 2-deoxyglucose studies. *Ann. Neurol.* 15, 521–529.
- Deuel, R.K., Farrar, C.A., 1993. Stimulus cancellation by macaques with unilateral frontal or parietal lesions. *Neuropsychologia* 31, 29–38.
- Deuel, R.K., Regan, D.J., 1985. Parietal hemineglect and motor deficits in the monkey. *Neuropsychologia* 23, 305–314.
- Di Pellegrino, G., Basso, G., Frassinetti, F., 1997. Spatial extinction on double asynchronous stimulation. *Neuropsychologia* 35, 1215–1223.
- Di Pellegrino, G., De Renzi, E., 1995. An experimental investigation on the nature of extinction. *Neuropsychologia* 33, 153–170.
- Dias, E.C.E.C., Segraves, M.A., 1999. Muscimol-induced inactivation of monkey frontal eye field: effects on visually and memory-guided saccades. *J. Neurophysiol.* 81, 2191–2214.
- Dijkhuizen, R.M., Ren, J., Mandeville, J.B., Wu, O., Ozdag, F.M., Moskowitz, M.A., Rosen, B.R., Finklestein, S.P., 2001. Functional magnetic resonance imaging of reorganization in rat brain after stroke. *Proc. Natl. Acad. Sci. U. S. A.* 98, 12766–71.
- Dijkhuizen, R.M., Singhal, A.B., Mandeville, J.B., Wu, O., Halpern, E.F., Finklestein, S.P., Rosen, B.R., Lo, E.H., 2003. Correlation between brain reorganization, ischemic damage, and neurologic status after transient focal cerebral ischemia in rats: a functional magnetic resonance imaging study. *J. Neurosci.* 23, 510–517.
- Dijkhuizen, R.M., van der Marel, K., Otte, W.M., Hoff, E.I., van der Zijden, J.P., van der Toorn, A., van Meer, M.P.A., 2012. Functional MRI and Diffusion Tensor Imaging of Brain Reorganization After Experimental Stroke. *Transl. Stroke Res.* 3, 36–43.
- Doricchi, F., Thiebaut de Schotten, M., Tomaiuolo, F., Bartolomeo, P., 2008. White matter (dis)connections and gray matter (dys)functions in visual neglect: Gaining insights into the brain networks of spatial awareness. *Cortex* 44, 983–995.
- Doricchi, F., Tomaiuolo, F., 2003. The anatomy of neglect without hemianopia: a key role for parietal-frontal disconnection? *Cogn. Neurosci. Neuropsychol.* 14, 2239–2243.
- Driver, J., Vuilleumier, P., 2001. Perceptual awareness and its loss in unilateral neglect and extinction. *Cognition* 79, 39–88.
- Ekstrom, L.B., Roelfsema, P.R., Arsenault, J.T., Bonmassar, G., Vanduffel, W., 2008.

- Bottom-up dependent gating of frontal signals in early visual cortex. *Science* 321, 414–417.
- Ellison, A., Schindler, I., Pattison, L.L., Milner, A.D., 2004. An exploration of the role of the superior temporal gyrus in visual search and spatial perception using TMS. *Brain* 127, 2307–2315.
- Ettlinger, G., Kalsbeck, J.E., 1962. Changes in tactile discrimination and in visual reaching after successive and simultaneous bilateral posterior parietal ablations in the monkey. *J. Neurol. Neurosurg. Psychiatry*.
- Everling, S., Tinsley, C.J., Gaffan, D., Duncan, J., 2006. Selective representation of task-relevant objects and locations in the monkey prefrontal cortex. *Eur. J. Neurosci.* 23, 2197–2214.
- Everling, S., Tinsley, C.J., Gaffan, D., Duncan, J., 2002. Filtering of neural signals by focused attention in the monkey prefrontal cortex. *Nat. Neurosci.* 5, 671–676.
- Fan, J., Li, Y., Fu, X., Li, L., Hao, X., Li, S., 2017. Nonhuman primate models of focal cerebral ischemia. *Neural Regen. Res.* 12, 321–328.
- Farne, A., 2004. Patterns of spontaneous recovery of neglect and associated disorders in acute right brain-damaged patients. *J. Neurol. Neurosurg. Psychiatry* 75, 1401–1410.
- Fecteau, J.H., Munoz, D.P., 2006. Saliency, relevance, and firing: a priority map for target selection. *Trends Cogn. Sci.* 10, 382–390.
- Feeney, D.M., Baron, J.C., 1986. Diaschisis. *Stroke* 17, 817–830.
- Ferrier, D., 1886. *The functions of the brain*, Smith, Elder, and Company. London.
- Fornito, A., Zalesky, A., Breakspear, M., 2015. The connectomics of brain disorders. *Nat. Rev. Neurosci.* 16, 159–172.
- Fox, M.D., Raichle, M.E., 2007. Spontaneous fluctuations in brain activity observed with functional magnetic resonance imaging. *Nat. Rev. Neurosci.* 8, 700–11.
- Friedrich, F.J., Egly, R., Rafal, R.D., Beck, D., 1998. Spatial attention deficits in humans: a comparison of superior parietal and temporal-parietal junction lesions. *Neuropsychology* 12, 193–207.
- Fries, W., 1984. Cortical projections to the superior colliculus in the macaque monkey: a retrograde study using horseradish peroxidase. *J. Comp. Neurol.* 230, 55–76.
- Fruhmann Berger, M., Johannsen, L., & Karnath, H.-O. (2008). Time course of eye and head deviation in spatial neglect. *Neuropsychology*, 22(6), 697–702.
- Fuchs, A.F., 1967. Saccadic and smooth pursuit eye movements in the monkey. *J. Physiol.* 191, 609–631.
- Fukuda, S., del Zoppo, G.J., 2003. Models of focal cerebral ischemia in the nonhuman primate. *ILAR J.* 44, 96–104.
- Funahashi, S., Bruce, C., Goldman-Rakic, P., 1991. Neuronal activity related to saccadic

- eye movements in the monkey's dorsolateral prefrontal cortex. *J. Neurophysiol.* 65, 1464–1483.
- Funahashi, S., Bruce, C., Goldman-Rakic, P., 1989. Mnemonic Coding of Visual Space in the Monkey's Dorsolateral Prefrontal Cortex. *J. Neurophysiol.* 61, 331–349.
- Funahashi, S., Bruce, C.J., Goldman-Rakic, P.S., 1990. Visuospatial coding in primate prefrontal neurons revealed by oculomotor paradigms. *J. Neurophysiol.*
- Fuster, J.M., 2008. *The Prefrontal Cortex, The Prefrontal Cortex.*
- Fuxe, K., Bjelke, B., Andbjør, B., Grahn, H., Rimondini, R., Agnati, L.F., 1997. Endothelin-1 induced lesions of the frontoparietal cortex of the rat. A possible model of focal cortical ischemia. *Neuroreport* 8, 2623–2629.
- Gaffan, D., Hornak, J., 1997. Visual neglect in the monkey: Representation and disconnection. *Brain* 120, 1647–1657.
- Geeraerts, S., Lafosse, C., Vandebussche, E., Verfaillie, K., 2005. A psychophysical study of visual extinction: Ipsilesional distractor interference with contralesional orientation thresholds in visual hemineglect patients. *Neuropsychologia* 43, 530–541.
- Gharabaghi, A., Fruhmann Berger, M., Tatagiba, M., Karnath, H.-O., 2006. The role of the right superior temporal gyrus in visual search—Insights from intraoperative electrical stimulation. *Neuropsychologia* 44, 2578–2581.
- Goldman-Rakic, P.S., Porrino, L.J., 1985. The primate mediodorsal (MD) nucleus and its projection to the frontal lobe. *J. Comp. Neurol.* 242, 535–560.
- Goldman, P.S., Nauta, W.J.H.H., 1976. Autoradiographic demonstration of a projection from prefrontal association cortex to the superior colliculus in the rhesus monkey. *Brain Res.* 116, 145–149.
- Gonzalez, C.L.R., Kolb, B., 2003. A comparison of different models of stroke on behaviour and brain morphology. *Eur. J. Neurosci.* 18, 1950–1962.
- Gottlieb, J., 2007. From thought to action: the parietal cortex as a bridge between perception, action, and cognition. *Neuron* 53, 9–16.
- Gottlieb, J., Goldberg, M.E., 1999. Activity of neurons in the lateral intraparietal area of the monkey during an antisaccade task. *Nat. Neurosci.* 2, 906–912.
- Gottlieb, J., Kusunoki, M., Goldberg, M.E., 2005. Simultaneous Representation of Saccade Targets and Visual Onsets in Monkey Lateral Intraparietal Area. *Cereb. Cortex* 15, 1198–1206.
- Gottlieb, J.P., Kusunoki, M., Goldberg, M.E., 1998. The representation of visual salience in monkey parietal cortex. *Nature* 391, 481–484.
- Grayson, D.S., Bliss-Moreau, E., Bennett, J., Lavenex, P., Amaral, D.G., 2017. Neural Reorganization Due to Neonatal Amygdala Lesions in the Rhesus Monkey: Changes in Morphology and Network Structure. *Cereb. Cortex* 27, 3240–3253.

- Grefkes, C., Fink, G.R., 2014. Connectivity-based approaches in stroke and recovery of function. *Lancet Neurol.* 13, 206–216.
- Grefkes, C., Fink, G.R., 2011. Reorganization of cerebral networks after stroke: New insights from neuroimaging with connectivity approaches. *Brain* 134, 1264–1276.
- Grefkes, C., Fink, G.R., 2005. The functional organization of the intraparietal sulcus in humans and monkeys. *J. Anat.* 207, 3–17.
- Greicius, M.D., Kiviniemi, V., Tervonen, O., Vainionpää, V., Alahuhta, S., Reiss, A.L., Menon, V., 2008. Persistent default-mode network connectivity during light sedation. *Hum. Brain Mapp.* 29, 839–847.
- Greicius, M.D., Krasnow, B., Reiss, A.L., Menon, V., 2003. Functional connectivity in the resting brain: a network analysis of the default mode hypothesis. *Proc. Natl. Acad. Sci. U. S. A.* 100, 253–8.
- Greicius, M.D., Supekar, K., Menon, V., Dougherty, R.F., 2009. Resting-state functional connectivity reflects structural connectivity in the default mode network. *Cereb. Cortex* 19, 72–78.
- Grosbras, M.H., Laird, A.R., Paus, T., 2005. Cortical regions involved in eye movements, shifts of attention, and gaze perception. *Hum. Brain Mapp.* 25, 140–154.
- Hagler, D.J., Sereno, M.I., 2006. Spatial maps in frontal and prefrontal cortex. *Neuroimage* 29, 567–577.
- Halligan, P.W., Marshall, J.C., 1993. The history and clinical presentation of neglect. *Unilateral Negl. Clin. Exp. Stud.*
- Harlow, J.M., 1848. Passage of an Iron Rod through the Head. *Bost. Med. Surg. J.* 39, 389–393.
- Harris, N.G., Verley, D.R., Gutman, B.A., Sutton, R.L., 2016. Bi-directional changes in fractional anisotropy after experiment TBI: Disorganization and reorganization? *Neuroimage* 133, 129–143.
- Hasegawa, R.P., Matsumoto, M., Mikami, A., 2000. Search target selection in monkey prefrontal cortex. *J. Neurophysiol.* 84, 1692–1696.
- Hattori, T., Ito, K., Nakazawa, C., Numasawa, Y., Watanabe, M., Aoki, S., Mizusawa, H., Ishiai, S., Yokota, T., 2018. Structural connectivity in spatial attention network: reconstruction from left hemispatial neglect. *Brain Imaging Behav.* 12, 309–323.
- He, B.J., Snyder, A.Z., Vincent, J.L., Epstein, A., Shulman, G.L., Corbetta, M., 2007. Breakdown of functional connectivity in frontoparietal networks underlies behavioral deficits in spatial neglect. *Neuron* 53, 905–18.
- Heilman, K.M., Pandya, D.N., Geschwind, N., 1970. Trimodal inattention following parietal lobe ablations. *Trans. Am. Neurol. Assoc.*
- Heilman, K.M., Valenstein, E., 1972. Frontal lobe neglect in man. *Neurology* 22, 660–660.

- Heilman, K.M., Valenstein, E., Watson, R.T., 1984. Neglect and related disorders. *Semin. Neurol.* 4, 209–219.
- Heilman, K.M., Van Den Abell, T., 1980. Right hemisphere dominance for attention: the mechanism underlying hemispheric asymmetries of inattention (neglect). *Neurology* 30, 327–330.
- Heilman, K.M., Watson, R.T., 1977. Mechanisms underlying the unilateral neglect syndrome. *Adv. Neurol.* 18, 93–106.
- Herbert, W.J., Powell, K., Buford, J.A., 2015. Evidence for a role of the reticulospinal system in recovery of skilled reaching after cortical stroke: initial results from a model of ischemic cortical injury. *Exp. Brain Res.* 233, 3231–3251.
- Hernandez-Castillo, C.R., Nashed, J.Y., Fernandez-Ruiz, J., Wang, J., Gallivan, J., Cook, D.J., 2017. Increased functional connectivity after stroke correlates with behavioral scores in non-human primate model. *Sci. Rep.* 7, 6701.
- Hier, D., Mondlock, J., Caplan, L., 1983. Recovery of behavioral abnormalities after right hemisphere stroke. *Neurology* 33, 345–350.
- Hikosaka, O., Wurtz, R.H., 1985. Modification of saccadic eye movements by GABA-related substances. I. Effect of muscimol and bicuculline in monkey superior colliculus. *J. Neurophysiol.*
- Hoffman, J.E., Subramaniam, B., 1995. The role of visual attention in saccadic eye movements. *Percept. Psychophys.* 57, 787–795.
- Holmes, G., 1918. Disturbances of vision by cerebral lesions. *Br. J. Ophthalmol.* 2, 353–384.
- Honey, C.J., Sporns, O., Cammoun, L., Gigandet, X., Thiran, J.P., Meuli, R., Hagmann, P., 2009. Predicting human resting-state functional connectivity from structural connectivity. *Proc. Natl. Acad. Sci. U. S. A.* 106, 2035–2040.
- Hori, Y., Schaeffer, D.J., Gilbert, K.M., Hayrynen, L.K., Cléry, J.C., Gati, J.S., Menon, R.S., Everling, S., 2020. Comparison of resting-state functional connectivity in marmosets with tracer-based cellular connectivity. *Neuroimage* 204.
- Husain, M., Kennard, C., 1996. Visual neglect associated with frontal lobe infarction. *J. Neurol.* 243, 652–657.
- Hutchison, R.M., Everling, S., 2012. Monkey in the middle: why non-human primates are needed to bridge the gap in resting-state investigations. *Front. Neuroanat.* 6, 29.
- Hutchison, R.M., Gallivan, J.P., Culham, J.C., Gati, J.S., Menon, R.S., Everling, S., 2012. Functional connectivity of the frontal eye fields in humans and macaque monkeys investigated with resting-state fMRI. *J. Neurophysiol.* 107, 2463–74.
- Hutchison, R.M., Hutchison, M., Manning, K.Y., Menon, R.S., Everling, S., 2014. Isoflurane induces dose-dependent alterations in the cortical connectivity profiles and dynamic properties of the brain's functional architecture. *Hum. Brain Mapp.* 35,

5754–5775.

- Hutchison, R.M., Leung, L.S., Mirsattari, S.M., Gati, J.S., Menon, R.S., Everling, S., 2011. Resting-state networks in the macaque at 7 T. *Neuroimage* 56, 1546–55.
- Hutchison, R.M., Mirsattari, S.M., Jones, C.K., Gati, J.S., Leung, L.S., 2010. Functional networks in the anesthetized rat brain revealed by independent component analysis of resting-state fMRI. *J. Neurophysiol.* 103, 3398–3406.
- Iba, M., Sawaguchi, T., 2003. Involvement of the dorsolateral prefrontal cortex of monkeys in visuospatial target selection. *J. Neurophysiol.* 89, 587–99.
- Ipata, A.E., Gee, A.L., Goldberg, M.E., Bisley, J.W., 2006. Activity in the lateral intraparietal area predicts the goal and latency of saccades in a free-viewing visual search task. *J. Neurosci.* 26, 3656–3661.
- Jackson, J.H., 1876. Case of large cerebral tumour without optic neuritis, and with left hemiplegia and imperception ... [Harrison & Sons, printers], [London].
- Jacobsen, C.F., Nissen, H.W., 1937. Studies of cerebral function in primates. IV. The effects of frontal lobe lesions on the delayed alternation habit in monkeys. *J. Comp. Psychol.* 23, 101–112.
- Johnston, K., Everling, S., 2012. Frontal cortex and flexible control of saccades, *The Oxford Handbook of Eye Movements*.
- Johnston, K., Everling, S., 2006. Monkey dorsolateral prefrontal cortex sends task-selective signals directly to the superior colliculus. *J. Neurosci.* 26, 12471–12478.
- Johnston, K., Lomber, S.G., Everling, S., 2016. Unilateral Deactivation of Macaque Dorsolateral Prefrontal Cortex Induces Biases in Stimulus Selection. *J. Neurophysiol.* 115, 1468–1476.
- Jones, T.A., Schallert, T., 1992. Overgrowth and pruning of dendrites in adult rats recovering from neocortical damage. *Brain Res.* 581, 156–160.
- Jones, T.H., Morawetz, R.B., Crowell, R.M., Marcoux, F.W., FitzGibbon, S.J., DeGirolami, U., Ojemann, R.G., 1981. Thresholds of focal cerebral ischemia in awake monkeys. *J. Neurosurg.* 54, 773–782.
- Juan, C.H., Shorter-Jacobi, S.M., Schall, J.D., 2004. Dissociation of spatial attention and saccade preparation. *Proc. Natl. Acad. Sci. U. S. A.* 101, 15541–15544.
- Kaping, D., Vinck, M., Hutchison, R.M., Everling, S., Womelsdorf, T., 2011. Specific contributions of ventromedial, anterior cingulate, and lateral prefrontal cortex for attentional selection and stimulus valuation. *PLoS Biol.* 9.
- Karnath, H.-O., Ferber, S., Himmelback, M., 2001. Spatial awareness is a function of the temporal not the posterior parietal lobe. *Nature* 411, 950-.
- Karnath, H.O., Berger, M.F., Küker, W., Rorden, C., 2004. The anatomy of spatial neglect based on voxelwise statistical analysis: A study of 140 patients. *Cereb. Cortex* 14, 1164–1172.

- Karnath, H.O., Rennig, J., Johannsen, L., Rorden, C., 2011. The anatomy underlying acute versus chronic spatial neglect: A longitudinal study. *Brain* 134, 903–912.
- Kastner, S., Ungerleider, L.G., 2000. Mechanisms of Visual Attention in the Human Cortex. *Annu. Rev. Neurosci.* 23, 315–341.
- Katsuki, F., Constantinidis, C., 2012. Unique and shared roles of the posterior parietal and dorsolateral prefrontal cortex in cognitive functions. *Front. Integr. Neurosci.*
- Keller, T.A., Just, M.A., 2009. Altering Cortical Connectivity: Remediation-Induced Changes in the White Matter of Poor Readers. *Neuron* 64, 624–631.
- Kennard, M.A., 1939a. Alterations in response to visual stimuli following lesions of frontal lobe in monkeys. *Arch. Neurol. Psychiatry* 41, 1153–1165.
- Kennard, M.A., 1939b. Alterations in response to visual stimuli following lesions of frontal lobe in monkeys. *Arch. Neurol. Psychiatry* 41, 1153–1165.
- Kennard, M.A., 1938. Reorganization of motor function in the cerebral cortex of monkeys deprived of motor and pre-motor areas in infancy. *J. Neurophysiol.* 1, 477–496.
- Kennard, M.A., Ectors, L., 1938. Forced circling in monkeys following lesions of the frontal lobes. *J. Neurophysiol.* 1, 45–54.
- Kinsbourne, M., 1987. Mechanisms of unilateral neglect. *Neurophysiol. Neuropsychol. Asp. Spat. Negl.* 69–86.
- Kinsbourne, M., 1970. The cerebral basis of lateral asymmetries in attention. *Acta Psychol. (Amst)*. 33, 193–201.
- Kleinman, J.T., Newhart, M., Davis, C., Heidler-Gary, J., Gottesman, R.F., Hillis, A.E., 2007. Right hemispatial neglect: frequency and characterization following acute left hemisphere stroke. *Brain Cogn.* 64, 50–59.
- Koval, M.J., Hutchison, R.M., Lomber, S.G., Everling, S., 2014. Effects of unilateral deactivations of dorsolateral prefrontal cortex and anterior cingulate cortex on saccadic eye movements. *J. Neurophysiol.* 111, 787–803.
- Kowler, E., Anderson, E., Doshier, B., Blaser, E., 1995. The role of attention in the programming of saccades. *Vision Res.* 35, 1897–1916.
- Koyama, M., Hasegawa, I., Osada, T., Adachi, Y., Nakahara, K., Miyashita, Y., 2004. Functional magnetic resonance imaging of macaque monkeys performing visually guided saccade tasks: Comparison of cortical eye fields with humans. *Neuron* 41, 795–807.
- Krauzlis, R.J., 2014. Attentional functions of the superior colliculus, in: Nobre, A.C. (Kia), Kastner, S. (Eds.), *The Oxford Handbook of Attention*. Oxford University Press, pp. 423–445.
- Krauzlis, R.J., Lovejoy, L.P., Zénon, A., 2013. Superior Colliculus and Visual Spatial Attention. *Annu. Rev. Neurosci.* 36, 165–182.

- Kubanek, J., Li, J.M., Snyder, L.H., 2015. Motor role of parietal cortex in a monkey model of hemispatial neglect. *Proc. Natl. Acad. Sci. U. S. A.* 112, E2067–E2072.
- Kunzle, H., Akert, K., 1977. Efferent connections of cortical area 8 (frontal eye field) in. *J Comp Neurol* 173, 147–164.
- Kwasnica, C.M., 2002. Unilateral neglect syndrome after stroke: Theories and management issues. *Crit. Rev. Phys. Rehabil. Med.* 14, 25–40.
- Lamotte, R.H., Acuña, C., 1978. Defects in accuracy of reaching after removal of posterior parietal cortex in monkeys. *Brain Res.*
- Latto, R., Cowey, A., 1971a. Fixation changes after frontal eye-field lesions in monkeys. *Brain Res.* 30, 25–36.
- Latto, R., Cowey, A., 1971b. Visual field defects after frontal eye field lesions in monkeys. *Brain Res.* 30, 1–24.
- Lebedev, M.A., Messinger, A., Kralik, J.D., Wise, S.P., 2004. Representation of attended versus remembered locations in prefrontal cortex. *PLoS Biol.* 2.
- Lee, R.G., van Donkelaar, P., 1995. Mechanisms underlying functional recovery following stroke. *Can.J.Neurol.Sci.* 22, 257–263.
- Lewis, J.W., Van Essen, D.C., 2000. Corticocortical connections of visual, sensorimotor, and multimodal processing areas in the parietal lobe of the macaque monkey. *J. Comp. Neurol.* 428, 112–137.
- Li, K., Malhotra, P.A., 2015. Spatial neglect. *Pract. Neurol.* 15, 333–339.
- Liepert, J., Storch, P., Fritsch, A., Weiller, C., 2000. Motor cortex disinhibition in acute stroke. *Clin. Neurophysiol.* 111, 671–676.
- Lin, Y.C., Daducci, A., Meskaldji, D.E., Thiran, J.P., Michel, P., Meuli, R., Krueger, G., Menegaz, G., Granziera, C., 2015. Quantitative analysis of myelin and axonal remodeling in the uninjured motor network after stroke. *Brain Connect.* 5, 401–412.
- Lindenberg, R., Renga, V., Zhu, L.L., Betzler, F., Alsop, D., Schlaug, G., 2010. Structural integrity of corticospinal motor fibers predicts motor impairment in chronic stroke. *Neurology* 74, 280–287.
- Lindenberg, R., Zhu, L.L., Rüber, T., Schlaug, G., 2012. Predicting functional motor potential in chronic stroke patients using diffusion tensor imaging. *Hum. Brain Mapp.* 33, 1040–1051.
- Liu, G., Dang, C., Chen, X., Xing, S., Dani, K., Xie, C., Peng, K., Zhang, Jingna, Li, J., Zhang, Jian, Chen, L., Pei, Z., Zeng, J., 2015. Structural remodeling of white matter in the contralesional hemisphere is correlated with early motor recovery in patients with subcortical infarction. *Restor. Neurol. Neurosci.* 33, 309–319.
- Liu, Y., D’Arceuil, H.E., Westmoreland, S., He, J., Duggan, M., Gonzalez, R.G., Pryor, J., De Crespigny, A.J., 2007. Serial diffusion tensor MRI after transient and permanent cerebral ischemia in nonhuman primates. *Stroke* 38, 138–145.

- Liu, Y., Yttri, E.A., Snyder, L.H., 2010. Intention and attention: different functional roles for LIPd and LIPv. *Nat. Neurosci.* 13, 495–500.
- Liu, Z., Li, Y., Zhang, X., Savant-Bhonsale, S., Chopp, M., 2008. Contralesional axonal remodeling of the corticospinal system in adult rats after stroke and bone marrow stromal cell treatment. *Stroke* 39, 2571–2577.
- Liversedge, S.P., Gilchrist, I.D., Everling, S., 2012. *The Oxford Handbook of Eye Movements*, The Oxford Handbook of Eye Movements.
- Logothetis, N.K., 2002. The neural basis of the blood-oxygen-level-dependent functional magnetic resonance imaging signal. *Philos. Trans. R. Soc. B Biol. Sci.* 357, 1003–1037.
- Lomber, S.G., Payne, B.R., 2000. Translaminar Differentiation of Visually Guided Behaviors Revealed by Restricted Cerebral Cooling Deactivation. *Cereb. Cortex* 10, 1066–1077.
- Lomber, S.G., Payne, B.R., Horel, J.A., 1999. The cryoloop: An adaptable reversible cooling deactivation method for behavioral or electrophysiological assessment of neural function. *J. Neurosci. Methods* 86, 179–194.
- Lunven, M., Bartolomeo, P., 2017. Attention and spatial cognition: Neural and anatomical substrates of visual neglect. *Ann. Phys. Rehabil. Med.* 60, 124–129.
- Lunven, M., De Schotten, M.T., Bourlon, C., Duret, C., Migliaccio, R., Rode, G., Bartolomeo, P., 2015. White matter lesion predictors of chronic visual neglect: A longitudinal study. *Brain* 138, 746–760.
- Lynch, J.C., Graybiel, A.M., Lobeck, L.J., 1985. The differential projection of two cytoarchitectonic subregions of the inferior parietal lobule of macaque upon the deep layers of the superior colliculus. *J. Comp. Neurol.* 235, 241–254.
- Lynch, J.C., McLaren, J.A.Y.W., 1989. Deficits of Visual Attention and Saccadic Eye Movements After Lesions of Parietooccipital Cortex in Monkeys. *J. Neurophysiol.* 6, 74–90.
- Macrae, I.M., Robinson, M.J., Graham, D.I., Reid, J.L., McCulloch, J., 1993. Endothelin-1-induced reductions in cerebral blood flow: dose dependency, time course, and neuropathological consequences. *J. Cereb. Blood Flow Metab.* 13, 276–284.
- Maioli, M.G., Squatrito, S., Galletti, C., Battaglini, P.P., Sanseverino, E.R., 1983. Cortico-cortical connections from the visual region of the superior temporal sulcus to frontal eye field in the macaque. *Brain Res.* 265, 294–299.
- Majchrzak, M., Di Scala, G., 2000. GABA and muscimol as reversible inactivation tools in learning and memory. *Neural Plast.* 7, 19–29.
- Mattingley, J.B., Driver, J., Beschin, N., Robertson, I.H., 1997. Attentional competition between modalities: Extinction between touch and vision after right hemisphere damage. *Neuropsychologia* 35, 867–880.

- McFie, J., Piercy, M.F., Zangwill, O.L., 1950. Visual-spatial agnosia associated with lesions of the right cerebral hemisphere. *Brain* 73, 167–190.
- McIntosh, A.R., 1999. Mapping Cognition to the Brain Through Neural Interactions. *Memory* 7, 523–548.
- McPeck, R.M., Keller, E.L., 2004. Deficits in saccade target selection after inactivation of superior colliculus. *Nat. Neurosci.* 7, 757–63.
- Meng, Y., Hu, X., Bachevalier, J., Zhang, X., 2016. Decreased functional connectivity in dorsolateral prefrontal cortical networks in adult macaques with neonatal hippocampal lesions: Relations to visual working memory deficits. *Neurobiol. Learn. Mem.* 134, 31–37.
- Mesulam, M.-M., 1999. Spatial attention and neglect: parietal, frontal and cingulate contributions to the mental representation and attentional targeting of salient extrapersonal events. *Philos. Trans. R. Soc. Lond. B. Biol. Sci.* 354, 1325–1346.
- Mesulam, M. -Marchsel, 1981. A cortical network for directed attention and unilateral neglect. *Ann. Neurol.*
- Miller, E.K., Cohen, J.D., 2001. An Integrative Theory of Prefrontal Cortex Function. *Annu. Rev. Neurosci.* 24, 167–202.
- Milner, A.D., Mcintosh, R.D., 2005. The neurological basis of visual neglect. *Curr. Opin. Neurol.* 18, 748–753.
- Monakow, C.V., 1914. *Die Lokalisation im Grosshirn und der Funktion durch kortikale Herde.* Wiesbaden.
- Monakow, C.V., 1897. *Gehirnpathologie.* Vienna.
- Monosov, I.E., Thompson, K.G., 2009. Frontal eye field activity enhances object identification during covert visual search. *J. Neurophysiol.* 102, 3656–3672.
- Moore, T., Armstrong, K.M., 2003. Selective gating of visual signals by microstimulation of frontal cortex. *Nature* 421, 370–373.
- Moore, T., Fallah, M., 2001. Control of eye movements and spatial attention. *Proc. Natl. Acad. Sci. U. S. A.* 98, 1273–1276.
- Mori, S., Zhang, J., 2006. Principles of Diffusion Tensor Imaging and Its Applications to Basic Neuroscience Research. *Neuron* 51, 527–539.
- Mort, D.J., Malhotra, P., Mannan, S.K., Rorden, C., Pambakian, A., Kennard, C., Husain, M., 2003. The anatomy of visual neglect. *Brain* 126, 1986–1997.
- Müller, J.R., Philiastides, M.G., Newsome, W.T., 2005. Microstimulation of the superior colliculus focuses attention without moving the eyes. *Proc. Natl. Acad. Sci. U. S. A.* 102, 524–529.
- Munoz, D.P., Everling, S., 2004. Look away: The anti-saccade task and the voluntary control of eye movement. *Nat. Rev. Neurosci.* 5, 218–228.

- Murata, Y., Higo, N., 2016. Development and Characterization of a Macaque Model of Focal Internal Capsular Infarcts. *PLoS One* 11, e0154752.
- Murphy, T.H., Corbett, D., 2009. Plasticity during stroke recovery: from synapse to behaviour. *Nat. Rev. Neurosci.* 10, 861–872.
- Murthy, A., Ray, S., Shorter, S.M., Schall, J.D., Thompson, K.G., 2009. Neural control of visual search by frontal eye field: Effects of unexpected target displacement on visual selection and saccade preparation. *J. Neurophysiol.* 101, 2485–2506.
- Napieralski, J.A., Butler, A.K., Chesselet, M.F., 1996. Anatomical and functional evidence for lesion-specific sprouting of corticostriatal input in the adult rat. *J. Comp. Neurol.* 373, 484–497.
- Nobre, A.C., Gitelman, D.R., Dias, E.C., Mesulam, M.M., 2000. Covert visual spatial orienting and saccades: Overlapping neural systems. *Neuroimage* 11, 210–216.
- Nomura, E.M., Gratton, C., Visser, R.M., Kayser, A., Perez, F., D’Esposito, M., 2010. Double dissociation of two cognitive control networks in patients with focal brain lesions. *Proc. Natl. Acad. Sci.* 107, 12017–12022.
- Ogawa, S., Lee, T.M., Kay, A.R., Tank, D.W., 1990. Brain magnetic resonance imaging with contrast dependent on blood oxygenation. *Proc. Natl. Acad. Sci. U. S. A.* 87, 9868–72.
- Ogawa, S., Tank, D.W., Menon, R., Ellermann, J.M., Kim, S.G., Merkle, H., Ugurbil, K., 1992. Intrinsic signal changes accompanying sensory stimulation: Functional brain mapping with magnetic resonance imaging. *Proc. Natl. Acad. Sci. U. S. A.* 89, 5951–5955.
- Oppenheim, H., 1885. Über eine, durch eine klinisch bisher nicht verwertete Untersuchungsmethode, ermittelte Form der Sensibilitätsstörung bei einseitigen Erkrankungen des Grosshirns. *Neurol. Cent.* 4, 529–533.
- Opris, I., Barborica, A., Ferrera, V.P., 2005. Microstimulation of the dorsolateral prefrontal cortex biases saccade target selection. *J. Cogn. Neurosci.* 17, 893–904.
- Pandya, D.N., Seltzer, B., 1982. Intrinsic connections and architectonics of posterior parietal cortex in the rhesus monkey. *J. Comp. Neurol.*
- Paré, M., Dorris, M.C., 2012. The role of posterior parietal cortex in the regulation of saccadic eye movements. *Oxford Handb. Eye Movements* 257–278.
- Park, C.H., Chang, W.H., Ohn, S.H., Kim, S.T., Bang, O.Y., Pascual-Leone, A., Kim, Y.H., 2011. Longitudinal changes of resting-state functional connectivity during motor recovery after stroke. *Stroke* 42, 1357–1362.
- Paterson, A., Zangwill, O.L., 1944. Disorders of visual space perception associated with lesions of the right cerebral hemisphere. *Brain* 67, 331–358.
- Paus, T., 1996. Location and function of the human frontal eye-field: A selective review. *Neuropsychologia* 34, 475–483.

- Payne, B.R., Lomber, S.G., Villa, A.E., Bullier, J., 1996. Reversible deactivation of cerebral network components. *Trends Neurosci.* 19, 535–542.
- Peel, T.R., Johnston, K., Lomber, S.G., Corneil, B.D., 2014. Bilateral saccadic deficits following large and reversible inactivation of unilateral frontal eye field. *J. Neurophysiol.* 111, 415–433.
- Perry, R.J., Zeki, S., 2000. The neurology of saccades and covert shifts in spatial attention: An event-related fMRI study. *Brain* 123, 2273–2288.
- Petcu, E.B., Sherwood, K., Popa-Wagner, A., Buga, A.M., Aceti, L., Miroiu, R.I., 2016. Artistic Skills Recovery and Compensation in Visual Artists after Stroke. *Front. Neurol.* 7.
- Petersen, S.E., Posner, M.I., 2012. The Attention System of the Human Brain: 20 Years After. *Annu. Rev. Neurosci.* 35, 73–89.
- Petrides, M., Pandya, D.N., 2002. Comparative cytoarchitectonic analysis of the human and the macaque ventrolateral prefrontal cortex and corticocortical connection patterns in the monkey. *Eur. J. Neurosci.* 16, 291–310.
- Petrides, M., Pandya, D.N., 1999. Dorsolateral prefrontal cortex: comparative cytoarchitectonic analysis in the human and the macaque brain and corticocortical connection patterns. *Eur. J. Neurosci.* 11, 1011–36.
- Petrides, M., Pandya, D.N., 1984. Projections to the frontal cortex from the posterior parietal region in the rhesus monkey. *J. Comp. Neurol.* 116, 105–116.
- Pierpaoli, C., Barnett, A., Pajevic, S., Chen, R., Penix, L.R., Virta, A., Basser, P., 2001. Water diffusion changes in wallerian degeneration and their dependence on white matter architecture. *Neuroimage* 13, 1174–1185.
- Pinéas, H., 1931. Ein Fall von räumlicher Orientierungsstörung mit Dyschirie. *Zeitschrift für die gesamte Neurol. und Psychiatr.*
- Poppelreuter, W., 1917. Die psychischen schaedungen durch kopfschuss in kriege 1914–1916. Voss, Leipzig, Germany.
- Posner, M.I., 1980. Orienting of attention. *Q. J. Exp. Psychol.* 32, 3–25.
- Posner, M.I., Cohen, Y., 1984. Components of visual orienting. *Atten. Perform.*
- Posner, M.I., Petersen, S.E., 1990. The Attention System of the Human Brain. *Annu. Rev. Neurosci.* 13, 25–42.
- Posner, M.I., Walker, J.A., Friedrich, F.J., Rafal, R.D., 1984. Effects of parietal injury on covert orienting of attention. *J. Neurosci.* 4, 1863–1874.
- Pouget, P., Stepniewska, I., Crowder, E.A., Leslie, M.W., Emeric, E.E., Nelson, M.J., Schall, J.D., 2009. Visual and motor connectivity and the distribution of calcium-binding proteins in macaque frontal eye field: implications for saccade target selection. *Front. Neuroanat.* 3, 2.

- Powell, K.D., Goldberg, M.E., 2000. Response of neurons in the lateral intraparietal area to a distractor flashed during the delay period of a memory-guided saccade. *J. Neurophysiol.* 84, 301–310.
- Premereur, E., Vanduffel, W., Roelfsema, P.R., Janssen, P., 2012. Frontal eye field microstimulation induces task-dependent gamma oscillations in the lateral intraparietal area. *J. Neurophysiol.* 108, 1392–1402.
- Rainer, G., Asaad, W.F., Miller, E.K., 1998. Selective representation of relevant information by neurons in the primate prefrontal cortex. *Nature* 393, 577–579.
- Rajkowska, G., Goldman-Rakic, P.S., 1995. Cytoarchitectonic definition of prefrontal areas in the normal human cortex: II. Variability in locations of areas 9 and 46 and relationship to the Talairach coordinate system. *Cereb. Cortex* 5, 323–337.
- Ramkumar, P., Fernandes, H., Kording, K., Segraves, M., 2015. Modeling peripheral visual acuity enables discovery of gaze strategies at multiple time scales during natural scene search. *J. Vis.* 15, 1–20.
- Ramsey, L.E., Siegel, J.S., Baldassarre, A., Metcalfe, N. V., Zinn, K., Shulman, G.L., Corbetta, M., 2016. Normalization of network connectivity in hemispatial neglect recovery. *Ann. Neurol.* 80, 127–141.
- Ramsey, L.E., Siegel, J.S., Lang, C.E., Strube, M., Shulman, G.L., Corbetta, M., 2017. Behavioural clusters and predictors of performance during recovery from stroke. *Nat. Hum. Behav.* 1, 0038.
- Rapcsak, S.Z., Watson, R.T., Heilman, K.M., 1987. Hemispace-visual field interactions in visual extinction. *J. Neurol. Neurosurg. Psychiatry* 50, 1117–1124.
- Rehme, A.K., Eickhoff, S.B., Wang, L.E., Fink, G.R., Grefkes, C., 2011. Dynamic causal modeling of cortical activity from the acute to the chronic stage after stroke. *Neuroimage* 55, 1147–1158.
- Rehme, A.K., Grefkes, C., 2013. Cerebral network disorders after stroke: evidence from imaging-based connectivity analyses of active and resting brain states in humans. *J. Physiol.* 591, 17–31.
- Rengachary, J., He, B.J., Shulman, G.L., Corbetta, M., 2011. A behavioral analysis of spatial neglect and its recovery after stroke. *Front. Hum. Neurosci.* 5, 29.
- Rizzolatti, G., Matelli, M., Pavesi, G., 1983. Deficits in attention and movement following the removal of postarcuate (area 6) and prearcuate (area 8) cortex in macaque monkeys. *Brain* 106, 655–673.
- Rizzolatti, G., Riggio, L., Dascola, I., Umiltá, C., 1987. Reorienting attention across the horizontal and vertical meridians: Evidence in favor of a premotor theory of attention. *Neuropsychologia* 25, 31–40.
- Rizzolatti, G., Luppino, G., Matelli, M., 1998. The organization of the cortical motor system: New concepts. *Electroencephalogr. Clin. Neurophysiol.*

- Ro, T., Rorden, C., Driver, J., Rafal, R., 2001. Ipsilesional biases in saccades but not perception after lesions of the human inferior parietal lobule. *J. Cogn. Neurosci.* 13, 920–929.
- Robinson, D.A., Fuchs, A.F., 1969. Eye movements evoked by stimulation of frontal eye fields. *J. Neurophysiol.* 32, 637–648.
- Robinson, D.L., Bowman, E.M., Kertzman, C., 1995. Covert orienting of attention in macaques. II. Contributions of parietal cortex. *J. Neurophysiol.* 74, 698–712.
- Robinson, D.L., Goldberg, M.E., Stanton, G.B., 1978. Parietal association cortex in the primate: sensory mechanisms and behavioral modulations. *J. Neurophysiol.* 41, 910–932.
- Rode, G., Pagliari, C., Huchon, L., Rossetti, Y., Pisella, L., 2017. Semiology of neglect: An update. *Ann. Phys. Rehabil. Med.* 60, 177–185.
- Rorden, C., Jelsek, L., Simon-Dack, S., Baylis, L.L., Baylis, G.C., 2009. Visual extinction: The effect of temporal and spatial bias. *Neuropsychologia* 47, 321–329.
- Rorden, C., Mattingley, J.B., Karnath, H.O., Driver, J., 1997. Visual extinction and prior entry: Impaired perception of temporal order with intact motion perception after unilateral parietal damage. *Neuropsychologia* 35, 421–433.
- Ross, D.T., Ebner, F.F., 1990. Thalamic retrograde degeneration following cortical injury: An excitotoxic process? *Neuroscience* 35, 525–550.
- Saalman, Y.B., Pigarev, I.N., Vidyasagar, T.R., 2007. Neural mechanisms of visual attention: How top-down feedback highlights relevant locations. *Science* (80-.). 316, 1612–1615.
- Sato, T., Murthy, A., Thompson, K.G., Schall, J.D., 2001. Search efficiency but not response interference affects visual selection in frontal eye field. *Neuron* 30, 583–591.
- Sato, T.R., Schall, J.D., 2003. Effects of stimulus-response compatibility on neural selection in frontal eye field. *Neuron* 38, 637–648.
- Saxena, S., Caroni, P., 2011. Selective Neuronal Vulnerability in Neurodegenerative Diseases: From Stressor Thresholds to Degeneration. *Neuron* 71, 35–48.
- Schaechter, J.D., Fricker, Z.P., Perdue, K.L., Helmer, K.G., Vangel, M.G., Greve, D.N., Makris, N., 2009. Microstructural status of ipsilesional and contralesional corticospinal tract correlates with motor skill in chronic stroke patients. *Hum. Brain Mapp.* 30, 3461–3474.
- Schall, J., 1991. Neuronal Activity related to Visually Guided Saccades in Frontal Eye Fields of Monkeys. *J. Neurophysiol.* 66, 559–579.
- Schall, J.D., 2004. On the role of frontal eye field in guiding attention and saccades. *Vision Res.* 44, 1453–1467.
- Schall, J.D., 2002. The neural selection and control of saccades by the frontal eye field.

- Philos. Trans. R. Soc. Lond. B. Biol. Sci. 357, 1073–82.
- Schall, J.D., Hanes, D.P., 1993. Neural basis of saccade target selection in frontal eye field during visual search. *Nature* 366, 467–469.
- Schall, J.D., Hanes, D.P., Thompson, K.G., King, D.J., 1995. Saccade target selection in frontal eye field of macaque. I. Visual and premovement activation. *J. Neurosci.* 15, 6905–6918.
- Schall, J.D., Thompson, K.G., 1999. NEURAL SELECTION AND CONTROL OF VISUALLY GUIDED EYE MOVEMENTS. *Annu. Rev. Neurosci.* 22, 241–259.
- Schiller, P.H., Chou, I., 2000. The effects of anterior arcuate and dorsomedial frontal cortex lesions on visually guided eye movements in the rhesus monkey: 1. Single and sequential targets. *Vision Res.* 40, 1609–1626.
- Schiller, P.H., Chou, I., 1998. The effects of frontal eye field and dorsomedial frontal cortex lesions on visually guided eye movements. *Nat. Neurosci.* 1, 248–253.
- Schiller, P.H., Sandell, J.H., Maunsell, J.H., 1987. The effect of frontal eye field and superior colliculus lesions on saccadic latencies in the rhesus monkey. *J. Neurophysiol.* 57, 1033–1049.
- Schiller, P.H., Tehovnik, E.J., 2003. Cortical inhibitory circuits in eye-movement generation. *Eur. J. Neurosci.* 18, 3127–3133.
- Schmahmann, J.D., Pandya, D.N., 1997. Anatomic Organization of the Basilar Pontine Projections from Prefrontal Cortices in Rhesus Monkey. *J. Neurosci.* 17, 438 LP – 458.
- Scholz, J., Klein, M.C., Behrens, T.E.J., Johansen-Berg, H., 2009. Training induces changes in white-matter architecture. *Nat. Neurosci.* 12, 1370–1371.
- Scoville, W.B., Milner, B., 1957. Loss of recent memory after bilateral hippocampal lesions. *J. Neurol. Neurosurg. Psychiatry* 20, 11–21.
- Segraves, M.A., Kuo, E., Caddigan, S., Berthiaume, E.A., Kording, K.P., 2017. Predicting rhesus monkey eye movements during natural image search. *J. Vis.* 17, 1–17.
- Sharkey, J., Ritchie, I.M., Kelly, P.A.T., 1993. Perivascular microapplication of endothelin-1: A new model of focal cerebral ischaemia in the rat. *J. Cereb. Blood Flow Metab.* 13, 865–871.
- Sommer, M.A., Tehovnik, E.J., 1999. Reversible inactivation of macaque dorsomedial frontal cortex: Effects on saccades and fixations. *Exp. Brain Res.* 124, 429–446.
- Sommer, M.A., Tehovnik, E.J., 1997. Reversible inactivation of macaque frontal eye field. *Exp. Brain Res.* 116, 229–249.
- Song, S.K., Yoshino, J., Le, T.Q., Lin, S.J., Sun, S.W., Cross, A.H., Armstrong, R.C., 2005. Demyelination increases radial diffusivity in corpus callosum of mouse brain. *Neuroimage* 26, 132–140.

- Sotak, C.H., 2002. The role of diffusion tensor imaging in the evaluation of ischemic brain - A review. *NMR Biomed.* 15, 561–569.
- Stanton, G., Bruce, C., Goldberg, M., 1993. Topography of projections to the frontal lobe from the macaque frontal eye fields. *J. Comp. Neurol.* 330, 286–301.
- Stanton, G., Goldberg, M., Bruce, C., 1988a. Frontal eye field efferents in the macaque monkey: I. Subcortical pathways and topography of striatal and thalamic terminal fields. *J. Comp. Neurol.* 271, 473–492.
- Stanton, G., Goldberg, M., Bruce, C., 1988b. Frontal eye field efferents in the macaque monkey: II. Topography of terminal fields in midbrain and pons. *J. Comp. Neurol.* 271, 493–506.
- Stanton, G.B., Deng, S. -Y, Goldberg, E.M., McMullen, N.T., 1989. Cytoarchitectural characteristic of the frontal eye fields in macaque monkeys. *J. Comp. Neurol.* 282, 415–427.
- Stone, S.P., Halligan, P.W., Greenwood, R.J., 1993. The incidence of neglect phenomena and related disorders in patients with an acute right or left hemisphere stroke. *Age Ageing.*
- Stroemer, R.P., Kent, T.A., Hulsebosch, C.E., 1995. Neocortical neural sprouting, synaptogenesis, and behavioral recovery after neocortical infarction in rats. *Stroke* 26, 2135–2144.
- Szczepanski, S.M., Konen, C.S., Kastner, S., 2010. Mechanisms of spatial attention control in frontal and parietal cortex. *J. Neurosci.* 30, 148–160.
- Teasell, R., Hussein, N., Mrehabmed, M., Viana, R., Donaldson Bhsc, S., Madady Msc, M., 2016. Clinical Consequences of Stroke. *Stroke Rehabil. Clin. Handb.*
- Tehovnik, E.J., Sommer, M. a., Chou, I.H., Slocum, W.M., Schiller, P.H., 2000. Eye fields in the frontal lobes of primates. *Brain Res. Rev.* 32, 413–448.
- Teo, L., Bourne, J., 2014. A Reproducible and Translatable Model of Focal Ischemia in the Visual Cortex of Infant and Adult Marmoset Monkeys. *Brain Pathol.* 24, 459–474.
- Thiebaut De Schotten, M., Dell’Acqua, F., Ratiu, P., Leslie, A., Howells, H., Cabanis, E., Iba-Zizen, M.T., Plaisant, O., Simmons, A., Dronkers, N.F., Corkin, S., Catani, M., 2015. From phineas gage and monsieur leborgne to H.M.: Revisiting disconnection syndromes. *Cereb. Cortex* 25, 4812–4827.
- Thiebaut de Schotten, M., Dell’Acqua, F., Valabregue, R., Catani, M., 2012. Monkey to human comparative anatomy of the frontal lobe association tracts. *Cortex* 48, 82–96.
- Thiebaut De Schotten, M., Tomaiuolo, F., Aiello, M., Merola, S., Silvetti, M., Lecce, F., Bartolomeo, P., Doricchi, F., 2014. Damage to white matter pathways in subacute and chronic spatial neglect: A group study and 2 single-case studies with complete virtual “in vivo” tractography dissection. *Cereb. Cortex* 24, 691–706.

- Thiebaut de Schotten, M., Urbanski, M., Duffau, H., Volle, E., Lévy, R., Dubois, B., Bartolomeo, P., 2005. Direct evidence for a parietal-frontal pathway subserving spatial awareness in humans. *Science* (80-.). 309, 2226–2228.
- Thomalla, G., Glauche, V., Koch, M.A., Beaulieu, C., Weiller, C., Röther, J., 2004. Diffusion tensor imaging detects early Wallerian degeneration of the pyramidal tract after ischemic stroke. *Neuroimage* 22, 1767–1774.
- Thompson, K.G., Bichot, N.P., 2005. A visual salience map in the primate frontal eye field, in: *Brain*. pp. 249–262.
- Thompson, K.G., Bichot, N.P., Schall, J.D., 2001. From attention to action in frontal cortex., in: *Visual Attention and Cortical Circuits*. The MIT Press, Cambridge, MA, US, pp. 137–157.
- Thompson, K.G., Bichot, N.P., Schall, J.D., 1997. Dissociation of visual discrimination from saccade programming in macaque frontal eye field. *J. Neurophysiol.* 77, 1046–1050.
- Thompson, K.G., Biscoe, K.L., Sato, T.R., 2005. Neuronal basis of covert spatial attention in the frontal eye field. *J. Neurosci.* 25, 9479–9487.
- Tian, J., Lynch, J.C., 1997. Subcortical Input to the Smooth and Saccadic Eye Movement Subregions of the Frontal Eye Field in Cebus Monkey. *J. Neurosci.* 17, 9233 LP – 9247.
- Umarova, R.M., Beume, L., Reisert, M., Kaller, C.P., Klöppel, S., Mader, I., Glauche, V., Kiselev, V.G., Catani, M., Weiller, C., 2017. Distinct white matter alterations following severe stroke. *Neurology* 88, 1546–1555.
- Umarova, R.M., Reisert, M., Beier, T.U., Kiselev, V.G., Klöppel, S., Kaller, C.P., Glauche, V., Mader, I., Beume, L., Hennig, J., Weiller, C., 2014. Attention-network specific alterations of structural connectivity in the undamaged white matter in acute neglect. *Hum. Brain Mapp.* 35, 4678–4692.
- Umarova, R.M., Saur, D., Kaller, C.P., Vry, M.S., Glauche, V., Mader, I., Hennig, J.J., Weiller, C., 2011. Acute visual neglect and extinction: Distinct functional state of the visuospatial attention system. *Brain* 134, 3310–3325.
- Urbanski, M., Thiebaut de Schotten, M., Rodrigo, S., Oppenheim, C., Touzé, E., Méder, J.F., Moreau, K., Loeper-Jeny, C., Dubois, B., Bartolomeo, P., 2011. DTI-MR tractography of white matter damage in stroke patients with neglect. *Exp. Brain Res.* 208, 491–505.
- Vallar, G., 2001. Extrapersonal visual unilateral spatial neglect and its neuroanatomy. *Neuroimage* 14, 52–58.
- Vallar, G., 1998. Spatial hemineglect in humans. *Trends Cogn. Sci.* 2, 87–97.
- Vallar, G., Sandroni, P., Rusconi, M.L., Barbieri, S., 1991. Hemianopia, hemianesthesia, and spatial neglect: A study with evoked potentials. *Neurology* 41, 1918–1922.

- Van der Stigchel, S., Nijboer, T.C.W., 2018. Temporal order judgements as a sensitive measure of the spatial bias in patients with visuospatial neglect. *J. Neuropsychol.* 12, 427–441.
- van der Zijden, J.P., van der Toorn, A., van der Marel, K., Dijkhuizen, R.M., 2008. Longitudinal in vivo MRI of alterations in perilesional tissue after transient ischemic stroke in rats. *Exp. Neurol.* 212, 207–212.
- van Meer, M.P. a, Otte, W.M., van der Marel, K., Nijboer, C.H., Kavelaars, A., van der Sprenkel, J.W.B., Viergever, M. a, Dijkhuizen, R.M., 2012. Extent of bilateral neuronal network reorganization and functional recovery in relation to stroke severity. *J. Neurosci.* 32, 4495–507.
- van Meer, M.P. a, van der Marel, K., Otte, W.M., Berkelbach van der Sprenkel, J.W., Dijkhuizen, R.M., 2010a. Correspondence between altered functional and structural connectivity in the contralesional sensorimotor cortex after unilateral stroke in rats: a combined resting-state functional MRI and manganese-enhanced MRI study. *J. Cereb. Blood Flow Metab.* 30, 1707–1711.
- van Meer, M.P. a, van der Marel, K., Wang, K., Otte, W.M., El Bouazati, S., Roeling, T. a P., Viergever, M. a, Berkelbach van der Sprenkel, J.W., Dijkhuizen, R.M., 2010b. Recovery of sensorimotor function after experimental stroke correlates with restoration of resting-state interhemispheric functional connectivity. *J. Neurosci.* 30, 3964–72.
- Vincent, J.L., Patel, G.H., Fox, M.D., Snyder, A.Z., Baker, J.T., Van Essen, D.C., Zempel, J.M., Snyder, L.H., Corbetta, M., Raichle, M.E., 2007. Intrinsic functional architecture in the anaesthetized monkey brain. *Nature* 447, 83–86.
- Walker, R., Findlay, J.M., 1996. Saccadic eye movement programming in unilateral neglect. *Neuropsychologia* 34, 493–508.
- Wang, C., Stebbins, G.T., Nyenhuis, D.L., deToledo-Morrell, L., Freels, S., Gencheva, E., Pedelty, L., Sripathirathan, K., Moseley, M.E., Turner, D.A., Gabrieli, J.D.E., Gorelick, P.B., 2006. Longitudinal changes in white matter following ischemic stroke: A three-year follow-up study. *Neurobiol. Aging* 27, 1827–1833.
- Wang, L., Yu, C., Chen, H., Qin, W., He, Y., Fan, F., Zhang, Y., Wang, M., Li, K., Zang, Y., Woodward, T.S., Zhu, C., 2010. Dynamic functional reorganization of the motor execution network after stroke. *Brain* 133, 1224–1238.
- Ward, N.S., Cohen, L.G., 2004. Mechanisms Underlying Recovery of Motor Function After Stroke. *Arch. Neurol.* 61, 1844–1848.
- Ward, N.S., Newton, J.M., Swayne, O.B.C., Lee, L., Frackowiak, R.S.J., Thompson, A.J., Greenwood, R.J., Rothwell, J.C., 2007. The relationship between brain activity and peak grip force is modulated by corticospinal system integrity after subcortical stroke. *Eur. J. Neurosci.* 25, 1865–1873.
- Ward, N.S.S., Brown, M.M.M., Thompson, A.J.J., Frackowiak, R.S.J.S.J., 2003. Neural correlates of motor recovery after stroke: A longitudinal fMRI study. *Brain* 126,

2476–2496.

- Wardak, C., Ibos, G., Duhamel, J.-R.R., Olivier, E., 2006. Contribution of the monkey frontal eye field to covert visual attention. *J. Neurosci.* 26, 4228–4235.
- Wardak, C., Olivier, E., Duhamel, J.-R., 2002. Saccadic target selection deficits after lateral intraparietal area inactivation in monkeys. *J. Neurosci.* 22, 9877–84.
- Wardak, C., Olivier, E., Duhamel, J.R., 2011. The relationship between spatial attention and saccades in the frontoparietal network of the monkey. *Eur. J. Neurosci.* 33, 1973–1981.
- Wardak, C., Olivier, E., Duhamel, J.R., 2004. A Deficit in covert attention after parietal cortex inactivation in the monkey. *Neuron* 42, 501–508.
- Wardak, C., Vanduffel, W., Orban, G.A., 2010. Searching for a salient target involves frontal regions. *Cereb. Cortex* 20, 2464–2477.
- Weber, R., Ramos-Cabrer, P., Justicia, C., Wiedermann, D., Strecker, C., Sprenger, C., Hoehn, M., 2008. Early prediction of functional recovery after experimental stroke: functional magnetic resonance imaging, electrophysiology, and behavioral testing in rats. *J. Neurosci.* 28, 1022–1029.
- Welch, K., Stuteville, P., 1958. Experimental production of unilateral neglect in monkeys. *Brain* 81, 341–347.
- Wernicke, C., 1874. *Der Aphasische Symptomencomplex. Ein psychologische Studie auf anatomischer Basis.* Breslau.
- Werring, D.J., Toosy, A.T., Clark, C.A., Parker, G.J.M., Barker, G.J., Miller, D.H., Thompson, A.J., 2000. Diffusion tensor imaging can detect and quantify corticospinal tract degeneration after stroke. *J. Neurol. Neurosurg. Psychiatry* 69, 269–272.
- West, G.A., Golshani, K.J., Doyle, K.P., Lessov, N.S., Hobbs, T.R., Kohama, S.G., Pike, M.M., Kroenke, C.D., Grafe, M.R., Spector, M.D., Tobar, E.T., Simon, R.P., Stenzel-Poore, M.P., 2009. A new model of cortical stroke in the rhesus macaque. *J. Cereb. Blood Flow Metab.* 29, 1175–1186.
- White, I.M., Wise, S.P., 1999. Rule-dependent neuronal activity in the prefrontal cortex. *Exp. Brain Res.* 126, 315–335.
- Wilke, M., Kagan, I., Andersen, R., 2012. Functional imaging reveals rapid reorganization of cortical activity after parietal inactivation in monkeys. *Proc. Natl. Acad. Sci.* 109, 8274–8279.
- Yanagisawa, M., Kurihara, H., Kimura, S., Tomobe, Y., Kobayashi, M., Mitsui, Y., Yazaki, Y., Goto, K., Masaki, T., 1988. A novel potent vasoconstrictor peptide produced by vascular endothelial cells. *Nature.*
- Yantis, S., Schwarzbach, J., Serences, J.T., Carlson, R.L., Steinmetz, M.A., Pekar, J.J., Courtney, S.M., 2002. Transient neural activity in human parietal cortex during

spatial attention shifts. *Nat. Neurosci.* 5, 995–1002.

Yeterian, E.H., Pandya, D.N., 1991. Prefrontostriatal connections in relation to cortical architectonic organization in rhesus monkeys. *J. Comp. Neurol.* 312, 43–67.

Zhang, J., Zhang, Y., Xing, S., Liang, Z., Zeng, J., 2012. Secondary neurodegeneration in remote regions after focal cerebral infarction: A new target for stroke management? *Stroke* 43, 1700–1705.

Zhou, H.H., Thompson, K.G., 2009. Cognitively directed spatial selection in the frontal eye field in anticipation of visual stimuli to be discriminated. *Vision Res.* 49, 1205–1215.

CHAPTER 2

2. Recovery of contralesional saccade choice and reaction time deficits after a unilateral lesion in the macaque prefrontal cortex

2.1. Introduction

The caudal prefrontal cortex (PFC) is involved in visual search through both covert attention and overt orienting eye movements (Passingham and Wise 2012). In macaque monkeys, the caudal PFC includes the frontal eye fields (FEF) in area 8 and the caudal part of the principal sulcus (area 9/46). Unilateral damage to the caudal PFC often results in a phenomenon referred to as ‘visual extinction’ which reflects an ipsilesional bias in selective attention. Visual extinction has been characterized by the failure to respond to a visual stimulus presented in the contralesional hemifield when it is presented simultaneously with an ipsilesional stimulus (Bisiach 1991; Corbetta and Shulman 2011; Di Pellegrino et al. 1997). It is a topic of debate as to whether extinction is a mild form of neglect or a separate phenomenon altogether (Driver and Vuilleumier 2001; Geeraerts et al. 2005; Milner and McIntosh 2005). Patients with neglect are unable to detect a stimulus in the contralesional hemifield even in the absence of any competing ipsilesional stimulus; whereas those with extinction can still detect a contralesional stimulus presented alone (de Haan et al. 2012). Lesions in the macaque caudal PFC have resulted in an initial, yet transient, neglect-like impairment with longer-lasting extinction-like deficits of the contralesional visual hemifield (Bianchi 1895; Deuel and Collins 1984; Deuel and Farrar 1993; Eidelberg and Schwartz 1971; Johnston et al. 2016; Latto and

Cowey 1971a; Rizzolatti et al. 1983; Schiller and Chou 1998; Welch and Stuteville 1958).

The severity of visual extinction has been investigated using double stimulation paradigms in which two stimuli are presented, with one in each visual hemifield, either simultaneously or in rapid succession. In humans, visual extinction is most often tested using temporal order-judgment tasks in which patients are asked to report which stimulus appeared first with a verbal response (Baylis 2002; Rorden et al. 1997, 2009) or saccade response (Ro et al. 2001). In monkeys, early work focused on the initial transient neglect-like deficit seen following unilateral FEF lesions and observed the presence or absence of a response to food or frightening visual stimuli that were brought towards the monkey from its contralesional side (Bianchi 1895; Clark and Lashley 1947; Ferrier 1886; Jacobsen and Nissen 1937; Kennard 1938; Kennard and Ectors 1938; Welch and Stuteville 1958). A decade later in the 1970s, Alan Cowey and Richard Latto conducted the first experiments in which eye movements were measured in monkeys with unilateral FEF lesions (Latto and Cowey 1971b, 1971a). In their task, monkeys were required to respond to a flashing visual stimulus that appeared in either hemifield by directing their gaze towards the stimulus while the researchers photographed the eye. They reported an ipsilesional bias in the monkey's gaze that gradually recovered over time to varying degrees across monkeys (Latto and Cowey 1971a). More recently, visual target selection has been measured using eye-tracking on temporal order-judgment tasks where monkeys are rewarded for correctly selecting the first appearing stimulus (Kubanek et al. 2015; Port and Wurtz 2009) or free-choice tasks where the monkey is rewarded for selecting either stimulus (Johnston, Lomber, & Everling, 2016; Schiller & Chou, 1998; Wardak, Olivier, & Duhamel, 2002). In the free-choice task, two stimuli are presented, one in each

hemifield, with a variable time delay between their onset and monkeys are free to look toward either stimulus so that their hemifield preference can be measured.

It has yet to be resolved whether these deficits in contralesional target selection following unilateral PFC lesions are tied to oculomotor impairments. In other words: is the decreased target selection of a contralesional stimulus for an upcoming saccade primarily due to slower contralesional reaction times? Several studies that temporarily inactivated the PFC have reported large increases in contralesional reaction time in addition to the contralesional target selection deficit (Dias and Segraves 1999; Johnston et al. 2016; Sommer and Tehovnik 1997; Wardak et al. 2006), however temporary inactivation studies are limited in that they are unable to study post-lesion recovery and cannot answer the question of whether slower contralesional reaction time recovers prior to the recovery of contralesional target selection deficits. Longitudinal studies are necessary to answer this question, but unfortunately those studies have been limited in number. In one such study, Schiller and Chou (1998) unilaterally ablated the macaque FEF and at three weeks post-lesion reported severe deficits in contralesional target selection on the free-choice task and increased contralesional reaction times.

Here, we investigated whether contralesional target selection deficits (i.e., an ipsilesional saccade choice bias) following a right caudal PFC lesion can be explained by impaired contralesional oculomotor programming. If the underlying cause of the saccade choice deficit was impaired contralesional oculomotor programming, then the saccadic reaction time to the preferred (ipsilesional) and non-preferred (contralesional) stimulus should differ in the presence of a choice bias, with slower reaction times to a contralesional stimulus than to a ipsilesional stimulus (Rincon-Gonzalez et al. 2016). We also tested whether contralesional oculomotor processing could account for the subsequent recovery of the saccade choice deficit. We created a more clinically relevant model of focal

cerebral ischemia than traditional aspiration lesions by injecting the vasoconstrictor endothelin-1 in the right caudal PFC of four male macaque monkeys. Endothelin-1 induces a focal occlusion with subsequent reperfusion, allowing the study of post-lesion recovery, and has recently been validated in marmoset and macaque monkeys (Dai et al. 2017; Herbert et al. 2015; Murata and Higo 2016; Teo and Bourne 2014). We collected behavioural data on the free-choice saccade task prior to the lesion and at weeks 1-16 following the lesion. We found that unilateral lesions of the caudal PFC impaired saccadic performance to targets in the contralesional visual hemifield. Neglect-like deficits to single contralesional targets were transient and recovered within 2 weeks post-lesion, yet the extinction-like contralesional target selection deficits persisted and gradually recovered over 2-4 months. Contralesional reaction times returned to pre-lesion baseline before the target selection deficit had recovered, suggesting that reaction times were insufficient in accounting for the degree of the choice deficit. These findings indicate that impaired attentional processing contribute to the contralesional target selection deficit observed following right caudal PFC lesions.

2.2. Methods

2.2.1. Subjects

Data were collected from four adult male macaque monkeys (*Macaca mulatta*) aged 5 – 7 years old and weighing 7 – 10 kg. Animals are individually described as Monkey L, Monkey S, Monkey B, and Monkey F and are ordered based on smallest to largest lesion size, described later in the text. All surgical and experimental procedures were carried out in accordance with the Canadian Council of Animal Care policy on the use of laboratory

animals and approved by the Animal Care Committee of the University of Western Ontario Council.

A custom-built acrylic head post was fixed to the skull using dental acrylic and 6-mm ceramic bone screws (Thomas Recording, Giessen, Germany) as previously described (Johnston and Everling, 2006). A head post was necessary for restraining the head for eye-tracking during training on the oculomotor task. Animals received postoperative analgesics and antibiotics and were monitored by a university veterinarian.

2.2.2. Behavioural paradigm

Prior to the induction of an experimental lesion, we trained the monkeys on a free-choice saccade task (Fig. 2.1) as previously described (Johnston, Lomber, and Everling, 2016; Schiller and Chou, 1998). We used the CORTEX behavioural control system (National Institute of Mental Health, Bethesda, MD) to control the behavioural paradigm and reward delivery. Visual stimuli were presented on a CRT monitor (60 Hz refresh rate). Eye movements were recorded at 1000 Hz using an infrared video eye tracker (Eyelink 1000, SR Research, ON, Canada).

In the task, monkeys were required to direct a saccade toward one of two stimuli that appeared in the left and right hemifield with a variable stimulus onset asynchrony (SOA) between the presentation of the two stimuli. Trials began with the presentation of a fixation point (white-filled circle, 0.3°) located in the center of a black screen on the display monitor. Animals were required to fixate this stimulus within 1000 ms of its presentation and maintain fixation within a $2^\circ \times 2^\circ$ window for a duration that varied between 500 to 1000 ms. Then, two peripheral stimuli (white-filled circles, 0.5°) were presented in the left and right hemifield at an equal eccentricity of 10° at a variable SOA.

Monkeys received a liquid reward for directing a single saccade to either stimulus of their choice within a $4^\circ \times 4^\circ$ target window. The SOA values were selected to anchor the psychometric function between 0% and 100% saccade choice. This resulted in an SOA range between -256 to 256 ms (-256, -128, -64, -32, 0, 32, 64, 128, 256 ms) for Monkeys L, S, and B, and between -512 to 512 ms (-512, -256, -128, -64, 0, 64, 128, 256, 512 ms) for Monkey F. Negative SOA values indicate trials on which the right stimulus was presented before the left; an SOA value of zero indicates trials in which both stimuli were presented simultaneously; and positive SOA values indicate trials on which the left stimulus was presented before the right.

In addition to the paired stimuli trials, we randomly interleaved an equal proportion of single stimulus trials to measure contralesional/ipsilesional saccadic reaction time, duration, peak velocity, and amplitude separately. The single stimulus trials involved the presentation of a left or right stimulus following fixation and the animal simply had to direct a saccade to that stimulus. Monkey S was the first animal used in this study before we included the single stimulus trials. Saccadic reaction time, duration, peak velocity, and amplitude for Monkey S were calculated from the paired stimulus trials with the largest SOA (256 ms) as described previously (Johnston et al. 2016). We collected baseline behavioural data prior to the induced lesion until performance on the task was stable across sessions for several weeks. After the experimental lesion was induced, we continued daily collection of eye-tracking data until behavioural performance stabilized without further improvement, a time point hereby denoted as “behavioural recovery” (week 8 post-lesion for Monkeys L and S and week 16 post-lesion for Monkeys B and F).

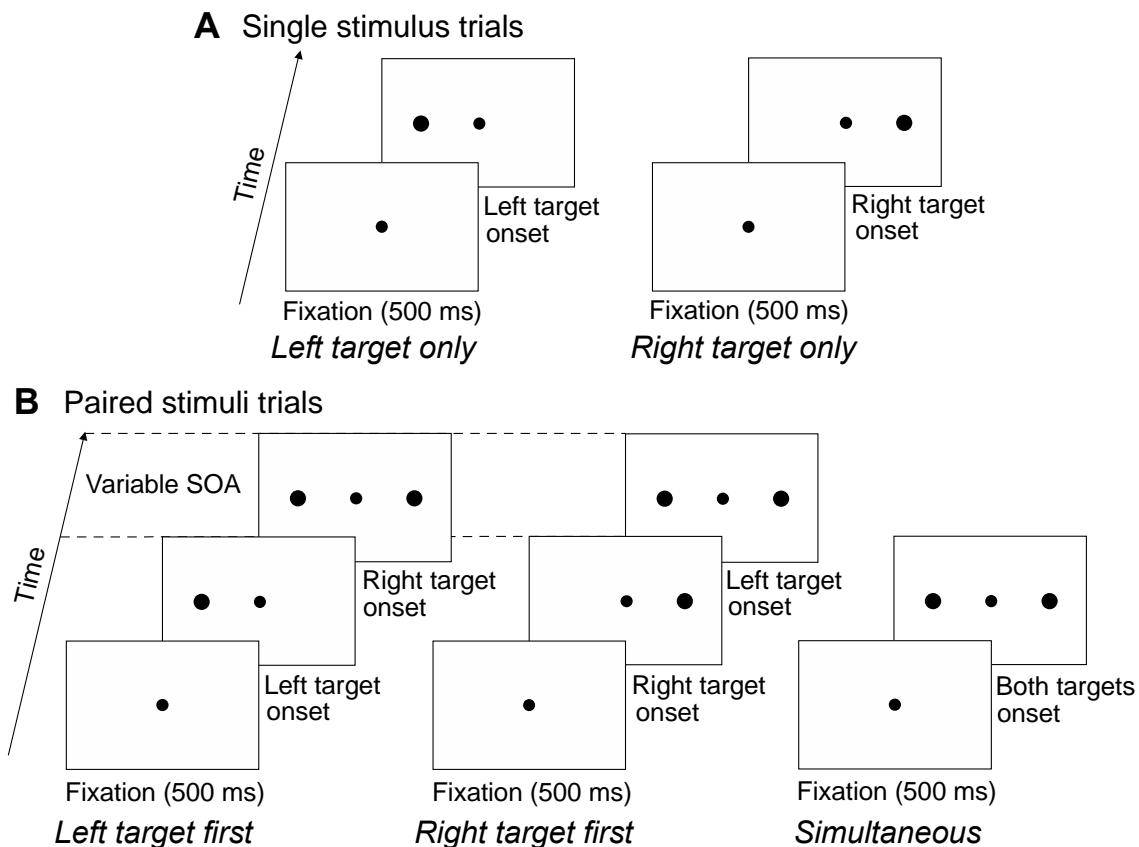


Figure 2.1. Free-choice saccade task.

Each trial began with the presentation of a central fixation point, followed by either one stimulus in the left or right hemifield (single stimulus trials) or two stimuli, with one in the left and one in the right hemifield (paired stimuli trials) presented at a variable stimulus onset asynchrony (SOA). SOA is the timing difference between presentation of the left and right stimulus. (A) Single stimulus trials included two conditions: 1) only the left stimulus was presented or 2) only the right stimulus was presented. (B) Paired stimuli trials included three conditions: 1) the left stimulus was presented before the right stimulus by a variable SOA, 2) the right stimulus was presented before the left stimulus, or 3) both left and right stimuli were presented at the same time. Single stimulus and paired stimuli trials were included in equal proportion and randomly interleaved throughout the behavioural session.

2.2.3. Endothelin-1-induced focal cerebral ischemia

Monkeys were initially sedated with 15.0 mg/kg ketamine, followed by intravenous administration of 2.5 mg/kg Propofol via the saphenous vein. Animals were then intubated and anaesthesia was maintained with 1-2% isoflurane mixed with oxygen and continuous rate infusion of propofol in saline. The animal's head was held in position using a stereotaxic frame with ear and eye bars (Model 1404 Stereotaxic Instrument, Kopf Instruments, CA, USA). A craniotomy was made above the right arcuate sulcus and caudal portion of the right principal sulcus and the dura was then removed to confirm the location of the arcuate and principal sulci by visual inspection. A 10 μ l-capacity syringe was held in position with a microinjection unit (Model 5000 Microinjection Unit, Kopf Instruments, CA, USA) that was mounted to a stereotaxic frame assembly and filled with endothelin-1 (E7764, Sigma-Aldrich).

We experimentally induced a small lesion in Monkey L and Monkey S and a larger lesion in Monkey B and Monkey F by varying the number of injections and concentration of endothelin-1 for each animal. Each injection contained 2 μ l of endothelin-1 and was injected at a flow rate of 0.75 μ l/min. Monkey L received a total of six injections of endothelin-1 (0.5 μ g/ μ l) in the anterior bank of the right arcuate sulcus at three injection sites separated by 2 mm along the mediolateral axis and at two depths at each site along the dorsoventral axis at 2 mm and 4 mm below dura. Monkey S received a total of 12 injections of endothelin-1 (0.5 μ g/ μ l) with six in the anterior bank of the right arcuate sulcus (as described for Monkey L) and an additional six in the caudal portion of the right principal sulcus at three injection sites separated by 2 mm along the rostrocaudal axis and at two depths at each site along the dorsoventral axis at 2 mm and 4 mm below dura. Monkey B received a total of 16 injections of endothelin-1 (0.5 μ g/ μ l), with eight in the anterior bank of the right arcuate sulcus (as described for Monkey L) and eight in the

caudal portion of the right principal sulcus (as described for Monkey S). Monkey F received a total of 16 injections of endothelin-1 (1.0 $\mu\text{g}/\mu\text{l}$), with eight in the anterior bank of the right arcuate sulcus (as described for Monkey L) and eight in the caudal portion of the right principal sulcus (as described for Monkey S).

At each injection site, the syringe needle was lowered to the greatest depth below the cortical surface and remained in situ for four minutes to allow the cortex to settle before the first endothelin-1 injection, after which the needle remained in situ for another four minutes to allow the solution to spread and reduce backflow of the solution through the needle track (Murata and Higo 2016). The needle was then retracted to the second depth and remained in situ for four minutes before the second injection of endothelin-1 was made, after which the needle remained in situ for another four minutes. The needle was then retracted from the cortex and repositioned over the next injection site and the procedure was repeated for the remaining injection sites. Following the last needle retraction, the dura flap was put back in place and the skull trephination was covered with medical grade silicon and left undisturbed to harden before the area was sealed by application of dental acrylic.

2.2.4. Lesion volume analysis

Before and after the lesion induction, we acquired T1-weighted MP2RAGE anatomical images (TR = 6500 ms, TE = 3.15 ms, TI1 = 800 ms, TI2 = 2700 ms, field of view = 128 x 128 mm, 0.5 mm isotropic resolution) and T2-weighted turbo spin echo anatomical MR images (TR = 7500 ms, TE = 90 ms, slices = 42, matrix size = 256 x 256, field of view = 128 x 128 mm, acquisition voxel size = 0.5 mm x 0.5 mm x 1 mm) on a 7-Tesla Siemens MAGNETOM scanner (Erlangen, Germany) using an in-house designed and manufactured 8-channel transmit, 24-channel receive primate head radiofrequency

coil (Gilbert et al. 2016). We used FMRIB's Automated Segmentation Tool (FAST) (Zhang et al. 2001) to segment tissue from each animal's T1-weighted anatomical acquired one week post-lesion. We segmented the T1 into four tissue types: grey matter, white matter, cerebrospinal fluid, and lesioned tissue. Segmented masks representing lesioned tissue were first inspected to ensure that they captured areas of hypointensity on the T1-weighted image and hyperintensity from the T2-weighted image acquired in the same session. Segmented T1 lesion masks were then normalized to the standard F99 space and lesion volumes were determined using MRIcron Toolbox (<http://www.cabiatl.com/mricro/mricron/index.html>). Lesioned tissue was visualized by projecting the lesion masks onto the macaque F99 template brain using MRIcron and the CARET toolbox (<http://www.nitrc.org/projects/caret>). Although there is no standard consensus on the nomenclature and boundaries for cytoarchitectonic subdivisions within the macaque prefrontal cortex, we have adopted labels from the Paxinos et al. (2000) rhesus monkey brain atlas to label lesioned cortical areas (Paxinos et al. 2000).

2.2.5. Data analysis

The following trials were excluded from further analysis: 1) trials in which the monkey blinked around the time of stimulus or saccade onset, 2) trials with broken or incorrect fixation, and 3) trials with saccadic reaction times less than 80 ms (anticipations) or greater than 1000 ms (no response). Saccade onset was defined as the time at which eye velocity exceeded 30°/s following stimulus onset, while saccade end was defined as the time at which eye velocity then fell below 30°/s (Johnston et al., 2016). All analyses were performed for each monkey individually using custom-designed software written in MATLAB (Mathworks, Natick, MA).

Performance on the free-choice saccade task was assessed by summing the proportion of saccades made to the contralesional (left) stimulus as a function of the SOA. For each animal, data was pooled into groups representing distinct time points: pre-lesion, week 1-2, 4, 8, and 16 post-lesion. For each time point, we generated a probability curve from the pooled data with a logistic function, $y=1/(1 + e^{-k(x-x_0)})$, where y is the proportion of contralesional saccade choice at a given SOA value (x), k is the slope of the curve, and x_0 is the x -value at the midpoint of the curve. The midpoint of the curve represents the point of equal selection, which is the SOA value at which the probability of choosing the contralesional or ipsilesional stimulus is equal; the greater the point of equal selection (with a contralesional lead time), the greater the contralesional target selection deficit. Contralesional and ipsilesional saccadic reaction time, duration, peak velocity, and amplitude to a single stimulus were calculated from the single stimulus trials for Monkey L, Monkey B, and Monkey F or from trials with longest SOA values ($|256|$ ms) for Monkey S at each time point. At the time of behavioural data collection for Monkey S, the first animal in the study, we had not yet introduced the single stimulus trials. However, the longest SOA values can effectively be used as single stimulus trials since these values exceeded the average reaction time of the animal (about 150-200 ms); by the time the second stimulus appeared, the animal would theoretically already have initiated a saccade to the first appearing stimulus (Johnston et al., 2016). We additionally measured the saccadic reaction time to a stimulus during the paired stimuli trials at each SOA value less than $|256|$ ms for all animals. Reaction time was defined as the length of time in milliseconds between stimulus onset and saccade onset. Duration was defined as the length of time in milliseconds between saccade onset and saccade end. Peak velocity was defined as the maximum velocity in degrees per second between saccade onset and saccade end. Saccade amplitude was defined as the angular distance in degrees that the eye traveled during the saccade. For data that was normally distributed (point of equal

selection, proportion contralesional choice, performance), we performed one-way analyses of variance (ANOVA) tests with time as a factor (variables: pre-lesion, week 1-2, 4, 8, 16 post-lesion) to test for significant differences from pre-lesion to post-lesion time points. Significant differences were further investigated using the post-hoc Tukey's Honestly Significant Difference (HSD) test ($p < 0.05$). For data that was not normally distributed (saccadic reaction time, duration, peak velocity, amplitude), we performed Kruskal-Wallis tests, a non-parametric equivalent of the one-way ANOVA, with post-hoc Tukey-Kramer tests. Effect sizes were measured using Hedges' g (Hedges 1981; Hedges and Olkin 1985).

To investigate whether prolonged contralesional reaction times can account for the severity of a saccade choice bias after a right caudal PFC lesion, we compared the mean difference between contralesional and ipsilesional reaction times to the point of equal selection. The idea is that if mean reaction time underlies the saccade choice bias, then the difference in reaction time to single contralesional or ipsilesional stimulus should account for the increased contralesional lead time necessary to reach the point of equal selection. However, the mean reaction time does not capture all of the information present in reaction time data (Ratcliff 1979; Wardak et al. 2012). Changes in the mean reaction time can be a result of changes in a host of parameters from the reaction time distribution (Ratcliff, 1979). For example, increased mean reaction time may reflect a shift of the whole distribution or just an increase in the tail of the distribution.

Alternatively, it is also possible that changes in the reaction time distribution may not be reflected in the mean reaction time. We investigated whether the saccade choice bias was the outcome of differences between the reaction time distributions for contralesional and ipsilesional saccades by simulating saccade choice using the reaction time distributions for single contralesional and ipsilesional saccades under the assumptions of the LATER

(Linear Approach to Threshold with Ergodic Rate) model (Carpenter and Williams 1995). See Supplemental Figure 2.S1 for the cumulative reaction time distributions for contralesional and ipsilesional saccades. The LATER model proposes that a decision signal rises linearly in response to a stimulus, at a rate that varies from trial to trial with a Gaussian distribution, until it reaches a threshold at which point a response is finally initiated (Carpenter & Williams, 1995; Reddi, 2003). Leach and Carpenter (2001) use the LATER model to show that reaction time distributions were able to predict the saccade choice probabilities at various stimulus onset asynchronies in healthy human participants (Leach and Carpenter 2001). We generated a linear race model with two decision signals (for an ipsilesional or contralesional saccade) using the reaction time distributions from the single stimulus trials and tested whether it could account for the observed saccade choice probabilities after a caudal PFC lesion (Carpenter and Williams 1995; Leach and Carpenter 2001; Rincon-Gonzalez et al. 2016). We first obtained the reaction time distributions for contralesional and ipsilesional saccades from single stimulus trials for Monkey L, Monkey B, and Monkey F and in trials with an SOA of $|256|$ ms for Monkey S (effectively single stimulus trials). Since the linear race model assumes that the reciprocal reaction times are directly related to the rate of rise and the variance of the decision signal for a single target, we generated 10000 simulated reaction times using the mean and standard deviation of the reciprocal observed contralesional and ipsilesional reaction times. Next, we modeled a race between the two decision signals and staggered them by each SOA value. We did this for each SOA condition by randomly selecting a contralesional and ipsilesional rate of rise (from the simulated reaction time distributions) 500 times and subtracted the SOA value from the first appearing stimulus in that condition. For example, when we modeled a race for an SOA condition of 128 ms-ipsilesional first, a randomly sampled ipsilesional rate of rise was first converted back to a reaction time by taking its reciprocal and then subtracting 128 from that simulated

reaction time to stagger the decision signals. Then, we compared this simulated ipsilesional reaction time to the simulated contralesional reaction time for the same condition and selected the ‘winner’ as the saccade with the shorter reaction time. This procedure was repeated 500 times at each of the nine SOA conditions which resulted in 500 simulated saccade choice probabilities at each SOA. We then compared the simulated saccade choice probabilities with the observed choice using a two-sample Chi-square goodness of fit test at each SOA value with FDR correction for multiple comparisons.

2.3. Results

2.3.1. Endothelin-1-induced focal cerebral ischemia in the right caudal PFC

The lesion analysis revealed an infarct volume of 0.43 cm³ for Monkey L, 0.51 cm³ for Monkey S, 1.28 cm³ for Monkey B, and 1.41 cm³ for Monkey F (Fig. 2.2). Since the infarct volumes for Monkeys B and F were more than double that of Monkeys L and S, we categorized Monkeys L and S as animals with a small lesion and Monkeys B and F as animals with a large lesion. All four animals sustained lesions within the right caudal PFC, however the lesion extended into nearby locations that varied across the animals (Fig. 2.2). In Monkey L, the lesion was mostly confined to the FEF (areas 8Ad, 8B), but extended slightly into the dorsal premotor cortex (areas 6DC/6DR). In Monkey S, the lesion affected the FEF (areas 8A, 8Ad, 8Av, 8B), dorsolateral PFC (areas 9/46, 9/46D, 46D), and ventrolateral PFC (areas 46v, 9/46v, 44, 45A, 45B, 47/12o). In Monkey B, the lesion affected the FEF (areas 8A, 8Ad, 8B), dorsolateral PFC (areas 9/46, 9/46D), dorsal premotor cortex (areas 6DC, 6DR) and slightly extended into the ventrolateral PFC (areas 46v, 9/46v) and ventral premotor cortex (area 6VC). In Monkey F, the lesion affected the

FEF (areas 8A, 8Ad, 8Av, 8B), dorsolateral PFC (areas 9/46, 9/46D, 46D), ventrolateral PFC (areas 46v, 9/46v, 45A, 45B), dorsal premotor cortex (area 6DC), and ventral premotor cortex (areas 6VC, 6VR). Overall, the right FEF was lesioned in all four animals. Of the two animals who sustained a smaller lesion, Monkey L only sustained a lesion to the FEF whereas the lesion in Monkey S extended into the dorsolateral and ventrolateral PFC. Of the two animals who sustained a larger lesion, Monkey B sustained a lesion which extended dorsally into the dorsal premotor cortex whereas in Monkey F the lesion extended into the dorsolateral and ventrolateral PFC and slightly into the ventral premotor cortex.

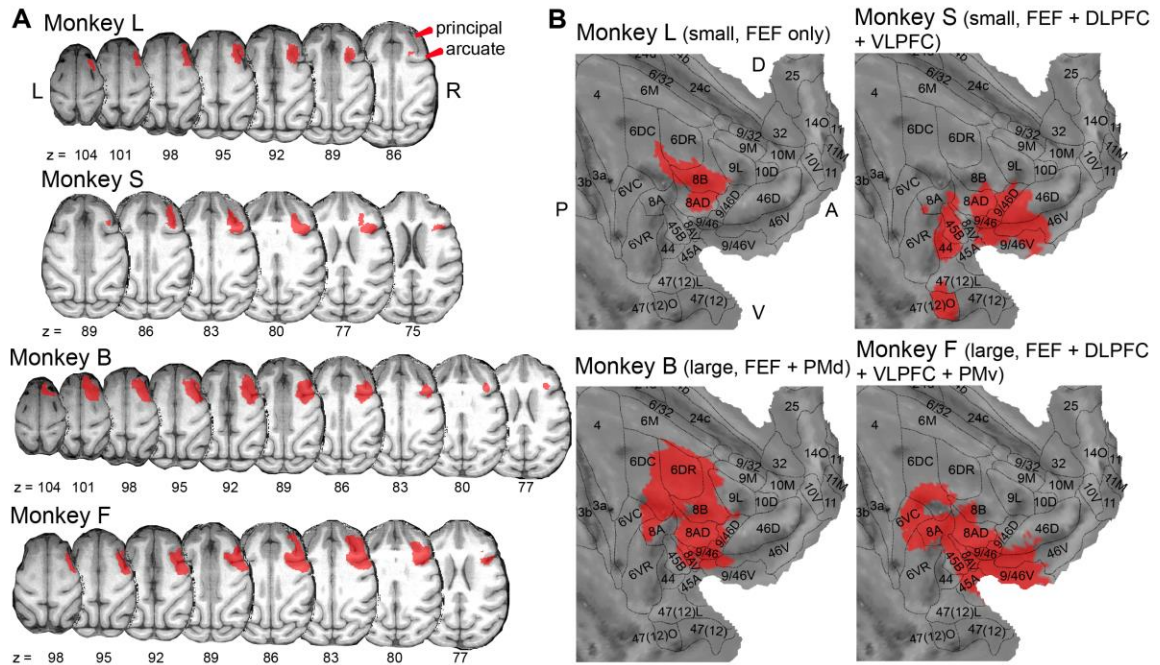


Figure 2.2. Lesion maps superimposed on the macaque F99 template brain.

For each animal, T1-weighted MRI images obtained one week post-lesion were segmented based on tissue type. Segmented masks representing lesioned tissue were registered to standard F99 space. Lesion masks were projected onto (A) axial slices of the macaque F99 template brain using the MRIcron Toolbox and (B) cortical flat map right hemisphere representations of the macaque F99 brain using CARET with Paxinos et al. (2000) area labels. Z-axis slice coordinates are in standard F99 space. Abbreviations: principal = principal sulcus; arcuate = arcuate sulcus, L = left hemisphere, R = right hemisphere, A = anterior, P = posterior, D = dorsal, V = ventral, small = small lesion, large = large lesion, FEF = frontal eye field, DLPFC = dorsolateral prefrontal cortex, VLPFC = ventrolateral prefrontal cortex, PMd = dorsal premotor cortex, PMv = ventral premotor cortex.

2.3.2. *Effects of a right caudal PFC lesion on free-choice saccade performance*

We used the free-choice saccade task to assess the extent of a saccade choice bias by measuring the proportion of saccades directed to a contralesional or ipsilesional stimulus before and after a right caudal PFC lesion. Figure 2.3A shows the proportion of contralesional saccade choices as a function of the SOA. Data shown in these figures represent task performance pre-lesion and at weeks 1-2, 4, 8, and 16 post-lesion. At pre-lesion, we observed only a small bias in the point of equal selection across all animals. Following a right caudal PFC lesion, the psychometric function shifted substantially to the right indicating a choice bias towards the ipsilesional stimulus, and then gradually shifted back to the left in the weeks following the lesion approaching baseline free-choice performance (Fig. 2.3A). At week 1-2 post-lesion, the two animals with lesions in both the FEF and dorsolateral/ventrolateral PFC [Monkey S (small lesion) and Monkey F (large lesion)] exhibited free-choice behaviour that resembled contralesional neglect more than extinction. For example, in the trials with the longest contralesional lead time (Monkey S: 256 ms contralesional-first; Monkey F: 512 ms contralesional-first), Monkey S and Monkey F still only made about 50% of saccades to the contralesional stimulus, whereas Monkeys L and B were making between 70-80% contralesional saccades on the same trial condition. Shifts in the midpoint of the curves, the point of equal selection, were further quantified and statistically compared for each animal across time in Figure 2.3B. One-way ANOVAs revealed significant differences in the point of equal selection across time in all four animals (Monkey L: $F(3, 19) = 19.62$, $p = 4.83 \times 10^{-6}$; Monkey S: $F(3, 23) = 24.95$, $p = 2.05 \times 10^{-7}$; Monkey B: $F(4, 40) = 47.56$, $p = 1.10 \times 10^{-14}$; Monkey F: $F(4, 24) = 27.12$, $p = 1.36 \times 10^{-8}$). Tukey's post-hoc tests revealed significant rightward shifts in the point of equal selection ($p < 0.05$) from pre-lesion to week 1-2 post-lesion for all four animals (Monkey L: 115 ms shift; Monkey S: 163 ms shift; Monkey B: 223 ms

shift; Monkey F: 386 ms shift). The point of equal selection then gradually returned to pre-lesion baseline performance and stabilized without further improvement in performance by week 8 in Monkey L and Monkey S and by week 16 in Monkey B and Monkey F (Table 2.1).

We examined the degree of a contralesional choice deficit by calculating the proportion of contralesional saccades on trials in which both stimuli appeared simultaneously (SOA = 0 ms) (Fig. 2.3C and Table 2.2). One-way ANOVAs revealed significant differences in the proportion of contralesional saccade choice at an SOA of 0 ms across time in all four animals (Monkey L: $F(3, 19) = 14.45$, $p = 3.85 \times 10^{-5}$; Monkey S: $F(3, 23) = 12.01$, $p = 6.19 \times 10^{-5}$; Monkey B: $F(4, 41) = 13.37$, $p = 4.64 \times 10^{-7}$; Monkey F: $F(4, 24) = 6.26$, $p = 0.0013$). At pre-lesion, the proportion of contralesional saccade choice was near 0.50 for all animals (Monkey L: 0.43; Monkey S: 0.44; Monkey B: 0.63; Monkey F: 0.50), indicating there was a roughly equal proportion of saccades made to both stimuli when presented simultaneously. Tukey's post-hoc tests revealed a significant decrease in the proportion of contralesional saccades ($p < 0.05$) from pre-lesion to week 1-2 post-lesion for all four animals [Monkey L: 0.06 ($p < 0.0001$); Monkey S: 0.06 ($p = 0.0002$); Monkey B: 0.17 ($p < 0.0001$); Monkey F: 0.12 ($p = 0.0026$)]. At week 4 post-lesion, the proportion of contralesional saccades remained less than pre-lesion for all animals [Monkey L: 0.22 ($p = 0.051$); Monkey S: 0.03 ($p = 0.0008$); Monkey B: 0.28 ($p = 0.0156$); Monkey F: 0.13 ($p = 0.0047$)]. The proportion of contralesional saccade choice gradually increased over time, approaching pre-lesion baseline performance, and stabilized without further improvement by week 8 for Monkey L and Monkey S and by week 16 for Monkey B and Monkey F (Table 2.2 and Fig. 2.3C). Interestingly, the two animals with lesions in both the FEF and dorsolateral/ventrolateral PFC (Monkeys S and F) showed only a partial recovery of function, whereas the two animals with lesions that did not extend into the

dorsolateral/ventrolateral PFC (Monkeys L and B) showed a more complete recovery (i.e., smaller difference between pre-lesion and post-lesion contralesional saccade choice performance). Correlations between lesion volume and behavioural deficits are included as supplemental material (Supplemental Fig. 2.S5).

In sum, an experimental lesion in the right caudal PFC that encompassed the FEF in all four animals and extended into the dorsolateral and ventrolateral PFC in Monkeys S and F led to an overall reduction in saccades to the contralesional (left) stimulus when a competing stimulus was also presented in the ipsilesional (right) visual hemifield. This contralesional choice deficit resembled contralesional visual extinction that gradually recovered over 2-4 months post-lesion. When the contralesional stimulus was presented well before the ipsilesional stimulus, the animals were more likely to respond to the contralesional stimulus without having the competing ipsilesional stimulus override their ability to detect or respond to the contralesional stimulus. The SOA between presentation of the contralesional and ipsilesional stimulus in which an equal proportion of saccades were made to both stimuli (i.e., the point of equal selection) was significantly longer at week 1-2 post-lesion, with the animals favouring the stimulus in the ipsilesional hemifield. Trials in which both stimuli were presented at the same time (SOA = 0 ms) showed the degree of contralesional target selection deficits as a drastic decrease in the proportion of saccades made to the contralesional stimulus. This ipsilesional saccade choice bias (or contralesional choice deficit) gradually recovered by week 8 post-lesion for Monkey L and Monkey S and by week 16 post-lesion for Monkey B and Monkey F.

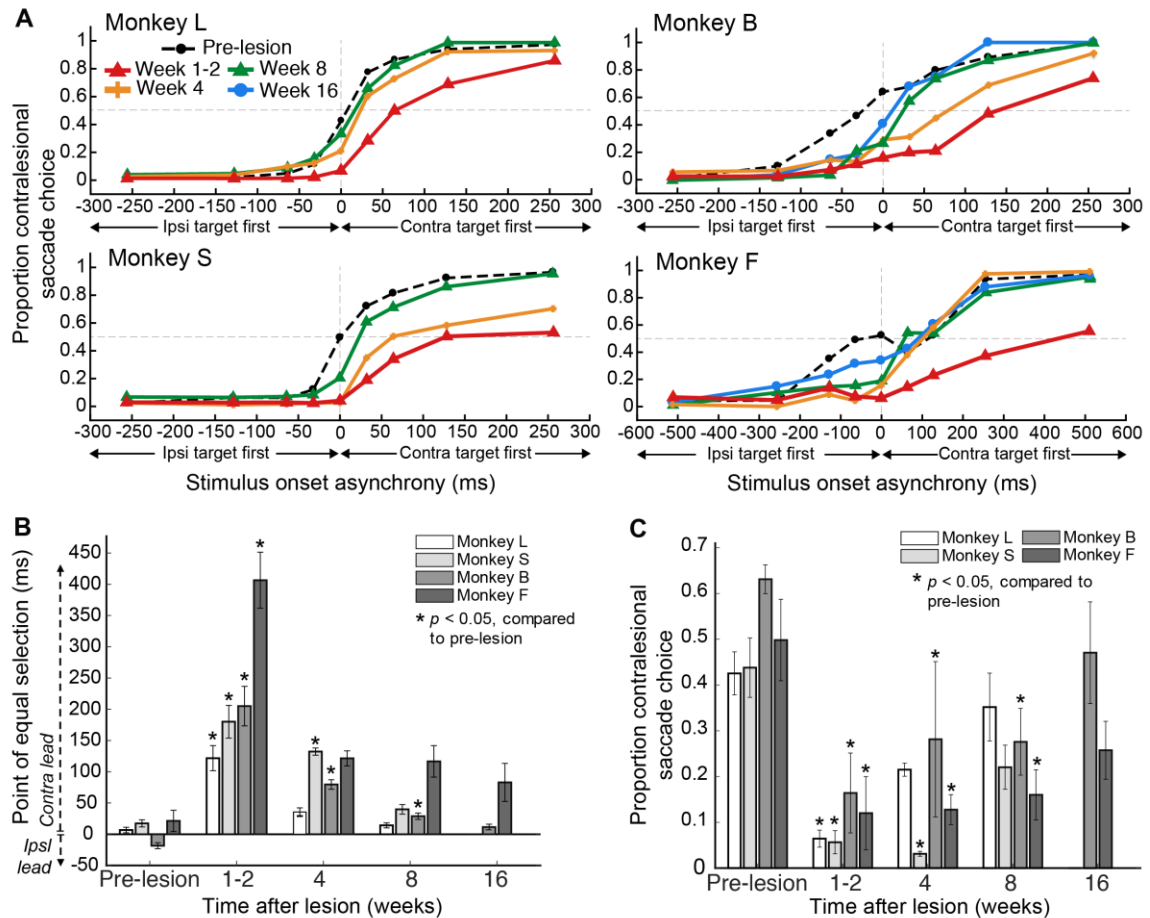


Figure 2.3. Performance on the free-choice saccade task.

(A) Proportion of saccades made to the contralesional stimulus as a function of the SOA at each time point. In each panel, black dotted lines represent pre-lesion data, red represents week 1-2 post-lesion, orange represents week 4 post-lesion, green represents week 8 post-lesion, and blue represents week 16 post-lesion. Positive x-axis values indicate trials in which the contralesional (left) stimulus appeared first and negative x-axis values indicate trials in which the ipsilesional (right) stimulus appeared first. (B) Recovery of the point of equal selection on the free-choice task. The point of equal selection is the temporal delay between presentation of the left and right stimuli at which an equal proportion of saccades were made to both stimuli. Positive y-axis values indicate that the point of equal selection was reached at a temporal delay in which the contralesional (left) stimulus was presented before the ipsilesional (right); negative y-axis values indicate a temporal delay in which the ipsilesional stimulus was presented first. Error bars indicate standard error of the mean. Statistical comparisons were made within subjects using a one-way ANOVA with post-hoc Tukey's test ($p < 0.05$) to compare the

point of equal selection at each post-lesion time point to pre-lesion. (C) Recovery of contralesional saccade choice on true simultaneous trials. Trials with an SOA value of 0 ms were deemed ‘true simultaneous trials’ in which both stimuli appeared at exactly the same time. We plotted the proportion of saccades made to the contralesional stimulus on those trials for each time point. Statistical comparisons were made using a one-way ANOVA with post-hoc Tukey’s test ($p < 0.05$). Abbreviations: ipsi = ipsilesional; contra = contralesional.

Table 2.1. Point of equal selection on the free-choice saccade task.

	Time after lesion	PES (ms)	No. of trials	No. of sessions	<i>p value</i>	Hedges' <i>g</i>
Monkey L	Pre-lesion	6.8 ± 4.5	3303	9		
	Week 1-2 post-lesion	121.7 ± 20.1	1198	7	<0.0001	3.17
	Week 4 post-lesion	35.7 ± 6.6	689	3	0.5282	2.23
	Week 8 post-lesion	14.2 ± 4.0	701	4	0.9790	0.61
Monkey S	Pre-lesion	17.3 ± 5.7	3226	11		
	Week 1-2 post-lesion	180.1 ± 26.1	1879	7	<0.0001	3.63
	Week 4 post-lesion	132.2 ± 5.7	1392	4	0.0006	3.99
	Week 8 post-lesion	39.9 ± 7.7	651	4	0.7539	1.22
Monkey B	Pre-lesion	-18.4 ± 4.8	3566	27		
	Week 1-2 post-lesion	205.0 ± 31.7	741	8	<0.0001	5.78
	Week 4 post-lesion	79.7 ± 7.6	330	3	0.0005	4.01
	Week 8 post-lesion	28.9 ± 5.1	467	4	0.1130	1.97
	Week 16 post-lesion	11.5 ± 4.6	259	4	0.6404	1.25
Monkey F	Pre-lesion	21.3 ± 17.0	1239	8		
	Week 1-2 post-lesion	406.5 ± 44.8	848	6	<0.0001	4.1
	Week 4 post-lesion	121.5 ± 12.1	1175	4	0.1292	2.31
	Week 8 post-lesion	116.7 ± 25.2	789	4	0.2011	1.88
	Week 16 post-lesion	82.9 ± 30.5	847	4	0.6671	1.18

Values are means ± SEM for point of equal selection (PES) on the free-choice saccade task and statistical comparisons between pre- and post-lesion time points using a one-way ANOVA with post hoc Tukey's test ($p < 0.05$). *P* values indicate significance level and Hedges' *g* is effect size.

Table 2.2. The proportion of saccades made to the contralesional stimulus during simultaneous presentation of both stimuli.

	Time after lesion	Proportion Contralesional Saccade Choice	No. of trials	No. of sessions	<i>p</i> value	Hedges' <i>g</i>
Monkey L	Pre-lesion	0.43 ± 0.05	357	9		
	Week 1-2 post-lesion	0.06 ± 0.02	129	7	<0.0001	-3.34
	Week 4 post-lesion	0.22 ± 0.01	76	3	0.0508	-1.67
	Week 8 post-lesion	0.35 ± 0.07	75	4	0.7014	-0.56
Monkey S	Pre-lesion	0.44 ± 0.07	303	11		
	Week 1-2 post-lesion	0.06 ± 0.03	219	7	0.0002	-2.12
	Week 4 post-lesion	0.03 ± 0.01	142	4	0.0008	-2.12
	Week 8 post-lesion	0.22 ± 0.05	54	4	0.0655	-1.1
Monkey B	Pre-lesion	0.63 ± 0.03	391	27		
	Week 1-2 post-lesion	0.17 ± 0.07	54	8	<0.0001	-2.64
	Week 4 post-lesion	0.28 ± 0.17	35	3	0.0156	-1.97
	Week 8 post-lesion	0.28 ± 0.07	52	4	0.0038	-2.2
	Week 16 post-lesion	0.47 ± 0.11	33	4	0.4276	-0.96
Monkey F	Pre-lesion	0.50 ± 0.09	150	8		
	Week 1-2 post-lesion	0.12 ± 0.08	64	6	0.0026	-1.75
	Week 4 post-lesion	0.13 ± 0.03	187	4	0.0047	-1.73
	Week 8 post-lesion	0.16 ± 0.05	79	4	0.0170	-1.55
	Week 16 post-lesion	0.26 ± 0.06	82	4	0.1881	-1.09

Values are means ± SE for proportion of saccades made to the contralesional stimulus during simultaneous presentation of both stimuli [stimulus onset asynchrony (SOA) = 0 ms] and statistical comparisons between pre- and postlesion time points using a one-way ANOVA with post hoc Tukey's test ($p < 0.05$). Total number of trials refers to trials with an SOA of 0 ms. *P* values indicate significance level, and Hedges' *g* is effect size.

2.3.3. *Effects of a right caudal PFC lesion on saccades to single targets*

We randomly interleaved single stimulus trials within the paired stimuli trials in the free-choice task to assess the presence of neglect-like deficits to single contralesional stimuli and to determine changes in contralesional and ipsilesional saccade metrics. Figure 2.4 shows each monkey's performance on single stimulus trials (or on trials with an SOA value of |256| ms for Monkey S) for contralesional and ipsilesional saccades over time. One-way ANOVAs revealed significant differences in the proportion of correct contralesional and ipsilesional saccades across time for Monkey S [Contralesional: $F(3,23) = 91.63$, $p = 6.15 \times 10^{-13}$; Ipsilesional: $F(3,23) = 5.61$, $p = 0.005$], Monkey B [Contralesional: $F(4,40) = 12.12$, $p = 1.51 \times 10^{-6}$; Ipsilesional: $F(4,40) = 9.36$, $p = 1.95 \times 10^{-5}$], and Monkey F [Contralesional: $F(4,24) = 11.80$, $p = 1.93 \times 10^{-5}$; Ipsilesional: $F(4,24) = 13.67$, $p = 6.07 \times 10^{-6}$]. Post-hoc Tukey's tests revealed that at week 1-2 post-lesion there was a significant decrease in the proportion of correct contralesional saccade performance compared to pre-lesion for Monkey S (pre-lesion: 0.94 ± 0.01 , week 1-2 post-lesion: 0.26 ± 0.03 , $p < 0.0001$, $g = -2.65$), Monkey B (pre-lesion: 0.99 , week 1-2 post-lesion: 0.84 ± 0.03 , $p < 0.0001$, $g = -2.50$), and Monkey F (pre-lesion: 0.95 ± 0.01 , week 1-2 post-lesion: 0.64 ± 0.04 , $p = 0.0001$, $g = -2.17$). Monkey L also showed a decrease in the proportion of correct contralesional saccades (about 75% correct contralesional performance at week 1-2 post-lesion compared to about 93% at pre-lesion), however this effect was not significant. Of the contralesional errors made that led to reduced performance at weeks 1-2 post-lesion, more than 85% were due to (1) no response after the contralesional stimulus presentation or (2) an incorrect saccade in which the saccade was made in the wrong direction. Recall that the saccade performance for Monkey S was from choice trials with the largest SOA value of |256| ms, so in this case all of the contralesional errors were due to either (1) incorrect saccades made

towards the second-appearing stimulus or (2) incorrect saccades made in any other direction except towards the stimuli. Only a small proportion of the contralesional errors were due to inaccurate saccades made towards the contralesional stimulus (13% in Monkey L, 0% in Monkey S, 0% in Monkey B, and 3% in Monkey F).

Monkey S had significantly decreased contralesional saccade performance at week 4 post-lesion (0.70 ± 0.02 , $p = 0.006$, $g = -0.91$) compared to pre-lesion. Post-hoc Tukey's tests also revealed a significant decrease in ipsilesional saccade performance at week 1-2 post-lesion compared to pre-lesion for Monkey S (pre-lesion: 0.94 ± 0.01 , week 1-2 post-lesion: 0.68 ± 0.08 , $p = 0.0059$, $g = -1.50$) and Monkey B (pre-lesion: 0.99 ± 0.01 , week 1-2 post-lesion: 0.95 ± 0.03 , $p < 0.0001$, $g = -2.16$). At week 16 post-lesion, Monkey F had significantly decreased ipsilesional (week 16 post-lesion: 0.86 ± 0.02 , $p = 0.0012$, $g = -2.44$) and contralesional (week 16 post-lesion: 0.76 ± 0.02 , $p = 0.0484$, $g = -8.10$) single saccade performance compared to pre-lesion (0.95 ± 0.01). In sum, at least in the early post-lesion stage (weeks 1-2), the monkeys were impaired in directing saccades to a single contralesional stimulus (without a competing ipsilesional target) which resembled contralesional visual neglect. This neglect-like deficit was more severe in the two monkeys with lesions that affected both the FEF and DLPFC/VLPFC (Monkey S and Monkey F) compared to Monkeys L and B (with more dorsal lesions). By week 4 post-lesion, the neglect-like deficit had attenuated and the performance level for saccades to single stimuli in either hemifield was comparable to pre-lesion baseline, with the exception of contralesional performance in Monkey F.

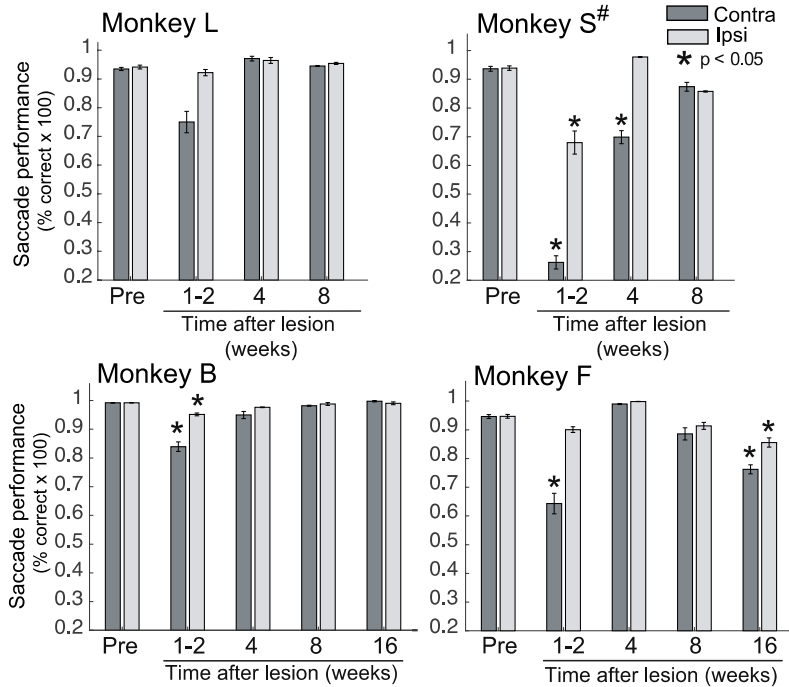


Figure 2.4. Saccade performance on single stimulus trials.

For each time point, we calculated the proportion of correct contralesional or ipsilesional saccades made on single contralesional or ipsilesional stimulus trials. Trials with an SOA value of $|256|$ ms were used as single stimulus trials for Monkey S (see *Data Analysis* above). Significant differences from pre-stroke to each post-stroke time point were evaluated using a one-way ANOVA with post-hoc Tukey's test ($p < 0.05$). Error bars indicate standard error of the mean. Abbreviations: # = trials with the largest SOA value were treated as single stimulus trials; contra = contralesional; ipsi = ipsilesional; pre = pre-lesion.

2.3.4. *Effects of a right caudal PFC lesion on saccade metrics*

Based on a previous cooling study of the caudal dorsolateral PFC (Johnston et al. 2016), we predicted that reaction time and duration would increase for contralesional saccades and decrease for ipsilesional saccades (vice versa for peak velocity) and that these metrics would return to pre-lesion baseline in the weeks following lesion (Schiller & Chou, 2000). Figure 2.5A shows the contralesional and ipsilesional saccadic reaction time across time for each animal. Kruskal-Wallis H tests showed that there was a statistically significant difference in contralesional reaction times across time in Monkey L [$\chi^2(3) = 141.91$, $p = 1.47 \times 10^{-30}$], Monkey B [$\chi^2(4) = 7.14$, $p = 2.21 \times 10^{-36}$], and Monkey F [$\chi^2(4) = 240.62$, $p = 6.81 \times 10^{-51}$]. Tukey-Kramer post-hoc tests revealed significantly increased contralesional reaction time at week 1-2 post-lesion compared to pre-lesion for Monkey L (pre-lesion: 172.8 ± 0.2 ms, week 1-2 post-lesion: 216.3 ± 0.2 ms, $p < 0.0001$, $g = 0.44$), Monkey B (pre-lesion: 170.5 ± 0.1 ms, week 1-2 post-lesion: 260.6 ± 0.6 ms, $p < 0.0001$, $g = 1.35$), and Monkey F (pre-lesion: 266.5 ± 0.1 ms, week 1-2 post-lesion: 310.3 ± 0.4 ms, $p < 0.0001$, $g = 0.83$). There were no significant changes in contralesional reaction time for Monkey S over time. Contralesional reaction time returned to pre-lesion baseline by week 4 post-lesion for Monkey L and by week 8 for Monkey B. For Monkey F, contralesional reaction time was significantly decreased at week 8 post-lesion (239.9 ± 0.3 ms, $p < 0.0001$, $g = -0.27$) compared to pre-lesion. Kruskal-Wallis tests also revealed a significant difference in ipsilesional reaction times over time in Monkey S [$\chi^2(3) = 35.92$, $p = 7.77 \times 10^{-8}$], Monkey B [$\chi^2(4) = 439.70$, $p = 7.33 \times 10^{-94}$], and Monkey F [$\chi^2(4) = 91.83$, $p = 5.39 \times 10^{-19}$]. Tukey-Kramer post-hoc tests revealed a significant decrease in ipsilesional reaction times at weeks 1-2 and 4 post-lesion for Monkey S, at weeks 1-2, 8, and 16 post-lesion for Monkey B, and at week 4 post-lesion for Monkey F (Figure 2.5A and Table 2.3).

Figure 2.5B shows the contralesional and ipsilesional saccadic duration for each animal statistically compared across time using one-way Kruskal-Wallis tests with post-hoc Tukey-Kramer's tests. Although changes in contralesional and ipsilesional saccadic duration across time were significant for Monkey L and Monkey F, these changes were quite small (Fig. 5B and Table 2.4). In Monkey S, saccadic duration significantly decreased at week 8 post-lesion compared to pre-lesion for both directions (Fig. 5B and Table 2.4). This effect was likely due to the late addition of single stimulus trials for Monkey S which were introduced after week 4 post-lesion. In Monkey B, contralesional saccade duration was significantly increased at week 1-2 through week 8 post-lesion compared to pre-lesion (Fig. 5B and Table 2.4). Overall, there was a minimal change in ipsilesional saccadic duration over time. Figure 2.5C shows the changes in saccadic peak velocity for contralesional and ipsilesional saccades in each animal statistically compared across time using one-way Kruskal-Wallis tests with post-hoc Tukey-Kramer's tests (Fig. 2.5C and Table 2.5). In Monkey L, peak velocity significantly increased for both directions post-lesion. In Monkey S, ipsilesional peak velocity decreased at week 1-2 post-lesion and then increased for both directions at week 4 post-lesion. In Monkey B, peak velocity for both directions decreased at week 1-2 post-lesion and then returned to baseline. In Monkey F, contralesional peak velocity decreased at weeks 8-16 post-lesion (Fig. 2.5C and Table 2.5). In Figure 2.5D, we show the saccade amplitude before and after the lesion; we found that changes in amplitude were minimal (at most, about a 2-3 degree change over time). In summary, (1) contralesional reaction time increased in all four animals at week 1-2 post-lesion and subsequently returned to pre-lesion by weeks 4 to 8 post-lesion; (2) ipsilesional reaction time decreased in Monkeys S, B, and F post-lesion; and (3) there was no consistent change in saccadic duration or peak velocity across all four animals over time.

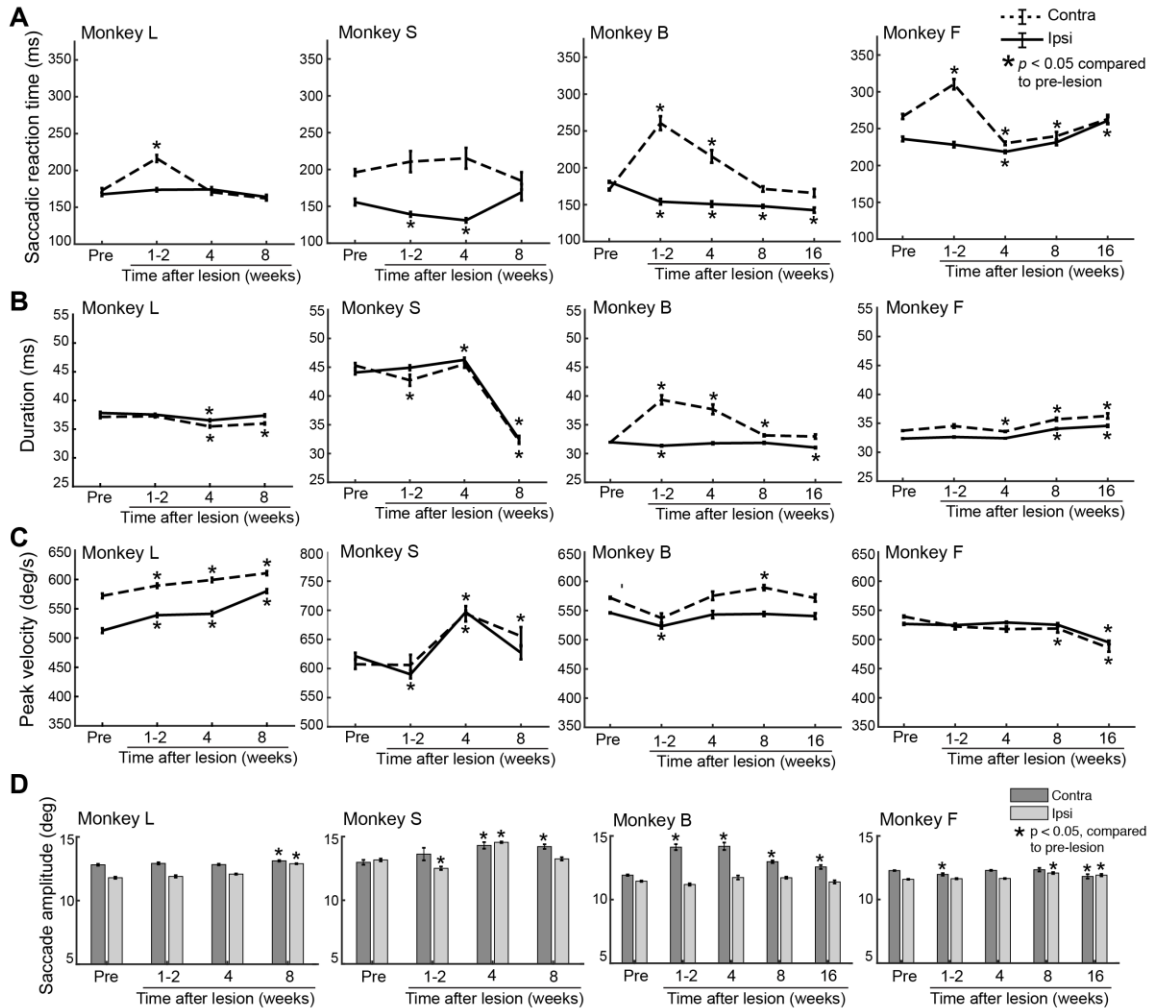


Figure 2.5. Effects of a right PFC lesion on saccade metrics to single targets.

Saccade metrics include (A) saccadic reaction time, (B) duration, (C) peak velocity, and (D) amplitude to a single contralesional or ipsilesional stimulus. Data for contralesional saccades (dashed line) and ipsilesional saccades (solid line) are shown for Monkey L (first column), Monkey S (second column), Monkey B (third column), and Monkey F (fourth column). Data for Monkey S was obtained from trials with an SOA of [256] ms which were treated as equivalent to single stimulus trials (see *Data Analysis in Methods*). Error bars indicate standard error of the mean. Statistical comparisons were made within subjects using one-way Kruskal-Wallis tests with post-hoc Tukey-Kramer's tests to compare each post-lesion time point to pre-lesion. Abbreviations: contra = contralesional; ipsi = ipsilesional; pre = pre-lesion.

Table 2.3. Saccadic reaction times to a single contralesional and ipsilesional stimulus.

	Time after lesion	Contralesional stimulus			Ipsilesional stimulus		
		SRT (ms)	No. of trials	<i>p</i>	SRT (ms)	No. of trials	<i>p</i>
Monkey L	Pre-lesion	172.8 ± 0.2	463		167.6 ± 0.1	480	
	Week 1-2 post-lesion	216.3 ± 0.2	604	<0.0001	173.8 ± 0.1	673	0.2820
	Week 4 post-lesion	170.6 ± 0.2	291	0.9165	174.2 ± 0.2	276	0.4527
	Week 8 post-lesion	162.0 ± 0.1	391	0.0083	164.0 ± 0.1	391	0.3125
Monkey S	Pre-lesion	196.1 ± 0.3	327		155.8 ± 0.3	344	
	Week 1-2 post-lesion	210.7 ± 0.2	86	0.9941	139.2 ± 0.2	209	0.0431
	Week 4 post-lesion	215.3 ± 0.2	104	0.3588	131.0 ± 0.2	152	<0.0001
	Week 8 post-lesion	184.6 ± 0.1	80	0.0825	169.1 ± 1.3	71	0.0852
Monkey B	Pre-lesion	170.5 ± 0.0	1876		181.0 ± 0.0	1920	
	Week 1-2 post-lesion	260.6 ± 0.6	215	<0.0001	154.0 ± 0.3	235	<0.0001
	Week 4 post-lesion	215.4 ± 0.9	88	<0.0001	150.8 ± 0.4	114	<0.0001
	Week 8 post-lesion	171.4 ± 0.2	241	0.8960	147.8 ± 0.1	243	<0.0001
	Week 16 post-lesion	165.8 ± 0.5	118	0.1410	142.5 ± 0.3	129	<0.0001
Monkey F	Pre-lesion	266.5 ± 0.1	653		236.0 ± 0.1	644	
	Week 1-2 post-lesion	310.3 ± 0.4	354	<0.0001	228.3 ± 0.2	426	0.2239
	Week 4 post-lesion	230.2 ± 0.1	958	<0.0001	218.6 ± 0.1	959	<0.0001
	Week 8 post-lesion	239.9 ± 0.3	393	<0.0001	231.4 ± 0.2	428	0.5671
	Week 16 post-lesion	263.1 ± 0.3	373	0.2716	260.9 ± 0.3	373	<0.0001

Values are means ± SE for saccadic reaction time (SRT) to a single contralesional and ipsilesional stimulus and statistical comparisons between pre- and post-lesion time points from a post hoc Tukey-Kramer's test. P values indicate significance level.

Table 2.4. Saccadic duration to a single contralesional and ipsilesional stimulus.

	Time after lesion	Contralesional stimulus			Ipsilesional stimulus		
		Duration (ms)	No. of trials	<i>p</i>	Duration (ms)	No. of trials	<i>p</i>
Monkey L	Pre-lesion	35.3 ± 0.01	462		35.9 ± 0.01	472	
	Week 1-2 post-lesion	35.4 ± 0.01	604	0.9706	35.7 ± 0.01	673	0.8790
	Week 4 post-lesion	33.9 ± 0.01	291	<0.0001	34.8 ± 0.01	276	0.0014
	Week 8 post-lesion	34.3 ± 0.01	392	<0.0001	35.5 ± 0.01	391	0.1585
Monkey S	Pre-lesion	45.3 ± 0.02	323		44.1 ± 0.02	340	
	Week 1-2 post-lesion	42.7 ± 0.10	86	0.0252	44.9 ± 0.03	209	0.6523
	Week 4 post-lesion	45.5 ± 0.06	103	0.8409	46.3 ± 0.03	153	0.0026
	Week 8 post-lesion	32.2 ± 0.06	73	<0.0001	32.5 ± 0.07	67	<0.0001
Monkey B	Pre-lesion	32.0 ± 0.01	1876		32.0 ± 0.00	1920	
	Week 1-2 post-lesion	39.3 ± 0.06	208	<0.0001	31.4 ± 0.01	234	<0.0001
	Week 4 post-lesion	37.7 ± 0.09	88	<0.0001	31.8 ± 0.02	114	0.6872
	Week 8 post-lesion	33.2 ± 0.01	241	<0.0001	31.9 ± 0.01	243	0.1012
	Week 16 post-lesion	32.8 ± 0.04	118	0.9840	31.1 ± 0.01	129	<0.0001
Monkey F	Pre-lesion	33.7 ± 0.00	653		32.4 ± 0.00	644	
	Week 1-2 post-lesion	34.5 ± 0.02	347	0.0742	32.6 ± 0.00	425	0.0146
	Week 4 post-lesion	33.6 ± 0.00	958	<0.0001	32.4 ± 0.00	959	0.2577
	Week 8 post-lesion	35.7 ± 0.01	393	<0.0001	34.1 ± 0.01	428	<0.0001
	Week 16 post-lesion	36.3 ± 0.04	373	<0.0001	34.6 ± 0.02	373	<0.0001

Values are means ± SE for saccadic duration to a single contralesional and ipsilesional stimulus and statistical comparisons between pre- and post-lesion time points from a post hoc Tukey-Kramer's test. *P* values indicate significance level.

Table 2.5. Saccadic peak velocity to a single contralesional and ipsilesional stimulus.

	Time after lesion	Contralesional stimulus			Ipsilesional stimulus		
		Peak velocity (ms)	No. of trials	<i>p</i>	Peak velocity (ms)	No. of trials	<i>p</i>
Monkey L	Pre-lesion	542.5 ± 0.2	467		490.9 ± 0.2	485	
	Week 1-2 post-lesion	557.6 ± 0.1	604	<0.0001	513.8 ± 0.1	673	<0.0001
	Week 4 post-lesion	566.1 ± 0.2	291	<0.0001	515.9 ± 0.2	276	0.0014
	Week 8 post-lesion	576.1 ± 0.2	392	<0.0001	549.5 ± 0.2	391	<0.0001
Monkey S	Pre-lesion	607.3 ± 0.5	320		621.2 ± 0.3	342	
	Week 1-2 post-lesion	605.9 ± 2.0	86	0.5351	590.0 ± 0.5	209	0.0006
	Week 4 post-lesion	694.1 ± 1.2	102	<0.0001	696.9 ± 0.2	153	<0.0001
	Week 8 post-lesion	655.6 ± 1.9	71	0.0466	627.0 ± 1.3	70	0.6774
Monkey B	Pre-lesion	571.7 ± 0.0	1876		546.0 ± 0.0	1920	
	Week 1-2 post-lesion	537.1 ± 0.5	215	0.1503	546.0 ± 0.4	235	<0.0001
	Week 4 post-lesion	575.1 ± 0.8	88	0.9414	543.0 ± 0.6	114	0.9654
	Week 8 post-lesion	589.2 ± 0.3	241	0.0044	544.1 ± 0.2	243	0.9965
	Week 16 post-lesion	571.4 ± 0.6	118	0.9706	540.4 ± 0.4	129	0.8915
Monkey F	Pre-lesion	539.3 ± 0.1	653		526.7 ± 0.1	644	
	Week 1-2 post-lesion	310.3 ± 0.3	354	0.9193	524.6 ± 0.1	426	0.9422
	Week 4 post-lesion	517.8 ± 0.1	958	0.2948	529.1 ± 0.1	959	0.6276
	Week 8 post-lesion	518.8 ± 0.3	393	0.0135	525.2 ± 0.1	428	0.9767
	Week 16 post-lesion	485.5 ± 0.3	373	<0.0001	495.0 ± 0.2	373	<0.0001

Values are means ± SE for saccadic peak velocity to a single contralesional and ipsilesional stimulus and statistical comparisons between pre- and post-lesion time points from a post hoc Tukey-Kramer's test. *P* values indicate significance level.

2.3.5. *Does the mean reaction time to single targets account for the contralesional saccade choice deficit?*

Following a right caudal PFC lesion, monkeys made a higher proportion of saccades toward an ipsilesional stimulus compared to a contralesional stimulus (Fig. 2.3) and the saccadic reaction times to an ipsilesional stimulus were shorter than to a contralesional stimulus (Fig. 2.5). Thus, we wanted to determine whether the post-lesion contralesional choice deficit was due to slower contralesional reaction times. The idea is that if prolonged contralesional reaction times underlie the contralesional choice deficit, then the difference in contralesional vs ipsilesional reaction times should equal the contralesional stimulus-lead time necessary to reach the point of equal selection. To this end, we plotted the mean reaction time difference between contralesional and ipsilesional saccades (left–right) against the point of equal selection (i.e., the SOA value at which there was an equal probability of selecting either stimulus) at each time point for each animal (Fig. 2.6). At pre-lesion, there was no significant difference between the point of equal selection and the mean reaction time difference for Monkey L, Monkey B, and Monkey F (Fig. 2.6). At week 1-2 post-lesion, a one-sample t-test ($p < 0.05$) showed that the point of equal selection was significantly greater than the mean reaction time difference for all four animals; the difference between the point of equal selection and the mean left-right reaction time difference was 79 ms for Monkey L ($g = 1.49$), 109 ms for Monkey S ($g = 1.57$), 98 ms for Monkey B ($g = 1.43$), and 324 ms for Monkey F ($g = 2.42$). In Monkeys L and S, the point of equal selection remained longer than the mean reaction time difference across week 4 (Monkey L: 39 ms difference, $g = 3.45$; Monkey S: 48 ms difference, $g = 0.98$) and week 8 post-lesion (Monkey L: 16 ms difference, $g = 2.00$; Monkey S: 24 ms difference, $g = 1.42$), although this difference was not significant at week 4 post-lesion in Monkey S. In Monkey F, the point of equal selection was longer

than the reaction time difference at weeks 4, 8, and 16 post-lesion, but this effect was only significant at week 4 (110 ms difference, $g = 3.72$) and week 8 (108 ms difference, $g = 1.92$). In Monkey B, the difference between the point of equal selection and the mean reaction time difference was both small and insignificant across weeks 4-16 post-lesion. In sum, following a right caudal PFC lesion, the prolonged reaction time to a contralesional (left) stimulus did not account for the much longer contralesional lead time necessary to achieve an equal probability of selecting either stimulus (i.e., the point of equal selection).

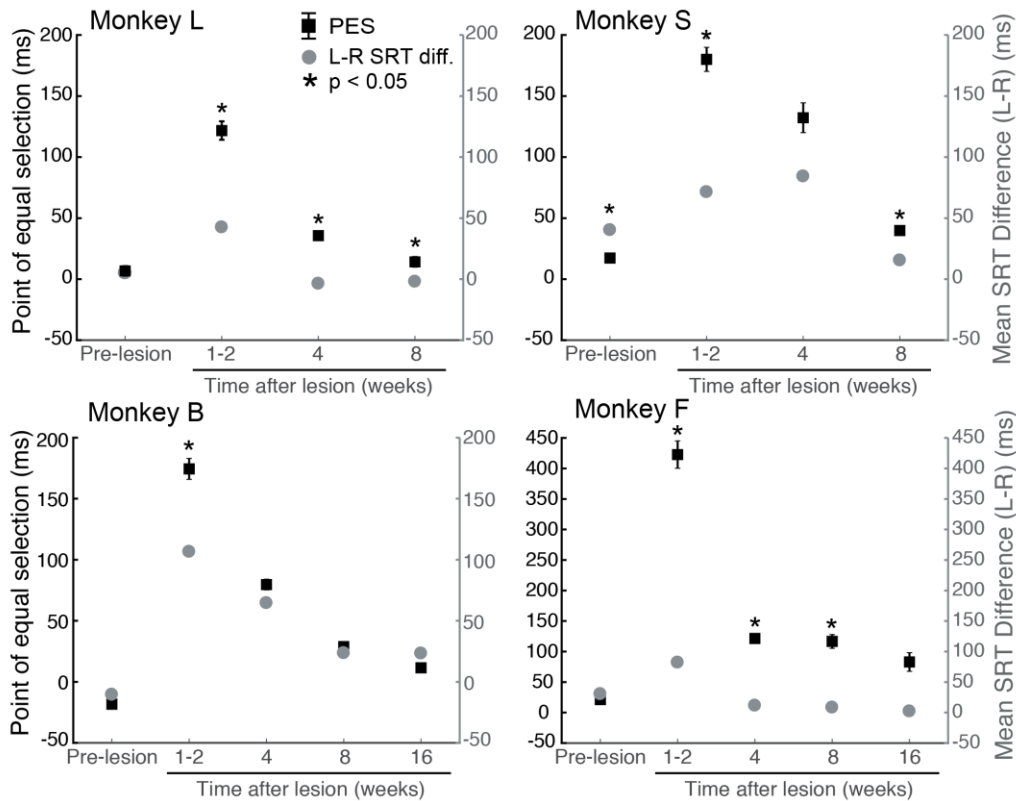


Figure 2.6. Point of equal selection on the free-choice task and the mean reaction time difference towards a contralesional vs ipsilesional stimulus.

The difference in contralesional and ipsilesional mean reaction time was plotted against the point of equal selection for each time point for all four animals. Note that Monkey F has a larger range of y-axis values. Positive y-axis values on the left side indicate a point of equal selection in which the contralesional stimulus was presented before the ipsilesional stimulus. Statistical comparisons were made within subjects using one-sample t-tests to compare the point of equal selection to the mean reaction time difference (contralesional SRT – ipsilesional SRT) at each time point. Error bars indicate standard error of the mean. Abbreviations: PES = point of equal selection; contra = contralesional; ipsi = ipsilesional; SRT = saccadic reaction time.

2.3.6. Does the reaction time distribution account for the contralesional saccade choice deficit?

Next, we examined whether the saccadic reaction time distribution, rather than the mean reaction time, to a single contralesional or ipsilesional stimulus could account for the contralesional choice deficit. We modeled a race with two decision signals arising from two targets and staggered by the SOA, using the LATER model with data from the contralesional and ipsilesional reaction time distributions. We plotted the simulated proportion of contralesional saccade choice for each SOA value and compared the simulated choice to the observed choice using a two-sided Chi-square test with FDR correction for multiple comparisons (Fig. 2.7). We then obtained the observed and simulated point of equal selection values for each animal at each time point.

At pre-lesion, the difference in the point of equal selection ($|\text{real} - \text{simulated}|$) was ~10 ms for Monkey L, ~8 ms for Monkey S, ~14 ms for Monkey B, and ~4 ms for Monkey F. This small difference between the observed and simulated choice suggests that, prior to the lesion, the reaction time distributions to single stimuli can account for the saccade choice on the free-choice task.

At week 1-2 post-lesion, the point of equal selection difference was ~82 ms for Monkey L, ~160 ms for Monkey S, ~115 ms for Monkey B, and ~422 ms for Monkey F. At week 4 post-lesion, point of equal selection differences ranged from 40–94 ms across the four animals. At week 8 post-lesion, differences were less than 30 ms for Monkey L, Monkey S, and Monkey B. Monkey F still had a difference of ~94 ms at week 4 and ~56 ms at week 8 post-lesion. The larger differences post-lesion between the point of equal selection for observed versus simulated saccade choice demonstrate that reaction time distributions can no longer sufficiently account for the saccade choice bias on the free-

choice task. Additionally, we used predictions from the LATER model to interpret the nature of the changes in the contralesional reaction time distributions and found that increased accumulation rate variability (i.e., variability in contralesional reaction times) best accounted for the changes in the reaction time distribution (see Supplemental Fig. 2.S6-10 for the results and discussion).

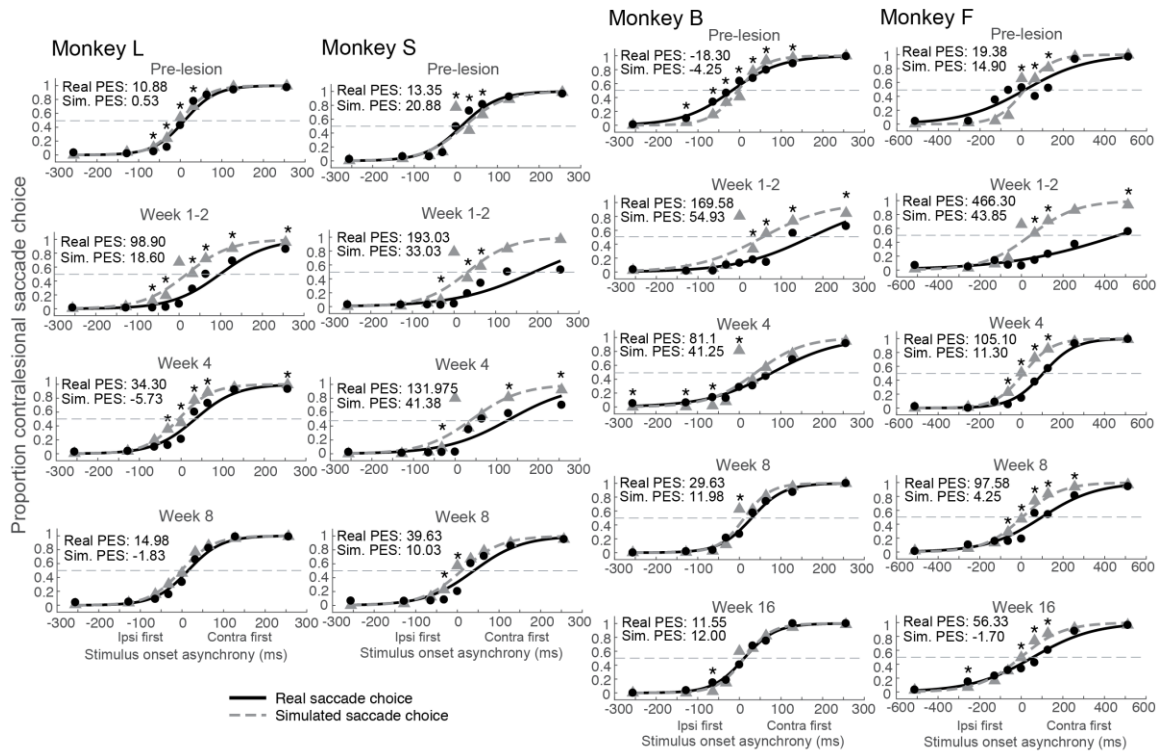


Figure 2.7. Observed versus simulated contralesional saccade choice on the free-choice saccade task.

Saccadic reaction time distributions were used to model saccade choice on a free-choice task staggered by the SOA based on a linear race model (Carpenter & Williams, 1995). Simulated contralesional choices at each SOA value are shown in grey dots and dotted grey lines and observed choices are shown in black dots and black lines. For each animal at each time point, the real and simulated point of equal selection is stated. Statistical comparisons between real and simulated choice at each SOA value were tested using a two-sided Chi-square test for proportions. Abbreviation: PES = point of equal selection; Sim. = simulated; contra = contralesional target; ipsi = ipsilesional target.

2.3.7. Does the mean reaction time on paired SOA trials account for the contralesional saccade choice?

Finally, we examined whether the reaction time to a selected stimulus on paired SOA trials could explain the contralesional choice deficit. We plotted the mean reaction time for saccades made towards the contralesional or ipsilesional stimulus at each SOA value (Fig. 2.8). On trials with a simultaneous presentation (SOA = 0 ms), the contralesional reaction time was significantly longer than the ipsilesional reaction time at weeks 1-2 post-lesion in Monkey L and at weeks 1-2, 4, and 8 post-lesion in Monkey B. However, in Monkeys L, S, and F, the contralesional reaction time was not significantly longer than the ipsilesional reaction time on true simultaneous trials during the later weeks post-lesion, even though there was a severe contralesional choice deficit on these trials at those time points (see Figure 2.3C). On trials in which the contralesional stimulus was presented first (SOA > 0ms), we find either no significant difference in reaction times or significantly decreased contralesional reaction times compared to ipsilesional post-lesion (in Monkeys L, S, and B). If the decreased proportion of contralesional saccade choice on paired trials was due to prolonged contralesional reaction times, then we would expect to see increased contralesional reaction times relative to ipsilesional reaction times. Our findings that contralesional saccades on paired trials were faster than ipsilesional saccades instead suggest that the drastic impairment in contralesional saccade choice post-lesion was also not accounted for by prolonged reaction times on paired trials.

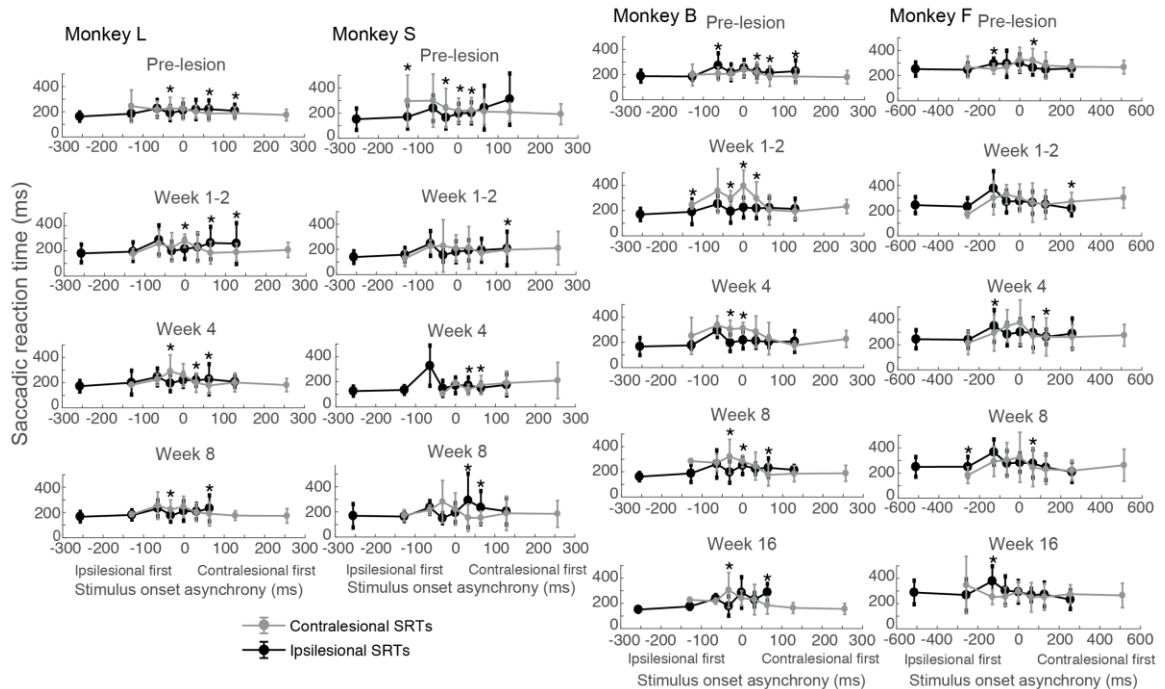


Figure 2.8. Saccadic reaction times to the selected contralesional or ipsilesional stimulus at each SOA condition on paired trials.

Mean reaction times to the contralesional (left) stimulus are shown in gray and mean reaction times to the ipsilesional (right) stimulus are shown in black. Weeks represent weeks post-lesion. Statistical comparisons were performed between contralesional and ipsilesional reaction times at each SOA value using two-sample Wilcoxon rank sum tests corrected for multiple comparisons. Error bars indicate standard error of the mean. Abbreviation: SRT = saccadic reaction time.

2.4. Discussion

The caudal PFC is involved in target selection and top-down control of visually-guided saccadic eye movements via reciprocal connections to cortical and subcortical oculomotor areas (Bruce & Goldberg, 1985; Hanes & Schall, 1996; Johnston & Everling, 2006; Johnston, Lomber, & Everling, 2016; Pierrot-Deseilligny, Rivaud, Gaymard, & Agid, 1991; Schall, 2004; Schall, 2002). Previous work in macaque monkeys has shown that a unilateral lesion (Rizzolatti et al. 1983; Schiller and Chou 1998) or reversible deactivation (Johnston et al. 2016; Schiller and Tehovnik 2003; Sommer and Tehovnik 1997; Wardak et al. 2006) of the caudal PFC leads to decreased selection of a contralesional target during simultaneous presentation of an ipsilesional target – an impairment that resembles visual extinction in humans. Here, we investigated whether these post-lesion deficits in contralesional target selection were largely due to contralesional motor deficits (i.e., slowed contralesional reaction times). We experimentally induced a right caudal PFC lesion in four male macaque monkeys using the vasoconstrictor endothelin-1 and studied the functional recovery.

We found that (1) injections of endothelin-1 in the macaque caudal PFC induced deficits in contralesional target selection that slightly varied depending on lesion size and location; (2) the neglect-like deficit in directing a saccade to a single contralesional target was transient and recovered by week 4 post-lesion; (3) contralesional target selection deficits on bilateral target trials were longer lasting and recovered gradually until no further improvement by 8 weeks post-lesion in Monkeys L and S and by 16 weeks post-lesion in Monkeys B and F; (4) contralesional reaction time returned to pre-lesion baseline by week 4 post-lesion in Monkey L, Monkey S, and Monkey F and by week 8 post-lesion in Monkey B; (3) the mean reaction time for contralesional and ipsilesional

saccades did not account for the degree of contralesional target selection deficits on the free-choice saccade task; and (4) simulated saccade choices modeled from the reaction time distribution were also unable to capture the degree of the ipsilesional saccade choice bias throughout recovery. Our findings suggest that the saccade choice bias observed after an endothelin-1-induced right caudal PFC lesion is not simply due to a contralesional motor processing deficit and may instead reflect the combination of motor biases and longer-lasting impairments in contralesional attentional selection.

2.4.1. Focal cerebral ischemia in the macaque caudal PFC using endothelin-1

To the best of our knowledge, this is the first study to use endothelin-1 to induce ischemic lesions in the PFC to study oculomotor function in macaque monkeys. Previous lesion studies in monkeys examining the oculomotor system have used reversible inactivation methods including cooling loops (Chan et al. 2015; Johnston et al. 2016; Peel et al. 2014), muscimol (Dias and Segraves 1999; Sommer and Tehovnik 1997), and lidocaine (Hanes and Wurtz 2001) or permanent inactivation by ablation (Heilman et al. 1995; Rizzolatti et al. 1983; Schiller et al. 1979) and electrocoagulation (Wurtz and Goldberg 1972). Although these lesion methods have been effective and reproducible in macaques, they are not representative of the underlying anatomical and cellular pathology of clinical focal cerebral ischemia. Traditional monkey models of ischemic stroke surgically occlude the middle cerebral artery (West et al. 2009), however this often produces widespread lesions affecting large swaths of cortical tissue which does not permit the study of specific behavioural effects following focal lesions. Endothelin-1 is a 21-amino acid peptide produced by vascular endothelial cells that was first isolated by Yanagisawa et al. (1988) and shown to have potent and long-acting vasoconstriction properties (Yanagisawa et al. 1988). Endothelin-1 has been used to induce focal cerebral

ischemia in rats (Fuxe et al. 1997; Macrae et al. 1993; Sharkey et al. 1993) and more recently in nonhuman primates, specifically in the visual cortex of marmosets (Teo and Bourne 2014) and in the motor cortex of macaque monkeys (Dai et al. 2017; Herbert et al. 2015; Murata and Higo 2016). This study adds to the growing line of research using endothelin-1 in nonhuman primate models of focal cerebral ischemia.

2.4.2. Effects of lesion volume and location on the severity and duration of choice deficits

We found that lesion size is related to the length of time to recovery (i.e., stable behavioural performance without further improvement) such that the two monkeys with the small lesion (Monkeys L and S) recovered after 8 weeks, and the two monkeys with a larger lesion (Monkeys B and F) recovered after 16 weeks post-lesion. This effect has also been reported in an early clinical stroke study by Hier et al. (1983) who found that patients with smaller lesions recovered more quickly from post-stroke cognitive deficits compared to those with larger lesions (Hier et al. 1983). We also found that lesion size appeared related to the point of equal selection at week 1-2 post-lesion; monkeys with a larger lesion volume showed an increased point of equal selection. At weeks 1-2 post-lesion, the contralesional lead time needed to reach the point of equal selection was 120 ms for Monkey L (smallest lesion volume), 180 ms for Monkey S, 205 ms for Monkey B, and 406 ms for Monkey F (largest lesion volume). Schiller and Chou (1998) unilaterally ablated the FEF in a monkey and found that two weeks after the lesion, the contralesional target had to be presented 116 ms before the ipsilesional target to achieve an equal probability of contralesional and ipsilesional saccade choice. The larger magnitude of the choice bias in our study compared to Schiller and Chou (1998) may first be due to our inclusion of choice performance at week 1 post-lesion which would capture the greatest

post-lesion deficits. Secondly, although Monkeys L's lesion was similar in size and location (FEF only) to the monkey reported in Schiller and Chou (1998) and showed a comparable deficit, Monkeys S, B, and F had larger lesion volumes that encompassed areas surrounding the FEF which may account for the larger contralesional deficits. The concept that larger lesions or inactivation leads to more severe deficits in contralesional target selection has been shown in both human and nonhuman primate studies (Johnston et al. 2016; Peers et al. 2005). Johnston et al. (2016) unilaterally cooled the dorsal and caudal principal sulcus in monkeys and found that inactivating both areas together induced larger shifts in the point of equal selection than inactivating individual areas alone. In human stroke patients, Peers et al. (2005) also found that the severity of an ipsilesional spatial bias was related to the lesion volume such that patients with larger lesions were the most spatially biased.

We also observed behavioural effects which appeared related to lesion location. We found that the two animals with lesions in both the FEF and dorsolateral/ventrolateral PFC [Monkey S (small lesion) and Monkey F (large lesion)] exhibited only a partial recovery of target selection deficits (i.e., proportion of contralesional choice at simultaneous presentation) at the time in which behavioural performance stabilized without further improvement. The proportion of contralesional saccade choice during simultaneous presentation was 22% in Monkey S and 26% in Monkey F, at the time in which there was no further recovery. However, there was a more complete recovery of function in the two animals with lesions that did not fully extend into the dorsolateral/ventrolateral PFC. The proportion of contralesional saccade choice during simultaneous presentation was 35% in Monkey L and 47% in Monkey B at the time in which there was no further recovery. Previous work has shown that unilateral inactivation of the FEF or dorsolateral PFC individually induces deficits in contralesional target

selection (Johnston et al. 2016; Schiller and Chou 1998), thus it is possible that the combined inactivation of both areas as in Monkeys S and F led to longer lasting impairments due to a reduction in intact task-related tissue remaining for post-lesion compensation (Nudo 2007, 2013). We also found that the severity of neglect-like deficits at weeks 1-2 post-lesion appeared related to lesion location. Monkeys S and F, with lesions in both the FEF and dorsolateral/ventrolateral PFC, showed larger deficits in directing a saccade to a single contralesional target at week 1-2 post-lesion, compared to Monkeys L and B.

2.4.3. Recovery of visuospatial deficits within the contralesional hemifield after unilateral caudal PFC lesions

We found that a right caudal PFC lesion resulted in decreased saccades to a single contralesional stimulus (Fig. 2.4) and contralesional target selection deficits during simultaneous presentation (Fig. 2.3). At weeks 1-2 post lesion, the monkeys were poor at responding to a single contralesional stimulus in the absence of a competing ipsilesional stimulus. In humans, this impairment is generally classified as neglect (e.g., failure to respond to a single contralesional stimulus), whereas extinction is when patients fail to respond to a contralesional stimulus during simultaneous presentation of an ipsilesional stimulus (de Haan et al. 2012). As mentioned above, deficits to single contralesional stimuli were more severe in Monkeys S and F, with lesions in both the FEF and dorsolateral/ventrolateral PFC. In stroke patients with neglect, one of the frontal areas most commonly lesioned is the middle frontal gyrus (He et al. 2007), which is considered the human homolog of the macaque dorsolateral PFC (Hutchison et al. 2012; Petrides and Pandya 1999). This might explain why our two monkeys with damage to the dorsolateral PFC show more severe neglect-deficits. The majority of contralesional errors made on

single stimulus trials were either largely due to an absence of a response when the contralesional stimulus was presented. This suggests that the errors reflected perceptual, rather than motor, deficits since motor deficits would likely appear as inaccurate saccades still directed towards the contralesional target. Deficits to single contralesional stimuli were transient and recovered by week 4 post-lesion, however contralesional target selection deficits on bilateral stimulus trials persisted until week 8 post-lesion in Monkeys L and S (small lesion) and until week 16 post-lesion in Monkeys B and F (large lesion).

This recovery pattern that we describe in which saccade behaviours resembling neglect and extinction occur together in the acute stage followed by a dissociation in which neglect recovers but extinction persists has been documented in stroke patients (Bender and Furlow 1945; Heilman et al. 1984, 2012; Milner and McIntosh 2005; Robertson and Halligan 1999). Since many lesion studies in animals have used temporary inactivation methods (Hier et al. 1983; Johnston et al. 2016; Kubanek et al. 2015; McPeck and Keller 2004; Wardak et al. 2002; Wilke et al. 2012), investigation into the longitudinal changes in behaviour during recovery has been limited. However, in one such study, Rizzolatti et al. (1983) reported that a unilateral aspiration lesion of the FEF in two macaque monkeys initially resulted in the absence of orientation to a single food stimulus presented in the contralesional hemifield, but that about two weeks post-lesion, this neglect-like impairment had recovered but there was a strong preference for ipsilesional food when the monkey was presented with two stimuli (Rizzolatti et al. 1983). They noted that this contralesional extinction-like deficit persisted until about eight weeks post-lesion. Our findings show that recovery of lateralized contralesional impairments after an ischemic lesion in the caudal PFC in monkeys is comparable to the recovery profile seen in stroke patients and one FEF lesion study in monkeys.

Our time course of recovery is also similar to what has been reported in stroke patients, where the greatest magnitude of behavioural recovery occurs within a few months post-lesion and plateaus afterwards. Ramsey et al. (2016) measured the extent of unilateral neglect deficits using the Posner Visual Orienting Task at 2 weeks, 3 months, and 12 months post-stroke (Ramsey et al. 2016). The Posner task is comparable to the free-choice saccade task in that a visual field bias can be determined by comparing saccade choice towards contralesional or ipsilesional visual fields. Comparable to our findings in macaques, the authors found significant visuospatial biases in the stroke patients with neglect at 2 weeks post-stroke. This impairment improved by 3 months post-stroke and plateaued with no further improvement when measured again one year later. This recovery time course has also been shown in macaque monkeys with deficits in contralesional choice after FEF lesions (Schiller and Chou 1998).

Immediately after the caudal PFC lesions, the reduced contralesional saccade performance may have worsened the contralesional target selection on the double and single stimulus trials through imbalanced reward expectations for each hemifield. Since the monkeys were impaired in directing saccades to the contralesional hemifield following the lesion, they would have been receiving more rewards overall for ipsilesional saccades, especially since they were rewarded for selecting either target on the double stimulus trials. The reward was not contingent on selecting the first appearing target because we wanted to ensure that the monkey was motivated to perform the task immediately post-lesion (Schiller and Chou 1998). Given that the monkey was severely impaired in directing saccades to the contralesional stimulus immediately post-lesion, the monkey would have been rewarded less if they were contingent on selecting the first target which would likely have decreased the monkey's motivation to perform the task. This imbalanced reward expectation may have affected the monkey's choice performance

on the double stimulus trials by causing the monkey to prefer the ipsilesional stimulus due to the increased reward for the ipsilesional stimulus overall on the single stimulus trials. The severe ipsilesional bias especially immediately post-lesion may have also caused the monkey to adopt a behavioural strategy to maximize reward delivery by always selecting the ipsilesional stimulus, which may have prolonged the time to recovery. There is only one study that we are aware of which did not reinforce inherent biases in behaviour through rewards and studied the longitudinal recovery in monkeys. Welch and Stuteville (1958) lesioned the macaque FEF and recorded whether the monkey responded to a single stimulus in either visual hemifield and reported a similar time to recovery of two weeks post-lesion without the imbalanced reward expectation. Although this is only one other study that we could relate our findings to, it suggests that the potential imbalance in reward expectations in our study did not prolong deficits to single targets in the monkeys.

As mentioned above, Monkey S continued to show contralesional neglect-like deficits at week 4 post-lesion whereas this impairment had recovered in the other monkeys by this time point. Recall that the behavioural paradigm for Monkey S did not have any single stimulus trials, so this monkey was not “forced” to direct saccades into the contralesional hemifield to receive a reward. Since Monkey S only had choice trials in which a saccade to either stimulus was rewarded, it is possible that this monkey developed a strategy to direct most saccades to the ipsilesional stimulus since it would always lead to a reward (since there were no single trials interleaved). It is possible that reduced contralesional choice led to imbalanced reward expectations which might have slowed this animal’s behavioural recovery and led to a more severe deficit than the other animals.

2.4.4. Recovery of oculomotor deficits after unilateral caudal PFC lesions

We observed changes in the reaction times for contralesional and ipsilesional saccades on single stimulus trials for Monkeys L, B, and F. We also observed decreased ipsilesional reaction times following the lesion in Monkeys S, B, and F. Previous work in our laboratory and by others have reported increased contralesional and decreased ipsilesional reaction times following caudal PFC inactivation (Johnston, Koval, Lomber, & Everling, 2014; Johnston et al., 2016b; Schiller & Chou, 1998). However, Peel et al. (2014) reported increased ipsilesional reaction times during unilateral cooling of the FEF (Peel et al. 2014). This inconsistent finding may be due to a greater inactivation of ipsilaterally-tuned FEF neurons which might have transiently increased ipsilesional reaction times in the Peel et al. (2014) study. Since the cooling session was only about 10 minutes long, it is possible that it only revealed the immediate effects of unilaterally deactivating the FEF (i.e., increased reaction time for both contralesional and ipsilesional saccades). Johnston et al. (2016) used a cooling period of 15-20 minutes; thus, it might be that more time was needed to see the decreased ipsilesional reaction times following a unilateral PFC inactivation. Longer inactivation times might be needed to observe the compensatory effects from the contralaterally-tuned FEF neurons of the intact left caudal PFC that lead to decreased ipsilesional reaction times.

Changes in saccadic duration, peak velocity, and amplitude following the lesion were minor and inconsistent across all four monkeys. Since these saccade parameters reflect motor output following the decision to look at a stimulus, we do not consider them to affect the choice bias. Previous work has also reported minor changes in contralesional duration and peak velocity following dorsolateral PFC deactivations (Koval et al. 2014).

2.4.5. Deficits in contralesional target selection are not only due to oculomotor impairments

If the saccade choice bias reflected a motor bias, we would expect to see the recovery of reaction times and the choice bias occurring simultaneously. Instead, we found that contralesional reaction times returned to pre-lesion baseline 4-8 weeks before the choice bias recovered. We explored this further by comparing the point of equal selection to the difference between contralesional and ipsilesional reaction times; we found that the contralesional lead time required to reach the point of equal selection was significantly greater than the difference in reaction times to either hemifield. This suggests that the mean reaction times to a single contralesional or ipsilesional stimulus were insufficient in explaining the degree of the contralesional choice deficit. Similarly, Schiller and Chou (1998) showed that at three weeks after a FEF ablation lesion in one animal, there is a pronounced choice bias where a 100 ms contralesional lead was required to reach the point of equal selection, however the difference in mean left/right reaction times was only about 68 ms at that time point. This is comparable to our findings suggesting that reaction times do not fully explain the lasting choice bias. However, they did not report the mean reaction times at the timepoint when the choice bias had recovered.

Leach and Carpenter (2001) showed that reaction time distributions to a single stimulus were able to predict saccade choice probabilities at various SOA values using a linear race model in humans. We modeled free-choice task performance using reaction time distributions to a single contralesional or ipsilesional stimulus and found that the model was unable to predict the ipsilesional choice bias following the caudal PFC lesion. This effect was most pronounced at a 0 ms SOA value (simultaneous presentation) where the linear race model from reaction time distributions predicted considerably more contralesional saccade choices than what was observed on the free-choice task. In other

words, the observed contralesional deficit on the free-choice task was larger than what would be expected based on reaction times to single contralesional targets alone and this effect lasted throughout recovery. Altogether, our findings indicate that the saccade choice bias following a caudal PFC lesion is not simply the result of a contralesional oculomotor deficit but likely reflects impaired attentional processing for competing target selection.

2.5. Supplemental Material

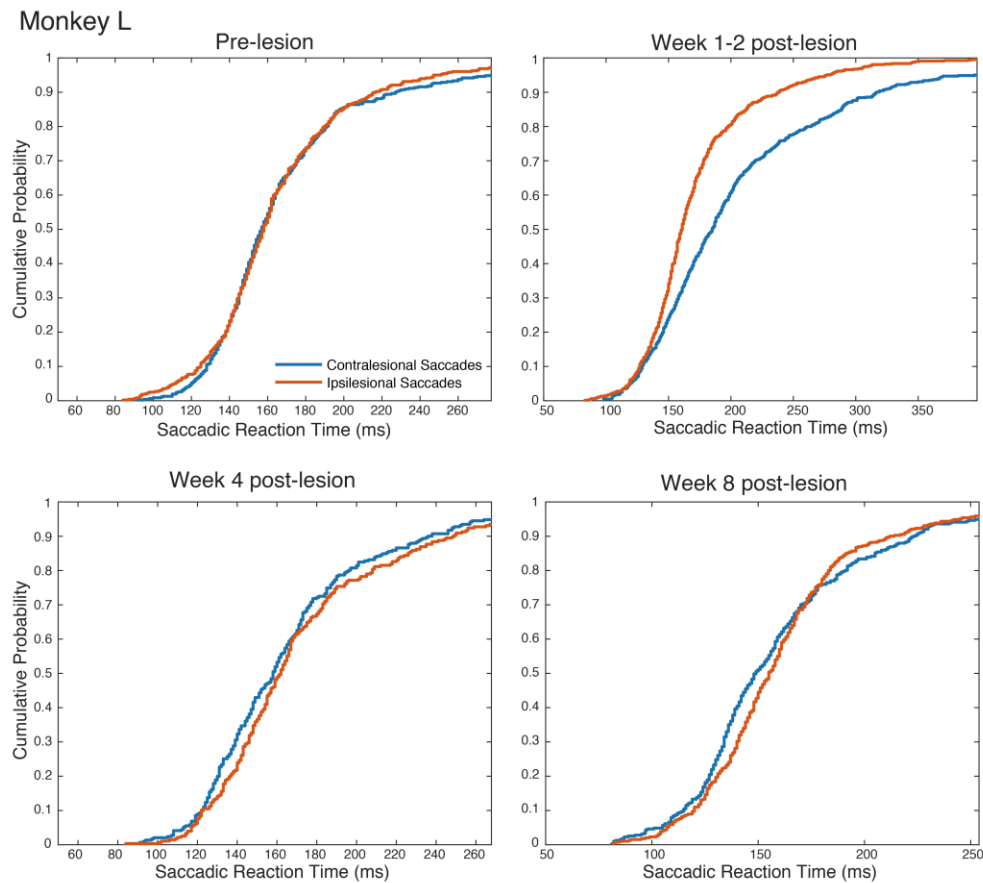


Figure 2.S1. Cumulative reaction time distributions for Monkey L.

Saccadic reaction times to a single contralesional (blue) or ipsilesional (red) stimulus are plotted cumulatively for each time point.

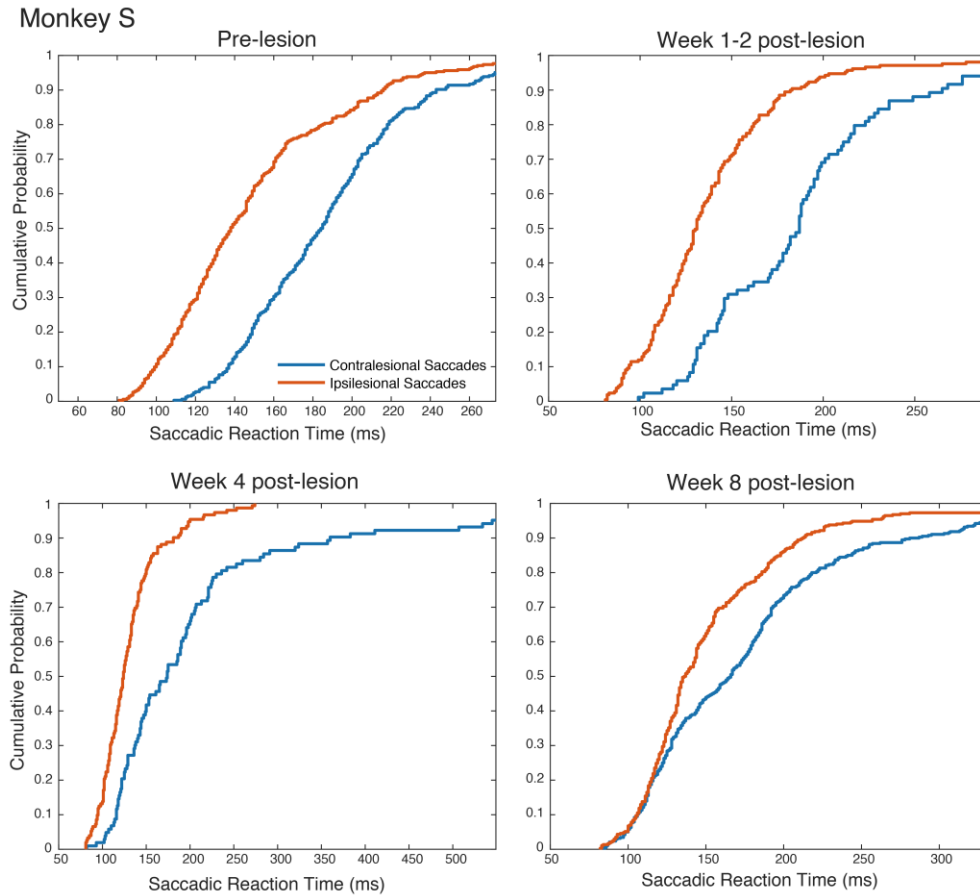


Figure 2.S2. Cumulative reaction time distributions for Monkey S.

Saccadic reaction times to a single contralesional (blue) or ipsilesional (red) stimulus are plotted cumulatively for each time point.

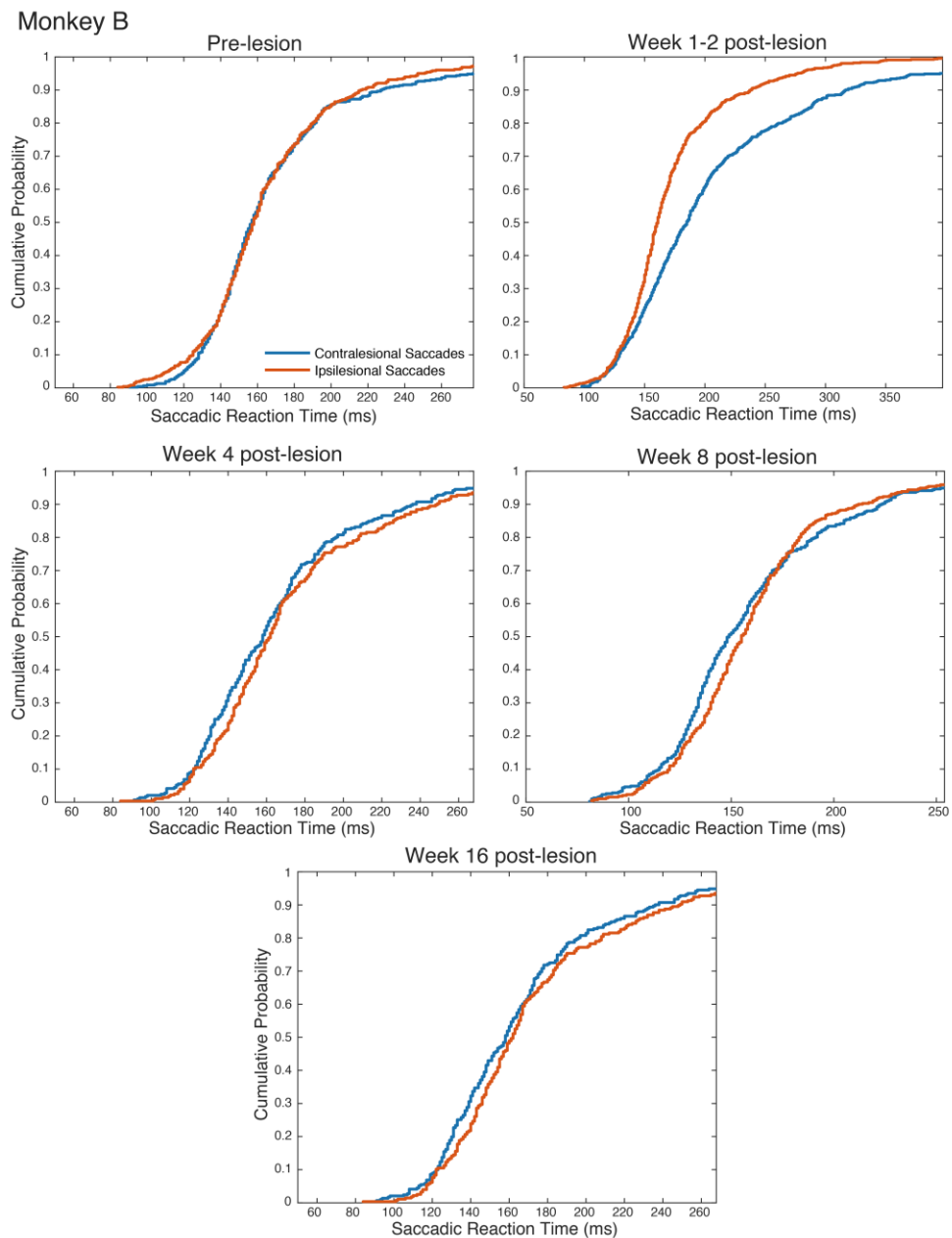


Figure 2.S3. Cumulative reaction time distributions for Monkey B.

Saccadic reaction times to a single contralesional (blue) or ipsilesional (red) stimulus are plotted cumulatively for each time point.

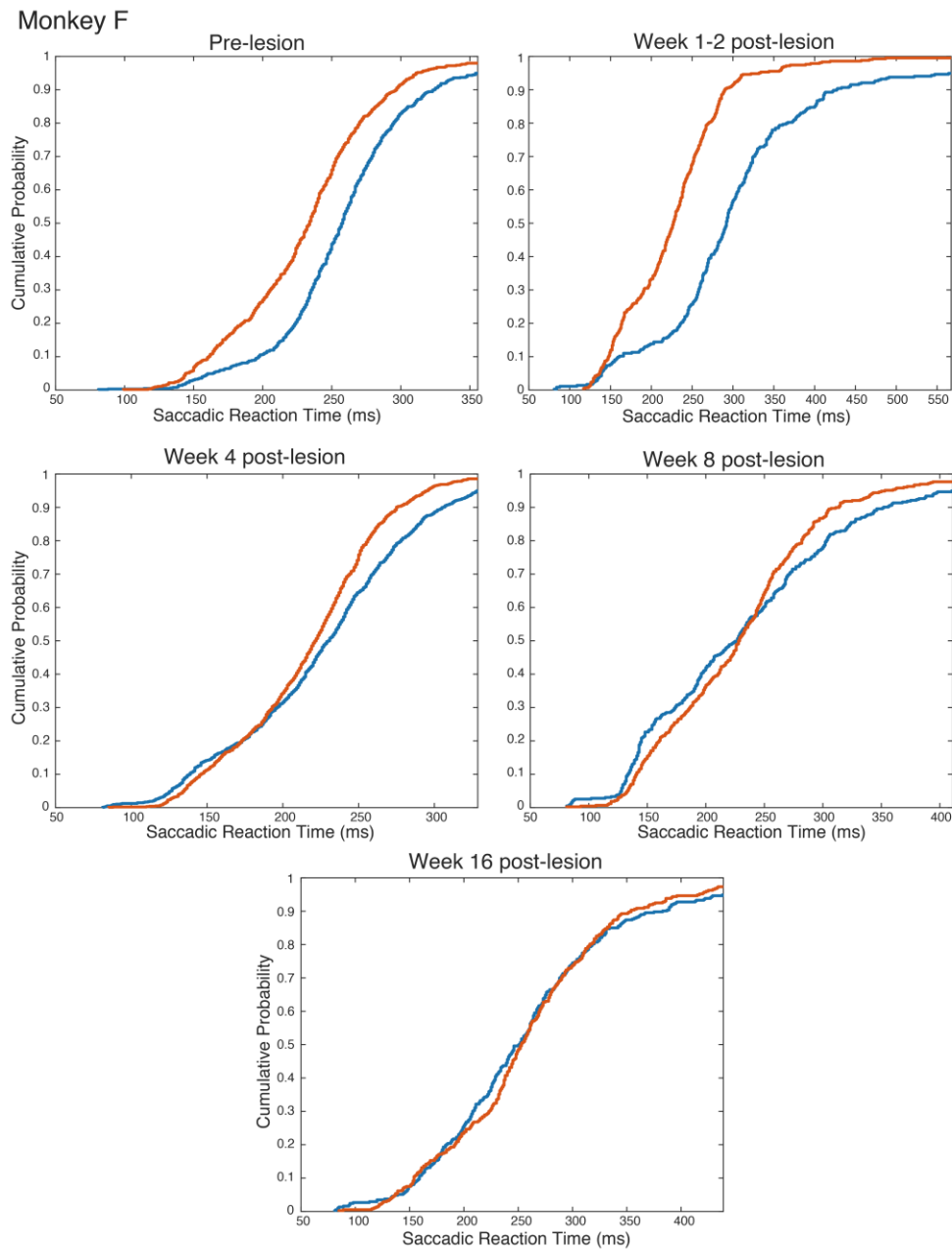


Figure 2.S4. Cumulative reaction time distributions for Monkey F.

Saccadic reaction times to a single contralesional (blue) or ipsilesional (red) stimulus are plotted cumulatively for each time point.

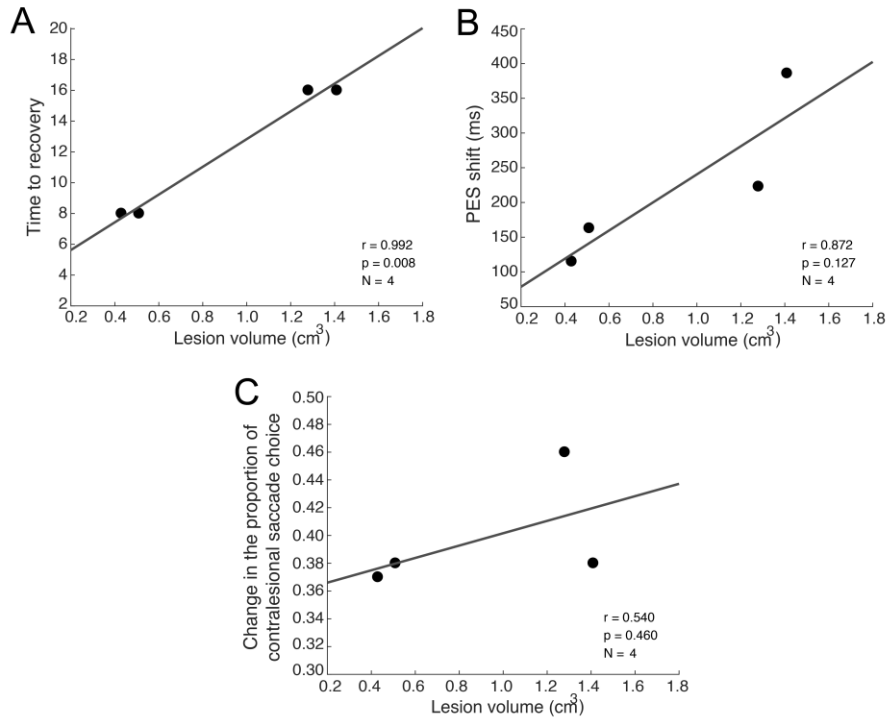


Figure 2.S5. Correlations between lesion volumes and the duration and severity of contralesional target selection deficits in each monkey.

(A) There is a strong and significant positive correlation between lesion volume and the time to recovery in weeks post-lesion. (B) There is a strong, but insignificant, positive correlation between lesion volume and the shift in the point of equal selection (PES) from pre-lesion to week 1 post-lesion. (C) There is a mild, but insignificant, positive correlation between lesion volume and the change in the proportion of contralesional saccade choice from pre-lesion to week 1 post-lesion. Abbreviations: PES = point of equal selection; r = Pearson's correlation coefficient; p = significance value; N = sample size.

2.5.1. Changes in the contralesional reciprocals after a right caudal PFC lesion

We used predictions from the LATER model to interpret the changes in the contralesional saccadic reaction time distribution throughout recovery (Supplementary Figure 2.S6). We plotted the cumulative probability of the reciprocal reaction time on a probit scale (reciprobit plot) with a line of best fit, where each line represents a reaction time distribution for each time point (see Supplementary Figures 2.S7-10 for reciprobital plots). The LATER model proposes that a decision signal rises linearly in response to a stimulus, at a rate that varies from trial to trial with a Gaussian distribution, until it reaches a threshold at which point a response is finally initiated (Supplementary Figure 2.S5A; Carpenter & Williams, 1995; Reddi, 2003). There are three possible interpretations for the changes in reaction time distributions (Supplementary Figure 2.S6B). A change in the accumulation rate of the model appears as a parallel “shift” in the line representing the reaction time distribution. A change in the threshold level would appear such that the line “swivels” about the infinite-time intercept. Lastly, a change in the variability of the accumulation rate appears such that the line “rotates” about the median. This third possibility was proposed more recently by Madelain et al. (2007). We found that all four monkeys show increased accumulation rate variability after the caudal PFC lesion (Supplementary Figure 2.S6C). This increased rate variability remains even in the later stages of recovery at weeks 8-16 post-lesion. Studies have shown that reaction times to rewarded locations are less variable than to non-rewarded locations (Takikawa et al., 2002; Montagnini and Chelazzi, 2005). We suspect that the increased reaction time variability in our study is due to the overall reduction in rewards to contralesional targets compared to ipsilesional targets following a right PFC lesion, which may have led to more variable contralesional reaction times.

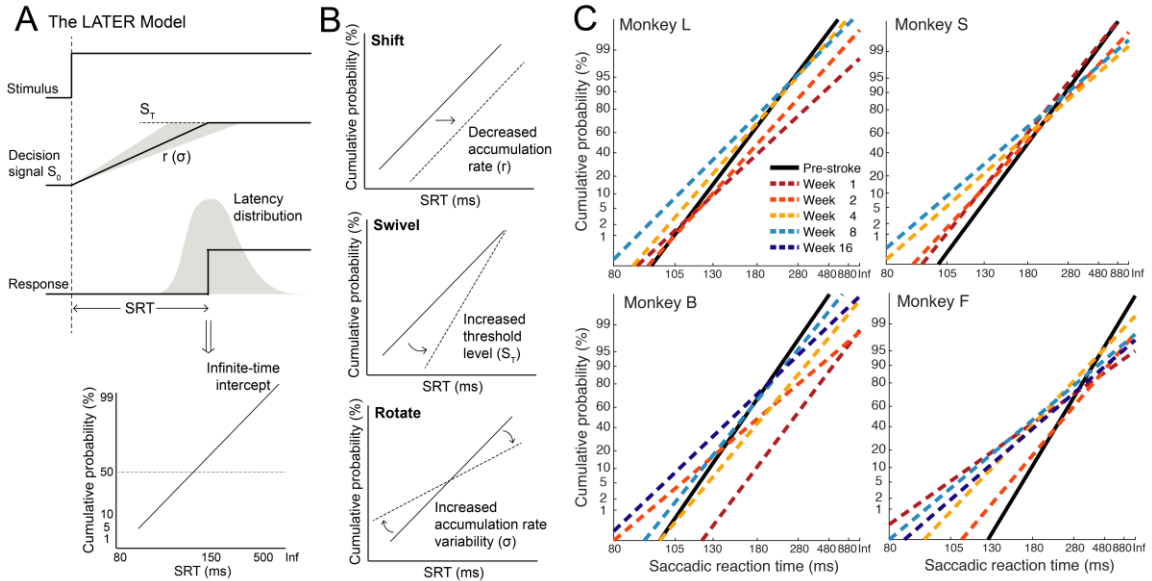


Figure 2.S6. The LATER model and longitudinal reciprob plots of contralesional reaction time distributions.

(A) A schematic of the LATER model. A decision signal S rises linearly in response to a stimulus, at an accumulation rate r that has a variance σ with a Gaussian distribution, until it reaches a threshold (S_T) at which point a response is finally initiated. The cumulative reaction times distribution can then be plotted on a probit scale (y-axis) with reciprocal reaction times (x-axis) resulting in a reciprob plot where distributions become straight lines (bottom). (B) Predictions of the LATER model. Top, a change in the accumulation rate of the model appears as a parallel shift in the line representing the reaction time distribution. Middle, a change in the threshold level would appear such that the line swivels about the infinite-time intercept. Bottom, a change in the variability of the accumulation rate appears such that the line rotates about the median. (C) Longitudinal reciprob plots of contralesional reaction time distributions. Contralesional saccadic reaction time data was obtained from the single stimulus trials. All monkeys show post-lesion changes in the reciprob plots that are consistent with increased accumulation rate variability; “rotation”.

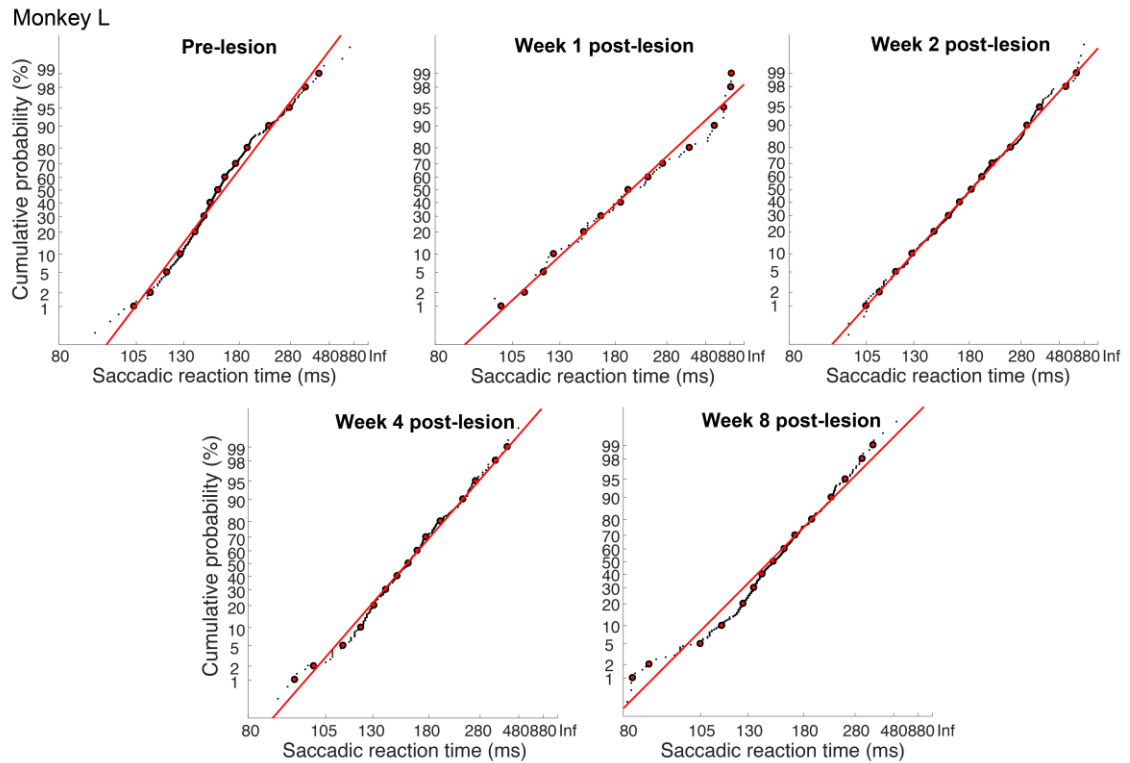


Figure 2.S7. Data points for the reciprobital plots of the contralesional reaction time distributions for Monkey L.

The y-axis represents the cumulative probability (%) on a probit scale and the x-axis represents the contralesional saccadic reaction time.

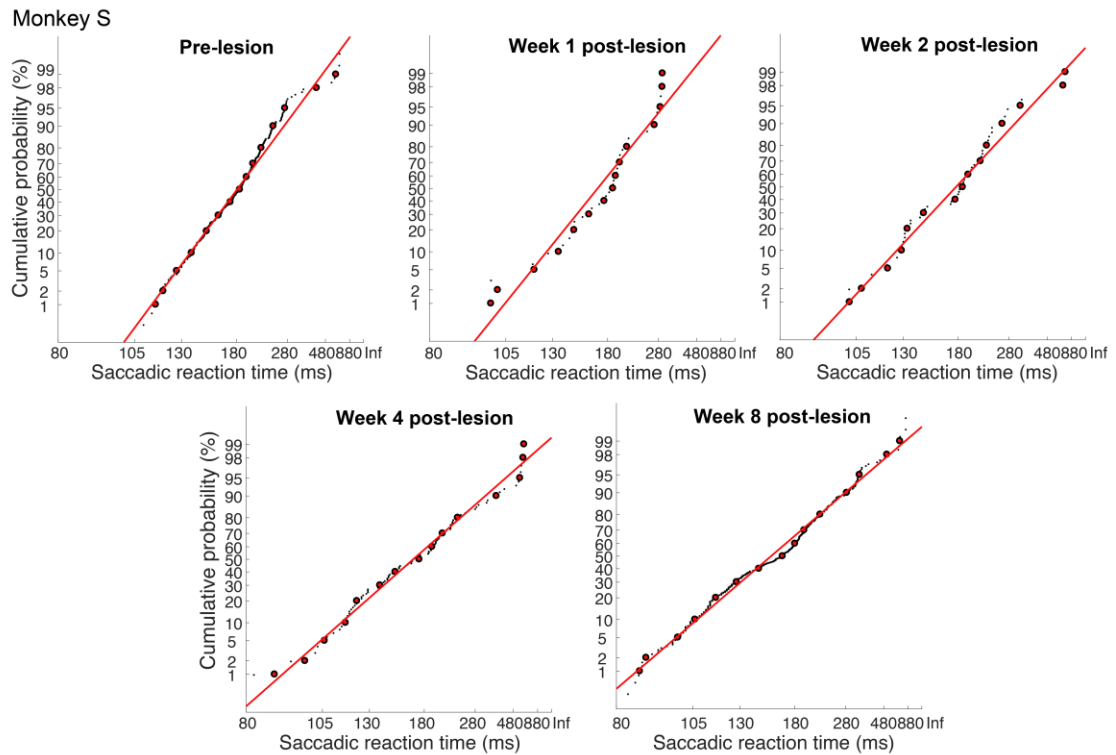


Figure 2.S8. Data points for the reciprob plots of the contralesional reaction time distributions for Monkey S.

The y-axis represents the cumulative probability (%) on a probit scale and the x-axis represents the contralesional saccadic reaction time.

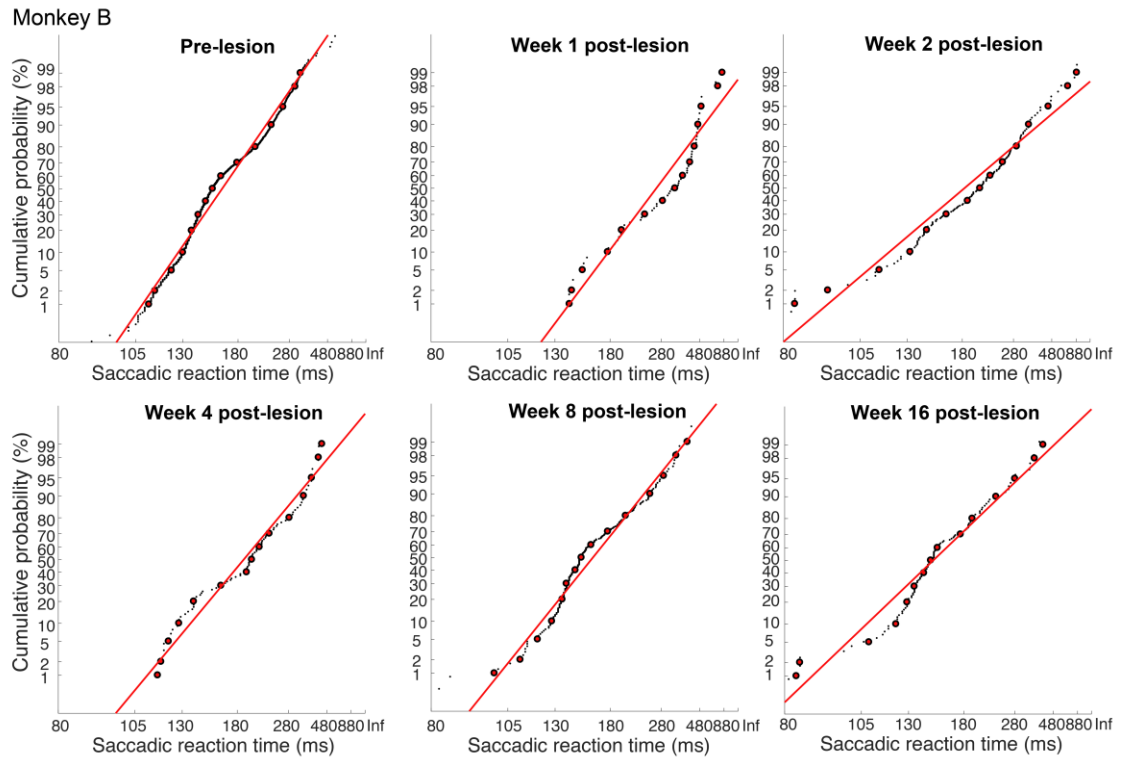


Figure 2.S9. Data points for the reciprocit plots of the contralesional reaction time distributions for Monkey B.

The y-axis represents the cumulative probability (%) on a probit scale and the x-axis represents the contralesional saccadic reaction time.

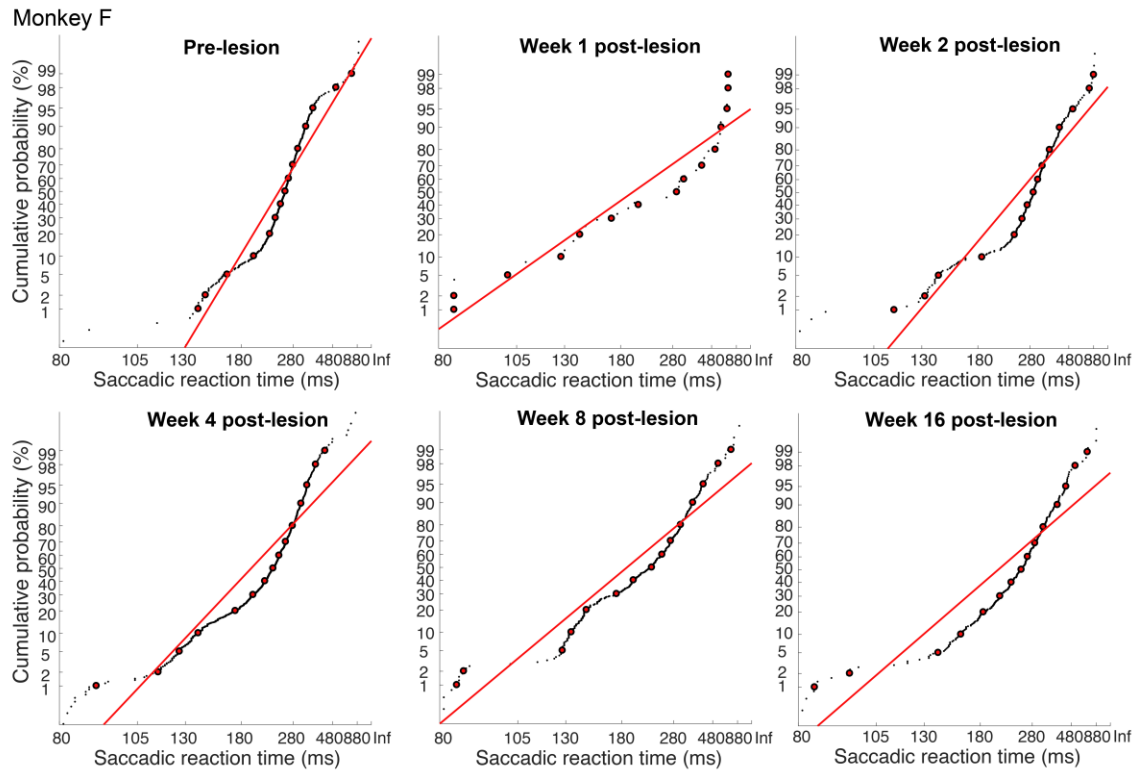


Figure 2.S10. Data points for the reciprocit plots of the contralesional reaction time distributions for Monkey F.

The y-axis represents the cumulative probability (%) on a probit scale and the x-axis represents the contralesional saccadic reaction time.

2.6. References

- Baylis G. Visual extinction with double simultaneous stimulation: what is simultaneous? *Neuropsychologia* 40: 1027–1034, 2002.
- Bender MB, Furlow LT. Phenomenon of visual extinction in homonymous fields and psychologic principles involved. *Arch Neurol Psychiatry* 53: 29–33, 1945.
- Bianchi L. The functions of the frontal lobes. *Brain* 18: 497–522, 1895.
- Bisiach E. Extinction and neglect: Same or different? 1991.
- Bruce CJ, Goldberg ME. Primate frontal eye fields. I. Single neurons discharging before saccades. *J Neurophysiol* 53: 603–635, 1985.
- Carpenter RHS, Williams MLL. Neural computation of log likelihood in control of saccadic eye movements. *Lett to Nat* 377: 69–62, 1995.
- Chan JL, Koval MJ, Womelsdorf T, Lomber SG, Everling S. Dorsolateral prefrontal cortex deactivation in monkeys reduces preparatory beta and gamma power in the superior colliculus. *Cereb Cortex* 25: 4704–4714, 2015.
- Clark G, Lashley KS. Visual disturbances following frontal ablations in the monkey. *Anat Rec* 97: 326, 1947.
- Corbetta M, Shulman GL. Spatial Neglect and Attention Networks. *Annu Rev Neurosci* 34: 569–599, 2011.
- Dai P, Huang H, Zhang L, He J, Zhao X, Yang F, Zhao N, Yang J, Ge L, Lin Y, Yu H, Wang J. A pilot study on transient ischemic stroke induced with endothelin-1 in the rhesus monkeys. *Sci Rep* 7: 45097, 2017.
- Deuel RK, Collins RC. The functional anatomy of frontal lobe neglect in the monkey: behavioral and quantitative 2-deoxyglucose studies. *Ann Neurol* 15: 521–529, 1984.
- Deuel RK, Farrar CA. Stimulus cancellation by macaques with unilateral frontal or parietal lesions. *Neuropsychologia* 31: 29–38, 1993.
- Dias EC, Segraves M. Muscimol-induced inactivation of monkey frontal eye field: effects on visually and memory-guided saccades. *J Neurophysiol* 81: 2191–2214, 1999.
- Driver J, Vuilleumier P. Perceptual awareness and its loss in unilateral neglect and extinction. *Cognition* 79: 39–88, 2001.
- Eidelberg E, Schwartz AS. Experimental analysis of the extinction phenomenon in monkeys. *Brain* 94: 91–108, 1971.
- Ferrier D. The functions of the brain. London: 1886.
- Fuxe K, Bjelke B, Andbjør B, Grahn H, Rimondini R, Agnati LF. Endothelin-1 induced lesions of the frontoparietal cortex of the rat. A possible model of focal cortical ischemia. *Neuroreport* 8: 2623–2629, 1997.

- Geeraerts S, Lafosse C, Vandenbussche E, Verfaillie K. A psychophysical study of visual extinction: Ipsilesional distractor interference with contralesional orientation thresholds in visual hemineglect patients. *Neuropsychologia* 43: 530–541, 2005.
- Gilbert KM, Gati JS, Barker K, Everling S, Menon RS. Optimized parallel transmit and receive radiofrequency coil for ultrahigh-field MRI of monkeys. *Neuroimage* 125: 153–161, 2016.
- de Haan B, Karnath HO, Driver J. Mechanisms and anatomy of unilateral extinction after brain injury. *Neuropsychologia* 50: 1045–1053, 2012.
- Hanes DP, Schall JD. Neural control of voluntary movement initiation. *Science* (80-) 274: 427–430, 1996.
- Hanes DP, Wurtz RH. Interaction of the frontal eye field and superior colliculus for saccade generation. *J Neurophysiol* 85: 804–815, 2001.
- He BJ, Snyder AZ, Vincent JL, Epstein A, Shulman GL, Corbetta M. Breakdown of functional connectivity in frontoparietal networks underlies behavioral deficits in spatial neglect. *Neuron* 53: 905–18, 2007.
- Hedges LV. *Distribution Theory for Glass's Estimator of Effect size and Related Estimators*. 1981.
- Hedges LV, Olkin I. *Statistical Methods for Meta-Analysis*. 1985.
- Heilman KM, Valenstein E, Day A, Watson R. Frontal lobe neglect in monkeys. *Neurology* 45: 1205–1210, 1995.
- Heilman KM, Valenstein E, Watson RT. Neglect and related disorders. *Semin Neurol* 4: 209–219, 1984.
- Heilman KM, Watson RT, Valenstein E. Neglect and Related Disorders. In: *Clinical Neuropsychology*, edited by Heilman KM, Valenstein E. New York: Oxford University Press, 2012.
- Herbert WJ, Powell K, Buford JA. Evidence for a role of the reticulospinal system in recovery of skilled reaching after cortical stroke: initial results from a model of ischemic cortical injury. *Exp Brain Res* 233: 3231–3251, 2015.
- Hier D, Mondlock J, Caplan L. Recovery of behavioral abnormalities after right hemisphere stroke. *Neurology* 33: 345–350, 1983.
- Hutchison RM, Gallivan JP, Culham JC, Gati JS, Menon RS, Everling S. Functional connectivity of the frontal eye fields in humans and macaque monkeys investigated with resting-state fMRI. *J Neurophysiol* 107: 2463–74, 2012.
- Jacobsen CF, Nissen HW. Studies of cerebral function in primates. IV. The effects of frontal lobe lesions on the delayed alternation habit in monkeys. *J Comp Psychol* 23: 101–112, 1937.
- Johnston K, Everling S. Monkey Dorsolateral Prefrontal Cortex Sends Task-Selective Signals Directly to the Superior Colliculus. *J Neurosci* 26: 12471–12478, 2006.

- Johnston K, Koval MJ, Lomber SG, Everling S. Macaque dorsolateral prefrontal cortex does not suppress saccade-related activity in the superior colliculus. *Cereb Cortex* 24: 1373–1388, 2014.
- Johnston K, Lomber SG, Everling S. Unilateral Deactivation of Macaque Dorsolateral Prefrontal Cortex Induces Biases in Stimulus Selection. *J Neurophysiol* 115: 1468–1476, 2016.
- Kennard MA. Reorganization of motor function in the cerebral cortex of monkeys deprived of motor and pre-motor areas in infancy. *J Neurophysiol* 1: 477–496, 1938.
- Kennard MA, Ectors L. Forced circling in monkeys following lesions of the frontal lobes. *J Neurophysiol* 1: 45–54, 1938.
- Koval MJ, Hutchison RM, Lomber SG, Everling S. Effects of unilateral deactivations of dorsolateral prefrontal cortex and anterior cingulate cortex on saccadic eye movements. *J Neurophysiol* 111: 787–803, 2014.
- Kubanek J, Li JM, Snyder LH. Motor role of parietal cortex in a monkey model of hemispatial neglect. *Proc Natl Acad Sci* 112: E2067–E2072, 2015.
- Latto R, Cowey A. Visual field defects after frontal eye field lesions in monkeys. *Brain Res* 30: 1–24, 1971a.
- Latto R, Cowey A. Fixation changes after frontal eye-field lesions in monkeys. *Brain Res* 30: 25–36, 1971b.
- Leach JCD, Carpenter RHS. Saccadic choice with asynchronous targets: Evidence for independent randomisation. *Vision Res* 41: 3437–3445, 2001.
- Macrae IM, Robinson MJ, Graham DI, Reid JL, McCulloch J. Endothelin-1-induced reductions in cerebral blood flow: dose dependency, time course, and neuropathological consequences. *J Cereb Blood Flow Metab* 13: 276–284, 1993.
- McPeck RM, Keller EL. Deficits in saccade target selection after inactivation of superior colliculus. *Nat Neurosci* 7: 757–63, 2004.
- Milner AD, McIntosh RD. The neurological basis of visual neglect. *Curr Opin Neurol* 18: 748–753, 2005.
- Murata Y, Higo N. Development and Characterization of a Macaque Model of Focal Internal Capsular Infarcts. *PLoS One* 11: e0154752, 2016.
- Nudo RJ. Postinfarct cortical plasticity and behavioral recovery. *Stroke* 38: 840–845, 2007.
- Nudo RJ. Recovery after brain injury: mechanisms and principles. *Front Hum Neurosci* 7: 1–14, 2013.
- Passingham RE, Wise SP. Caudal prefrontal cortex: searching for goals. In: *The Neurobiology of the Prefrontal Cortex: Anatomy, Evolution, and the Origin of Insight*. Oxford University Press, 2012.

- Paxinos G, Huang X, Toga A. *The Rhesus Monkey Brain in Stereotaxic Coordinates*. San Diego: Academic Press, 2000.
- Peel TR, Johnston K, Lomber SG, Corneil BD. Bilateral saccadic deficits following large and reversible inactivation of unilateral frontal eye field. *J Neurophysiol* 111: 415–433, 2014.
- Peers P V., Ludwig CJH, Rorden C, Cusack R, Bonfiglioli C, Bundesen C, Driver J, Antoun N, Duncan J. Attentional functions of parietal and frontal cortex. *Cereb Cortex* 15: 1469–1484, 2005.
- Di Pellegrino G, Basso G, Frassinetti F. Spatial extinction on double asynchronous stimulation. *Neuropsychologia* 35: 1215–1223, 1997.
- Petrides M, Pandya DN. Dorsolateral prefrontal cortex: comparative cytoarchitectonic analysis in the human and the macaque brain and corticocortical connection patterns. *Eur J Neurosci* 11: 1011–36, 1999.
- Pierrot-Deseilligny CH, Rivaud S, Gaymard B, Agid Y. Cortical control of reflexive visually-guided saccades. *Brain* 114: 1473–1485, 1991.
- Port NL, Wurtz RH. Target selection and saccade generation in monkey superior colliculus. *Exp Brain Res* 192: 465–477, 2009.
- Ramsey LE, Siegel JS, Baldassarre A, Metcalf N V., Zinn K, Shulman GL, Corbetta M. Normalization of network connectivity in hemispatial neglect recovery. *Ann Neurol* 80: 127–141, 2016.
- Ratcliff R. Group reaction time distributions and an analysis of distribution statistics. *Psychol Bull* 86: 446–461, 1979.
- Reddi BAJ. Accuracy, Information, and Response Time in a Saccadic Decision Task. *J Neurophysiol* 90: 3538–3546, 2003.
- Rincon-Gonzalez L, Selen LPJ, Halfwerk K, Corneil BD, Koppen M, Medendorp WP. Decisions in motion: vestibular contributions to saccadic target selection. *J Neurophysiol* 116: 977–985, 2016.
- Rizzolatti G, Matelli M, Pavesi G. Deficits in attention and movement following the removal of postarcuate (area 6) and prearcuate (area 8) cortex in macaque monkeys. *Brain* 106: 655–673, 1983.
- Ro T, Rorden C, Driver J, Rafal R. Ipsilesional biases in saccades but not perception after lesions of the human inferior parietal lobule. *J Cogn Neurosci* 13: 920–929, 2001.
- Robertson IH, Halligan PW. *Spatial neglect: A clinical handbook for diagnosis and treatment*. Hove, England: Psychology Press/Taylor & Francis (UK), 1999.
- Rorden C, Jelse L, Simon-Dack S, Baylis LL, Baylis GC. Visual extinction: The effect of temporal and spatial bias. *Neuropsychologia* 47: 321–329, 2009.
- Rorden C, Mattingley JB, Karnath HO, Driver J. Visual extinction and prior entry: Impaired perception of temporal order with intact motion perception after unilateral

- parietal damage. *Neuropsychologia* 35: 421–433, 1997.
- Schall JD. The neural selection and control of saccades by the frontal eye field. *Philos Trans R Soc Lond B Biol Sci* 357: 1073–82, 2002.
- Schall JD. On the role of frontal eye field in guiding attention and saccades. *Vision Res* 44: 1453–1467, 2004.
- Schiller PH, Chou I. The effects of frontal eye field and dorsomedial frontal cortex lesions on visually guided eye movements. *Nat Neurosci* 1: 248–253, 1998.
- Schiller PH, Chou I. The effects of anterior arcuate and dorsomedial frontal cortex lesions on visually guided eye movements: 2. Paired and multiple targets. *Vision Res* 40: 1627–1638, 2000.
- Schiller PH, Tehovnik EJ. Cortical inhibitory circuits in eye-movement generation. *Eur J Neurosci* 18: 3127–3133, 2003.
- Schiller PH, True S, Conway J. Effects of Frontal Eye Field and Superior Colliculus Ablations on Eye Movements. *Science* (80-) 206: 590–592, 1979.
- Sharkey J, Ritchie IM, Kelly PAT. Perivascular microapplication of endothelin-1: A new model of focal cerebral ischaemia in the rat. *J Cereb Blood Flow Metab* 13: 865–871, 1993.
- Sommer MA, Tehovnik EJ. Reversible inactivation of macaque frontal eye field. *Exp Brain Res* 116: 229–249, 1997.
- Teo L, Bourne J. A Reproducible and Translatable Model of Focal Ischemia in the Visual Cortex of Infant and Adult Marmoset Monkeys. *Brain Pathol* 24: 459–474, 2014.
- Wardak C, Hamed S Ben, Olivier E, Duhamel J-R. Differential effects of parietal and frontal inactivations on reaction times distributions in a visual search task. *Front Integr Neurosci* 6: 1–13, 2012.
- Wardak C, Ibos G, Duhamel J-R, Olivier E. Contribution of the Monkey Frontal Eye Field to Covert Visual Attention. *J Neurosci* 26: 4228–4235, 2006.
- Wardak C, Olivier E, Duhamel J-R. Saccadic target selection deficits after lateral intraparietal area inactivation in monkeys. *J Neurosci* 22: 9877–84, 2002.
- Welch K, Stuteville P. Experimental production of unilateral neglect in monkeys. *Brain* 81: 341–347, 1958.
- West GA, Golshani KJ, Doyle KP, Lessov NS, Hobbs TR, Kohama SG, Pike MM, Kroenke CD, Grafe MR, Spector MD, Tobar ET, Simon RP, Stenzel-Poore MP. A new model of cortical stroke in the rhesus macaque. *J Cereb Blood Flow Metab* 29: 1175–1186, 2009.
- Wilke M, Kagan I, Andersen R. Functional imaging reveals rapid reorganization of cortical activity after parietal inactivation in monkeys. *Proc Natl Acad Sci* 109: 8274–8279, 2012.

- Wurtz RH, Goldberg ME. Activity of superior colliculus in behaving monkey. IV. Effects of lesions on eye movements. *J Neurophysiol* 35: 587–596, 1972.
- Yanagisawa M, Kurihara H, Kimura S, Tomobe Y, Kobayashi M, Mitsui Y, Yazaki Y, Goto K, Masaki T. A novel potent vasoconstrictor peptide produced by vascular endothelial cells. *Nature* 332: 411–415, 1988.
- Zhang Y, Brady M, Smith S. Segmentation of brain MR images through a hidden Markov random field model and the expectation-maximization algorithm. *IEEE Trans Med Imaging* 20: 45–57, 2001.

CHAPTER 3

3. Functional reorganization during the recovery of contralesional target selection deficits after prefrontal cortex lesions in macaque monkeys

3.1. Introduction

Unilateral brain damage commonly results in a phenomenon referred to as ‘visual extinction’ which reflects an ipsilesional visuospatial bias in selective attention. Visual extinction has been characterized by the failure to respond to a stimulus in the contralesional hemifield when it is presented simultaneously with an ipsilesional stimulus (Bisiach, 1991; Corbetta and Shulman, 2011; Di Pellegrino et al., 1997). Unlike visual neglect, patients with extinction can still detect a single stimulus presented alone in either hemifield (de Haan et al., 2012). In humans, extinction is typically seen following right hemisphere lesions in the posterior parietal cortex (PPC), most commonly in the temporoparietal junction (de Haan et al., 2012; Di Pellegrino et al., 1997; Rorden et al., 2009, 1997). Extinction-like deficits have also been observed in neurologically-normal humans following transcranial magnetic stimulation over the PPC (Fierro et al., 2000; Meister et al., 2006) and in macaque monkeys following permanent lesions or reversible deactivation of the PPC (Wardak et al., 2002; Schiller and Tehovnik, 2003; Lynch and McLaren, 1989). Although impairments in contralesional attention are most often associated with damage to the PPC, it has also been observed following damage to the prefrontal cortex (PFC) in humans (Damasio et al., 1980; Husain and Kennard, 1996; Mesulam, 1999) and macaque monkeys (Bianchi, 1895; Deuel and Collins, 1984; Deuel

and Farrar, 1993; Eidelberg and Schwartz, 1971; Ferrier, 1886; Jacobsen and Nissen, 1937; Johnston et al., 2016; Kennard and Ectors, 1938; Latto and Cowey, 1971b, 1971a; Schiller and Chou, 1998; Welch and Stuteville, 1958). Thus, it has been suggested that disruptions of visuospatial attention are better accounted for by damage to a distributed frontoparietal network that mediates attention, rather than from damage to a single brain area (Corbetta and Shulman, 2011, 2002; Mesulam, 1981).

Two core regions of the macaque caudal PFC comprise the anterior portion of the frontoparietal network, namely the frontal eye field (FEF; area 8A) and dorsolateral PFC (area 9/46D) which are both strongly implicated in visual target selection and attentional control (Hutchison et al., 2012; Womelsdorf and Everling, 2015). The FEF is located in the anterior bank of the arcuate sulcus and the dorsolateral PFC is located in the caudal portion of the dorsal bank of the principal sulcus, just anterior to the FEF. Both regions share extensive reciprocal connections with each other and with other cortical oculomotor structures, including the lateral intraparietal area (LIP), other higher order visual areas, and the contralateral PFC (Barbas et al., 2005; Barbas and Mesulam, 1985; Borra et al., 2019; Kunzle and Akert, 1977; Maioli et al., 1983; Petrides and Pandya, 1999, 1984; Stanton et al., 1993). The FEF and dorsolateral PFC send projections to subcortical oculomotor areas, including the superior colliculus (Fries, 1984; Goldman and Nauta, 1976; Stanton et al., 1988a), caudate and putamen (Stanton et al., 1988b; Yeterian and Pandya, 1991), and pontine nuclei (Kunzle and Akert, 1977; Schmahmann and Pandya, 1997; Stanton et al., 1988b), and in turn receive subcortical input via the mediodorsal thalamus (Goldman-Rakic and Porrino, 1985; Tian and Lynch, 1997). Previous work has shown that caudal PFC lesions in monkeys results in impaired contralesional target selection that resembles visual extinction in humans (Johnston et al., 2016; Schiller and Chou, 1998).

Saccade target selection has been investigated using double stimulation oculomotor paradigms (e.g., temporal order-judgement (TOJ) and free-choice saccade tasks) in which two peripheral visual stimuli are presented in rapid succession in either hemifield with a variable temporal delay between stimulus onsets (stimulus onset asynchrony, SOA) and a randomized order of side of the first-presented stimulus. In the TOJ task, monkeys are rewarded for correctly selecting the first-appearing stimulus (Kubaneck et al., 2015; Port and Wurtz, 2009), whereas on the free-choice task, selection of either stimulus is rewarded in order to measure the naturally-occurring visuospatial bias (Johnston et al., 2016; Schiller and Chou, 1998; Wardak et al., 2002). In permanently lesioned monkeys, requiring the selection of the first-appearing stimulus in order to receive a reward (i.e., on the TOJ task) might be too difficult and may reduce the number of completed trials. The free-choice task has been used to measure visuospatial target selection biases in monkeys after reversible inactivation (Johnston et al., 2016; Wardak et al., 2002; Wilke et al., 2012) and after permanent lesions where the gradual behavioural recovery has been reported (Adam et al., 2019; Schiller and Chou, 1998). Schiller and Chou (1998) permanently lesioned the left FEF in monkeys and reported an ipsilesional bias on the free-choice task, with gradual improvements in target selection of the contralesional stimulus over the following months (Schiller and Chou, 2000, 1998). We have also previously reported on the behavioural recovery of contralesional attention deficits over 2-4 months post-lesion in the monkeys described in the present study (Adam et al., 2019).

The compensatory neural processes underlying post-lesion behavioural recovery are poorly understood. Although structural damage from a stroke or lesion may be focal, functional disruptions to distant and intact areas that are functionally connected to the lesion site have been reported and shown to correlate with behavioural recovery (Carter et al., 2012; He et al., 2007). Therefore, studying the effects of a cortical lesion on a

widespread functional network, rather than on local structures alone, may provide a more comprehensive understanding of the recovery process following brain damage. Resting-state fMRI (rsfMRI) has emerged as a powerful method to study functional brain networks using measures of functional connectivity (FC). One of the major advantages of rsfMRI over task-based fMRI is that it measures the blood-oxygen level-dependent (BOLD) signal at rest, which makes it possible to collect data from subjects who are severely impaired following brain damage without requiring them to perform complex tasks in the scanner. RsfMRI also avoids potential confounds of FC between subjects whose task performance may rely on different means of behavioural compensation. Previous studies in stroke patients and animal models of stroke have shown a link between recovery of behavioural deficits and changes in FC (Ainsworth et al., 2018; Carter et al., 2010; Grefkes and Fink, 2011; He et al., 2007; van Meer et al., 2010; Westlake and Nagarajan, 2011).

Here, we used rsfMRI to investigate longitudinal changes in FC of the frontoparietal network during the recovery of contralesional target selection deficits after unilateral caudal PFC lesions in macaque monkeys. Macaque monkeys share similar oculomotor behaviour, cortical organization, and resting-state functional networks with humans (Wurtz and Goldberg, 1989; Petrides and Pandya, 1999; Hutchison et al., 2011; Hutchison and Everling, 2012; Sallet et al., 2013), which uniquely positions them as a valuable animal model in the study of post-lesion functional brain reorganization. The use of an animal model of focal cerebral ischemia was beneficial since it allowed us to collect pre-lesion baseline behavioural and imaging data and study the effects of location-specific lesions. We injected the vasoconstrictor endothelin-1 (ET-1) in the right caudal PFC to create a well-controlled and clinically-relevant model of focal cerebral ischemia, compared to traditional aspiration or clipping methods. ET-1 induces focal occlusion with

subsequent reperfusion and has recently been validated in marmosets and macaque monkeys (Dai et al., 2017; Herbert et al., 2015; Murata and Higo, 2016; Teo and Bourne, 2014). We measured behavioural performance on a free-choice saccade task and have previously reported the recovery of deficits in contralesional target selection over 2-4 months after PFC lesions (Adam et al., 2019). Functional imaging data was collected using rsfMRI at 7-Tesla (7T) prior to the lesion and at weeks 1-16 following the lesion during behavioural recovery. Since the frontoparietal network plays an important role in mediating visuospatial attention (Corbetta and Shulman, 2011, 2002; Mesulam, 1981) and the areas of the caudal PFC form the core anterior portion of the frontoparietal network (Hutchison et al., 2011; Babapoor-Farrokhran et al., 2013), we hypothesized that a caudal PFC lesion would alter the frontoparietal network FC and that these changes in FC might be associated with the behavioural recovery of deficits in contralesional target selection.

3.2. Methods

3.2.1. Subjects

Data were collected from four adult male macaque monkeys (*Macaca mulatta*) aged 5 to 7 years old and weighing 7 to 10 kg. Animals are individually described as Monkey L, Monkey S, Monkey B, and Monkey F and are ordered from smallest to largest lesion size, as described in Section 3.1. All surgical and experimental procedures were carried out in accordance with the Canadian Council of Animal Care policy on the use of laboratory monkeys and approved by the Animal Care Committee of the University of Western Ontario Council. A custom-built acrylic head post was fixed to the skull using dental acrylic and 6-mm ceramic bone screws (Thomas Recording, Giessen, Germany) as

previously described (Johnston and Everling, 2006). We opted for an acrylic head post to minimize signal drop out. A head post was necessary to restrain the head for eye-tracking during training on the oculomotor task. Animals received postoperative analgesics and antibiotics and were monitored by a university veterinarian.

3.2.2. Experimental focal ischemic lesions

Monkeys were initially sedated with 15.0 mg/kg ketamine (Vetalar 100 mg/ml), followed by intravenous administration of 2.5 mg/kg propofol (10 mg/ml) via the saphenous vein. Animals were then intubated with an endotracheal tube and anaesthesia was maintained with 1-2% isoflurane mixed with oxygen (1 L/min) and continuous rate infusion of propofol (2.5 mg/ml) in saline. The animal's head was held in position using a stereotaxic frame with ear and eye bars (Model 1404 Stereotaxic Instrument, Kopf Instruments, CA, USA). A craniotomy was made above the right arcuate sulcus and caudal portion of the right principal sulcus using coordinates derived from each animal's anatomical MRI. The dura was then removed to confirm the location of the arcuate and principal sulci by visual inspection. A 10 μ l-capacity syringe (26 gauge) was held in position with a microinjection unit (Model 5000 Microinjection Unit, Kopf Instruments, CA, USA) that was mounted to a stereotaxic frame assembly and filled with ET-1 (E7764, Sigma-Aldrich).

We experimentally induced a small lesion in Monkeys L and S and a larger lesion in Monkeys B and F by varying the number of injections and concentration of ET-1. Each injection contained 2 μ l of ET-1 and was injected at a flow rate of 0.75 μ l/min. Monkey L received a total of six injections of ET-1 (0.5 μ g/ μ l) in the anterior bank of the right arcuate sulcus at three injection sites separated by 2 mm along the mediolateral axis and at two depths at each site along the dorsoventral axis at 2 mm and 4 mm below dura.

Monkey S received a total of 12 injections of ET-1 (0.5 $\mu\text{g}/\mu\text{l}$) with six in the anterior bank of the right arcuate sulcus (as described for Monkey L) and an additional six in the caudal portion of the right principal sulcus at three injection sites separated by 2 mm along the rostrocaudal axis and at two depths at each site along the dorsoventral axis at 2 mm and 4 mm below dura. Monkey B received a total of 16 injections of ET-1 (0.5 $\mu\text{g}/\mu\text{l}$), with eight in the anterior bank of the right arcuate sulcus (as described for Monkey L) and eight in the caudal portion of the right principal sulcus (as described for Monkey S). Monkey F received a total of 16 injections of ET-1 (1.0 $\mu\text{g}/\mu\text{l}$), with eight in the anterior bank of the right arcuate sulcus (as described for Monkey L) and eight in the caudal portion of the right principal sulcus (as described for Monkey S). Following the last needle retraction, the dura flap was put back in place and the skull trephination was covered with medical grade silicon and left undisturbed to dry before the area was sealed by application of dental acrylic. More details on the lesion induction methods have been previously described (Adam et al., 2019).

3.2.3. Behavioural task

Prior to the induction of an experimental lesion, monkeys were trained to perform the free-choice saccade task (see Fig. 3.3A), as previously described (Adam et al., 2019; Johnston et al., 2016; Schiller and Chou, 1998). Each trial began with the presentation of a central fixation point (white-filled circle, 0.3°) against a black background on the display monitor. Monkeys were required to maintain fixation for a duration that varied between 500 to 1000 ms. Two peripheral visual stimuli (white-filled circles, 0.5°) were then presented in the left and right hemifields at an equal eccentricity of 10° and with a variable stimulus onset asynchrony (SOA) between the presentation of both stimuli. For example, in some trials the left (or right) target was presented at an SOA that varied

between 32-256 ms before the right (or left) target or both stimuli were presented simultaneously (SOA = 0 ms). Monkeys were required to direct a single saccade towards either stimulus and received a liquid reward for either choice. The behavioural paradigm also included single stimulus trials to measure the degree of neglect-like impairment. We randomly interleaved an equal proportion of single stimulus trials with the free-choice double stimulus trials. The single stimulus trials involved the presentation of either a left or right target following fixation and the monkey simply had to direct a saccade to that single target to receive a liquid reward.

The behavioural paradigm and reward delivery were controlled with the CORTEX behavioural control system (National Institute of Mental Health, Bethesda, MD). Stimuli were presented on a CRT monitor (refresh rate = 60 Hz) centered in front of the monkey. Eye movements were recorded at 1000 Hz using an infrared video eye tracker (Eyelink 1000, SR Research, ON, Canada). Monkeys performed this task for about an hour daily. We have previously published a detailed report of the behavioural paradigm and task performance (Adam et al., 2019).

3.2.4. Behavioural data analysis

Analyses were performed using custom-designed software written in MATLAB (Mathworks, Natick, MA). Saccade onset was defined as the time at which eye velocity exceeded 30°/s following stimulus onset, while saccade end was defined as the time at which eye velocity then fell below 30°/s (Johnston et al., 2016). The following trials were excluded from further analysis: 1) trials in which the animal blinked around the time of stimulus or saccade onset and 2) trials with broken or incorrect fixation. We were interested in how a unilateral focal ischemic lesion in the right caudal PFC would affect contralesional target selection when competing stimuli were presented in the left and

right visual hemifields simultaneously. Behavioural data was grouped into time points that aligned with the functional imaging sessions: pre-lesion, and weeks 1-2, 4, 8, and 16 post-lesion. We assessed the degree of contralesional target selection on the double stimulus trials using two behavioural metrics. The first metric was the point of equal selection, which was the SOA value at which the probability of choosing the contralesional or ipsilesional stimulus was equal; the greater the point of equal selection (with a contralesional lead time), the greater the contralesional target selection deficit. The second metric was the proportion of contralesional saccade choice, which was the number of saccades directed towards the contralesional stimulus during simultaneous presentation of both stimuli divided by the total number of saccades made to either stimulus. Since extinction deficits are maximal when both stimuli are presented simultaneously (Baylis, 2002; Di Pellegrino et al., 1997), we correlated FC with the proportion of contralesional saccade choice on trials with an SOA of 0 ms. Performance on the single stimulus trials was used to measure neglect-like saccadic behaviour. Monkey S was the first subject in the study and we had not yet introduced the single stimulus trials at that time, so we used double stimulus trials with the longest SOA (256 ms) as single stimulus trials. The longest SOA values can effectively be used as single stimulus trials since these values exceeded the average reaction time of the animal (about 150-200 ms). Thus, by the time the second stimulus appeared, the animal would theoretically have already initiated a saccade to the first appearing stimulus (Adam et al., 2019; Johnston et al., 2016). We performed one-way analyses of variance (ANOVA) with time as a factor (variables: pre-lesion, week 1-2, 4, 8, 16 post-lesion) on these data to test for significant differences in performance between pre-lesion and post-lesion time points. Significant differences were further investigated using post-hoc Tukey's Honestly Significant Difference (HSD) tests ($p < 0.05$). All analyses were performed for each monkey individually.

Pre-lesion baseline behavioural data was collected until task performance was stable across sessions for several weeks (i.e., when the point of equal selection was no longer significantly different when compared across weeks). After the experimental lesion was induced, daily behavioural data collection continued until performance stabilized without further improvement (i.e., when the point of equal selection was no longer significantly different when compared across weeks). We denoted this final time point as “behavioural recovery”, which was week 8 post-lesion for Monkeys L and S (small lesion) and week 16 post-lesion for Monkeys B and F (large lesion).

3.2.5. Animal preparation for MR image acquisition

One hour prior to scanning, monkeys were sedated with intramuscular injections of 0.05 – 0.2 mg/kg acepromazine (Acevet 25 mg/ml) and 5.0 – 7.5 mg/kg ketamine (Vetalar 100 mg/ml), followed by intravenous administration of 2.5 mg/kg propofol (10 mg/ml) via the saphenous vein. Animals were then intubated with an endotracheal tube and anaesthesia was maintained with 1.0 – 1.50% isoflurane mixed with 100% oxygen. Each monkey was then placed in a custom-built primate chair with its head restrained to reduce motion and then inserted into the magnet bore for image acquisition, at which time the isoflurane level was lowered to 1.0%. Animals were spontaneously ventilating throughout the duration of image acquisition. Physiological parameters were monitored [rectal temperature via a fiber-optic temperature probe (FISO, Quebec City, QC, Canada), respiration via bellows (Siemens, Union, NJ), and end-tidal CO₂ via a capnometer (Covidien-Nellcor, Boulder, CO)]. Body temperature was maintained using thermal insulation and a heating disk (Snugglesafe, Littlehampton, West Sussex, UK). Light anaesthesia was used because it reduces motion artifacts, physiological stress, and avoids the need to train monkeys to undergo MRI scanning. Although isoflurane has vasodilator

properties that could affect cerebrovascular activity (Farber et al., 1997), resting-state FC and synchronous BOLD fluctuations measured under 1.0 – 1.5% isoflurane have been robustly reported in previous studies (Hutchison et al., 2014; Vincent et al., 2007). These animal preparation procedures has been previously reported (Hutchison et al., 2011).

3.2.6. MR image acquisition at 7T

We acquired rsfMRI data at the following time points: pre-lesion (after behavioural training), and at week 1, 4, 8, and 16 post-lesion. Since data collection was ceased for Monkeys L and S at the time of behavioural recovery at week 8 post-lesion (see Section 2.5), only Monkeys B and F had rsfMRI data at week 16 post-lesion. Data were acquired on an actively shielded 7T Siemens MAGNETOM Step 2.3 68-cm horizontal bore scanner (Erlangen, Germany) operating at a slew rate of 300 mT/m/s. An in-house designed and manufactured 8-channel transmit, 24-channel receive primate head radiofrequency coil was used for all MR image acquisitions (Gilbert et al., 2016). Magnetic field optimization (B_0 shimming with shims up to 4th order) was performed using an automated 3D mapping procedure over the specific imaging volume of interest. For each animal in each session, we acquired four to six 10-minute runs of 600 T2*-weighted continuous multi-band echo-planar imaging (EPI) functional volumes (TR = 1000 ms, TE = 18 ms, flip angle = 40°, slices = 42, matrix size = 96 x 96, field of view = 96 x 96 mm, acquisition voxel size = 1 x 1 x 1 mm). EPI functional volumes were acquired with GRAPPA at an acceleration factor of 2. Every image was corrected for physiological fluctuations using navigator echo correction. A standard T2-weighted turbo spin echo anatomical MR image was acquired along the same orientation as the functional images (TR = 7500 ms, TE = 90 ms, slices = 42, matrix size = 256 x 256, field of view = 128 x 128 mm, acquisition voxel size = 0.5 mm x 0.5 mm x 1 mm). A high-

resolution T2-weighted turbo spin echo anatomical MR image (TR = 7500 ms, TE = 80 ms, slices = 42, matrix size = 320 x 320, field of view = 128 x 128 mm, acquisition voxel size = 0.4 mm x 0.4 mm x 1 mm) and a T1-weighted MP2RAGE anatomical image (TR = 6500 ms, TE = 3.15 ms, TI1 = 800 ms, TI2 = 2700 ms, field of view = 128 x 128 mm, 0.5 mm isotropic resolution) were also acquired along the same orientation as the functional images.

3.2.7. MR image preprocessing

MR image preprocessing was implemented using the FMRIB Software Library (FSL; <http://www.fmrib.ox.ac.uk>). First, denoising was performed using FSL's Multivariate Exploratory Linear Optimized Decomposition into Independent Components (MELODIC), which outputs the functional data as a set of independent components for each session (Beckmann and Smith, 2004). Components that were labelled as noise, motion, or physiological artefact were removed (Griffanti et al., 2014). Functional data was then processed using FSL's fMRI Expert Analysis Tool (FEAT) that included brain extraction (Smith, 2002), MCFLIRT motion correction (6-parameter affine transformation) (Jenkinson et al., 2002), spatial smoothing (full-width at half-maximum = 3 mm), high-pass temporal filtering (Gaussian-weighted least-squares straight line fitting with $\sigma = 100$ s), and registration (12 DOF linear affine transformation in FLIRT and nonlinear registration in FNIRT) to the standard F99 macaque template (Van Essen, 2004). Temporal signal-to-noise ratio (tSNR) maps were calculated by dividing the mean and standard deviation for each resting-state functional run without spatial smoothing or registration. Figure 3.1 shows the coronal slices for each time point per monkey. There was no signal dropout related to the acrylic head post.

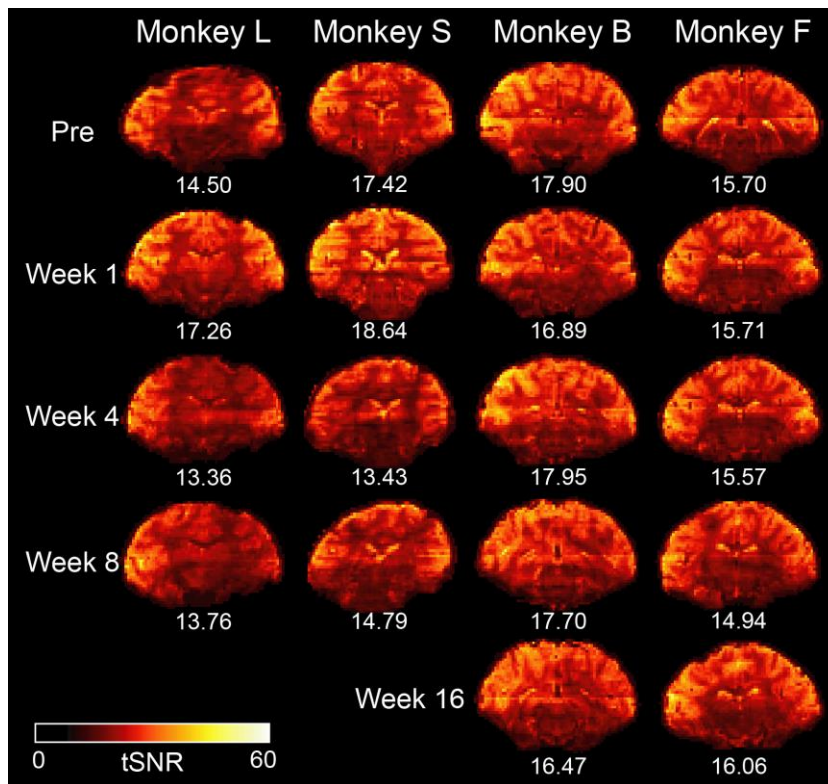


Figure 3.1. Temporal SNR maps for each resting-state fMRI session.

Coronal slices are shown at a level that corresponds to the location of the acrylic head post. The colour bar represents tSNR values and the mean tSNR for each time point are shown below each slice. Abbreviations: L = left, R = right, tSNR = temporal signal-to-noise ratio.

3.2.8. Lesion volume analysis

Automated tissue-type segmentation was performed on each animal's T1-weighted MP2RAGE anatomical image acquired one week post-lesion using FMRIB's Automated Segmentation Tool (FAST) (Zhang et al., 2001). We opted to use the T1 MP2RAGE images because they had higher overall resolution (0.5 mm isotropic) than the T2 images (1 mm resolution in the Z-plane), providing increased accuracy when determining the extent of the lesion. The T1 MP2RAGE sequence provides a higher tissue contrast between gray matter, white matter, and cerebrospinal fluid than traditional T1 MPRAGE and T2-weighted images and is thus more superior for tissue segmentation methods (Marques et al., 2010). We set the number of classes to be segmented to four: grey matter, white matter, cerebrospinal fluid, and lesioned tissue. Segmented masks representing lesioned tissue captured areas of hypointensity on the T1-weighted image and hyperintensity from the T2-weighted image acquired in the same session. Segmented lesion masks were not manually edited. Segmented T1-weighted lesion masks were then transformed to the standard F99 space using the transformation matrix from the co-registered T1-weighted image. Lesion volumes were determined using the lesion masks in standard F99 space (0.5 mm isotropic resolution) using the MRIcron Toolbox (<http://www.cabiatl.com/mricro/mricron/index.html>). We projected lesion masks onto the macaque F99 template brain using MRIcron and CARET (<http://www.nitrc.org/projects/caret>) and identified lesioned brain areas based on the cytoarchitectonic subdivisions from the Paxinos et al. (2000) rhesus monkey brain atlas (Paxinos et al., 2000).

3.2.9. Resting-state fMRI analysis

Frontoparietal network construction

A network is defined as a group of nodes and the edges between each pair of nodes (Rubinov and Sporns, 2010). Here, nodes represent brain areas and edges represent the statistical correlation in the BOLD time series between each pair of brain regions (i.e., FC), where edge weight refers to correlation strength. The primary interest of this study was to investigate the longitudinal changes in FC of the frontoparietal network during recovery of contralesional target selection deficits. We selected frontoparietal network regions-of-interest (ROIs) based on previously identified frontoparietal areas from fMRI studies in macaque monkeys (Vincent et al., 2007; Hutchison et al., 2011; Patel et al., 2015). Hutchison et al. (2011) found a resting-state frontoparietal network using an independent component analysis that included bilateral connectivity in the frontal eye fields and both banks of the intraparietal sulcus. Vincent et al. (2007) also localized a macaque frontoparietal network from a resting-state analysis which included correlations in the anterior arcuate sulcus and caudal principal sulcus (caudal PFC), both banks of the intraparietal sulcus, and the middle temporal area (MT) and medial superior temporal area (MST). Patel et al. (2015) identified the frontoparietal network from the BOLD activations during a visual attention task in monkeys, which included the LIP, FEF, and dorsolateral PFC. We used the stereotaxic macaque monkey atlas (Saleem and Logothetis, 2012) to localize all previously identified frontoparietal areas based on this anatomical parcellation. We defined 12 frontoparietal ROIs (see Table 3.1) in the four monkeys in our study using those anatomical landmarks and cross-referencing each ROI from the atlas with each monkey's T1 and T2 anatomical MRI. We created spherical seeds (radius = 2 mm) for each frontoparietal ROI and additionally created masks within

white matter and cerebrospinal fluid (CSF) to be used as covariates of no interest. White matter masks included three major areas: 1) corpus callosum, 2) bilaterally in tissue medioposterior to the dorsal premotor cortex, and 3) bilaterally medioposterior to somatosensory cortex. CSF masks included the lateral ventricle and third ventricle bilaterally. There was no overlap between the white matter masks, CSF masks, and the frontoparietal ROIs. We extracted the mean BOLD signal time series across all voxels within each frontoparietal ROI and computed Pearson's r correlation coefficients between the mean BOLD time series of every ROI pair, while controlling for the time series obtained from white matter and CSF. We then applied the Fisher's r -to- z transformation to convert the correlation coefficients into z-scores, where z-scores denote the FC between node pairs. This procedure was repeated for each pre-lesion and post-lesion functional run, which resulted in 4 pre-lesion FC matrices and 4-6 FC matrices for each post-lesion session (week 1, 4, 8, 16) per monkey.

Table 3.1. List of the cortical structures included as regions of interest in the frontoparietal network.

Abbreviation	Structure Name	Left			Right		
		x	y	z	x	y	z
9/46D	area 9/46 of cortex, dorsal part	16	18	15	-10	18	15
FEF	frontal eye field	17	7	15	-14	7	15
PE	parietal area PE (subdivision of superior parietal lobule)	16	-19	22	-11	-19	22
PEa	parietal area PEa (MIP) (subdivision of superior parietal lobule)	11	-20	18	-7	-20	18
PEC	parietal area PE, caudal part (subdivision of superior parietal lobule)	7	-27	23	-4	-27	24
PF	parietal area PF (subdivision of inferior parietal lobule, rostral)	21	-23	20	-17	-23	19
PFG	parietal area PFG (subdivision of inferior parietal lobule, rostral)	24	-17	18	-21	-14	17
POa	parietal area POa (LIP)	20	-16	15	-15	-16	16
POaE	parietal area POa, external part (LIPe)	16	-24	20	-12	-24	20
POaI	parietal area POa, internal part (LIPi)	14	-21	16	-10	-21	16
PPt	posterior parietal area	14	-28	19	-10	-28	19
MT/MST	middle temporal/medial superior temporal area	18	-24	11	-14	-24	11

Coordinates are in standard macaque F99 space.

Pairwise functional connectivity analysis of the frontoparietal network

We averaged across the 4-8 non-thresholded, fully weighted FC matrices for each session per animal, which resulted in one averaged matrix for each session: pre-lesion A, pre-lesion B, week 1, 4, 8, and 16 post-lesion. Note that only Monkeys B and F have a week 16 time point. First, we tested whether resting-state FC of the frontoparietal network significantly changed throughout post-lesion recovery. We statistically compared the absolute FC (|z-scores|) using two-sample t-tests with FDR correction for multiple comparisons ($p < 0.05$) from (1) pre-lesion to week 1 post-lesion, (2) week 1 to week 8 for Monkeys L and S or to week 16 post-lesion for Monkeys B and F, and (3) pre-lesion to week 8 for Monkeys L and S or to week 16 post-lesion for Monkeys B and F. Increased absolute FC was defined as either (1) a positive correlation that became more positive or (2) a negative correlation that became more negative. Decreased absolute FC was defined as either (1) a positive correlation that became less positive or (2) a negative correlation that became less negative.

Correlations between functional connectivity and behaviour

We investigated whether the change in FC between any pair of nodes correlated with recovery of contralesional saccade choice. We performed a Pearson's correlation analysis between the FC strengths of each ROI pair with the proportion of contralesional saccade choice at each post-lesion time point. We acknowledge that the sample size for this correlation analysis within each monkey is very small with $N = 3$ variables for Monkeys L and S (FC and behavioural values at 3 time points: week 1, 4, and 8 post-lesion) and with $N = 4$ variables for Monkeys B and F (FC and behavioural values at 4 time points: week 1, 4, 8, and 16 post-lesion). Nonetheless, we were interested in whether any strong correlations existed between FC and behavioural recovery. Significance values were

corrected using the Benjamini and Hochberg (1995) procedure for controlling the false-discovery rate (FDR) for multiple comparisons (Benjamini and Hochberg, 1995).

Functional connections that correlated with the proportion of contralesional saccade choices were visualized using BrainNet Viewer (Xia, Wang, and He, 2013; <https://www.nitrc.org/projects/bnv/>).

Graph theoretical analysis of degree centrality in the frontoparietal network

Graph theory was used to analyze changes in degree centrality using the graph theoretical network analysis (GRETNA) toolbox (Wang et al., 2015). Degree centrality is a measure of the number of edges connected to a given node (i.e., the number of brain areas functionally connected to the node), which reflects its communication ability within the functional network (Fornito et al., 2016). We used a sparsity-based threshold instead of an absolute threshold because it outputs normalized matrices with the same number of edges across networks (pre-lesion vs. post-lesion) which minimizes confounds relating to differences in overall correlation strengths between networks (Fornito et al., 2016; Lv et al., 2015). We used a wide threshold level range (sparsity: 0.05 – 0.5, with 0.05 intervals) and then calculated the area under the curve (AUC) for each metric across the sparsity range to avoid arbitrariness in thresholding (Achard and Bullmore, 2007; Itahashi et al., 2014; Zhang et al., 2011). Negative correlations were ignored in this study as suggested in (Rubinov and Sporns, 2010). The AUC of the nodal degree centrality was calculated for each monkey at each pre-lesion and post-lesion time point. Significant differences across time were evaluated using one-way ANOVAs with post-hoc Tukey's tests ($p < 0.05$).

Seed-based functional connectivity analysis

We used area 9/46D in the contralesional hemisphere as a seed region (2 mm radius) and extracted the mean BOLD signal time series across the seed voxels for each functional run per monkey. The general linear model was then implemented using FSL's FEAT (fMRI Expert Analysis Tool, <http://fsl.fmrib.ox.ac.uk/fsl/fslwiki/FEAT>) where the BOLD signal time course was used as a predictor in a multiple regression model for each individual functional run. We included the mean time series for white matter and cerebrospinal fluid as nuisance covariates in this model. At the individual subject level and for each time point, a fixed effects analysis was performed across all functional runs. Corrections for multiple comparisons were implemented at the cluster level with Gaussian random field theory with $z > 2.3$ and a cluster significance of $p < 0.05$. This within-subject, within-session analysis produced a contrast of parameter estimates (COPE) image for each time point that showed significant positive correlations across the whole brain with the seed region for each monkey. In a higher-level FEAT analysis using a fixed effects model, we performed a two-sample paired t-test to compare the pre-lesion COPE with each post-lesion COPE per monkey. This higher-level analysis produced a Z-statistic map with corrections for multiple comparisons determined at the cluster level by $Z > 2.3$ and a cluster significance of $p < 0.05$. Each monkey had a thresholded Z-statistic image showing significantly increased or decreased contralesional 9/46D FC for: pre-lesion to week 1, 4, 8, and 16 post-lesion. The volumetric z-statistic map was then projected to the macaque F99 cortical flat maps using the CARET enclosed-voxel method (Van Essen et al., 2001; <http://www.nitrc.org/projects/caret>).

3.3. Results

3.3.1. Intracortical injections of ET-1 induced lesions in the right caudal PFC

The following lesions have been described in a previously published paper (Adam et al., 2019). The lesion infarct volume was 0.43 cm³ for Monkey L, 0.51 cm³ for Monkey S, 1.28 cm³ for Monkey B, and 1.41 cm³ for Monkey F. Monkeys L and S were classified as having small lesions and Monkeys B and F as having larger lesions since the infarct volume was more than doubled. All four monkeys sustained lesions in the right caudal PFC with consistent lesions in area 8AD of the FEF (Fig. 3.2). Additionally, in Monkey L the lesion extended into area 8B and in Monkey S it extended into the dorsolateral PFC (areas 9/46D and 46D) and ventrolateral PFC (areas 44, 45B, 9/46V, 46V, and 47). Also in addition to area 8AD, the lesion in Monkey B extended into areas 8A, 8AV, 8B, 9/46 and dorsal premotor area 6D, and in Monkey F it extended into areas 8A, 8AV, 8B, 9/46, dorsolateral PFC (areas 9/46D, 46D), ventrolateral PFC (areas 45A, 45B, 9/46V, 46V) and into premotor areas 6D and 6V.

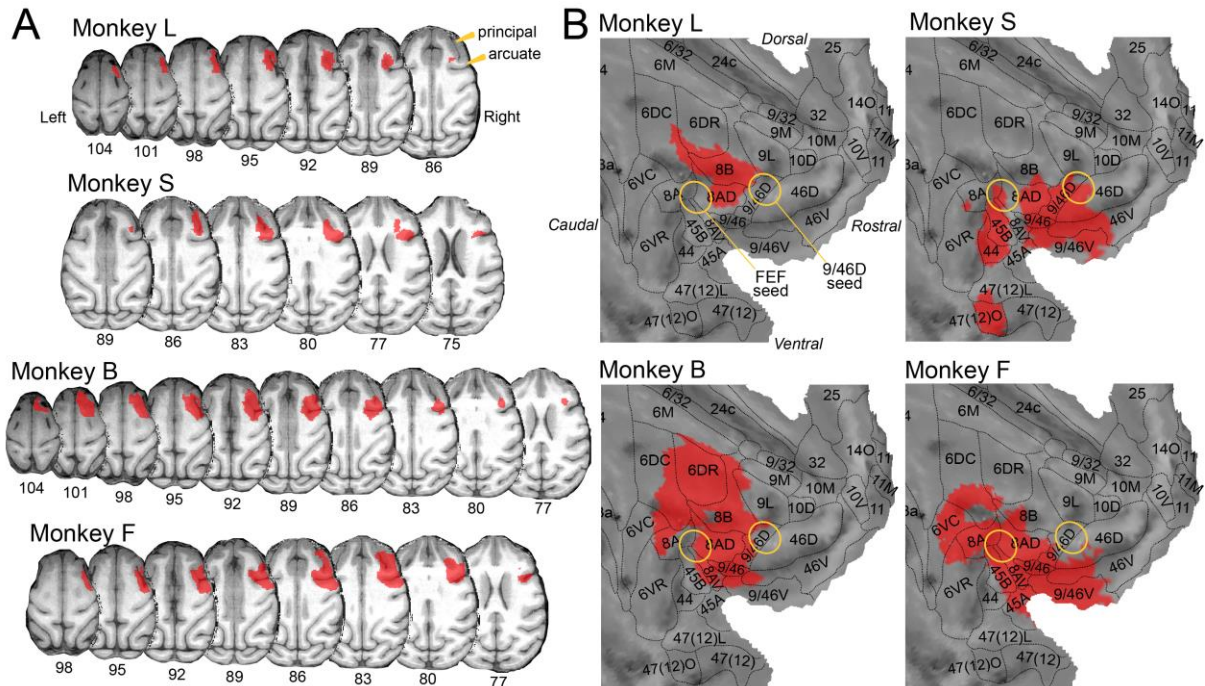


Figure 3.2. Reconstructed lesions superimposed on the macaque F99 template brain.

T1-weighted images obtained at week 1 post-lesion were segmented based on tissue type. Masks representing lesioned tissue were registered to standard F99 space and projected onto (A) axial slices of the macaque F99 template brain using MRIcron and (B) cortical flat map right hemisphere representations of the macaque F99 brain using CARET with surface outlines that we created based on the Paxinos et al. (2000) macaque cortical parcellation scheme. The network node placement for the right FEF and area 9/46D are shown as yellow outlines. Abbreviations: principal = principal sulcus; arcuate = arcuate sulcus, L = left hemisphere, R = right hemisphere, A = anterior, P = posterior, D = dorsal, V = ventral, small = small lesion, large = large lesion, FEF = frontal eye field, DLPFC = dorsolateral prefrontal cortex, VLPFC = ventrolateral prefrontal cortex, PMd = dorsal premotor cortex, PMv = ventral premotor cortex.

3.3.2. Unilateral caudal PFC lesions induced contralesional target selection deficits that recovered by 2-4 months

Monkeys performed the free-choice saccade task before and after the experimental lesion in the right caudal PFC (Fig. 3.3A). Neglect-like impairments in directing a saccade to a single contralesional stimulus were transient and recovered by 4 weeks post-lesion in Monkeys L, B, and F (Fig. 3.3B). In Monkey S, the deficit took longer to recover at 8 weeks post-lesion, which was likely due to the absence of true single stimulus trials in this monkey (see Methods). Contralesional target selection deficits were assessed using the point of equal selection (Fig. 3.3C) and the proportion of contralesional saccade choices (Fig. 3.3D) as measured on the free-choice double stimulus task. One-way ANOVAs revealed significant differences in the point of equal selection across time in all four animals (Monkey L: $F(3, 19) = 19.62$, $p = 4.83 \times 10^{-6}$; Monkey S: $F(3, 23) = 24.95$, $p = 2.05 \times 10^{-7}$; Monkey B: $F(4, 40) = 47.56$, $p = 1.10 \times 10^{-14}$; Monkey F: $F(4, 24) = 27.12$, $p = 1.36 \times 10^{-8}$). Tukey's post-hoc tests revealed significant rightward shifts in the point of equal selection ($p < 0.05$) from pre-lesion to week 1-2 post-lesion for all four animals (Monkey L: 115 ms shift; Monkey S: 163 ms shift; Monkey B: 223 ms shift; Monkey F: 386 ms shift). The point of equal selection then gradually returned to pre-lesion baseline performance and stabilized without further improvement in performance by week 8 in Monkey L and Monkey S and by week 16 in Monkey B and Monkey F.

As for the proportion of contralesional saccade choice, one-way ANOVAs also revealed significant differences across time in all four animals (Monkey L: $F(3, 19) = 14.45$, $p = 3.85 \times 10^{-5}$; Monkey S: $F(3, 23) = 12.01$, $p = 6.19 \times 10^{-5}$; Monkey B: $F(4, 41) = 13.37$, $p = 4.64 \times 10^{-7}$; Monkey F: $F(4, 24) = 6.26$, $p = 0.0013$). Before the lesion was induced, the proportion of contralesional saccade choices was near 0.50 for all animals (Monkey L: 0.43; Monkey S: 0.44; Monkey B: 0.63; Monkey F: 0.50), indicating a roughly equal

proportion of saccades made to the contralesional and ipsilesional stimulus when presented simultaneously. Tukey's post-hoc tests revealed a significant decrease in contralesional saccade choice ($p < 0.05$) from pre-lesion to week 1-2 post-lesion for all four animals [Monkey L: 0.06 ($p < 0.0001$); Monkey S: 0.06 ($p = 0.0002$); Monkey B: 0.17 ($p < 0.0001$); Monkey F: 0.12 ($p = 0.0026$)]. At week 4 post-lesion, contralesional saccade choice was still less than the proportion at pre-lesion for all animals, but this effect was not significant for Monkey L [Monkey L: 0.22 ($p = 0.051$); Monkey S: 0.03 ($p = 0.0008$); Monkey B: 0.28 ($p = 0.0156$); Monkey F: 0.13 ($p = 0.0047$)]. Overall, the proportion of contralesional saccade choice gradually recovered until no further improvement by week 8 for Monkeys L and S and by week 16 for Monkeys B and F (Fig. 3.3D). Behavioural performance on this task has been described in full previously (Adam et al., 2019). In sum, an experimental lesion in the right caudal PFC led to contralesional target selection deficits that gradually recovered over 2-4 months post-lesion.

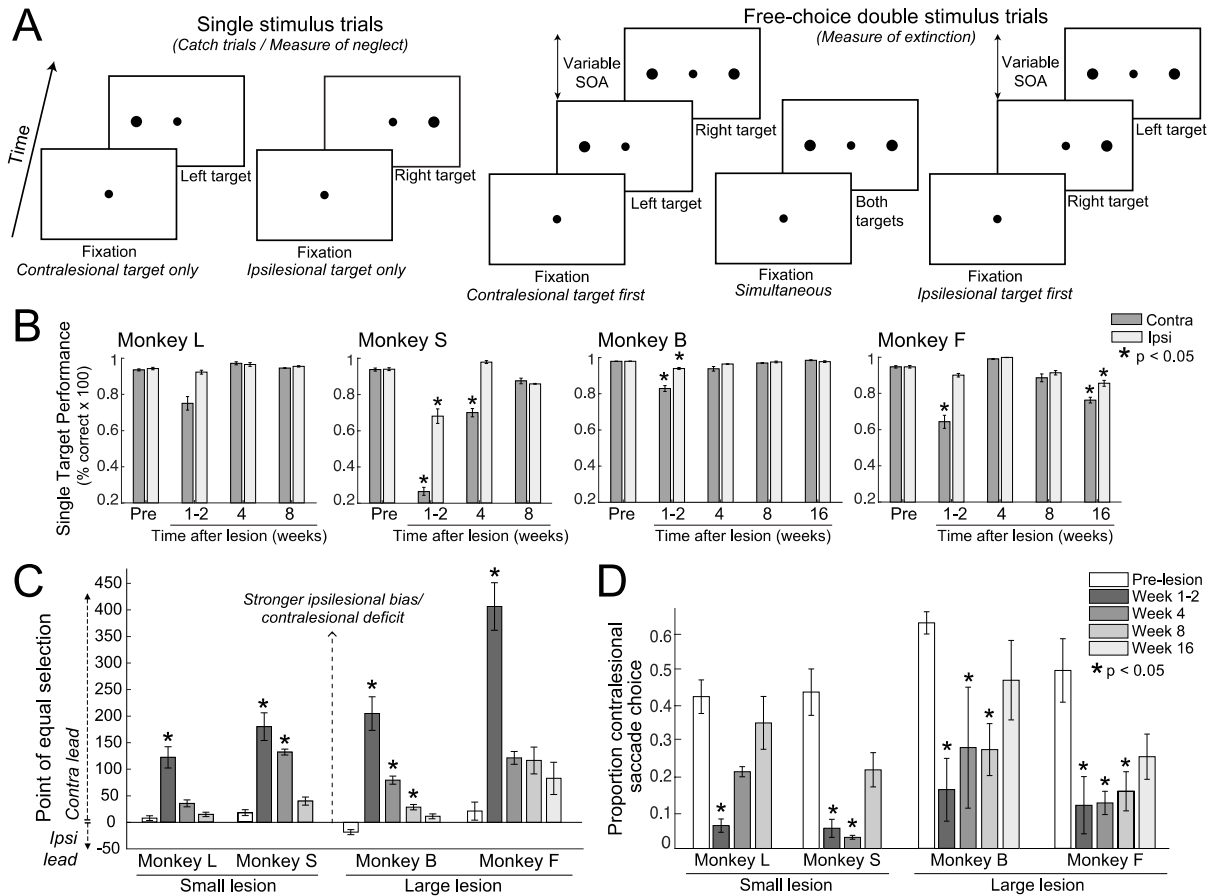


Figure 3.3. Contralateral saccade choice deficit and gradual recovery on the free-choice saccade task.

(A) Behavioural task. Each trial began with the presentation of a fixation point, followed by either one stimulus in the left or right hemifield (single stimulus trials) or two stimuli, with one in the left and one in the right hemifield (double stimulus trials) presented at a variable stimulus onset asynchrony (SOA). SOA is the variable time delay between presentation of the left and right stimulus on double stimulus trials. (B) Saccade performance on single stimulus trials. We calculated the proportion of correct contralateral/ipsilateral saccades made on single stimulus trials. Trials with an SOA value of $|256|$ ms were used as single stimulus trials for Monkey S (see Section 2.5). (C) Recovery of the point of equal selection on the free-choice double stimulus trials. The point of equal selection is the temporal delay between presentation of the left and right stimuli at which an equal proportion of saccades were made to both stimuli. Positive y-axis values indicate that the point of equal selection was reached at a temporal delay in which the contralateral (left) stimulus was presented before the ipsilateral (right) stimulus; negative y-axis values indicate a temporal delay in which the ipsilateral

stimulus was presented first. (D) Recovery of the contralesional saccade choice deficit on simultaneous trials before and after a right caudal PFC lesion. We plotted the proportion of saccades made to the contralesional stimulus on trials with simultaneous presentation of both stimuli for each monkey. Statistical comparisons between pre-lesion and post-lesion time points were made using one-way ANOVAs with post-hoc Tukey's tests ($p < 0.05$). Error bars represent standard error of the mean across sessions within each time point. Grayscale bars in the legend refer to each time point, with 'weeks' indicating the duration of time following the lesion.

3.3.3. *Pairwise FC changes of the frontoparietal network after a right caudal PFC lesion*

RsfMRI data were collected before the right caudal PFC lesion and at several time points during functional recovery at weeks 1, 4, 8, and 16 post-lesion. Here, we examined the changes in FC of the frontoparietal network from pre-lesion and throughout post-lesion recovery. We subtracted the absolute FC values ($|z\text{-scores}|$) for each node pair for the following comparisons: (1) pre-lesion to week 1, (2) week 1 to week 8 (or to week 16 for Monkeys B and F), and (3) pre-lesion to week 8 (or to week 16 for Monkeys B and F). We measured the effect sizes using Hedge's g and found that all significant pairwise FC changes shown in Figure 3.4 have a minimum effect size of $g = 1.2$, considered a large effect (Hedges, 1981). Figure 3.4A shows the significant changes in pairwise FC from pre-lesion to week 1 post-lesion (two-sample t-test, $p < 0.05$, FDR corrected). We found that the two small lesion monkeys (Monkeys L and S) showed an increase in network-wide FC one week after a right caudal PFC lesion (Fig. 3.4A, left). Of the two large lesion monkeys, Monkey B showed changes in only a few network nodes, whereas Monkey F showed substantially decreased network FC one week following the lesion (Fig. 3.4A, right).

Recall that contralesional target selection deficits improved from week 1 to week 8/week 16 post-lesion (see Fig. 3.3C,D). When comparing FC changes throughout behavioural recovery in the two small lesion monkeys (Monkeys L and S), we found that FC substantially decreased from week 1 to week 8 (Fig. 3.4B, top row, lower triangles). There were fewer significant changes in FC between pre-lesion and week 8 post-lesion in Monkeys L and S (Fig. 3.4B, top row, upper triangles). Notably, Monkey S had significantly increased FC of the contralesional (left) prefrontal area 9/46D with the frontoparietal network across both time point comparisons. Altogether, it appears that the

network-wide FC in Monkeys L and S (small lesion) initially increased one week after the lesion (Fig. 3.4A, left), and then decreased throughout recovery (Fig. 3.4B, top row, lower triangles) approaching pre-lesion baseline (Fig. 3.4B, top row, upper triangles).

In the two monkeys with a larger lesion (Monkeys B and F), we conversely found substantially increased pairwise FC from weeks 1 to 16 post-lesion (Fig. 3.4B, bottom row, lower triangles). Compared to pre-lesion, pairwise FC remained increased at week 16 post-lesion in Monkeys B and F, but Monkey F also had strongly decreased FC in the right FEF. Overall, following a larger lesion, it appears that network FC initially decreased (in Monkey F; Fig. 3.4A, right), and then increased throughout behavioural recovery (Fig. 3.4B, bottom row). In sum, in the two animals with a small lesion (Monkeys L and S), the FC between areas of the frontoparietal network initially increased and then decreased back to baseline during the time that the contralesional target selection deficit was improving following the lesion. However, in the two animals with a larger lesion (Monkeys B and F), FC increased throughout post-lesion recovery of contralesional target selection, with lasting changes to the functional network when compared to pre-lesion.

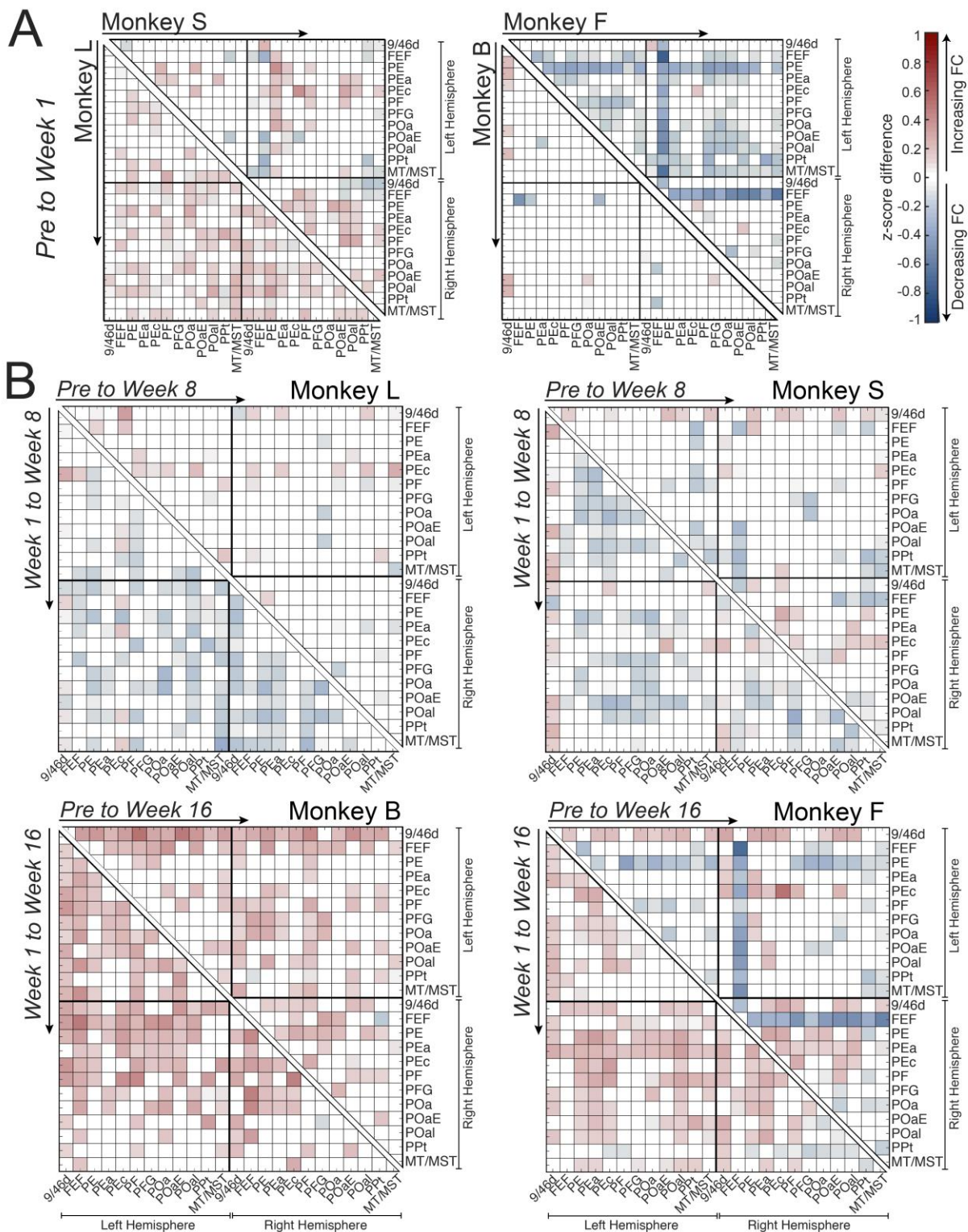


Figure 3.4. Pairwise functional connectivity changes of the frontoparietal network across time.

(A) FC changes from pre-lesion to week 1 post-lesion. Changes in the two small lesion monkeys are shown on the left, with Monkey L in the lower triangle and Monkey S in the upper triangle. Changes in the large lesion monkeys are shown on the right, with Monkey B in the lower triangle and Monkey F in the upper triangle. (B) FC changes from week 1 to week 8/16 post-lesion (lower triangles) and from pre-lesion to week 8/16 post-lesion (upper triangles). FC changes are represented as a difference in the absolute Fisher's z-transformed Pearson's correlation coefficient (i.e., |z-scores|) between two time points. Statistical differences were calculated using two-sample t-tests with FDR correction for multiple comparisons across all pair-wise correlations ($p < 0.05$). Red cells indicate a significant increase and blue cells indicate a significant decrease in FC. Non-significant changes are shown as white cells. The colour bar indicates the strength of change in FC. Abbreviations: FC = FC; pre = pre-lesion; week = week post-lesion.

3.3.4. Frontoparietal FC changes that correlate with the recovery of contralesional target selection

Next, we tested whether longitudinal FC changes from week 1 to week 8 or week 16 post-lesion correlated with improvements in contralesional target selection (i.e., an increasing proportion of contralesional saccade choice on double stimulus trials). We acknowledge the small sample size for this correlation analysis: Monkeys L and S only had three data points for each of the FC and behavioural values (week 1, 4, and 8 post-lesion); Monkeys B and F had four values (week 1, 4, 8, and 16 post-lesion). Pearson's correlation analysis revealed significant correlations ($p < 0.05$, FDR corrected) in Monkeys B and F, but not for Monkeys L and S (Fig. 3.5B). Since Monkeys L and S only had three data points in the correlation analysis, significance was not reached; however, the correlations were very strong. We show edges between nodes that represent these very strong correlations ($-0.95 > \text{Pearson's } r > 0.95$) between FC and behavioural performance for Monkeys L and S (Fig. 3.5B). Across all four monkeys, we found a strong positive correlation (Pearson's $r > 0.95$) between behavioural recovery and increasing FC of the contralesional prefrontal area 9/46D–ipsilesional parietal area PE (Fig. 3.5B). In other words, as the monkeys selected a higher proportion of contralesional targets throughout the weeks post-lesion, the FC between contralesional prefrontal area 9/46D and ipsilesional parietal area PE was also increasing at the same time points.

We also noted differences in FC-behaviour correlations based on lesion size. In both monkeys with a small lesion (Monkeys L and S), recovery of contralesional target selection correlated with decreasing FC between bilateral parietal areas that was absent in the large lesion monkeys. However, in Monkey L there was one positive FC-behaviour correlation between two parietal areas: contralesional area PEC and ipsilesional area PE. Monkey S also had some positive FC-behaviour correlations in bilateral parietal areas,

mostly with ipsilesional parietal area PEC. Those negative correlations involving bilateral parietal areas were not observed in Monkeys B and F; rather, these monkeys showed several positive FC-behaviour correlations involving bilateral parietal areas. Additionally, Monkeys B and F showed significant positive correlations between contralesional prefrontal FC and behavioural recovery. We also observed that the contralesional FEF in Monkey S (small lesion) showed increased FC with the perilesional dorsolateral PFC; whereas the contralesional FEF in Monkeys B and F (large lesion) showed increased FC with the parietal cortex during recovery. The location of the ipsilesional area 9/46D node was slightly affected by the lesion in Monkey S, but in perilesional cortex just outside the border of the lesion site for Monkeys L, B, and F. The ipsilesional FEF node was fully damaged in Monkeys B and F, but only slightly affected by the lesion in Monkeys L and S (see Fig. 3.2B).

Since FC between contralesional 9/46D and ipsilesional PE strongly positively correlated with the increasing proportion of contralesional saccade choices from weeks 1 to 8/16 across all four monkeys, we further examined how the contralesional 9/46D–ipsilesional PE FC changed over time. Statistical comparisons were made within subjects using one-way ANOVAs with post-hoc Tukey's tests ($p < 0.05$) to compare values between each pair of time points. We found that across all four monkeys, the contralesional 9/46D–ipsilesional PE FC slightly increased from pre-lesion to week 1 post-lesion, albeit not significantly (Fig. 3.5C). FC continued to gradually increase over time, reaching significance at week 4 post-lesion in Monkey S and Monkey F ($p < 0.05$), and by week 8 post-lesion in Monkey B. FC remained significantly greater than pre-lesion baseline in Monkeys S, B, and F at the time of behavioural recovery (week or 16), however this effect was only a trend in Monkey L.

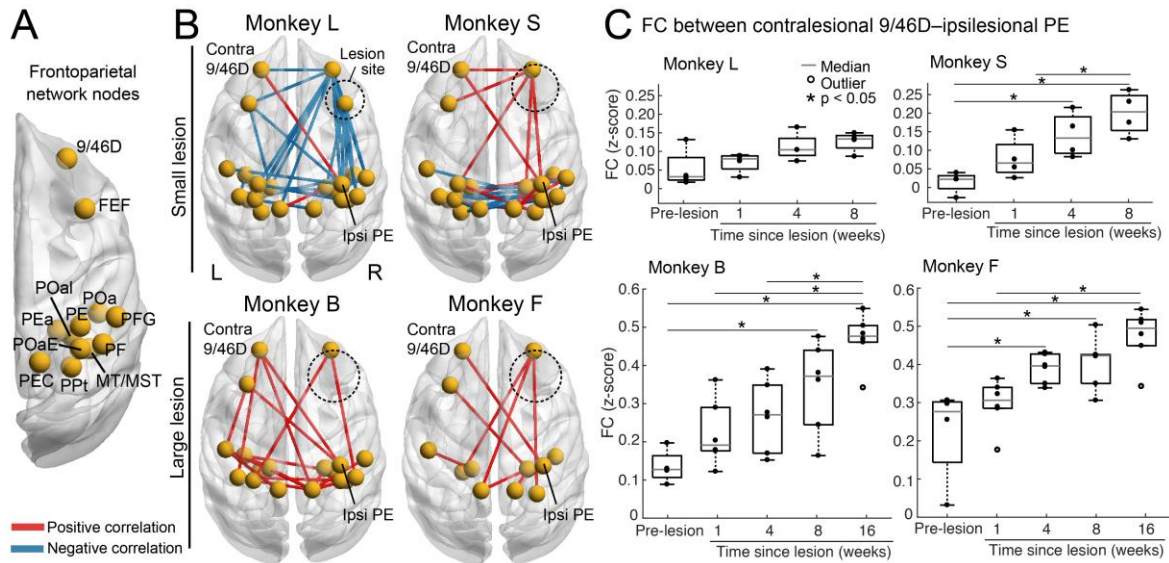


Figure 3.5. Functional connections that correlated with the recovery of contralesional saccade choice following a right caudal PFC lesion.

(A) Frontoparietal network nodes. We defined 24 bilateral regions-of-interest as the frontoparietal network (see Table 3.1 for abbreviations). (B) Significant correlations between pairwise FC and the proportion of contralesional saccade choice at each post-lesion time point. Correlations were assessed using a Pearson's correlation analysis with FDR correction of the significance values for multiple comparisons. Red lines indicate a positive correlation, such that increasing FC between those two nodes correlated with an increasing proportion of contralesional saccade choice over time. Blue lines indicate a negative correlation, such that decreasing FC between those two nodes correlated with an increasing contralesional choice over time. The rough lesion site is circled in black. (C) FC changes between contralesional area 9/46D and ipsilesional area PE over time. Note that the y-axis for Monkeys L and S is smaller than that for Monkeys B and F. Gray lines within each box indicate the median, the bottom and top edges of the box indicate the 25th and 75th percentiles, respectively, and the whiskers extend to the most extreme data points that are not considered outliers. Statistical comparisons were made within subjects using one-way ANOVAs with post-hoc Tukey's tests ($p < 0.05$) to compare values between each pair of time points. Abbreviations: L = left hemisphere; R = right hemisphere; contra = contralesional; ipsi = ipsilesional, FC = functional connectivity.

3.3.5. *Changes in regional node properties of the frontoparietal network from pre-lesion to post-lesion*

We investigated changes in the degree centrality of each node (i.e., ROI) within the frontoparietal network from pre-lesion to week 8 or 16 post-lesion using a graph theoretical approach. Degree centrality represents the number of connections that a given node maintains within the network (Fig. 3.6A). One-way ANOVAs revealed significant differences in degree centrality across time for contralesional (left) area 9/46D in all four monkeys [Monkey L: $F(3,12) = 17.21$, $p = 0.00012$; Monkey S: $F(3,12) = 15.97$, $p = 0.00017$; Monkey B: $F(4,23) = 6.79$, $p = 0.00092$; Monkey F: $F(4,23) = 14.53$, $p = 4.68 \times 10^{-4}$] (Fig. 3.6B). Tukey's post-hoc tests revealed significantly increased left 9/46D degree centrality from pre-lesion to week 8 post-lesion in the two small lesion monkeys (Monkey L: $p = 0.005$; Monkey S: $p = 0.0004$) or to week 16 post-lesion in the two large lesion monkeys (Monkey B: $p = 0.0005$; Monkey F: $p = 0.0001$). We found differences in the pattern of left 9/46D degree centrality changes over time based on lesion size. In the two small lesion monkeys (Monkeys L and S), degree decreased initially and then gradually increased, whereas in the large lesion monkeys (Monkeys B and F) degree increased at week 1 post-lesion and maintained that level over time (except for a brief decrease in degree at week 4 post-lesion in Monkey F). In sum, we found that the contralesional prefrontal area 9/46D demonstrated increased degree centrality within the frontoparietal network at the time of behavioural recovery compared to pre-lesion, suggesting that this area has increased its communicability within the network. Although there were no other nodes with changes in degree centrality that were consistent across monkeys, there were still several nodes that showed significant changes within each monkey. In Monkey L, increased degree was found in two contralesional (left 9/46D, PEc) and one ipsilesional node (right FEF); decreased degree was found in one

ipsilesional node (right PFG). In Monkey S, we found increased degree in one contralesional (left 9/46D) and two ipsilesional nodes (right PE, PEc); decreased degree was found in three contralesional (left PF, PFG, Opt) and one ipsilesional node (right FEF). In Monkey B, we only found increased degree in one contralesional node (left 9/46D). In Monkey F, increased degree was found in three contralesional (left 9/46D, PEa, PEc) and four ipsilesional nodes (right 9/46D, PE, PEa, PEc); decreased degree was found in two contralesional (left FEF, PE) and one ipsilesional node (right FEF).

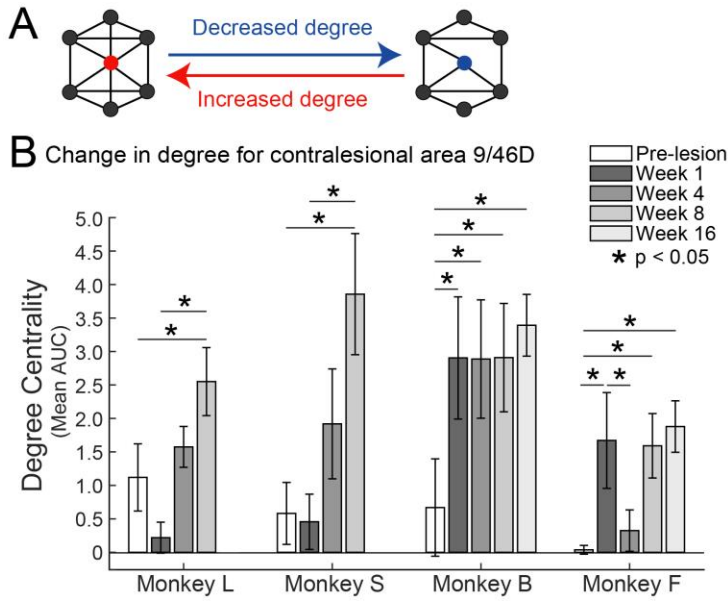


Figure 3.6. Degree centrality for contralesional dorsolateral PFC.

(A) Network schematic of increasing or decreasing degree centrality. The network on the left shows a red node with a high degree centrality, such that it is connected to every node in that network. The network on the right shows a blue node with a lower degree centrality in which it has lost some of those connections to other network nodes. The higher the degree of a given node, the more well-connected that node is within the network. (B) Changes in degree centrality of contralesional area 9/46D over time. All four monkeys showed significantly increased degree centrality of contralesional (left) area 9/46D from pre-lesion to the final post-lesion time point (week 8 or 16). Statistical comparisons between pre-lesion and post-lesion time points were made using one-way ANOVAs with post-hoc Tukey's tests ($p < 0.05$). Error bars denote standard error of the mean. Grayscale bars in the legend refer to each time point, with 'weeks' indicating the duration of time following the lesion. AUC = area under the curve.

3.3.6. Seed-based functional connectivity changes of contralesional area 9/46D

Since contralesional area 9/46D is located in the contralateral PFC that is homologous to the lesion site and showed increased degree centrality over time, we examined the longitudinal FC of contralesional 9/46D with the whole-brain using a seed-based analysis. We tested for changes in the contralesional 9/46D FC from pre-lesion to each post-lesion time point using two-sample paired t-tests (corrected cluster significance threshold: $p < 0.05$). In the two monkeys with a small lesion (Monkeys L and S), we found decreased FC of left dorsolateral PFC at week 1 post-lesion compared to pre-lesion across the entire brain, which decreased even further at week 4 and week 8 post-lesion (Fig. 3.7B, top half). In Monkey L, increased FC with left dorsolateral PFC was found in left orbitofrontal, ventral prefrontal, infero-temporal, and parieto-occipital areas and in right insular and superior parietal areas (Brodmann area 5 and 7), which gradually increased over weeks 4 and 8 post-lesion (Fig. 3.4B, top left). In Monkey S, dorsolateral PFC FC increased mostly with bilateral occipito-temporal and with small areas of parietal cortex (Fig. 3.7B, top right). Conversely in the two large lesion monkeys, there were no substantial decreases in FC from pre- to post-lesion. However, increased FC was found across the whole brain, but clustered around bilateral parietal cortex in Monkey B (Fig. 3.7B, bottom left) and left ventral prefrontal cortex and right parietal cortex in Monkey F (Fig. 3.7B, bottom right). Altogether, the contralesional dorsolateral PFC–whole brain FC mirror our earlier findings of decreasing network-wide FC in the two small lesion monkeys over time that was absent in the two large lesion monkeys. These findings are also in line with the pattern of changes in degree centrality of this seed region with the frontoparietal network (see Fig. 3.5B).

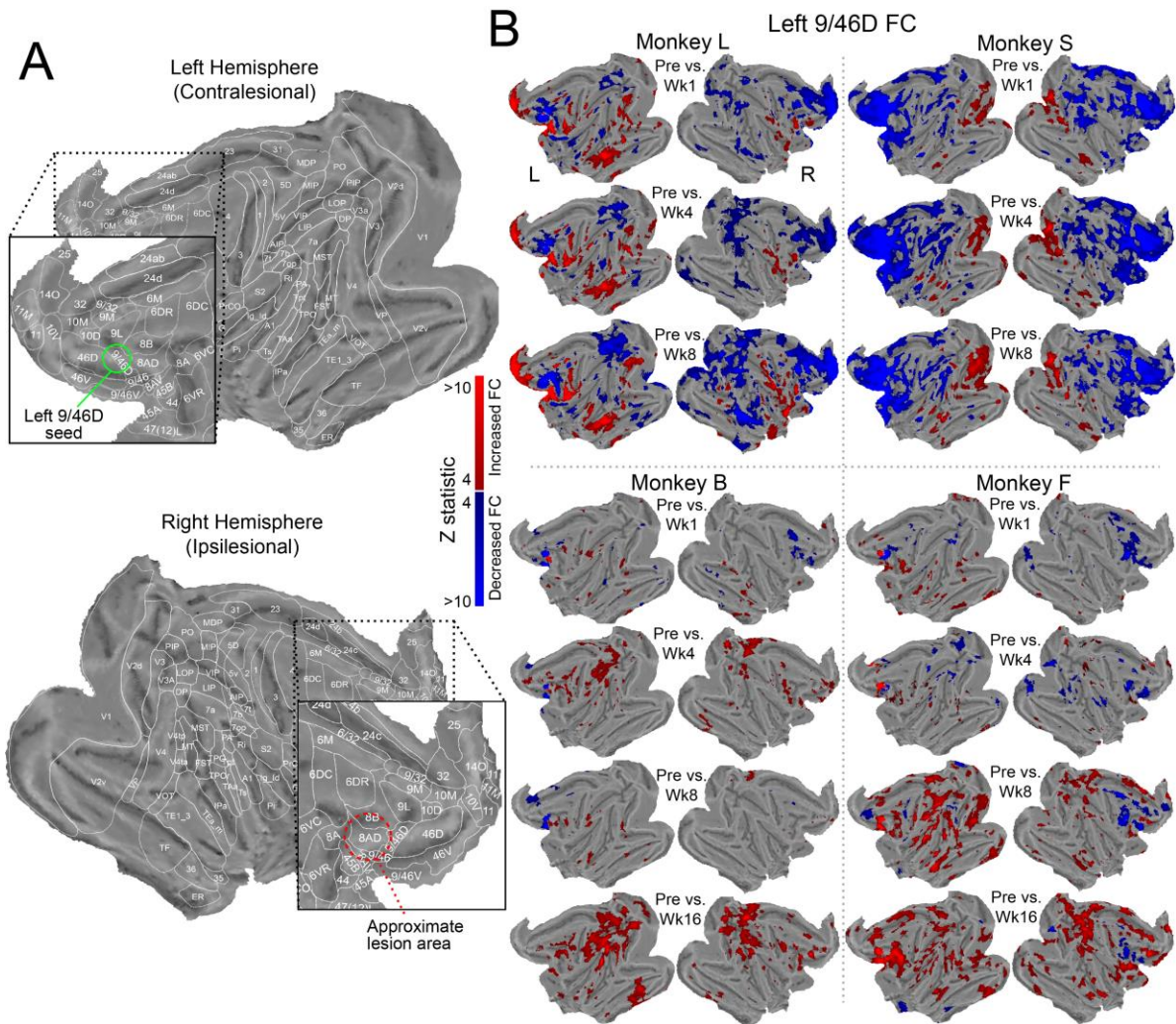


Figure 3.7. Changes in the whole-brain functional connectivity with contralesional dorsolateral PFC from pre-lesion to post-lesion.

(A) Flat map representations of the macaque F99 left and right hemispheres with surface outlines that we created based on the Paxinos et al. (2000) macaque cortical parcellation scheme. The left 9/46D seed region is outlined in green and the approximate lesion area is shown in red in the right hemisphere. (B) FC of the left dorsolateral PFC (area 9/46D) from pre-lesion to week 1, 4, 8, and 16. Z-statistic maps were thresholded according to the colour bar, with red showing significantly increased FC and blue showing a decreased FC.

3.4. Discussion

In the present study, we combined resting-state fMRI with the free-choice saccade task to investigate longitudinal changes in FC during recovery of contralesional target selection deficits after a unilateral caudal PFC lesion. We found a lesion size-dependent pattern of functional changes in the frontoparietal network over time. Pairwise frontoparietal FC acutely increased in the two small lesion monkeys, and then decreased back to pre-lesion baseline from week 1 to 8 post-lesion; conversely, network FC increased during recovery in the two large lesion monkeys. Within each monkey, we found that the FC between contralesional dorsolateral PFC (left 9/46D) and ipsilesional superior parietal lobule (right PE) strongly correlated with the proportion of contralesional target selection from week 1 to 8/16 post-lesion. Lastly, the contralesional dorsolateral PFC (left 9/46D) showed increased degree centrality with the frontoparietal network at the time of behavioural recovery (week 8 or 16) compared to pre-lesion across all four monkeys.

3.4.1. Recovery of contralesional target selection on a free-choice task

We found that a right caudal PFC lesion in macaque monkeys led to transient neglect-like deficits and longer lasting target selection deficits for contralesional stimuli. Neglect-like deficits were subtle and recovered within 4 weeks, whereas extinction-like deficits were more pronounced and took 8 weeks to recover in Monkeys L and S (small lesion) and 16 weeks to recover in Monkeys B and F (large lesion). However, Monkey S and Monkey F showed poor recovery of function, such that their behaviour plateaued at week 8 or 16 without full recovery (i.e., the proportion of contralesional saccade choice at week 8/week 16 post-lesion in both monkeys was much lower than pre-lesion baseline). We discuss these differences in the degree of behavioural recovery in terms of lesion

anatomy below (see Section 3.4.2). Previous studies in human stroke patients have also reported both neglect and extinction deficits acutely, with neglect recovering shortly after while extinction deficits were longer lasting (Bender and Furlow, 1945; Heilman et al., 2012, 1984; Milner and McIntosh, 2005; Robertson and Halligan, 1999). In monkeys, there are limited longitudinal studies that track post-lesion behavioural recovery since most monkey stroke models have used temporary inactivation methods (Hier et al., 1983; Johnston et al., 2016; Kubanek et al., 2015; McPeck and Keller, 2004; Wardak et al., 2002; Wilke et al., 2012). However, in one longitudinal monkey study following permanent unilateral FEF aspiration, the authors report a recovery profile similar to our findings (Rizzolatti et al., 1983). After the FEF lesion, they reported an absence of a response to a single food stimulus presented in the contralesional hemifield that recovered at two weeks post-lesion. However, the monkeys showed a lasting ipsilesional bias when presented with a food stimulus in either hemifield which recovered after eight weeks post-lesion.

Saccade performance on the single stimulus trials provided insight into the nature of the deficits in contralesional target selection on the double stimulus trials (i.e., whether the selection deficits were due to motor or perceptual impairments). In our previous report on the behavioural data alone (Adam et al., 2019), we showed that the contralesional errors on single stimulus trials were largely due to an absence of a saccade response when the contralesional stimulus was presented. These error types suggested that the target selection deficits reflected a contralesional perceptual impairment, rather than a motor impairment, since motor deficits would instead have resulted in inaccurate saccades that were still directed towards the contralesional stimulus. In other words, with a motor deficit we would have expected saccades to be directed towards the contralesional target, but with slower reaction times, reduced amplitude, slower peak velocity, or longer

duration, and for these metrics to co-occur with the target selection deficits. Instead, we showed that those contralesional saccade metrics returned to baseline well before the target selection deficits had recovered and thus could not completely account for the lasting contralesional target selection impairment (Adam et al., 2019).

In humans, visuospatial attention has been investigated using double stimulation paradigms similar to our free-choice saccade task, including the Posner spatial cueing task and the TOJ task. The Posner cueing task includes trials with valid or invalid cues, where a valid-cue trial is one in which the cue is presented in one of two peripheral boxes (either left or right of the fixation point) is followed by the target in that cued location. An invalidly cued trial is one in which a cue is presented in either peripheral box, but the subsequent target is presented in the opposite non-cued location. Participants must respond to the target location as quickly as possible. Patients with visual extinction show a “disengagement deficit” in which their responses on invalid trials are disproportionately slower when contralesional targets follow ipsilesional cues, compared to the opposite (Posner et al., 1982; Posner and Petersen, 1990). Posner and colleagues thus view extinction as a difficulty in disengaging attention from stimuli (cues) in the unaffected ipsilesional hemifield, which leads to impaired ability to attend to contralesional space. In a longitudinal study, Ramsey et al. (2016) used the Posner task to measure the severity of neglect in stroke patients and found severe visuospatial biases at 2 weeks post-stroke, with improvements over the first 12 weeks. They reported that the improvements then plateaued without completely reaching baseline performance and without further improvement one year later (Ramsey et al., 2016). Comparably, Farne et al. (2004) used a battery of paper-and-pencil neuropsychological tests to assess the recovery of visual extinction/neglect deficits in stroke patients and also reported initial contralesional visuospatial deficits that partially recovered over eight weeks post-stroke (Farne, 2004).

Although we used a free-choice task, the pattern of behavioural recovery we reported was similar to that of previous studies using different paradigms to measure neglect and extinction.

TOJ tasks are similar to the free-choice paradigm in that two stimuli are presented in rapid succession, with one on the left and one on the right side, with a variable delay between stimulus onsets (stimulus onset asynchrony, SOA) and randomized order of side of first-presented stimulus. Participants then report which stimulus was presented first using a verbal response (Baylis, 2002; Rorden et al., 2009, 1997) or saccade response (Ro et al., 2001). In a case study of a right hemisphere-lesioned patient, Di Pellegrino et al. (1997) used the TOJ task and showed that the patient was not only impaired at reporting the contralesional stimulus when it was presented with the ipsilesional stimulus, but also when the ipsilesional stimulus was presented within 300-400 ms before or after the contralesional stimulus. The authors suggest that visual extinction reflects more than just a disengagement deficit, since that would only explain the poor performance when the ipsilesional stimulus was presented first or simultaneously, not when it was presented second. The free-choice task we use in the present study is most comparable to the TOJ task, but also includes elements from the Posner task (e.g., fast response required). In the free-choice task, monkeys are rewarded for selecting either stimulus to ensure that they would continue performing the task after the lesion, especially when impaired at detecting the contralesional stimulus when it appeared first. Rewarding only correct judgements of temporal order would have been difficult for lesioned monkeys and likely resulted in a reduced number of completed trials. The free-choice task has been used to measure visuospatial target selection biases in monkeys after reversible inactivation (Johnston et al., 2016; Wardak et al., 2002; Wilke et al., 2012) and permanent lesions (Adam et al., 2019; Schiller and Chou, 1998) to frontoparietal areas. Similar to our

findings, Schiller and Chou (1998) showed a severe reduction in contralesional saccade choices on the free-choice task following FEF lesions in monkeys, with gradual improvements over 4 months that plateaued without reaching baseline.

3.4.2. Frontoparietal anatomical connectivity and functional models of visuospatial attention

Areas of the frontoparietal network are anatomically connected via the superior longitudinal fasciculus (SLF), a white matter pathway with three distinct branches identified in monkeys (Petrides and Pandya, 1984; Sani et al., 2019; Schmahmann et al., 2009, 2007) and in humans (Thiebaut de Schotten et al., 2012). In monkeys, SLF I connects dorsal frontal areas 6D and 9 with parietal areas PGm, PE, and PEc; SLF II connects areas 6DC, 6DR, 8AD, 9/46D, and 46D with parietal areas POa and PG; and SLF III connects ventral frontal areas 6V and 44 with parietal areas PF, POa, PFG, and PFop (Thiebaut de Schotten et al., 2012). It has been suggested that damage to the white matter pathways connecting frontal and parietal areas may be more crucial in the development of neglect than damage to those cortical areas alone (Bartolomeo, 2007; Bartolomeo et al., 2012, 2007). Bartolomeo et al. (2007) describe neglect as a “disconnection syndrome” and review the evidence linking the pathophysiology of neglect to SLF damage, specifically SLF II and III (Bartolomeo et al., 2012; Corbetta et al., 2005; Doricchi et al., 2008; Doricchi and Tomaiuolo, 2003; Gaffan and Hornak, 1997; Thiebaut de Schotten et al., 2005). In the present study, although each monkey sustained damage to the frontal areas of SLF II (areas 6DC, 6DR, 8AD, 9/46D, and 46D) to varying degrees (see Fig. 3.2B), only Monkey S and Monkey F sustained more ventral damage, affecting frontal portions of SLF III (area 44 in Monkey S and areas 6VR, 6VC in Monkey F). Interestingly, both Monkey S (small lesion) and Monkey F (large lesion)

showed stronger neglect-like deficits acutely and worse recovery of function (i.e., larger difference in behaviour between pre-lesion and final post-lesion time point) compared to the other two monkeys.

Monkeys S and F also showed more damage in ventral PFC areas 9/46V and 45, which are connected to temporoparietal areas IPa and TPO via the extreme capsule (Petrides and Pandya, 1984; Schmahmann et al., 2007). The extreme capsule is a white matter bundle that connects ventral PFC and temporoparietal areas and is increasingly being considered important for visuospatial processing and attention in monkeys (Bogadhi et al., 2018; Kagan et al., 2010; Sani et al., 2019; Wilke et al., 2012) and humans (Umarova et al., 2010). Altogether, the view that neglect manifests from damage to white matter pathways is interesting in the context of our finding that Monkeys S and F may have sustained more damage to the frontal portions of SLF III and extreme capsule and also showed a stronger initial neglect-like deficit with worse behavioural recovery.

It is worthwhile to mention the differences in hemispheric lateralization and contralateral organization for visuospatial processing between humans and monkeys (Kagan et al., 2010). Visuospatial functions of the frontoparietal network are strongly right hemisphere-lateralized in humans (Gazzaniga, 2000), as demonstrated by the observation that neglect and extinction deficits are more commonly seen following right hemisphere damage (Corbetta and Shulman, 2011; Heilman et al., 1984; Karnath and Rorden, 2012; Thiebaut De Schotten et al., 2011). In monkeys, visuospatial functions are less lateralized, with lesions to either hemisphere producing comparable contralateral deficits (Gaffan and Hornak, 1997). Conversely, responses to visual stimuli within these frontoparietal areas are strongly contralateral in monkeys (Barash et al., 1991; Funahashi et al., 1989), but less contralaterally-tuned in humans (Schluppeck et al., 2006; Srimal and Curtis, 2008). These interspecies differences may explain the observation that monkeys with

frontoparietal lesions do not often show severe and lasting neglect-like deficits (Gaffan and Hornak, 1997; Lynch and McLaren, 1989; Wardak et al., 2004, 2002; Wilke et al., 2012). A more symmetrical functional organization in monkeys might allow for faster recovery of lateralized impairment after unilateral damage.

3.4.3. Patterns of functional network reorganization differ based on lesion size

We found that the longitudinal pattern of frontoparietal FC changes differed between monkeys based on lesion size, such that network FC decreased back to baseline in Monkeys L and S (small lesion) from week 1 to 8 post-lesion, whereas FC substantially increased in Monkeys B and F (large lesion) from week 1 to 16 post-lesion. These findings are in line with previous studies of stroke patients and animal lesion models showing that the patterns of cortical reorganization that mediated post-stroke recovery largely depended on initial lesion size (Biernaskie et al., 2005; Grafman, 2000; Grefkes and Ward, 2014; Van Hees et al., 2014; van Meer et al., 2012; Zhu et al., 2014). In animal models of motor stroke, larger lesions of the primary motor cortex have been associated with greater recruitment of the contralesional premotor cortex during paretic forelimb recovery in rats (Touvykine et al., 2016) and larger post-lesion representations of the paretic hand in distant cortical areas in squirrel monkeys (Frost, 2003). Biernaskie et al. (2005) examined the degree of compensatory reorganization in rats with small or large motor cortex lesions after 4 weeks of rehabilitation with improved motor performance. When the authors temporarily inactivated the contralesional motor cortex, only the rats with large lesions showed a return of the initial motor deficits (Biernaskie et al., 2005). This suggests that the rats with smaller lesions did not rely on compensatory reorganization in distant/intact areas of the affected network to the same degree as large

lesion rats. Those findings support our results regarding the increased network-wide FC in large lesion monkeys, but a return to baseline FC in monkeys with smaller lesions.

Theoretical models have been proposed to explain how and why different lesion sizes might lead to different mechanisms of functional reorganization to provide effective compensation during post-lesion recovery. It has been suggested that functional recovery following small/incomplete lesions likely involves spared representations in adjacent perilesional cortex or transient recruitment of remote ipsilesional areas with similar function and connectivity as the lesion site (Grafman, 2000), as described in squirrel monkeys (Nudo et al., 1996), rodents (Biernaskie et al., 2005; Brown et al., 2009), and in a review of post-stroke rehabilitation in humans (Plow et al., 2015). On the other hand, a large lesion may completely impair functions that were normally carried out by the lesioned tissue and recovery of function may then rely on recruitment of brain areas distant to the lesion site, in both the ipsilesional and contralesional hemisphere, that are involved in similar functions (Grafman, 2000; Liu and Rouiller, 1999; Plautz et al., 2003; Zeiler et al., 2013). In the present study, there was a varying degree of spared perilesional tissue with similar function across monkeys, namely in areas 8AV and 45B. Both regions play a role in encoding the saliency or behavioural value of contralateral visual targets, which then modulates the allocation of attention (Schwedhelm et al., 2017). Areas 8AV and 45B are also densely interconnected with oculomotor structures in the surrounding PFC and higher order visual areas (Barbas and Mesulam, 1985, 1981; Yeterian et al., 2012). In Monkey L, both areas 8AV and 45B are spared; in Monkey S, area 8AV is spared; in Monkey B, area 45B is spared; and in Monkey F both areas are damaged (see Fig. 3.2B). These areas may have played a compensatory role in the functional recovery for Monkey L, with no lesions to 8AV/45B, and to a smaller degree in Monkeys S and B, with incomplete lesions to 8AV/45B. Complete damage to both 8AV and 45B may

explain the poor recovery of function in Monkey F, in which there was still a lasting ~60 ms difference (ipsilesional bias) in the point of equal selection at week 16 post-lesion compared to pre-lesion (see Fig. 3.3C).

We also observed differences in the network-wide FC changes between the two large lesion monkeys, such that Monkey B had substantially stronger increases in FC from week 1 to week 16 and from pre-lesion to week 16 than Monkey F (see Fig. 3.4B). It is interesting that Monkey F also had a worse recovery of function compared to Monkey B (see Fig. 3.3C,D). Dancause (2006) proposed that following large cortical lesions, when surviving tissue is either insufficient or non-existent, functionally-related intact areas are essential to take over the lost function; whereas following small/incomplete lesions, reorganization of remaining tissue is more beneficial than recruitment of functionally-related distant areas (Dancause, 2006; Grafman, 2000). This suggests that recruitment of the intact areas of the frontoparietal network may be important for behavioural improvement following larger lesions. The weaker increase in network FC in Monkey F may then be associated with the weaker behavioural recovery in this monkey. Ideally, these findings should be replicated in a study with larger sample sizes for each lesion group to better delineate the recovery patterns based on lesion size.

3.4.4. Compensatory role of distant and intact areas in the recovery of contralesional target selection

Across monkeys, we found that the increasing FC between contralesional dorsolateral PFC (area 9/46D) and ipsilesional superior parietal lobule (area PE) correlated with behavioural recovery. Using a graph theoretical approach, we also found increased degree centrality for contralesional dorsolateral PFC with the frontoparietal network at week 8/week 16 post-lesion compared to pre-lesion. The dorsolateral PFC is involved in

the cognitive control of visually-guided saccadic eye movements and target selection, as shown via single neuron electrophysiological recordings (Everling and DeSouza, 2005; Funahashi et al., 1991; Johnston and Everling, 2006b) and inactivation studies (Iba and Sawaguchi, 2003; Johnston et al., 2016), supporting a role in visuospatial processing. Anatomically, area 9/46D of the dorsolateral PFC is connected to the parietal lobe via SLF I and SLF II (Schmahmann et al., 2007), as described earlier in Section 4.2. Area PE of the superior parietal lobule (Brodmann area 5) has classically been regarded as a somatosensory association area (Duffy and Burchfiel, 1971), but more recent studies suggest a role in the visual control of movement (Caminiti et al., 2010; Kalaska et al., 1983). In monkeys, area PE monitors movement direction and updates its spatial maps using proprioceptive information (Kalaska et al., 1983) and has been shown to contain neurons sensitive to visual stimuli (Squatrito et al., 2001). Axonal tracing and diffusion tractography studies have shown that area PE is connected with the inferior parietal lobule, which is more directly involved in visuospatial processing as it relates to the oculomotor system (Caminiti et al., 2010; Catani et al., 2017; Rozzi et al., 2006). Our findings indicate that the functional connection between contralesional 9/46D and ipsilesional PE may contribute to the recovery of contralesional target selection following unilateral damage to the caudal PFC.

This present work suggests that intact areas of both the contralesional and ipsilesional frontoparietal networks are beneficial in the post-lesion functional recovery. Historically, there has been considerable debate about the role of the contralesional hemisphere in the recovery of visuospatial attention deficits after unilateral lesions (Corbetta and Shulman, 2011). The dominant view in the past was that contralesional attention deficits after right hemisphere lesions were due to an overactivation of the intact left hemisphere, due to the release of interhemispheric callosal inhibition, which would bias attention to the

ipsilesional hemifield (Kinsbourne, 1970). In support of Kinsbourne's theory of hemirivalry, an fMRI study in neglect patients showed an imbalance in functional activation between hemispheres that correlated with the degree of attentional bias (Corbetta et al., 2005). However, more recent studies have shown evidence that activation of the intact contralesional hemisphere may be adaptive in the recovery of attention deficits (Lunven and Bartolomeo, 2017; Saj et al., 2013; Thimm et al., 2008; Umarova et al., 2016, 2011), which supports the opposing theory that the contralesional hemisphere is beneficial for functional recovery (Heilman and Van Den Abell, 1980; Mesulam, 1981). Additionally, Umarova and colleagues (2011) reported increased task-related activation of the contralesional dorsolateral PFC on a visuospatial attention task in better recovered stroke patients with extinction, but not in poorly recovered patients with chronic neglect (Umarova et al., 2011). This suggests that recruitment of the intact dorsolateral PFC in the contralesional hemisphere is an important compensatory response for the recovery of visuospatial deficits, since only the patients with milder attention deficits (i.e., extinction) showed this activation pattern, not those with chronic neglect.

The findings from this present study support the view that involvement of the intact contralesional hemisphere is beneficial for recovery. This is in line with the studies described above and in a recent monkey fMRI study in which the right lateral intraparietal area (LIP) in the posterior parietal cortex was temporarily inactivated while monkeys performed a free-choice task (Wilke et al., 2012). The authors found an overall reduction in contralesional saccade choice during unilateral LIP inactivation, and more interestingly, that the selection of the contralesional target was associated with increased activation of the ipsilesional PFC and both contralesional LIP and PFC; all distant and intact nodes of the frontoparietal network. Our findings support and extend those in Wilke et al. (2012) to show that the longitudinal FC changes after a permanent lesion to a

single frontoparietal node (in our study, right PFC; in Wilke et al., right LIP) also involved a distant ipsilesional network area (in our study, right parietal cortex; in Wilke et al., right PFC) along with the contralesional homolog of the lesion site (in our study, left PFC; in Wilke et al., left LIP), which correlated with behavioural recovery over time.

3.4.5. Conclusions

In summary, we have found that recovery of contralesional target selection deficits following unilateral PFC lesions correlated with FC between contralesional dorsolateral PFC and ipsilesional superior parietal cortex. Contralesional dorsolateral PFC also showed increased degree centrality with the frontoparietal network from pre- to post-lesion. The assumption that these brain areas provide valuable functional compensation could be addressed in a future study in which those areas are inactivated in a recovered monkey during a choice task and observing whether target selection deficits reappear. Additionally, we have also shown that the pattern of longitudinal changes in functional reorganization during behavioural recovery varied according to lesion size. In general, network FC returned to pre-lesion baseline during recovery after small lesions, but instead strongly increased after larger lesions. Future research could explore this result further using task-based fMRI to test whether recovered monkeys with large lesions show greater task-related BOLD activation during selection of a contralesional target on a choice task, compared to recovered monkeys with smaller lesions. The broad implication of the present research is that both the contralesional and ipsilesional frontoparietal networks play a beneficial role during the recovery of function. Importantly, our findings provide evidence for greater recruitment of the bilateral frontoparietal network during recovery of target selection after large lesions, while recovery after smaller lesions was optimally supported by a normalization of the functional network.

3.5. References

- Achard, S., Bullmore, E., 2007. Efficiency and cost of economical brain functional networks. *PLoS Comput. Biol.* 3, 0174–0183.
- Adam, R., Johnston, K., Everling, S., 2019. Recovery of contralesional saccade choice and reaction time deficits after a unilateral endothelin-1-induced lesion in the macaque caudal prefrontal cortex. *J. Neurophysiol.* 122, 672–690.
- Ainsworth, M., Browncross, H., Mitchell, D.J., Mitchell, A.S., Passingham, R.E., Buckley, M.J., Duncan, J., Bell, A.H., 2018. Functional reorganisation and recovery following cortical lesions: A preliminary study in macaque monkeys. *Neuropsychologia* 119, 382–391.
- Babapoor-Farrokhran, S., Hutchison, R.M., Gati, J.S., Menon, R.S., Everling, S., 2013. Functional connectivity patterns of medial and lateral macaque frontal eye fields reveal distinct visuomotor networks. *J. Neurophysiol.* 109, 2560–70.
- Barash, S., Bracewell, R.M., Fogassi, L., Gnadt, J.W., Andersen, R. a, 1991. Saccade-related activity in the lateral intraparietal area. II. Spatial properties. *J. Neurophysiol.* 66, 1109–1124.
- Barbas, H., Medalla, M., Alade, O., Suski, J., Zikopoulos, B., Lera, P., 2005. Relationship of prefrontal connections to inhibitory systems in superior temporal areas in the rhesus monkey. *Cereb. Cortex* 15, 1356–1370.
- Barbas, H., Mesulam, M.-M., 1985. Cortical afferent input to the principals region of the rhesus monkey. *Neuroscience* 15, 619–637.
- Barbas, H., Mesulam, M. -M, 1981. Organization of afferent input to subdivisions of area 8 in the rhesus monkey. *J. Comp. Neurol.* 200, 407–431.
- Bartolomeo, P., 2007. Visual neglect. *Curr. Opin. Neurol.* 20, 381–386.
- Bartolomeo, P., Thiebaut de Schotten, M., Chica, A.B., 2012. Brain networks of visuospatial attention and their disruption in visual neglect. *Front. Hum. Neurosci.* 6, 1–10.
- Bartolomeo, P., Thiebaut De Schotten, M., Doricchi, F., 2007. Left unilateral neglect as a disconnection syndrome. *Cereb. Cortex* 17, 2479–2490.
- Baylis, G., 2002. Visual extinction with double simultaneous stimulation: what is simultaneous? *Neuropsychologia* 40, 1027–1034.
- Beckmann, C.F., Smith, S.M., 2004. Probabilistic independent component analysis for functional magnetic resonance imaging. *IEEE Trans. Med. Imaging* 23, 137–152.
- Bender, M.B., Furlow, L.T., 1945. Phenomenon of visual extinction in homonymous fields and psychologic principles involved. *Arch. Neurol. Psychiatry* 53, 29–33.
- Benjamini, Y., Hochberg, Y., 1995. Controlling the false discovery rate: a practical and powerful approach to multiple testing. *J. R. Stat. Soc. B.*

- Bianchi, L., 1895. The functions of the frontal lobes. *Brain* 18, 497–522.
- Biernaskie, J., Szymanska, A., Windle, V., Corbett, D., 2005. Bi-hemispheric contribution to functional motor recovery of the affected forelimb following focal ischemic brain injury in rats. *Eur. J. Neurosci.* 21, 989–999.
- Bisiach, E., 1991. Extinction and neglect: Same or different?, *Brain and space*.
- Bogadhi, A.R., Bollimunta, A., Leopold, D.A., Krauzlis, R.J., 2018. Brain regions modulated during covert visual attention in the macaque. *Sci. Rep.* 8, 1–15.
- Borra, E., Ferroni, C.G., Gerbella, M., Giorgetti, V., Mangiaracina, C., Rozzi, S., Luppino, G., 2019. Rostro-caudal Connectional Heterogeneity of the Dorsal Part of the Macaque Prefrontal Area 46. *Cereb. Cortex* 29, 485–504.
- Brown, C.E., Aminoltejari, K., Erb, H., Winship, I.R., Murphy, T.H., 2009. In Vivo Voltage-Sensitive Dye Imaging in Adult Mice Reveals That Somatosensory Maps Lost to Stroke Are Replaced over Weeks by New Structural and Functional Circuits with Prolonged Modes of Activation within Both the Peri-Infarct Zone and Distant Sites. *J. Neurosci.* 29, 1719–1734.
- Caminiti, R., Chafee, M. V., Battaglia-Mayer, A., Averbeck, B.B., Crowe, D.A., Georgopoulos, A.P., 2010. Understanding the parietal lobe syndrome from a neurophysiological and evolutionary perspective. *Eur. J. Neurosci.* 31, 2320–2340.
- Carter, A.R., Astafiev, S. V., Lang, C.E., Connor, L.T., Rengachary, J., Strube, M.J., Pope, D.L.W., Shulman, G.L., Corbetta, M., 2010. Resting interhemispheric functional magnetic resonance imaging connectivity predicts performance after stroke. *Ann. Neurol.* 67, 365–375.
- Carter, A.R., Shulman, G.L., Corbetta, M., 2012. Why use a connectivity-based approach to study stroke and recovery of function? *Neuroimage* 62, 2271–2280.
- Catani, M., Robertsson, N., Beyh, A., Huynh, V., de Santiago Requejo, F., Howells, H., Barrett, R.L.C., Aiello, M., Cavaliere, C., Dyrby, T.B., Krug, K., Pfitz, M., D’Arceuil, H., Forkel, S.J., Dell’Acqua, F., 2017. Short parietal lobe connections of the human and monkey brain. *Cortex* 97, 339–357.
- Corbetta, M., Kincade, M.J., Lewis, C., Snyder, A.Z., Sapir, A., 2005. Neural basis and recovery of spatial attention deficits in spatial neglect. *Nat. Neurosci.* 8, 1603–10.
- Corbetta, M., Shulman, G.L., 2011. Spatial Neglect and Attention Networks. *Annu. Rev. Neurosci.* 34, 569–599.
- Corbetta, M., Shulman, G.L., 2002. Control of goal-directed and stimulus-driven attention in the brain. *Nat. Rev. Neurosci.* 3, 201–15.
- Dai, P., Huang, H., Zhang, L., He, J., Zhao, X., Yang, F., Zhao, N., Yang, J., Ge, L., Lin, Y., Yu, H., Wang, J., 2017. A pilot study on transient ischemic stroke induced with endothelin-1 in the rhesus monkeys. *Sci. Rep.* 7, 45097.
- Damasio, A.R., Damasio, H., Chui, H.C., 1980. Neglect following damage to frontal lobe

- or basal ganglia. *Neuropsychologia* 18, 123–132.
- Dancause, N., 2006. Vicarious function of remote cortex following stroke: Recent evidence from human and animal studies. *Neuroscientist* 12, 489–499.
- de Haan, B., Karnath, H.O., Driver, J., 2012. Mechanisms and anatomy of unilateral extinction after brain injury. *Neuropsychologia* 50, 1045–1053.
- Deuel, R.K., Collins, R.C., 1984. The functional anatomy of frontal lobe neglect in the monkey: behavioral and quantitative 2-deoxyglucose studies. *Ann. Neurol.* 15, 521–529.
- Deuel, R.K., Farrar, C.A., 1993. Stimulus cancellation by macaques with unilateral frontal or parietal lesions. *Neuropsychologia* 31, 29–38.
- Di Pellegrino, G., Basso, G., Frassinetti, F., 1997. Spatial extinction on double asynchronous stimulation. *Neuropsychologia* 35, 1215–1223.
- Doricchi, F., Thiebaut de Schotten, M., Tomaiuolo, F., Bartolomeo, P., 2008. White matter (dis)connections and gray matter (dys)functions in visual neglect: Gaining insights into the brain networks of spatial awareness. *Cortex* 44, 983–995.
- Doricchi, F., Tomaiuolo, F., 2003. The anatomy of neglect without hemianopia: a key role for parietal-frontal disconnection? *Cogn. Neurosci. Neuropsychol.* 14, 2239–2243.
- Duffy, F.H., Burchfiel, J.L., 1971. Somatosensory system: Organizational hierarchy from single units in monkey area 5. *Science* (80-). 172, 273–275.
- Eidelberg, E., Schwartz, A.S., 1971. Experimental analysis of the extinction phenomenon in monkeys. *Brain* 94, 91–108.
- Everling, S., DeSouza, J.F.X., 2005. Rule-dependent Activity for Prosaccades and Antisaccades in the Primate Prefrontal Cortex. *J. Cogn. Neurosci.* 17, 1483–1496.
- Farber, N., Harkin, C., Niedfeldt, J., Hudetz, A., Kampine, J., Schmeling, W., 1997. Region-specific and agent-specific dilation of intracerebral microvessels by volatile anesthetics in rat brain slices. *Anesthesiology* 87, 1191–1198.
- Farne, A., 2004. Patterns of spontaneous recovery of neglect and associated disorders in acute right brain-damaged patients. *J. Neurol. Neurosurg. Psychiatry* 75, 1401–1410.
- Ferrier, D., 1886. *The functions of the brain*, Smith, Elder, and Company. London.
- Fierro, B., Brighina, F., Oliveri, M., Piazza, A., La Bua, V., Buffa, D., Bisiach, E., 2000. Contralateral neglect induced by right posterior parietal rTMS in healthy subjects. *Neuroreport* 11, 1519–1521.
- Fornito, A., Zalesky, A., Bullmore, E., 2016. *Fundamentals of brain network analysis*. *Fundam. brain Netw. Anal.*
- Fries, W., 1984. Cortical projections to the superior colliculus in the macaque monkey: a retrograde study using horseradish peroxidase. *J. Comp. Neurol.* 230, 55–76.

- Frost, S.B., 2003. Reorganization of Remote Cortical Regions After Ischemic Brain Injury: A Potential Substrate for Stroke Recovery. *J. Neurophysiol.* 89, 3205–3214.
- Funahashi, S., Bruce, C., Goldman-Rakic, P., 1991. Neuronal activity related to saccadic eye movements in the monkey's dorsolateral prefrontal cortex. *J. Neurophysiol.* 65, 1464–1483.
- Funahashi, S., Bruce, C., Goldman-Rakic, P., 1989. Mnemonic Coding of Visual Space in the Monkey's Dorsolateral Prefrontal Cortex. *J. Neurophysiol.* 61, 331–349.
- Gaffan, D., Hornak, J., 1997. Visual neglect in the monkey: Representation and disconnection. *Brain* 120, 1647–1657.
- Gazzaniga, M.S., 2000. Cerebral specialization and interhemispheric communication: Does the corpus callosum enable the human condition? *Brain* 123, 1293–1326.
- Gilbert, K.M., Gati, J.S., Barker, K., Everling, S., Menon, R.S., 2016. Optimized parallel transmit and receive radiofrequency coil for ultrahigh-field MRI of monkeys. *Neuroimage* 125, 153–161.
- Goldman-Rakic, P.S., Porrino, L.J., 1985. The primate mediodorsal (MD) nucleus and its projection to the frontal lobe. *J. Comp. Neurol.* 242, 535–560.
- Goldman, P.S., Nauta, W.J.H.H., 1976. Autoradiographic demonstration of a projection from prefrontal association cortex to the superior colliculus in the rhesus monkey. *Brain Res.* 116, 145–149.
- Grafman, J., 2000. Conceptualizing functional neuroplasticity. *J. Commun. Disord.* 33, 345–356.
- Grefkes, C., Fink, G.R., 2011. Reorganization of cerebral networks after stroke: New insights from neuroimaging with connectivity approaches. *Brain* 134, 1264–1276.
- Grefkes, C., Ward, N.S., 2014. Cortical reorganization after stroke: How much and how functional? *Neurosci.* 20, 56–70.
- Griffanti, L., Salimi-khorshidi, G., Beckmann, C.F., Auerbach, E.J., Douaud, G., Sexton, C.E., Ebmeier, K.P., Filippini, N., Mackay, C.E., Moeller, S., Xu, J., Yacoub, E., Baselli, G., Ugurbil, K., Miller, K.L., Smith, S.M., 2014. ICA-based artefact removal and accelerated fMRI acquisition for improved resting state network imaging. *Neuroimage* 95, 232–247.
- He, B.J., Snyder, A.Z., Vincent, J.L., Epstein, A., Shulman, G.L., Corbetta, M., 2007. Breakdown of functional connectivity in frontoparietal networks underlies behavioral deficits in spatial neglect. *Neuron* 53, 905–18.
- Hedges, L.V., 1981. Distribution Theory for Glass's Estimator of Effect size and Related Estimators, *Journal of Educational Statistics.*
- Heilman, K.M., Valenstein, E., Watson, R.T., 1984. Neglect and related disorders. *Semin. Neurol.* 4, 209–219.
- Heilman, K.M., Van Den Abell, T., 1980. Right hemisphere dominance for attention: the

- mechanism underlying hemispheric asymmetries of inattention (neglect). *Neurology* 30, 327–330.
- Heilman, K.M., Watson, R.T., Valenstein, E., 2012. Neglect and Related Disorders, in: Heilman, K.M., Valenstein, E. (Eds.), *Clinical Neuropsychology*. Oxford University Press, New York.
- Herbert, W.J., Powell, K., Buford, J.A., 2015. Evidence for a role of the reticulospinal system in recovery of skilled reaching after cortical stroke: initial results from a model of ischemic cortical injury. *Exp. Brain Res.* 233, 3231–3251.
- Hier, D., Mondlock, J., Caplan, L., 1983. Recovery of behavioral abnormalities after right hemisphere stroke. *Neurology* 33, 345–350.
- Husain, M., Kennard, C., 1996. Visual neglect associated with frontal lobe infarction. *J. Neurol.* 243, 652–657.
- Hutchison, R.M., Everling, S., 2012. Monkey in the middle: why non-human primates are needed to bridge the gap in resting-state investigations. *Front. Neuroanat.* 6, 29.
- Hutchison, R.M., Gallivan, J.P., Culham, J.C., Gati, J.S., Menon, R.S., Everling, S., 2012. Functional connectivity of the frontal eye fields in humans and macaque monkeys investigated with resting-state fMRI. *J. Neurophysiol.* 107, 2463–74.
- Hutchison, R.M., Hutchison, M., Manning, K.Y., Menon, R.S., Everling, S., 2014. Isoflurane induces dose-dependent alterations in the cortical connectivity profiles and dynamic properties of the brain's functional architecture. *Hum. Brain Mapp.* 35, 5754–5775.
- Hutchison, R. Matthew, Leung, L.S., Mirsattari, S.M., Gati, J.S., Menon, R.S., Everling, S., 2011. Resting-state networks in the macaque at 7T. *Neuroimage* 56, 1546–1555.
- Hutchison, R. Matthew, Leung, L.S., Mirsattari, S.M., Gati, J.S., Menon, R.S., Everling, S., 2011. Resting-state networks in the macaque at 7 T. *Neuroimage* 56, 1546–55.
- Iba, M., Sawaguchi, T., 2003. Involvement of the dorsolateral prefrontal cortex of monkeys in visuospatial target selection. *J. Neurophysiol.* 89, 587–99.
- Itahashi, T., Nakamura, M., Toriizuka, K., Kato, N., Hashimoto, R., Watanabe, H., Jimbo, D., Shioda, S., Yamada, T., 2014. Altered Network Topologies and Hub Organization in Adults with Autism: A Resting-State fMRI Study. *PLoS One* 9, e94115.
- Jacobsen, C.F., Nissen, H.W., 1937. Studies of cerebral function in primates. IV. The effects of frontal lobe lesions on the delayed alternation habit in monkeys. *J. Comp. Psychol.* 23, 101–112.
- Jamerson, E.C., Snyder, L.H., Corbetta, M., Patel, G.H., Yang, D., Jamerson, E.C., Snyder, L.H., Corbetta, M., Jamerson, E.C., Ferrera, V.P., 2015. Functional evolution of new and expanded attention networks in humans. *Proc. Natl. Acad. Sci.* 112, E5377–E5377.

- Jenkinson, M., Bannister, P., Brady, M., Smith, S., 2002. Improved optimization for the robust and accurate linear registration and motion correction of brain images. *Neuroimage* 17, 825–841.
- Johnston, K., Everling, S., 2006a. Monkey dorsolateral prefrontal cortex sends task-selective signals directly to the superior colliculus. *J. Neurosci.* 26, 12471–12478.
- Johnston, K., Everling, S., 2006b. Neural Activity in Monkey Prefrontal Cortex Is Modulated by Task Context and Behavioral Instruction during Delayed-match-to-sample and Conditional Prosaccade–Antisaccade Tasks. *J. Cogn. Neurosci.* 18, 749–765.
- Johnston, K., Lomber, S.G., Everling, S., 2016. Unilateral Deactivation of Macaque Dorsolateral Prefrontal Cortex Induces Biases in Stimulus Selection. *J. Neurophysiol.* 115, 1468–1476.
- Kagan, I., Iyer, A., Lindner, A., Andersen, R.A., 2010. Space representation for eye movements is more contralateral in monkeys than in humans. *Proc. Natl. Acad. Sci. U. S. A.* 107, 7933–7938.
- Kalaska, J., Caminiti, R., Georgopoulos, A.P., 1983. Cortical Mechanisms Related to the Direction of Two-Dimensional Arm Movements: Relations in Parietal Area 5 and Comparison with Motor Cortex. *Exp. brain Res.* 51, 247–260.
- Karnath, H.O., Rorden, C., 2012. The anatomy of spatial neglect. *Neuropsychologia* 50, 1010–1017.
- Kennard, M.A., Ectors, L., 1938. Forced circling in monkeys following lesions of the frontal lobes. *J. Neurophysiol.* 1, 45–54.
- Kinsbourne, M., 1970. The cerebral basis of lateral asymmetries in attention. *Acta Psychol. (Amst).* 33, 193–201.
- Kubanek, J., Li, J.M., Snyder, L.H., 2015. Motor role of parietal cortex in a monkey model of hemispatial neglect. *Proc. Natl. Acad. Sci. U. S. A.* 112, E2067–E2072.
- Kunzle, H., Akert, K., 1977. Efferent connections of cortical area 8 (frontal eye field) in. *J Comp Neurol* 173, 147–164.
- Latto, R., Cowey, A., 1971a. Fixation changes after frontal eye-field lesions in monkeys. *Brain Res.* 30, 25–36.
- Latto, R., Cowey, A., 1971b. Visual field defects after frontal eye field lesions in monkeys. *Brain Res.* 30, 1–24.
- Liu, Y., Rouiller, E.M., 1999. Mechanisms of recovery of dexterity following unilateral lesion of the sensorimotor cortex in adult monkeys. *Exp. Brain Res.* 128, 149–159.
- Lunven, M., Bartolomeo, P., 2017. Attention and spatial cognition: Neural and anatomical substrates of visual neglect. *Ann. Phys. Rehabil. Med.* 60, 124–129.
- Lv, Q., Yang, L., Li, G., Wang, Z.Z.Z., Shen, Z., Yu, W., Jiang, Q., Hou, B., Pu, J., Hu, H., Wang, Z.Z.Z., 2015. Large-scale Persistent Network Reconfiguration Induced by

- Ketamine in Anesthetized Monkeys: Relevance to Mood Disorders. *Biol. Psychiatry* 79, 765–775.
- Lynch, J.C., McLaren, J.A.Y.W., 1989. Deficits of Visual Attention and Saccadic Eye Movements After Lesions of Parietooccipital Cortex in Monkeys. *J. Neurophysiol.* 6, 74–90.
- Maioli, M.G., Squatrito, S., Galletti, C., Battaglini, P.P., Sanseverino, E.R., 1983. Cortico-cortical connections from the visual region of the superior temporal sulcus to frontal eye field in the macaque. *Brain Res.* 265, 294–299.
- Marques, J.P., Kober, T., Krueger, G., van der Zwaag, W., Van de Moortele, P.F., Gruetter, R., 2010. MP2RAGE, a self bias-field corrected sequence for improved segmentation and T1-mapping at high field. *Neuroimage* 49, 1271–1281.
- McPeck, R.M., Keller, E.L., 2004. Deficits in saccade target selection after inactivation of superior colliculus. *Nat. Neurosci.* 7, 757–63.
- Meister, I.G., Wienemann, M., Buelte, D., Grünewald, C., Sparing, R., Dambeck, N., Boroojerdi, B., 2006. Hemiextinction induced by transcranial magnetic stimulation over the right temporo-parietal junction. *Neuroscience* 142, 119–123.
- Mesulam, M.-M., 1999. Spatial attention and neglect: parietal, frontal and cingulate contributions to the mental representation and attentional targeting of salient extrapersonal events. *Philos. Trans. R. Soc. Lond. B. Biol. Sci.* 354, 1325–1346.
- Mesulam, M. -Marchsel, 1981. A cortical network for directed attention and unilateral neglect. *Ann. Neurol.*
- Milner, A.D., McIntosh, R.D., 2005. The neurological basis of visual neglect. *Curr. Opin. Neurol.* 18, 748–753.
- Murata, Y., Higo, N., 2016. Development and Characterization of a Macaque Model of Focal Internal Capsular Infarcts. *PLoS One* 11, e0154752.
- Nudo, R.J., Wise, B.M., SiFuentes, F., Milliken, G.W., 1996. Neural Substrates for the Effects of Rehabilitative Training on Motor Recovery After Ischemic Infarct. *Science* (80-.). 272, 1791–1794.
- Paxinos, G., Huang, X., Toga, A., 2000. *The Rhesus Monkey Brain in Stereotaxic Coordinates.* Academic Press.
- Petrides, M., Pandya, D.N., 1999. Dorsolateral prefrontal cortex: comparative cytoarchitectonic analysis in the human and the macaque brain and corticocortical connection patterns. *Eur. J. Neurosci.* 11, 1011–36.
- Petrides, M., Pandya, D.N., 1984. Projections to the frontal cortex from the posterior parietal region in the rhesus monkey. *J. Comp. Neurol.* 116, 105–116.
- Plautz, E.J., Barbay, S., Frost, S.B., Friel, K.M., Dancause, N., Zoubina, E. V., Stowe, A.M., Quaney, B.M., Nudo, R.J., 2003. Post-infarct cortical plasticity and behavioral recovery using concurrent cortical stimulation and rehabilitative training:

- A feasibility study in primates. *Neurol. Res.* 25, 801–810.
- Plow, E.B., Cunningham, D., Varnerin, N., Machado, A., Clinic, C., Clinic, C., Clinic, C., 2015. Rethinking stimulation of brain in stroke rehabilitation: Why higher-motor areas might be better alternatives for patients with greater impairments. *Neuroscientist* 21, 225–240.
- Port, N.L., Wurtz, R.H., 2009. Target selection and saccade generation in monkey superior colliculus. *Exp. Brain Res.* 192, 465–477.
- Posner, M.I., Cohen, Y., Rafal, R.D., 1982. Neural systems control of spatial orienting. *Philos. Trans. R. Soc. Lond. B. Biol. Sci.* 298, 187–198.
- Posner, M.I., Petersen, S.E., 1990. The Attention System of the Human Brain. *Annu. Rev. Neurosci.* 13, 25–42.
- Ramsey, L.E., Siegel, J.S., Baldassarre, A., Metcalfe, N. V., Zinn, K., Shulman, G.L., Corbetta, M., 2016. Normalization of network connectivity in hemispatial neglect recovery. *Ann. Neurol.* 80, 127–141.
- Rizzolatti, G., Matelli, M., Pavesi, G., 1983. Deficits in attention and movement following the removal of postarcuate (area 6) and prearcuate (area 8) cortex in macaque monkeys. *Brain* 106, 655–673.
- Ro, T., Rorden, C., Driver, J., Rafal, R., 2001. Ipsilesional biases in saccades but not perception after lesions of the human inferior parietal lobule. *J. Cogn. Neurosci.* 13, 920–929.
- Robertson, I.H., Halligan, P.W., 1999. Spatial neglect: A clinical handbook for diagnosis and treatment., *Spatial neglect: A clinical handbook for diagnosis and treatment., Brain damage, behaviour and cognition series.* Psychology Press/Taylor & Francis (UK), Hove, England.
- Rorden, C., Jelsone, L., Simon-Dack, S., Baylis, L.L., Baylis, G.C., 2009. Visual extinction: The effect of temporal and spatial bias. *Neuropsychologia* 47, 321–329.
- Rorden, C., Mattingley, J.B., Karnath, H.O., Driver, J., 1997. Visual extinction and prior entry: Impaired perception of temporal order with intact motion perception after unilateral parietal damage. *Neuropsychologia* 35, 421–433.
- Rozzi, S., Calzavara, R., Belmalih, A., Borra, E., Gregoriou, G.G., Matelli, M., Luppino, G., 2006. Cortical connections of the inferior parietal cortical convexity of the macaque monkey. *Cereb. Cortex* 16, 1389–1417.
- Rubinov, M., Sporns, O., 2010. Complex network measures of brain connectivity: Uses and interpretations. *Neuroimage* 52, 1059–1069.
- Saj, A., Cojan, Y., Vocat, R., Luaute, J., Vuilleumier, P., 2013. Prism adaptation enhances activity of intact fronto-parietal areas in both hemispheres in neglect patients. *Cortex.* 49, 107–119.
- Saleem, K.S., Logothetis, N.K., 2006. A combined MRI and histology atlas of the rhesus

monkey brain in stereotaxic coordinates.

- Sallet, J., Mars, R.B., Noonan, M.P., Neubert, F.-X., Jbabdi, S., O'Reilly, J.X., Filippini, N., Thomas, A.G., Rushworth, M.F., 2013. The Organization of Dorsal Frontal Cortex in Humans and Macaques. *J. Neurosci.* 33, 12255–12274.
- Sani, I., McPherson, B.C., Stemmann, H., Pestilli, F., Freiwald, W.A., 2019. Functionally defined white matter of the macaque monkey brain reveals a dorso-ventral attention network. *Elife* 8, 1–21.
- Schiller, P.H., Chou, I., 2000. The effects of anterior arcuate and dorsomedial frontal cortex lesions on visually guided eye movements: 2. Paired and multiple targets. *Vision Res.* 40, 1627–1638.
- Schiller, P.H., Chou, I., 1998. The effects of frontal eye field and dorsomedial frontal cortex lesions on visually guided eye movements. *Nat. Neurosci.* 1, 248–253.
- Schiller, P.H., Tehovnik, E.J., 2003. Cortical inhibitory circuits in eye-movement generation. *Eur. J. Neurosci.* 18, 3127–3133.
- Schluppeck, D., Curtis, C.E., Glimcher, P.W., Heeger, D.J., 2006. Sustained activity in topographic areas of human posterior parietal cortex during memory-guided saccades. *J. Neurosci.* 26, 5098–5108.
- Schmahmann, J.D., Pandya, D.N., 1997. Anatomic Organization of the Basilar Pontine Projections from Prefrontal Cortices in Rhesus Monkey. *J. Neurosci.* 17, 438 LP – 458.
- Schmahmann, J.D., Pandya, D.N., Schmahmann, J.D., Pandya, D.N., 2009. *Extreme Capsule, Fiber Pathways of the Brain.* Oxford University Press, New York.
- Schmahmann, J.D., Pandya, D.N., Wang, R., Dai, G., D'Arceuil, H.E., De Crespigny, A.J., Wedeen, V.J., 2007. Association fibre pathways of the brain: Parallel observations from diffusion spectrum imaging and autoradiography. *Brain* 130, 630–653.
- Schwedhelm, P., Baldauf, D., Treue, S., 2017. Electrical stimulation of macaque lateral prefrontal cortex modulates oculomotor behavior indicative of a disruption of top-down attention. *Sci. Rep.* 7, 1–10.
- Smith, S.M., 2002. Fast robust automated brain extraction. *Hum. Brain Mapp.* 17, 143–155.
- Squatrito, S., Raffi, M., Maioli, M.G., Battaglia-mayer, A., 2001. Visual Motion Responses of Neurons in the Caudal Area PE of Macaque Monkeys. *J. Neurosci.* 21, 1–5.
- Srimal, R., Curtis, C.E., 2008. Persistent neural activity during the maintenance of spatial position in working memory. *Neuroimage* 39, 455–468.
- Stanton, G., Bruce, C., Goldberg, M., 1993. Topography of projections to the frontal lobe from the macaque frontal eye fields. *J. Comp. Neurol.* 330, 286–301.

- Stanton, G., Goldberg, M., Bruce, C., 1988a. Frontal eye field efferents in the macaque monkey: I. Subcortical pathways and topography of striatal and thalamic terminal fields. *J. Comp. Neurol.* 271, 473–492.
- Stanton, G., Goldberg, M., Bruce, C., 1988b. Frontal eye field efferents in the macaque monkey: II. Topography of terminal fields in midbrain and pons. *J. Comp. Neurol.* 271, 493–506.
- Teo, L., Bourne, J., 2014. A Reproducible and Translatable Model of Focal Ischemia in the Visual Cortex of Infant and Adult Marmoset Monkeys. *Brain Pathol.* 24, 459–474.
- Thiebaut De Schotten, M., Dell’Acqua, F., Forkel, S.J., Simmons, A., Vergani, F., Murphy, D.G.M., Catani, M., 2011. A lateralized brain network for visuospatial attention. *Nat. Neurosci.* 14, 1245–1246.
- Thiebaut de Schotten, M., Dell’Acqua, F., Valabregue, R., Catani, M., 2012. Monkey to human comparative anatomy of the frontal lobe association tracts. *Cortex* 48, 82–96.
- Thiebaut de Schotten, M., Urbanski, M., Duffau, H., Volle, E., Lévy, R., Dubois, B., Bartolomeo, P., 2005. Direct evidence for a parietal-frontal pathway subserving spatial awareness in humans. *Science* (80-.). 309, 2226–2228.
- Thimm, M., Fink, G.R., Sturm, W., 2008. Neural correlates of recovery from acute hemispatial neglect. *Restor Neurol Neurosci* 26, 481–492.
- Tian, J., Lynch, J.C., 1997. Subcortical Input to the Smooth and Saccadic Eye Movement Subregions of the Frontal Eye Field in Cebus Monkey. *J. Neurosci.* 17, 9233 LP – 9247.
- Touvykine, B., Mansoori, B.K., Jean-Charles, L., Deffeyes, J., Quessy, S., Dancause, N., 2016. The effect of lesion size on the organization of the ipsilesional and contralesional motor cortex. *Neurorehabil. Neural Repair* 30, 280–292.
- Umarova, R.M., Nitschke, K., Kaller, C.P., Klöppel, S., Beume, L., Mader, I., Martin, M., Hennig, J., Weiller, C., 2016. Predictors and signatures of recovery from neglect in acute stroke. *Ann. Neurol.* 79, 673–686.
- Umarova, R.M., Saur, D., Kaller, C.P., Vry, M.S., Glauche, V., Mader, I., Hennig, J.J., Weiller, C., 2011. Acute visual neglect and extinction: Distinct functional state of the visuospatial attention system. *Brain* 134, 3310–3325.
- Umarova, R.M., Saur, D., Schnell, S., Kaller, C.P., Vry, M.S., Glauche, V., Rijntjes, M., Hennig, J., Kiselev, V., Weiller, C., 2010. Structural connectivity for visuospatial attention: Significance of ventral pathways. *Cereb. Cortex* 20, 121–129.
- Van Essen, D.C., 2004. Surface-based approaches to spatial localization and registration in primate cerebral cortex, in: *NeuroImage*.
- Van Essen, D.C., Drury, H.A., Dickson, J., Harwell, J., Hanlon, D., Anderson, C.H., 2001. An integrated software suite for surface-based analyses of cerebral cortex. *J. Am. Med. Informatics Assoc.* 8, 443–459.

- Van Hees, S., McMahon, K., Angwin, A., de Zubicaray, G., Read, S., Copland, D. a., 2014. A functional MRI study of the relationship between naming treatment outcomes and resting state functional connectivity in post-stroke aphasia. *Hum. Brain Mapp.* 35, 3919–3931.
- van Meer, M.P. a, Otte, W.M., van der Marel, K., Nijboer, C.H., Kavelaars, A., van der Sprenkel, J.W.B., Viergever, M. a, Dijkhuizen, R.M., 2012. Extent of bilateral neuronal network reorganization and functional recovery in relation to stroke severity. *J. Neurosci.* 32, 4495–507.
- van Meer, M.P. a, van der Marel, K., Wang, K., Otte, W.M., El Bouazati, S., Roeling, T. a P., Viergever, M. a, Berkelbach van der Sprenkel, J.W., Dijkhuizen, R.M., 2010. Recovery of sensorimotor function after experimental stroke correlates with restoration of resting-state interhemispheric functional connectivity. *J. Neurosci.* 30, 3964–72.
- Vincent, J.L., Patel, G.H., Fox, M.D., Snyder, A.Z., Baker, J.T., Van Essen, D.C., Zempel, J.M., Snyder, L.H., Corbetta, M., Raichle, M.E., 2007. Intrinsic functional architecture in the anaesthetized monkey brain. *Nature* 447, 83–86.
- Wang, J., Wang, X., Xia, M., Liao, X., Evans, A., He, Y., 2015. GRETNA: a graph theoretical network analysis toolbox for imaging connectomics. *Front. Hum. Neurosci.* 9, 1–16.
- Wardak, C., Olivier, E., Duhamel, J.-R., 2002. Saccadic target selection deficits after lateral intraparietal area inactivation in monkeys. *J. Neurosci.* 22, 9877–84.
- Wardak, C., Olivier, E., Duhamel, J.R., 2004. A Deficit in covert attention after parietal cortex inactivation in the monkey. *Neuron* 42, 501–508.
- Welch, K., Stuteville, P., 1958. Experimental production of unilateral neglect in monkeys. *Brain* 81, 341–347.
- Westlake, K.P., Nagarajan, S.S., 2011. Functional connectivity in relation to motor performance and recovery after stroke. *Front. Syst. Neurosci.* 5, 8.
- Wilke, M., Kagan, I., Andersen, R., 2012. Functional imaging reveals rapid reorganization of cortical activity after parietal inactivation in monkeys. *Proc. Natl. Acad. Sci.* 109, 8274–8279.
- Womelsdorf, T., Everling, S., 2015. Long-Range Attention Networks: Circuit Motifs Underlying Endogenously Controlled Stimulus Selection. *Trends Neurosci.* 38, 682–700.
- Wurtz, R.H., Goldberg, M.E., 1989. *The Neurobiology of Saccadic Eye Movements, Volume III.* ed. Elsevier, Amsterdam.
- Xia, M., Wang, J., He, Y., 2013. BrainNet Viewer: A Network Visualization Tool for Human Brain Connectomics. *PLoS One* 8.
- Yeterian, E.H., Pandya, D.N., 1991. Prefrontostriatal connections in relation to cortical architectonic organization in rhesus monkeys. *J. Comp. Neurol.* 312, 43–67.

- Yeterian, E.H., Pandya, D.N., Tomaiuolo, F., Petrides, M., 2012. The cortical connectivity of the prefrontal cortex in the monkey brain. *Cortex* 48, 68–81.
- Zeiler, S.R., Gibson, E.M., Hoesch, R.E., Li, M.Y., Worley, P.F., O'Brien, R.J., Krakauer, J.W., 2013. Medial Premotor Cortex Shows a Reduction in Inhibitory Markers and Mediates Recovery in a Mouse Model of Focal Stroke. *Stroke* 44, 483–489.
- Zhang, J., Wang, J., Wu, Q., Kuang, W., Huang, X., He, Y., Gong, Q., 2011. Disrupted brain connectivity networks in drug-naive, first-episode major depressive disorder. *Biol. Psychiatry* 70, 334–342.
- Zhang, Y., Brady, M., Smith, S., 2001. Segmentation of brain MR images through a hidden Markov random field model and the expectation-maximization algorithm. *IEEE Trans. Med. Imaging* 20, 45–57.
- Zhu, D., Chang, J., Freeman, S., Tan, Z., Xiao, J., Gao, Y., Kong, J., 2014. Changes of functional connectivity in the left frontoparietal network following aphasic stroke. *Front. Behav. Neurosci.* 8, 1–10.

CHAPTER 4

4. Structural alterations in cortical white matter tracts after recovery from prefrontal cortex lesions in macaques

4.1. Introduction

Impaired spatial attention and reduced gaze shifts toward the contralesional visual hemifield are commonly seen following unilateral damage to the primate frontoparietal network, which includes the caudal prefrontal cortex (PFC), posterior parietal cortex (PPC), and white matter pathways connecting the large-scale network (Bartolomeo et al., 2012; Corbetta and Shulman, 2011; Mesulam, 1999). In stroke patients, these deficits manifest as a decreased ability to respond or attend to a single visual target within the contralesional hemifield, a phenomenon known as visual neglect (Bartolomeo, 2007; Li and Malhotra, 2015). In many cases, deficits within the contralesional hemifield appear only in the presence of a competing stimulus in the ipsilesional hemifield, referred to as visual extinction (Bisiach, 1991; Damasio et al., 1980; B. de Haan et al., 2012; Di Pellegrino et al., 1997). Similar visuospatial deficits within the contralesional hemifield have been demonstrated in macaque monkeys after experimental lesions or reversible inactivation of PFC or PPC areas (Adam et al., 2019; Bianchi, 1895; Deuel and Farrar, 1993; Johnston et al., 2016; Latto and Cowey, 1971; Lynch and McLaren, 1989; Rizzolatti et al., 1983; Schiller and Chou, 1998; Wardak et al., 2002, 2006, 2004; Wilke et al., 2012). Functional imaging studies of lateralized attention deficits in neglect patients and animal lesion models have shown that functional changes across a distributed network correlated with the severity of deficits in the acute stage (Baldassarre et al., 2014;

Umarova et al., 2011; Wilke et al., 2012) and with the degree of behavioural recovery in the chronic stage (Deuel and Collins, 1983; He et al., 2007; Ramsey et al., 2016; Umarova et al., 2016).

Recently, we reported the longitudinal changes in resting-state functional connectivity (rsFC) within the frontoparietal network after a unilateral caudal PFC lesion in macaque monkeys (Adam et al., 2020). We showed that recovery of contralesional saccade choice deficits correlated with increasing rsFC between the contralesional PFC and ipsilesional PPC. Since network-wide rsFC has been shown to reflect properties of the underlying structural connections (Dijkhuizen et al., 2012; Greicius et al., 2009; Hagmann et al., 2008; Shen et al., 2015), here we expand on our previous study to examine the lesion-induced changes in white matter pathways connecting the bilateral frontoparietal network, including the superior longitudinal fasciculus (SLF) and transcallosal fibers connecting bilateral PFC and bilateral PPC. The SLF is a long-range association white matter pathway that connects frontoparietal areas within hemisphere (Petrides and Pandya, 1984; Schmahmann et al., 2007; Thiebaut de Schotten et al., 2012). Between hemispheres, the caudal PFC and PPC are connected to their respective contralateral homologs via transcallosal fibers which cross at the genu or isthmus of the corpus callosum, respectively (Barbas and Pandya, 1984; Hofer et al., 2008). It has not yet been explored whether recovery of contralesional target selection after a focal lesion is associated with changes in related white matter fibers. Moreover, the behavioural relevance of structural alterations in remote fiber tracts before and after focal damage have been understudied and are not well understood.

Diffusion-weighted imaging (DWI) has emerged as a valuable and non-invasive MRI technique that is sensitive to the rate of water diffusion in biological tissue (Moseley et al., 1991, 1990; Thomsen et al., 1987; Wesbey et al., 1984). Water diffusion can then be

modeled using diffusion tensor imaging (DTI) analysis which fits a three-dimensional tensor at each voxel to estimate local fiber orientations for tractography and outputs scalar diffusion maps to describe white matter microstructure (Basser et al., 1994a, 1994b). The behavioural relevance of white matter tract remodeling after focal lesions has been shown in previous DWI studies of stroke patients and animal models (Liu et al., 2007; Schaechter et al., 2009; Umarova et al., 2017; van der Zijden et al., 2008; Wang et al., 2016).

In the present study, we examined the microstructural changes of frontoparietal white matter tracts in those four macaque monkeys using high spatial and high angular resolution DWI acquired *in vivo* at 7T. DWI data were obtained at two time points: before the unilateral PFC lesion and at a late post-lesion stage (week 8 or 16 post-lesion) when contralesional saccade choice deficits had largely recovered. Probabilistic fiber tractography was used to reconstruct four fiber tracts of interest: contralesional and ipsilesional SLF and transcallosal PFC and PPC tracts. Tract-specific diffusion parameters, including fractional anisotropy (FA) and mean, axial, and radial diffusivity, were then calculated for each tract and compared over time. We speculated that the remote fiber tracts (i.e., contralesional SLF and transcallosal PPC) may have mediated the increased rsFC between contralesional PFC and ipsilesional PPC that was found in our previous study (Adam et al., 2020), since those tracts provide an undamaged pathway which indirectly links the cortical regions together. On the other hand, ipsilesional SLF and transcallosal PFC fibers were likely damaged by anterograde/retrograde degeneration since they directly innervate the lesioned right caudal PFC (Thomalla et al., 2004; Werring et al., 2000). Thus, we hypothesized that the remote contralesional SLF and transcallosal PPC tracts play a compensatory role to support behavioural recovery post-lesion, by potentially mediating increased rsFC of the frontoparietal network. We

predicted that if behaviour or rsFC relied on the contralesional SLF and transcallosal PPC tracts, then FA should increase within one or both of those remote tracts from pre-lesion to late post-lesion.

4.2. Methods

4.2.1. Subjects

Data were collected from four adult male macaque monkeys (*Macaca mulatta*) aged 5 – 7 years old and weighing 7 – 10 kg. All surgical and experimental procedures were carried out in accordance with the Canadian Council of Animal Care policy on the use of laboratory monkeys and approved by the Animal Care Committee of the University of Western Ontario Council. Experimental methods for these subjects has been previously published in our companion paper (Adam et al., 2020). Herein, animals are individually described as Monkey L, Monkey S, Monkey B, and Monkey F. We show behavioural data from these subjects at the following time points: pre-lesion, week 1-2 post-lesion (early post-lesion), and week 8 or 16 post-lesion (late post-lesion). The early post-lesion time point shows the acute behavioural deficits following the lesion and the late post-lesion time point shows the recovered behaviour months later. DWI data was acquired at pre-lesion at late post-lesion (described below) to examine how the white matter microstructure changed at the time of behavioural recovery compared to pre-lesion.

4.2.2. Lesions

Details of the experimental lesioning surgeries have been previously published in these subjects (Adam et al., 2020). Briefly, lesions were induced using the vasoconstrictor

endothelin-1, which induces focal occlusion with subsequent reperfusion and has been validated in marmosets and macaque monkeys (Dai et al., 2017; Herbert et al., 2015; Murata and Higo, 2016; Teo and Bourne, 2014). Intracortical injections were made in the right caudal PFC (along the anterior bank of the arcuate sulcus and the caudal portion of the principal sulcus). We varied the total amount of endothelin-1 administered to each animal to produce small lesions in Monkey L and Monkey S (6-12 μg) and large lesions in Monkey B and Monkey F (16-32 μg). Figure 4.1 shows the lesion extent in each animal. All monkeys sustained damage to the right caudal PFC with consistent lesions in area 8AD (Fig. 4.1B). The lesion in Monkey L was localized to area 8AD and 8B; in Monkey S, the lesion extended further into the dorsolateral and ventrolateral PFC. In Monkey B, the lesion extended into dorsal premotor areas and in Monkey F it extended into the dorsolateral and ventrolateral PFC and premotor areas. Lesion volume analysis showed that Monkey B and Monkey F sustained larger lesions than Monkey L and Monkey S with a lesion volume that was more than doubled (Monkey L = 0.43 cm^3 , Monkey S = 0.51 cm^3 , Monkey B = 1.28 cm^3 , Monkey F = 1.41 cm^3).

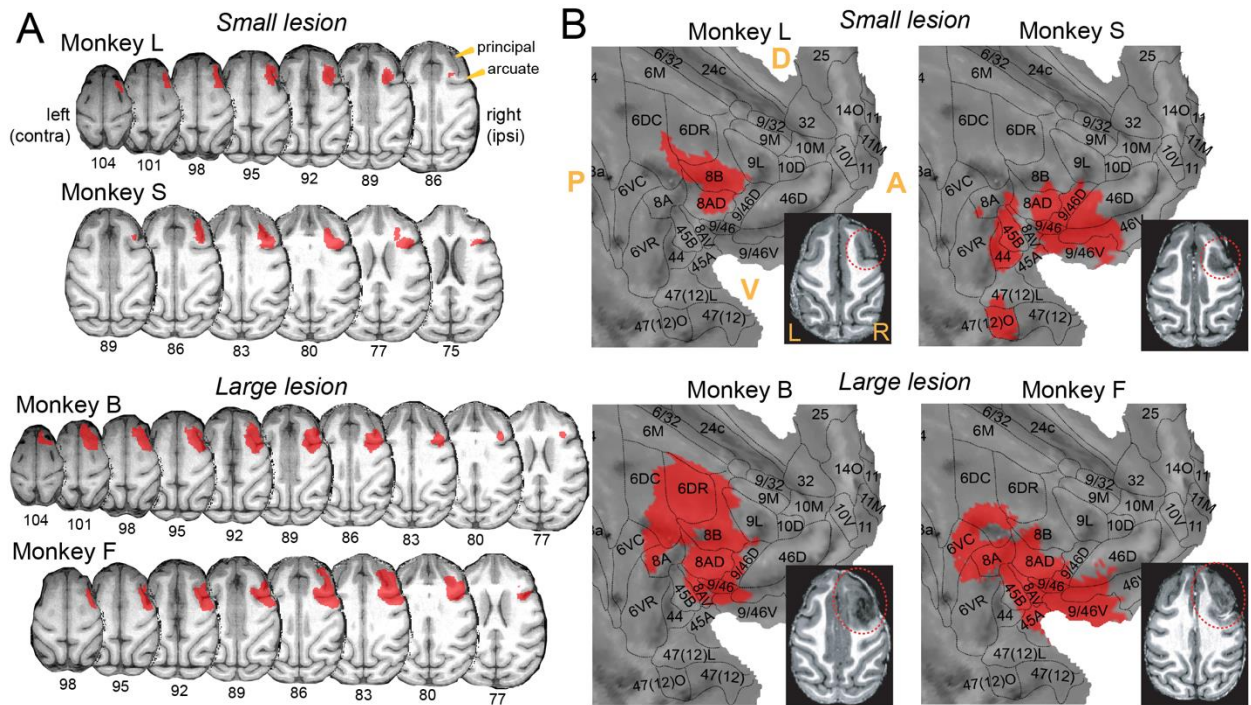


Figure 4.1. Lesion masks projected onto the macaque F99 template brain.

Each monkey's T1-weighted MP2RAGE anatomical image obtained one week post-lesion was segmented based on tissue type. Masks representing lesioned tissue were registered to the standard macaque F99 space and projected onto (A) axial slices of the macaque F99 brain and (B) cortical flat map representations of the macaque F99 right hemisphere with surface outlines that we created based on the Paxinos et al. (2000) macaque cortical parcellation scheme (Paxinos et al., 2000). Bottom right: one axial T1 image at one week post-lesion showing the lesioned tissue within the dotted red line boundary for each monkey. Abbreviations: principal = principal sulcus; arcuate = arcuate sulcus; contra = contralesional; ipsi = ipsilesional; D = dorsal; V = ventral; A = anterior; P = posterior; L = left; R = right.

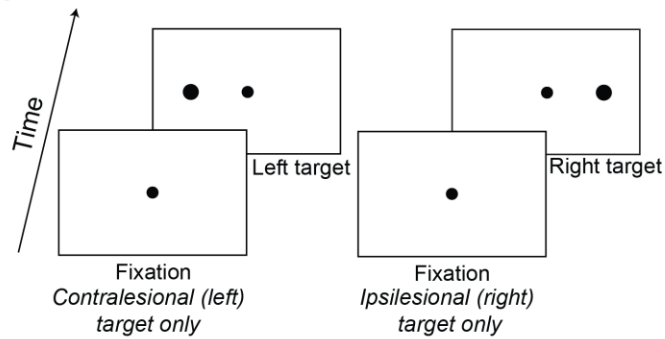
4.2.3. Behaviour

We have previously reported the saccade target selection at pre-lesion and late post-lesion (Adam et al., 2019) but here we compare behavioural performance with DW-MRI data. For a detailed report of the behavioural task design, see (Adam et al., 2019). Before the lesion was induced, monkeys were trained on a saccade task that included two randomly interleaved trial types: (1) visually-guided single target trials and (2) free-choice paired stimulus trials in which a single visual stimulus appeared in each hemifield either simultaneously or at varying stimulus onset asynchronies (SOAs) and monkeys were able to freely select either stimulus as a saccade target to receive a liquid reward (Fig. 4.2). SOA is the variable temporal delay between presentation of the contralesional and ipsilesional stimulus on the free-choice trials. Each trial began with the presentation of a fixation point, followed by either a single visual target in the contralesional (left) or ipsilesional (right) hemifield or two peripheral stimuli, with one in the contralesional and one in the ipsilesional hemifield presented at a variable SOA. Free-choice trials were used to measure the degree of extinction-like deficits, since those appear in the presence of a competing ipsilesional stimulus, whereas single target trials were used to measure the extent of neglect-like impairment. This task is able to show whether a monkey exhibits a spatially lateralized saccade selection deficit by measuring saccade choice for contralesional and ipsilesional visual stimuli.

In brief, we found that the right caudal PFC lesion induced deficits in contralesional target selection, such that there were decreased correct saccades made towards a single contralesional target (Fig. 4.3A) and decreased saccade choice of the contralesional stimulus on the free-choice trials (Fig. 4.3B,C). Deficits gradually recovered over 2-4 months post-lesion. We considered post-lesion behaviour as ‘compensated’ when task performance stabilized without further improvement. The time point for compensated

behaviour was week 8 post-lesion for the small lesion monkeys (Monkeys L and S) and week 16 post-lesion for the large lesion monkeys (Monkeys B and F); we refer to these time points collectively as ‘late post-lesion’. Detailed results on this behavioural paradigm have been previously published (Adam et al., 2020, 2019).

Single stimulus trials (*Catch trials / Measure of neglect*)



Free-choice trials (*Measure of extinction*)

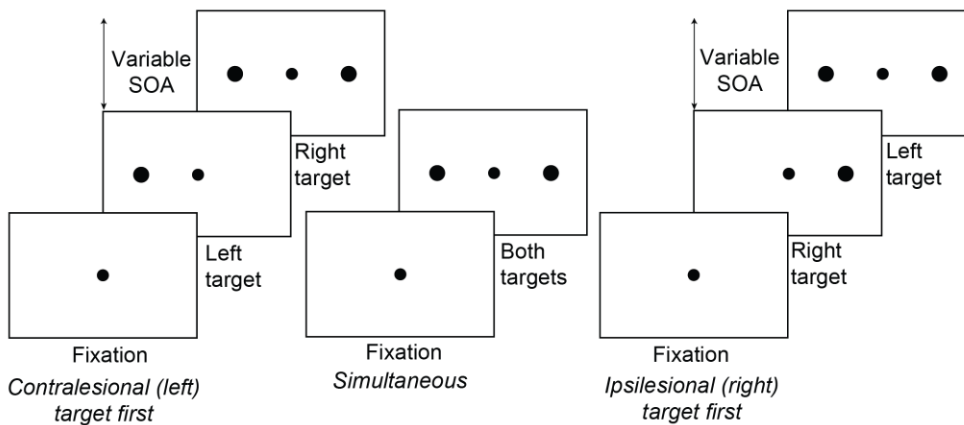


Figure 4.2. Behavioural task.

Single target and free-choice paired stimulus trials were randomly interleaved within a session. Each trial began with the presentation of a fixation point, followed by either a single target in the contralesional (left) or ipsilesional (right) hemifield or two visual stimuli in either hemifield presented at a variable stimulus onset asynchrony. Stimulus onset asynchrony was the variable temporal delay (0-256 ms) between presentation of the left and right stimulus on the free-choice paired stimulus trials. Abbreviation: SOA = stimulus onset asynchrony.

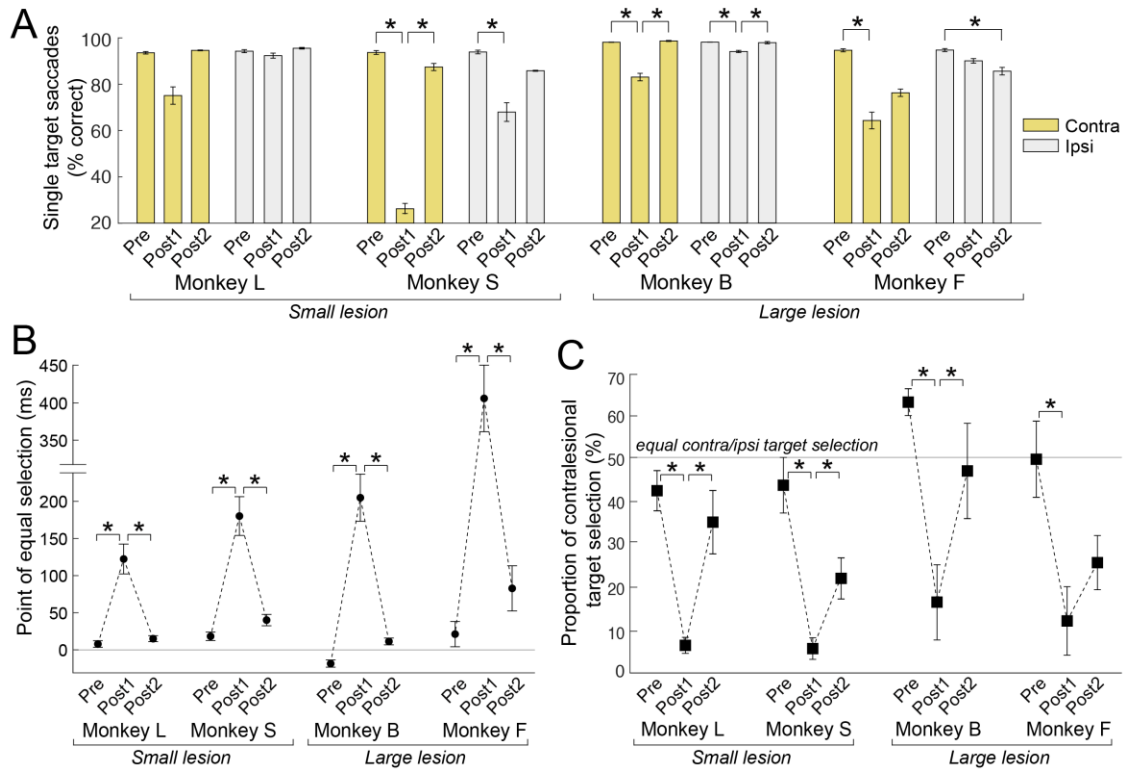


Figure 4.3. Saccade target selection deficits and compensation from pre-lesion to early and late post-lesion.

(A) The proportion of correct saccades made to a single contralesional (yellow) or ipsilesional (light grey) target. (B) Point of equal selection on the free-choice paired stimulus trials. The point of equal selection is the stimulus onset asynchrony value at which the probability of choosing the contralesional (left) or ipsilesional (right) stimulus was equal. Positive y-axis values indicate that the point of equal selection was reached at a stimulus onset asynchrony in which the contralesional stimulus was presented before the ipsilesional stimulus, which would indicate a contralesional deficit. Negative y-axis values indicate a stimulus onset asynchrony in which the ipsilesional stimulus was presented first. (C) The proportion of saccades made to contralesional stimuli on trials with simultaneous presentation of both stimuli (stimulus onset asynchrony = 0 ms) on the free-choice trials. Statistical comparisons between pre-lesion and post-lesion time points were made using one-way ANOVAs with post-hoc Tukey's tests ($p < 0.05$). Error bars represent standard error of the mean across sessions within each time point.

Abbreviations: pre = pre-lesion; post1 = early post-lesion (week 1-2 post-lesion); post2 = late post-lesion (small lesion: week 8 post-lesion; large lesion: week 16 post-lesion); contra = contralesional; ipsi = ipsilesional.

4.2.4. Image acquisition at 7T

One hour prior to scanning, monkeys were sedated with intramuscular injections of 0.05-0.2 mg/kg acepromazine (Acevet 25 mg/ml) and 5.0-7.5 mg/kg ketamine (Vetalar 100 mg/ml), followed by 2.5 mg/kg propofol (10 mg/ml). Monkeys were then intubated with an endotracheal tube and anesthesia was maintained with 1.0-1.5% isoflurane mixed with 100% oxygen. Each monkey was positioned in a custom-built MRI primate bed with its head restrained to reduce motion and then inserted into the magnet bore for image acquisition, at which point the isoflurane level was maintained at 1.0% for the duration of the image acquisition. Body temperature, respiration, heart rate, and blood oxygen saturation levels were continuously monitored and were within a normal range throughout the scans. Body temperature was maintained using thermal insulation and a heating disk.

Imaging data were collected at pre-lesion (after behavioural training), week 1 post-lesion (early post-lesion), and at week 8 or 16 post-lesion when behaviour had compensated near pre-lesion baseline (late post-lesion). Although behaviour had compensated by week 8 for Monkey S, we were only able to obtain DWI data at week 16 post-lesion. Data were acquired on a 7T Siemens MAGNETOM Step 2.3 68-cm horizontal bore scanner (Erlangen, Germany) operating at a slew rate of 300 mT/m/s. We used an in-house designed and manufactured 8-channel transmit, 24-channel receive primate head radiofrequency coil for all image acquisitions (Gilbert et al., 2016). A high-resolution T2-weighted anatomical MR image was acquired using a turbo spin echo sequence with the following parameters: TR = 7500 ms, TE = 80 ms, slices = 42, matrix size = 320 x 320, field of view = 128 x 128 mm, acquisition voxel size = 0.4 mm x 0.4 mm x 1 mm. A T1-weighted MP2RAGE anatomical image was also acquired with these parameters: TR = 6500 ms, TE = 3.15 ms, TI1 = 800 ms, TI2 = 2700 ms, field of view

= 128 x 128 mm, 0.5 mm isotropic resolution. Resting-state fMRI data were acquired and a detailed report of the fMRI acquisition has been previously published (Adam et al., 2020). In brief, we collected 4-6 10-minute runs of T2*-weighted continuous multi-band echo-planar imaging with 600 functional volumes per run using the following parameters: TR = 1000 ms, TE = 18 ms, slices = 42, slice thickness = 1 mm, and in-plane resolution = 1 mm x 1 mm.

DWI data were obtained using an interleaved echo planar imaging sequence with the following parameters: repetition time (TR) = 5100–7500 ms, echo time (TE) = 46.8–54.8 ms, number of averages = 1, number of slices = 46–54, slice thickness = 1 mm, in-plane resolution = 1 mm x 1 mm. We acquired 64 diffusion-encoding directions (b-value = 1000-1500 s/mm²) and one non-diffusion weighted volume (b-value = 0 s/mm²). Although there are slight within-subject variations in our TR (maximal difference of 1500 ms) and TE (maximal difference of 3 ms), previous work has shown no significant differences in the overall magnitude of diffusion between scans with larger differences in TR and TE (Celik, 2016). It has also been demonstrated that the mean FA in high angular resolution scans (e.g., 64 diffusion directions) was not significantly different between scans with a TR of 4000 ms or 13200 ms (Provenzale et al., 2018).

4.2.5. Image processing

Raw DWI data were converted from DICOM to NIFTI using MRIconvert (Lewis Center for Neuroimaging, University of Oregon) and reoriented to standard space using the FMRIB Software Library (FSL; <http://www.fmrib.ox.ac.uk>) tools ‘fslswapdim’ and ‘fslorient’. ASCII text files containing a list of gradient directions and b-values for each volume were also flipped and transposed to correspond with the reoriented DWI data. Data processing was then carried out using FMRIB’s Diffusion Toolbox (FDT)

implemented with FSL. First, eddy current-induced distortions and subject motion were corrected using ‘EDDY’ (Andersson and Sotiropoulos, 2016). We then performed a DTI analysis to obtain four scalar maps representing FA and mean, axial, and radial diffusivity. DTI analysis involved fitting a tensor model at each voxel using ‘DTIFIT’ on the eddy corrected DWI data. The output DTI scalar maps are directly related to the three major eigenvalues ($\lambda_1, \lambda_2, \lambda_3$) of the fitted tensor (i.e., the magnitude of diffusion for each eigenvector of the tensor). Axial diffusivity represents the magnitude of parallel diffusion and is defined as the first eigenvalue (λ_1). Radial diffusivity represents the magnitude of perpendicular diffusion and is the average of the second and third eigenvalues $[(\lambda_2 + \lambda_3)/2]$. Mean diffusivity represents the total magnitude of diffusion and is the average of all three eigenvalues $[(\lambda_1 + \lambda_2 + \lambda_3)/3]$. Fractional anisotropy represents the degree of anisotropy and is calculated as the relative difference of the first eigenvalue compared to the other two eigenvalues $[\sqrt{\frac{(\lambda_1 - \lambda_2)^2 + (\lambda_2 - \lambda_3)^2 + (\lambda_1 - \lambda_3)^2}{2(\lambda_1^2 + \lambda_2^2 + \lambda_3^2)}}]$ (Alexander et al., 2007; Basser et al., 1994; Basser and Pierpaoli, 1996; Beaulieu, 2002).

Next, a multiple tensor model was fit at each voxel using ‘BEDPOSTX’ which estimates two fiber orientations per voxel to account for crossing fibers and more accurately generate probability distributions of local fiber orientations (Behrens et al., 2007, 2003b). This Bayesian estimation of multiple fiber directions vastly improves sensitivity when fiber tracking non-dominant pathways through regions of crossing fibers, such as the SLF (anterior-posterior) that has been traditionally difficult to track due to crossing dorsal-ventral projections in the more dominant corona radiata white matter bundle (Behrens et al., 2007). Transformation matrices were derived within subjects for each session from diffusion space to pre-lesion structural T2 space using a rigid-body transformation with 6 degrees of freedom using FSL’s ‘FLIRT’ (Jenkinson et al., 2002). The inverse

transformation matrix from this registration was then used to register the seed masks from structural to diffusion space for the probabilistic tractography analysis. We have previously published preprocessing details for the resting-state fMRI data (Adam et al., 2020). Briefly, Resting-state fMRI data was processed using FSL and included brain extraction, MCFLIRT motion correction (6-parameter affine transformation), spatial smoothing (FWHM = 3 mm), high-pass temporal filtering, and registration to the standard macaque F99 template.

4.2.6. *DWI tractography analysis*

Regions of interest for tractography

We reconstructed the contralesional and ipsilesional SLF and the transcallosal PFC and PPC tracts using bilateral seed regions (radius = 2 mm) created in pre-lesion structural T2 space for each subject. Seeds were placed in the frontal eye field (FEF) of the caudal PFC and in the lateral intraparietal area (LIP) of the PPC based on the (Saleem and Logothetis, 2006) rhesus monkey anatomical atlas. FEF seeds were placed in the anterior bank of the arcuate sulcus (Tehovnik et al., 2000) and LIP seeds were in the lateral bank of the intraparietal sulcus (Lewis and Van Essen, 2000). FEF and LIP constitute the main cortical nodes of the frontoparietal network (Wardak et al., 2011) and have been previously used to track these fibers in rhesus macaques (Hofer et al., 2008). Figure 4.4A shows representative seed mask locations in pre-lesion structural T2 space. The following seed region pairs were used in a probabilistic tractography analysis (described below) to reconstruct the four tracts of interest: bilateral FEF seeds were used to track the transcallosal PFC fiber tracts (Barbas and Pandya, 1984; Hofer et al., 2008); bilateral LIP seeds were used to track the transcallosal PPC tracts (Hofer et al., 2008); contralesional

FEF and LIP seeds were used to track the contralesional SLF; and the ipsilesional FEF and LIP seeds were used to track the ipsilesional SLF (Petrides and Pandya, 1984; Schmahmann et al., 2007; Thiebaut de Schotten et al., 2012) (Fig. 4.4B). A midline sagittal exclusion mask was used to restrict tracking to the opposite hemisphere for the SLF association tracts and an axial exclusion mask at the anterior-posterior midpoint of the corpus callosum was used to restrict tracking to the anterior half of the brain for the transcallosal PFC tract or to the posterior half of the brain for the transcallosal PPC tract.

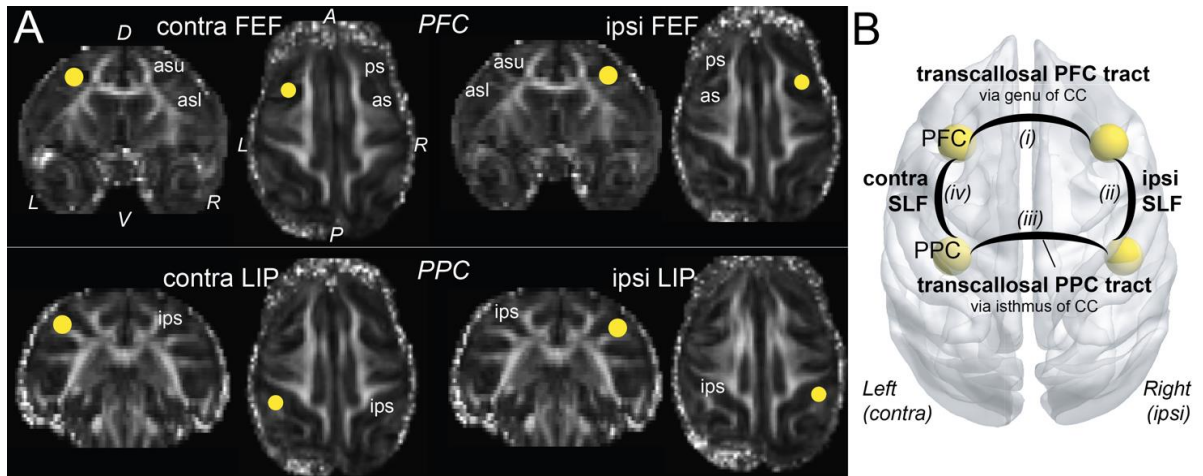


Figure 4.4. Seed masks to reconstruct fiber tracts of interest using probabilistic tractography.

(A) Representative seed masks in bilateral FEF and LIP overlaid on FA maps in native T2 space shown at coronal and axial sections. Similar seeds were created for each monkey in native pre-lesion T2 space. (B) Schematic of the white matter tracts of interest. Probabilistic streamlines were generated for the (i) transcallosal PFC tract using bilateral FEF seeds, (ii) ipsilesional SLF association tract connecting the PFC and PPC using ipsilesional FEF and LIP seeds, (iii) transcallosal PPC tract using bilateral LIP seeds, and (iv) contralesional SLF association tract connecting the PFC and PPC using contralesional FEF and LIP seeds. Abbreviations: D = dorsal, V = ventral, L = left, R = right, contra = contralesional, ipsi = ipsilesional, A = anterior, P = posterior, as = arcuate sulcus, asu = upper limb of the arcuate sulcus, asl = lower limb of the arcuate sulcus, ips = intraparietal sulcus, ps = principal sulcus, FEF = frontal eye field, LIP = lateral intraparietal area, PFC = prefrontal cortex, PPC = posterior parietal cortex, SLF = superior longitudinal fasciculus, CC = corpus callosum.

Probabilistic tractography analysis

Probabilistic tractography was computed with FDT's 'ProbtrackX' which uses the output from BEDPOSTX to estimate the number of streamlines that traveled between two seed regions for each voxel (Behrens et al., 2007, 2003a). We used the following ProbtrackX standard parameters: number of sample streamlines sent out per seed voxel = 5000, curvature threshold = 0.2, step length = 0.5, maximum number of steps = 2000, subsidiary fibre volume threshold = 0.01. Distance correction was additionally implemented to correct for the decrease in streamlines with distance from the seed region. For each of the 5000 streamlines per seed voxel sampled from the BEDPOSTX probability distribution, a 'successful' streamline was one that originated from one seed and reached the other. This algorithm outputs a streamline density map where individual voxel intensities represent the number of successful streamlines that passed through the voxel. This procedure also outputs the 'waytotal' for each seed, which is the total number of streamlines that originated from that seed and successfully made it to the other seed. The streamline density map was then normalized by dividing it by the waytotal sum ($\text{waytotal}_{\text{seedA}} + \text{waytotal}_{\text{seedB}}$), which yielded voxel intensities that now represent the probability of that voxel being part of that tract. In contrast to methods that normalize streamline density maps using a constant proportion of the total number of streamlines sent out per voxel, proportional normalization based on the waytotal sum is the preferred approach when comparing reconstructed fiber tracts across sessions since it accounts for any differences in seeded voxels across sessions that may have affected trackability (Bennett et al., 2011). Streamline probability maps were then thresholded to maintain only voxels with intensities of at least 50% (i.e., a minimum of 50% probability that the voxel belongs to that streamline) and then visually inspected to confirm anatomical plausibility. Note that these suprathreshold white matter voxels are not necessarily

exclusively part of the fiber tract of interest, but this probabilistic tractography approach gives a better approximation of the tract-related voxels compared to traditional approaches that use pre-defined region of interest FA mask without tractography. These normalization and thresholding procedures have been used for probabilistic tractography analysis (Cunningham et al., 2017; Galantucci et al., 2011; Gray et al., 2018; Latzman et al., 2015). Thresholded streamline probability maps representing the tracts of interest were generated for each subject and each session individually. These white matter fiber tracts have been previously identified in nonhuman primates using DWI tractography (Hofer et al., 2008; Hofer and Frahm, 2008; Schaeffer et al., 2017; Schmammann et al., 2007; Thiebaut de Schotten et al., 2012) and tracer methods (Barbas and Pandya, 1984; Petrides and Pandya, 1984). Figure 4.5 shows a representative sample of the reconstructed fiber tracts and the average streamline probability values for each tract are reported in Table 4.1.

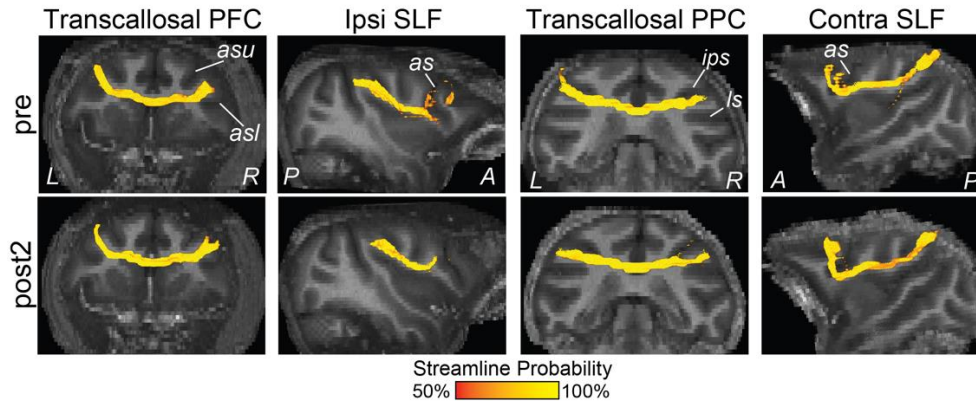


Figure 4.5. Representative white matter tracts reconstructed with probabilistic tractography.

First column: bilateral FEF seeds revealed transcallosal streamlines between the bilateral PFC that traveled across hemispheres through the rostral portion, or genu, of the corpus callosum. Second column: ipsilesional FEF and LIP seeds revealed the ipsilesional SLF association fibers connecting frontal and parietal areas. Third column: bilateral LIP seeds revealed transcallosal streamlines between bilateral PPC that traveled across hemispheres through a posterior region (isthmus) of the corpus callosum. Fourth column: contralesional FEF and LIP seeds revealed the contralesional SLF association fibers connecting frontal and parietal areas. The colour bar represents streamline probabilities for each voxel in the thresholded tracts. Streamline probability maps are shown overlaid on a T2 coronal or parasagittal slice. Abbreviations: pre = pre-lesion, post2 = late post-lesion, A = anterior, P = posterior, L = left, R = right, PFC = prefrontal cortex, PPC = posterior parietal cortex, SLF = superior longitudinal fasciculus, contra = contralesional, ipsi = ipsilesional, as = arcuate sulcus, asu = upper limb of the arcuate sulcus, asl = lower limb of the arcuate sulcus, ips = intraparietal sulcus, ls = lateral sulcus.

Table 4.1. Average streamline probability of the suprathreshold voxels in the reconstructed white matter fiber tracts.

Tract	Time since lesion	Monkey L			Monkey S			Monkey B			Monkey F		
		No. of voxels	Mean	SEM	No. of voxels	Mean	SEM	No. of voxels	Mean	SEM	No. of voxels	Mean	SEM
PFC–PFC	Pre	888	87.3	0.56	641	88.6	0.66	1199	83.5	0.52	1211	84.6	0.50
	Post2	926	87.3	0.56	1126	87.1	0.51	1119	87.5	0.5	1151	82.4	0.56
Ipsi SLF	Pre	1949	81.4	0.41	801	82.6	0.66	1073	84.6	0.55	995	80.7	0.58
	Post2	930	82.2	0.61	1943	77.7	0.41	865	81.9	0.64	1498	75.1	0.48
PPC–PPC	Pre	1519	85.2	0.46	917	84.6	0.6	1653	85.9	0.43	1763	84.5	0.43
	Post2	1797	95.3	0.27	1141	85	0.55	1819	85.2	0.42	1604	84.3	0.46
Contra SLF	Pre	936	85.7	0.6	1072	85	0.55	1089	82.4	0.56	1421	80.4	0.49
	Post2	912	85.5	0.59	1047	85.3	0.55	1011	84	0.57	1421	78.8	0.49

All values were derived from thresholded probabilistic tracts with a minimum streamline probability of 50%. Abbreviations: No. = number; PFC = prefrontal cortex, PPC = posterior parietal cortex, SLF = superior longitudinal fasciculus, SEM = standard error of the mean, pre = pre-lesion, post2 = late post-lesion, ipsi = ipsilesional, contra = contralesional.

4.2.7. *Tract-specific DTI parameters*

Here, we masked the four DTI scalar maps with the reconstructed tracts to obtain tract-specific measures of FA and mean, axial, and radial diffusivity at pre-lesion and late post-lesion. Previous studies have also obtained tract-specific measures of diffusivity and anisotropy since it takes fiber orientation into account, rather than only measuring diffusion parameters within pre-defined regions of interest without using masks generated from fiber tractography (Bennett et al., 2011; Galantucci et al., 2011; Ge et al., 2013; Gray et al., 2018; Lindenberg et al., 2012). First, the reconstructed thresholded tracts were binarized and only those voxels that overlapped in both the pre-lesion and late post-lesion binarized tracts were retained. This conservative approach accounts for any misalignment among individual tracts between time points. For the transcallosal tracts whose diffusion is largely oriented along the left-right x-direction (transcallosal PFC and PPC tracts), voxels within an x-coordinate range that were shared between pre-lesion and late pre-lesion tracts were retained. For the SLF association tracts whose diffusion is largely oriented along the anterior-posterior y-direction, voxels within a shared y-coordinate range in both pre-lesion and late post-lesion tracts were retained. Next, we masked DTI scalar maps with the binarized tracts to obtain tract-wise measures of FA and mean, axial, and radial diffusivity. We additionally calculated the average segment-wise FA values of three discrete segments along the length of each tract. Transcallosal PFC and PPC tracts were divided along the x-direction into contralesional/left, middle, and ipsilesional/right segments and SLF tracts were divided along the y-direction into anterior, middle, and posterior segments. This segment-wise spatial FA analysis may reveal important information about whether FA is uniform along the length of a tract and could identify whether local FA changes within one segment was driving changes in the average tract-wise FA (Colby et al., 2012; Davis et al., 2009). Tract-specific DTI metrics

were statistically compared between pre-lesion and late post-lesion using two-sample t-tests ($p < 0.05$) with FDR correction for multiple comparisons within each subject.

4.2.8. Relationship between tract-wise FA and the rsFC of grey matter areas connected by that white matter fiber tract

We have previously reported the rsFC changes in these subjects along similar time points (Adam et al., 2020). Here, we compared changes in tract-wise FA with rsFC between cortical areas connected by that fiber tract. Bilateral seed regions of interest (radius = 2 mm) for the rsFC analysis were placed in areas of the resting-state frontoparietal network (Hutchison et al., 2012), including two major caudal PFC areas [FEF and 9/46D (DLPFC)] and nine PPC areas [PE, PEa, PEC, PF, PFG, POa (LIP), POaE, POaI, Opt]. Caudal PFC areas are connected within hemisphere to the PPC areas via the SLF (Schmahmann et al., 2007). To compare tract-wise FA with rsFC, we extracted the average rsFC between groups of seed regions that corresponded to our tracts of interest: (1) contralesional and ipsilesional PFC seeds correspond with the transcallosal PFC tract, (2) ipsilesional PFC and PPC seeds correspond ipsilesional SLF, (3) contralesional and ipsilesional PPC seeds correspond with the transcallosal PPC tract, and (4) contralesional PFC and PPC seeds correspond with contralesional SLF. To obtain the rsFC between groups of seed regions, the average blood-oxygen level-dependent (BOLD) signal timecourse was first obtained for each seed and Pearson's r correlation coefficients were computed between the BOLD signal timecourse of every pair of seeds, while regressing out the white matter and cerebrospinal fluid BOLD timecourse as noise. Fisher's r -to- z transformation was applied to convert the correlation coefficients into z -scores, where z -scores denote the rsFC between seed regions. We averaged across the 4-6 z -score rsFC matrices for each session per subject, resulting in one rsFC matrix for pre-lesion and late

post-lesion. For instance, to calculate the rsFC between contralesional PFC and PPC seed regions for comparison with the FA of the contralesional SLF, we took the $|z\text{-score}|$ between the FEF and each of the nine PPC areas and the $|z\text{-score}|$ between area 9/46D (DLPFC) and the nine PPC areas in the contralesional hemisphere, and used the average $|z\text{-score}|$ as a rsFC index corresponding to the contralesional SLF. We statistically compared the $|z\text{-scores}|$ (absolute rsFC) using two-sample t-tests with FDR correction for multiple comparisons ($p < 0.05$) from pre-lesion to late post-lesion.

4.3. Results

4.3.1. Longitudinal changes in the tract-specific DTI parameters

White matter tracts of interest were reconstructed using probabilistic tractography and used to extract tract-specific DTI parameters (FA and mean, axial, and radial diffusivity) from DTI scalar maps. Average values were calculated across the voxels of each tract within an overlapping x- or y-coordinate range between pre-lesion and late post-lesion. While we show results from all four tracts of interest, our main focus is on the remote fiber tracts that were not directly affected by the lesion, namely the contralesional SLF and transcallosal PPC tract.

In Monkey L, two-sample t-tests revealed that all four tracts showed significantly increased FA and decreased radial diffusivity from pre-lesion to late post-lesion, when behaviour had compensated (Fig. 4.6A,D). In addition, transcallosal PFC, contralesional SLF, and transcallosal PPC tracts had significantly decreased mean diffusivity, whereas the ipsilesional SLF had decreased axial diffusivity (Fig. 4.6B,C). For Monkey S, transcallosal PFC tract showed decreased FA whereas contralesional SLF and

transcallosal PPC tracts showed increased FA (Fig. 4.6A). Both transcallosal PFC and ipsilesional SLF also showed increased mean, axial, and radial diffusivity, whereas transcallosal PPC and contralesional SLF showed decreased radial diffusivity (Fig. 4.6B–D). Lastly, contralesional SLF showed increased axial diffusivity (Fig. 4.6C). Findings shared by both small lesion monkeys were that the remote contralesional SLF and transcallosal PPC tracts showed increased FA and decreased radial diffusivity when behaviour had compensated.

In Monkey B, transcallosal PFC and ipsilesional SLF showed significantly decreased FA and increased mean, axial, and radial diffusivity (Fig. 4.6A–D). Transcallosal PPC showed decreased FA and increased mean and radial diffusivity and lastly, contralesional SLF showed decreased mean and axial diffusivity. In Monkey F, decreased FA and increased radial diffusivity was found in all four tracts from pre-lesion to late post-lesion (Fig. 4.6A,D). In addition, transcallosal PFC and PPC tracts showed increased mean diffusivity (Fig. 4.6B), whereas contralesional and ipsilesional SLF showed decreased axial diffusivity (Fig. 4.6C). Findings shared by both large lesion monkeys were that (1) transcallosal PFC and transcallosal PPC showed decreased FA and increased mean and radial diffusivity, (2) ipsilesional SLF showed decreased FA and increased radial diffusivity, and (3) contralesional SLF showed decreased axial diffusivity.

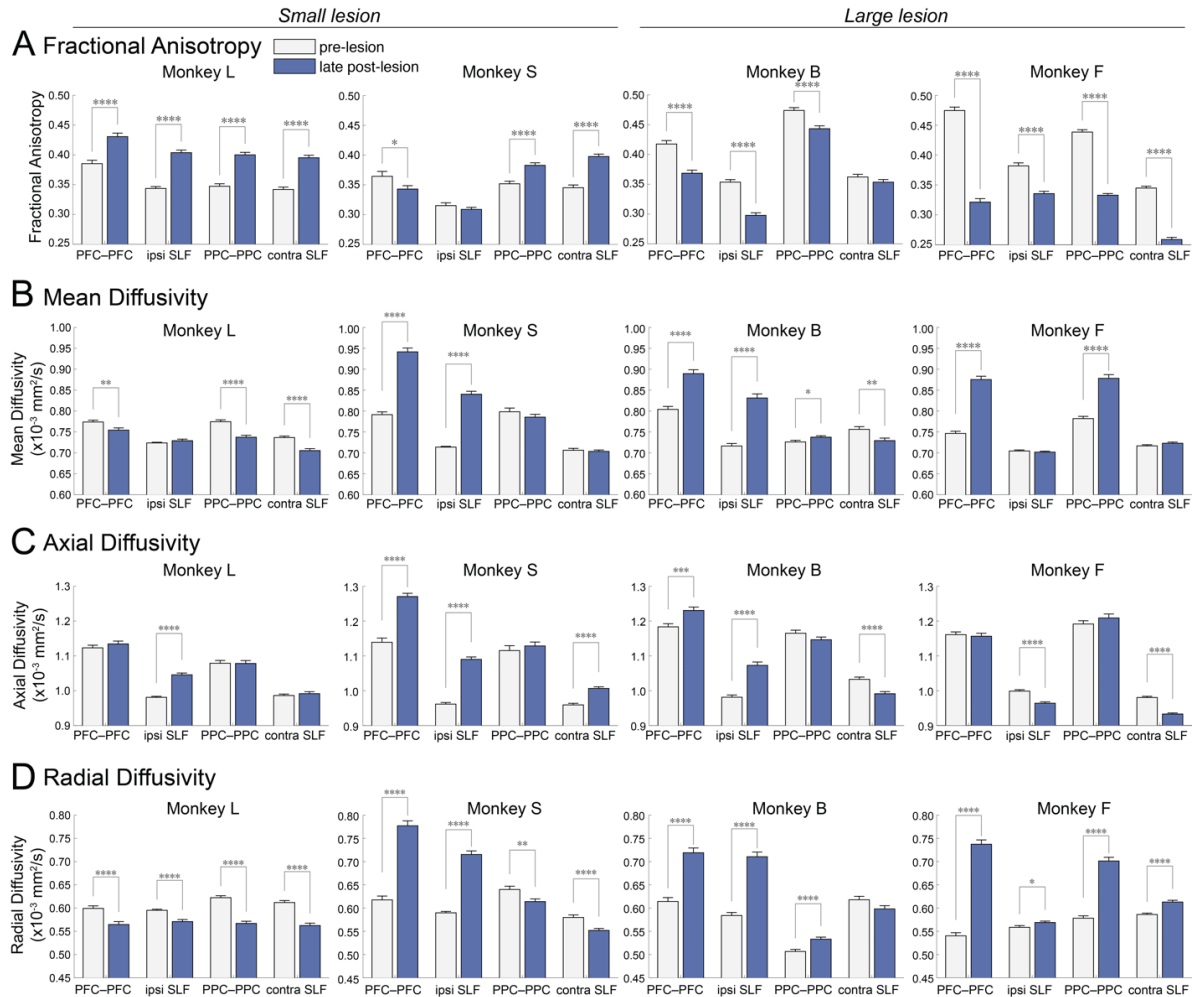


Figure 4.6. Changes in the average tract-wise DTI parameters over time.

White matter tracts of interest were reconstructed with probabilistic tractography and then used to extract tract-specific measures of (A) fractional anisotropy, (B) mean diffusivity, (C) axial diffusivity, and (D) radial diffusivity. Statistical comparisons between pre-lesion and late post-lesion were made using two-sample t-tests with FDR correction for multiple comparisons (* = $p < 0.05$, ** = $p < 0.01$, *** = $p < 0.001$, **** = $p < 0.0001$). Error bars represent standard error of the mean across voxels. Abbreviations: pre = pre-lesion, post2 = late post-lesion (behavioural compensation time point), PFC-PFC = transcallosal PFC tract, PPC-PPC = transcallosal PPC tract, SLF = superior longitudinal fasciculus, ipsi = ipsilesional, contra = contralesional.

4.3.2. Longitudinal changes of segment-wise FA in white matter fiber tracts

Here, we divided each tract into three segments to test whether FA changes were uniform along the length of the tract and to identify which segments likely drove the overall tract-wise FA. Transcallosal PFC and PPC tracts were divided along the x-direction into contralesional/left, middle, and ipsilesional/right segments and the SLF tracts were divided along the y-direction into anterior, middle, and posterior segments. Average FA was calculated for each segment and compared between pre-lesion and late post-lesion. In Monkey L, we found increased FA in the majority of segments across the four tracts (Fig. 4.7), except for the two segments closest to the lesion site (i.e., ipsilesional segment of the transcallosal PFC tract and anterior segment of the ipsilesional SLF) and the contralesional segment of the transcallosal PPC tract, which showed no change. In Monkey S, we found decreased FA in the middle segment of the transcallosal PFC tract and in the anterior segment of ipsilesional SLF (Fig. 4.7). In Monkey B, we found decreased segment-wise FA in the lesion-affected ipsilesional SLF and transcallosal PFC tracts and increased FA in the middle segment of the remote contralesional SLF and transcallosal PPC tracts (Fig. 4.7). In Monkey F, decreased FA was found in all tract segments, except for increased FA in the anterior segment of ipsilesional SLF (Fig. 4.7).

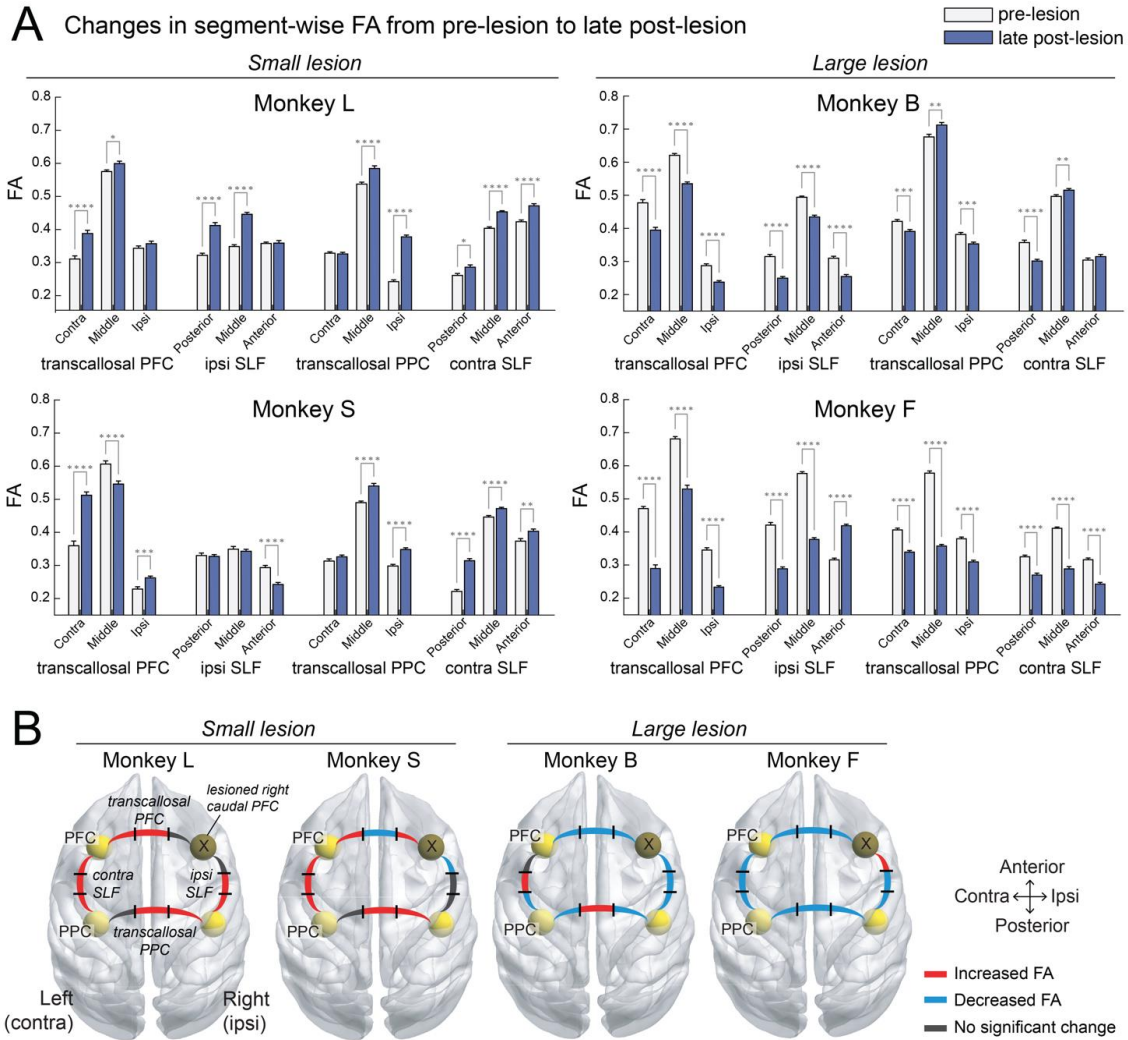


Figure 4.7. Changes in segment-wise FA from pre-lesion to late post-lesion.

(A) White matter tracts were divided into three segments. Transcallosal PFC and PPC tracts were divided into contralesional/left, middle, and ipsilesional/right segments, and SLF tracts were divided into anterior, middle, and posterior segments. Average FA was extracted for each segment and compared between pre-lesion and late post-lesion using two-sample t-tests with FDR correction (* = $p < 0.05$, ** = $p < 0.01$, *** = $p < 0.001$, **** = $p < 0.0001$). Error bars represent standard error of the mean across voxels. (B) Schematic summary of the segment-wise FA changes from pre-lesion to late post-lesion. Tract segments are illustrated with black lines dividing each segment. Red indicates increased FA ($p < 0.05$), blue indicates decreased FA ($p < 0.05$), and grey represents no significant change in FA. PFC = prefrontal cortex, SLF = superior longitudinal fasciculus, PPC = posterior parietal cortex, contra = contralesional, ipsi = ipsilesional.

4.3.3. Relationship between white matter microstructure and resting-state FC

We have previously published the changes in rsFC of the frontoparietal network in these subjects (Adam et al., 2020). Here, we examined the relationship between changes in the tract-wise FA with the corresponding change in rsFC (Table 4.2). We made the following rsFC–FA comparisons: (1) rsFC between contralesional PFC and PPC seeds with the FA of the contralesional SLF, (2) rsFC between ipsilesional PFC and PPC seeds with the FA of the ipsilesional SLF, (3) rsFC between bilateral PFC seeds with the FA of the transcallosal PFC tract, and (4) rsFC between bilateral PPC seeds with the FA of the transcallosal PPC tract.

The rsFC between contralesional PFC–PPC (corresponding to contralesional SLF) was increased from pre- to late post-lesion across the four monkeys, except this effect was not significant for Monkey F (Table 4.2). In the two small lesion monkeys, Monkey L and Monkey S, this increased rsFC corresponded with the increased tract-wise FA in the contralesional SLF (Fig. 4.8). However, the two large lesion monkeys (Monkeys B and F) did not show a corresponding FA increase in contralesional SLF; instead FA had decreased in both monkeys, but this effect was not significant for Monkey B (see Fig. 4.6). Monkey S additionally showed decreased rsFC between bilateral PFC, which corresponded with decreased FA in the transcallosal PFC tract (Fig. 4.8), and decreased rsFC in ipsilesional SLF (Table 4.2). In Monkey B, increased rsFC was found in all comparisons which were inconsistent with the decreased FA found in those tracts (Fig. 4.8). Monkey F showed decreased rsFC between bilateral PFC which corresponded with decreased FA in the transcallosal PFC tract. Overall, the direction of rsFC changes largely matched the changes in tract-wise FA in the small lesion monkeys, but not in the large lesion monkeys.

Table 4.2. Changes in resting-state FC between frontoparietal areas of interest.

Seed regions	Time	Monkey L			Monkey S			Monkey B			Monkey F		
		rsFC			rsFC			rsFC			rsFC		
		Mean	SEM	<i>p</i>	Mean	SEM	<i>p</i>	Mean	SEM	<i>p</i>	Mean	SEM	<i>p</i>
Bilateral PFC	Pre	0.11	0.01	0.649	0.25	0.02	0.028	0.26	0.04	0.003	0.38	0.06	0.054
	Post2	0.10	0.01		0.18	0.01		0.43	0.02		0.26	0.02	
Ipsilesional PFC-PPC	Pre	0.06	0.01	0.156	0.13	0.01	0.027	0.19	0.04	0.017	0.33	0.02	0.001
	Post2	0.08	0.01		0.08	0.01		0.30	0.02		0.21	0.01	
Bilateral PPC	Pre	0.10	0.01	0.997	0.19	0.03	0.492	0.27	0.04	0.019	0.51	0.03	0.873
	Post2	0.10	0.01		0.17	0.00		0.38	0.02		0.50	0.02	
Contralesional PFC-PPC	Pre	0.06	0.01	0.001	0.13	0.02	0.048	0.20	0.04	0.001	0.40	0.05	0.644
	Post2	0.12	0.01		0.19	0.01		0.47	0.03		0.42	0.02	

Abbreviations: pre = pre-lesion, post2 = late post-lesion (behavioural recovery time point), contra = contralesional, ipsi = ipsilesional, SEM = standard error of the mean. *P* values indicate significance value for rsFC comparisons between pre- and post-lesion.

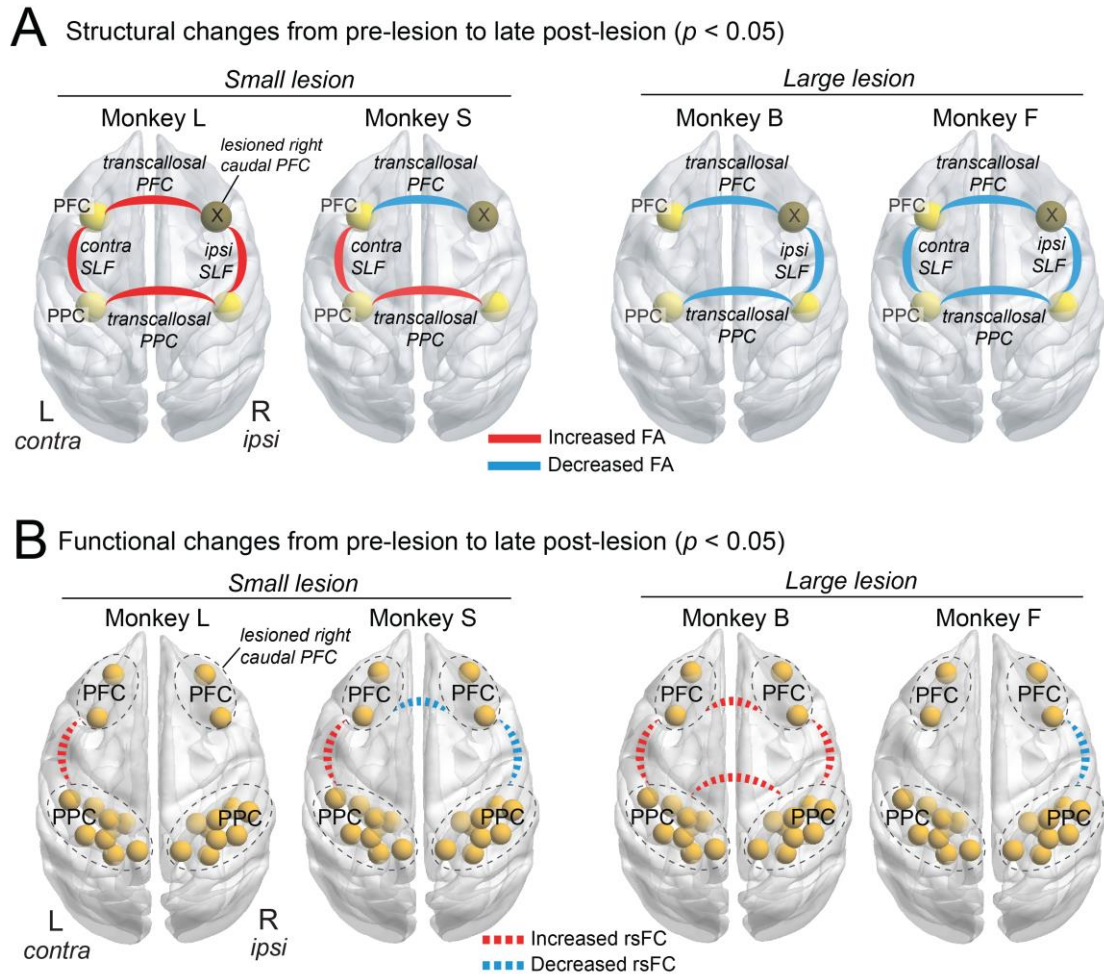


Figure 4.8. Schematic summary of the changes in tract-specific FA and rsFC.

(A) Changes in the tract-wise mean FA for each white matter tract of interest from pre-lesion to late post-lesion, when behavioural performance had compensated. Solid red lines indicate significantly increased FA and solid blue lines indicate significantly decreased FA. (B) Resting-state FC changes that correspond to the white matter tracts of interest. Resting-state FC was calculated as the average absolute z-score between all pairwise seed regions and compared with the FA of the corresponding white matter tract. Dotted red lines indicate significantly increased FC and dotted blue lines indicate significantly decreased FC. Statistical comparisons between pre-lesion and late post-lesion were made using two-sample t-tests with FDR correction for multiple comparisons ($p < 0.05$). Abbreviations: PFC = prefrontal cortex, SLF = superior longitudinal fasciculus, PPC = posterior parietal cortex, contra = contralesional, ipsi = ipsilesional.

4.4. Discussion

In this longitudinal DWI study, we used probabilistic tractography to investigate microstructural changes in frontoparietal white matter tracts after right caudal PFC lesions in macaque monkeys. DTI metrics were obtained within each tract and compared from pre-lesion to late post-lesion, when behavioural performance on a saccade choice task had largely recovered. We have previously published detailed reports of the behaviour and resting-state fMRI data in these subjects (Adam et al., 2020, 2019). Here, we found that tract-wise FA in remote contralesional SLF and transcallosal PPC tract was differentially altered based on lesion size, with increased FA after small PFC lesions (Monkeys L and S) and decreased FA after larger lesion (Monkeys B and F). This study also highlights the importance of evaluating segment-wise FA since the changes in FA were not always uniform along the length of a fiber tract. The lack of consistent or compensatory changes in network-wide rsFC and FA after larger lesions may suggest the recruitment of alternate pathways beyond the cortical frontoparietal network to support the behavioural recovery.

4.4.1. *White matter degeneration in the lesion-affected white matter tracts*

White matter alterations after a focal lesion initially occur locally in perilesional tissue and along fiber tracts directly connected to the site of the lesion by anterograde (i.e., Wallerian) and retrograde axonal degeneration (Beaulieu, 2002; Pierpaoli et al., 2001; Thomalla et al., 2004; Werring et al., 2000). These changes in perilesional tissue microstructure have been studied using measures of FA from DWI studies in stroke patients (Pierpaoli et al., 2001; Thomalla et al., 2004; Umarova et al., 2017; Werring et al., 2000). In this section, we discuss the microstructural changes in the lesion-affected

ipsilesional SLF and transcallosal PFC tracts (i.e. tracts that directly innervate the lesioned right caudal PFC).

Ipsilesional SLF and transcallosal PFC tracts in Monkey S, Monkey B, and Monkey F show decreased FA and increased radial diffusivity. DTI studies in stroke patients have also reported decreased FA and increased radial diffusivity in lesion-affected white matter tracts (Dacosta-Aguayo et al., 2014; Schaechter et al., 2009; Umarova et al., 2017). Previous reports of white matter degeneration on DWI suggest that this pattern of microstructural changes reflects myelin breakdown in axons directly connected to the lesion site (Beaulieu, 2002; Pierpaoli et al., 2001; Werring et al., 2000). Degeneration of the normal white matter tissue structure is thought to expand the extracellular space between axons, allowing water molecules to diffuse more freely (i.e., more isotropic diffusion) and manifesting as decreased FA. In Monkey S, segment-wise FA analysis of the transcallosal PFC tract revealed that only the middle segment showed a decreased FA, which likely drove the decreased tract-wise FA for that tract. This may be due to FA changes within other prefrontal fibers traversing the genu of the corpus callosum that were not picked up by our tractography analysis and may have been more impacted by the lesion.

In contrast, Monkey L showed increased FA in ipsilesional SLF and transcallosal PFC tracts at late post-lesion. Since Monkey L sustained the smallest and most focal lesion, it is possible that there was a relatively greater number of preserved/undamaged axonal fibers from the lesioned caudal PFC traveling within hemisphere via ipsilesional SLF or between hemispheres via transcallosal PFC fibers. Spared fibers may have allowed for optimal neural compensation strategies to take place by way of local plasticity in the perilesional tracts (Murphy and Corbett, 2009). While increased FA in ipsilesional SLF and transcallosal PFC tracts in Monkey L may be viewed as the outcome of adaptive

plasticity for behavioural recovery, these findings should be interpreted with caution since DWI changes in lesion-affected tracts may be confounded by direct lesion pathology (Pierpaoli et al., 2001).

4.4.2. Transneuronal degeneration or compensation in remote fiber tracts

Over several days to weeks following the initial degeneration of fibers directly connected to the lesion, white matter atrophy may take place in remote areas indirectly connected to the lesion. Fibers connected to the lesion across multiple synapses may undergo anterograde transneuronal degeneration due to loss of excitatory input and retrograde transneuronal degeneration due to loss of trophic support (Baron et al., 2014; Fornito et al., 2015; Grayson et al., 2017; Zhang et al., 2012). The extent of transneuronal degeneration likely depends on the initial lesion size and location (Thiel et al., 2010; Wasserman and Schlichter, 2008). Here, we focus on the remote fiber tracts that are indirectly connected to the lesioned right caudal PFC, namely the contralesional SLF and transcallosal PPC tracts. Transneuronal degeneration may appear on DWI as decreased FA, decreased axial diffusivity, and/or increased radial diffusivity in white matter tracts remote from the lesion (Beaulieu, 2002). These diffusion changes may reflect a combination of degenerative changes, including decreased fiber density, demyelination, and axonal loss (Sotak, 2002).

We found evidence of transneuronal degeneration in the contralesional SLF and transcallosal PPC tracts in the two large lesion monkeys, but not in the small lesion monkeys. Specifically, Monkey B showed decreased FA and increased radial diffusivity in transcallosal PPC and decreased axial diffusivity in contralesional SLF. Monkey F showed decreased FA and increased radial diffusivity in both tracts and additionally decreased axial diffusivity in contralesional SLF. Several lines of evidence support our

finding of decreased FA in remote fiber tracts only after larger lesions and more severe/lasting deficits. DWI studies have reported that, compared to patients with mild or recovered neglect, patients with severe or persistent deficits showed decreased FA in the posterior corpus callosum, which provides the communication link between parietal areas in the damaged and intact hemispheres (Bozzali et al., 2012; Lunven et al., 2015), or decreased FA between contralesional frontoparietal areas (Umarova et al., 2014). Similarly, in a longitudinal study of neglect, Umarova et al. (2017) reported that the degree of unrecovered neglect correlated strongly with white matter degeneration in the intact hemisphere between contralesional frontoparietal pathways (Umarova et al., 2017). This finding has also been demonstrated in one other study in chronic stroke patients recovering from motor-related deficits, such that poorly recovered patients had reduced FA in both ipsilesional and contralesional corticospinal tracts, whereas well-recovered patients showed increased FA in those tracts compared to healthy controls (Schaechter et al., 2009). Alternatively, decreased FA in remote tracts after larger lesions may not necessarily underlie the severity or persistence of deficits, but may instead reflect an epiphenomenon of larger lesions (Umarova et al., 2017). It is possible that the lesions in Monkeys L and S were not large enough to induce transneuronal degeneration. However, we are unable to conclude whether the white matter abnormalities in the remote contralesional SLF and transcallosal PPC tracts are a result of larger lesions (Thiel et al., 2010; Wasserman and Schlichter, 2008) or whether they are associated with the severity and persistence of behavioural deficits. In addition, the segment-wise FA analysis in Monkey B showed increased FA in the middle segments of contralesional SLF and transcallosal PPC tracts that were averaged out in the tract-wise mean FA. This increased FA may represent an adaptive change that supports behavioural recovery, since Monkey B showed a greater degree of recovery than Monkey F. However, It would be valuable for future studies to test whether these spatial differences in FA along fiber tracts are due

to true microstructural alterations or reflect artifacts from crossing fibers (Jones et al., 2013).

In contrast, the two small lesion monkeys (Monkeys L and S) showed increased FA and decreased radial diffusivity in the remote contralesional SLF and transcallosal PPC tracts. Increased FA combined with decreased radial diffusivity likely reflects increased myelination of these remote fiber tracts (Beaulieu, 2002). In line with this finding, immunohistochemical studies have reported increased myelin protein and oligodendrocyte density in perilesional and contralesional white matter tissue after experimental ischemic lesions in rats (Gregersen et al., 2001; Ishiguro et al., 1993; Tanaka et al., 2003). It is also possible that increased FA in remote fiber tracts after smaller lesions reflects an adaptive or compensatory change in white matter microstructure that may be related to the faster time to behavioural recovery in these animals (8 weeks) compared to those with larger lesions (16 weeks). This interpretation is supported by studies suggesting that remote areas in the intact hemisphere plays a beneficial role in the recovery of visuospatial attention deficits after a unilateral lesion (Heilman and Van Den Abell, 1980; Lunven et al., 2019, 2015; Lunven and Bartolomeo, 2017; Mesulam, 1981; Saj et al., 2013; Thimm et al., 2008; Umarova et al., 2011, 2017, 2016, 2014). Previous studies have highlighted an adaptive role for post-lesion changes in distant white matter tissue in both stroke patients (Bütefisch et al., 2003; Crofts et al., 2011; Lin et al., 2015; Liu et al., 2015; Schaechter et al., 2009) and animal models (Carmichael and Chesselet, 2002; Liu et al., 2008; Napieralski et al., 1996; Stroemer et al., 1995). Specifically, improved motor function in stroke patients correlated with increased FA in contralesional white matter (Lin et al., 2015; Liu et al., 2015; Schaechter et al., 2009). DWI studies in patients with congenital hemiparesis or multiple sclerosis (i.e., a non-ischemic etiology of white matter damage) have also reported microstructural

changes in functionally relevant contralesional white matter tracts (Audoin et al., 2007; Thomas et al., 2005).

Alternatively, another possibility is that the increased FA after small lesions and decreased FA after larger lesions in remote fiber tracts may reflect differences in the extent of disinhibition and potential downstream excitotoxicity. Focal lesions can lead to large-scale depolarization of connected areas resulting in disinhibition and hyperexcitability of widespread, functionally related networks (Buchkremer-Ratzmann and Witte, 1997; Fornito et al., 2015; Liepert et al., 2000). Adaptive structural plasticity after a focal lesion may be induced by this hyperexcitability, which has been associated with axonal and dendritic growth of undamaged fibers, myelin remodeling, synaptogenesis (Carmichael and Chesselet, 2002; Fornito et al., 2015; Gonzalez and Kolb, 2003; Jones and Schallert, 1992; Lin et al., 2015) and improved motor function (Reitmeir et al., 2011). However, larger lesions induce more widespread disinhibition and may lead to remote white matter degeneration across connected areas due to excitotoxicity and excessive metabolic stress from persistent hyperactivation (Buchkremer-Ratzmann and Witte, 1997; W. de Haan et al., 2012; Fornito et al., 2015; Ross and Ebner, 1990; Saxena and Caroni, 2011). Smaller lesions in Monkeys L and S may not have been sufficient enough to induce maladaptive hyperactivation in remote areas; here, the degree of disinhibition/hyperexcitability may have allowed for adaptive plasticity and contributed to compensatory changes across the functionally related network. On the other hand, larger lesions in Monkeys B and F likely induced more substantial disinhibition across the bilateral network and subsequently led to excessive hyperactivation, excitotoxicity, and metabolic stress, ultimately resulting in transneuronal degeneration of remote fiber tracts.

4.4.3. Relationship between white matter microstructure and resting-state FC

Although we found inconsistencies between DTI-derived metrics and resting-state FC, the magnitude of significant change reported for FA and rsFC are very robust. Thus, these discrepancies are unlikely to result from methodology, but instead may reflect variability in the compensatory response to lesions of different size or affecting different areas. Increased FA in the remote contralesional SLF and increased rsFC between corresponding grey matter areas (contralesional PFC–PPC) in both small lesion monkeys was the only consistent finding between FA and rsFC. We interpret this paired increase in contralesional FA and rsFC as support for a compensatory role of the contralesional hemisphere in the recovery of function after small PFC lesions. In our previous resting-state fMRI study, we reported that rsFC between areas in the contralesional PFC and ipsilesional PPC correlated with improving behavioural performance over time in all four monkeys (Adam et al., 2020). Since the contralesional SLF is one of the pathways that contributes to the indirect link between contralesional PFC and ipsilesional PPC, it is possible that the increased FA in contralesional SLF mediated the increased rsFC between contralesional PFC and ipsilesional PPC areas. This interpretation is supported by previous studies that showed positive correlations between rsFC and structural connectivity/FA in the white matter tracts that contribute to the indirect/polysynaptic pathway linking the functionally connected areas (Adachi et al., 2012; Greicius et al., 2009; Honey et al., 2009; Hori et al., 2020; Messé et al., 2014).

However, this compensatory response was not observed in the two large lesion monkeys. In Monkey B, rsFC increased between all areas from pre-lesion to late post-lesion, yet this was in contrast to the significantly decreased FA in ipsilesional SLF, transcallosal PFC, and transcallosal PPC tracts. Notably, there was no significant change in the tract-wise FA for contralesional SLF even though the corresponding rsFC was significantly

increased. One interpretation is that although functional and structural connectivity are often correlated, increased functional connectivity between two regions with a ‘weakened’ structural connection (e.g., decreased FA) may be mediated by strengthening of structural connections with a related third region (Honey et al., 2009; Koch et al., 2002). Another possible explanation for the opposite change in FA and rsFC in Monkey B comes from accumulating evidence demonstrating that network reorganization can maintain functional connectivity after loss of major structural pathways (O’Reilly et al., 2013; Tyszka et al., 2011; Uddin, 2013; Uddin et al., 2008). After major disconnections of the corpus callosum, sparing of even a few commissural fibers was sufficient to maintain normal levels of functional connectivity between hemispheres months later (O’Reilly et al., 2013; Tyszka et al., 2011; Uddin, 2013; Uddin et al., 2008). On the other hand, Monkey F did not show similar significant widespread increases in rsFC as in Monkey B, but instead only had significantly decreased rsFC in ipsilesional SLF. The lack of any significantly increased rsFC along with an overall decreased FA in all fiber tracts in Monkey F at the time of behavioural recovery suggests that neural compensation may have involved other brain areas or networks. Altogether, decreased FA in frontoparietal white matter tracts in both large lesion monkeys hint that behavioural recovery after larger PFC lesions may not be solely mediated by cortical connections in the frontoparietal network. Instead, there may be a functionally relevant third region/network that supports behavioural compensation and possibly works to maintain cortical rsFC (Damoiseaux and Greicius, 2009).

4.4.4. Conclusions

After the recovery of contralesional saccade choice deficits, FA in remote contralesional SLF and transcallosal PPC tracts was increased in monkeys with small PFC lesions, and

decreased in monkeys with larger lesions compared to pre-lesion. This suggests that the white matter tracts connecting remote areas of the frontoparietal network (i.e., distant to the lesion) may contribute an important compensatory response to support recovery of function after small PFC lesions. However, larger lesions may have induced more widespread damage to the structural network over time such that these remote fiber tracts are no longer sufficiently able to compensate for lost function. Future research is needed to clarify the behavioural relevance of the remote fiber tracts and to investigate an alternate source of neural compensation after greater frontoparietal network damage.

4.5. References

- Adachi, Y., Osada, T., Sporns, O., Watanabe, T., Matsui, T., Miyamoto, K., Miyashita, Y., 2012. Functional connectivity between anatomically unconnected areas is shaped by collective network-level effects in the macaque cortex. *Cereb. Cortex* 22, 1586–1592.
- Adam, R., Johnston, K., Everling, S., 2019. Recovery of contralesional saccade choice and reaction time deficits after a unilateral endothelin-1-induced lesion in the macaque caudal prefrontal cortex. *J. Neurophysiol.* 122, 672–690.
- Adam, R., Johnston, K., Menon, R.S., Everling, S., 2020. Functional reorganization during the recovery of contralesional target selection deficits after prefrontal cortex lesions in macaque monkeys. *Neuroimage* 207, 116339.
- Alexander, A., Lee, J., Lazar, M., Field, A., 2007. Diffusion Tensor Imaging of the Brain. *Neurother* 4, 316–329.
- Andersson, J.L.R., Sotiropoulos, S.N., 2016. An integrated approach to correction for off-resonance effects and subject movement in diffusion MR imaging. *Neuroimage* 125, 1063–1078.
- Audoin, B., Guye, M., Reuter, F., Au Duong, M. Van, Confort-Gouny, S., Malikova, I., Soulier, E., Viout, P., Chérif, A.A., Cozzone, P.J., Pelletier, J., Ranjeva, J.P., 2007. Structure of WM bundles constituting the working memory system in early multiple sclerosis: A quantitative DTI tractography study. *Neuroimage* 36, 1324–1330.
- Baldassarre, A., Ramsey, L.E., Hacker, C.L., Callejas, A., Astafiev, S. V., Metcalf, N. V., Zinn, K., Rengachary, J., Snyder, A.Z., Carter, A.R., Shulman, G.L., Corbetta, M., Zinn, K., Siegel, J.S., Metcalf, N. V., M., S., Snyder, A.Z., Corbetta, M., 2014. Large-scale changes in network interactions as a physiological signature of spatial neglect. *Brain* 137, 3267–3283.
- Barbas, H., Pandya, D., 1984. Topography of Commissural Fibers of the Prefrontal Cortex in the Rhesus Monkey. *Exp. Brain Res.* 55, 187–191.
- Baron, J.C., Yamauchi, H., Fujioka, M., Endres, M., 2014. Selective neuronal loss in ischemic stroke and cerebrovascular disease. *J. Cereb. Blood Flow Metab.* 34, 2–18.
- Bartolomeo, P., 2007. Visual neglect. *Curr. Opin. Neurol.* 20, 381–386.
- Bartolomeo, P., Thiebaut de Schotten, M., Chica, A.B., 2012. Brain networks of visuospatial attention and their disruption in visual neglect. *Front. Hum. Neurosci.* 6, 1–10.
- Basser, P., Mattiello, J., LeBihan, D., 1994a. MR diffusion tensor spectroscopy and imaging. *Biophys. J.* 66, 259–267.
- Basser, P., Mattiello, J., LeBihan, D., 1994b. Estimation of the effective self-diffusion tensor from the NMR spin echo. *J. Magn. Reson.* 103, 247–254.

- Basser, P., Pierpaoli, C., 1996. Microstructural and physiological features of tissues elucidated by quantitative-diffusion-tensor MRI. *J. Magn. Reson.* 111, 209–219.
- Beaulieu, C., 2002. The basis of anisotropic water diffusion in the nervous system - A technical review. *NMR Biomed.*
- Behrens, T.E.J., Berg, H.J., Jbabdi, S., Rushworth, M.F.S., Woolrich, M.W., 2007. Probabilistic diffusion tractography with multiple fibre orientations: What can we gain? *Neuroimage* 34, 144–155.
- Behrens, T.E.J., Johansen-Berg, H., Woolrich, M.W., Smith, S.M., Wheeler-Kingshott, C.A.M., Boulby, P.A., Barker, G.J., Sillery, E.L., Sheehan, K., Ciccarelli, O., Thompson, A.J., Brady, J.M., Matthews, P.M., 2003a. Non-invasive mapping of connections between human thalamus and cortex using diffusion imaging. *Nat. Neurosci.* 6, 750–757.
- Behrens, T.E.J., Woolrich, M.W., Jenkinson, M., Johansen-Berg, H., Nunes, R.G., Clare, S., Matthews, P.M., Brady, J.M., Smith, S.M., 2003b. Characterization and Propagation of Uncertainty in Diffusion-Weighted MR Imaging. *Magn. Reson. Med.* 50, 1077–1088.
- Bennett, I.J., Madden, D.J., Vaidya, C.J., Howard, J.H., Howard, D. V., 2011. White matter integrity correlates of implicit sequence learning in healthy aging. *Neurobiol. Aging* 32, 2317.e1-2317.e12.
- Bianchi, L., 1895. The functions of the frontal lobes. *Brain* 18, 497–522.
- Bisiach, E., 1991. Extinction and neglect: Same or different?, *Brain and space.*
- Bozzali, M., Mastropasqua, C., Cercignani, M., Giulietti, G., Bonni, S., Caltagirone, C., Koch, G., 2012. Microstructural Damage of the Posterior Corpus Callosum Contributes to the Clinical Severity of Neglect. *PLoS One* 7, 3–8.
- Buchkremer-Ratzmann, I., Witte, O.W., 1997. Extended brain disinhibition following small photothrombotic lesions in rat frontal cortex. *Neuroreport* 8, 519–522.
- Bütefisch, C.M., Netz, J., Weßling, M., Seitz, R.J., Hömberg, V., 2003. Remote changes in cortical excitability after stroke. *Brain* 126, 470–481.
- Carmichael, S.T., Chesselet, M.F., 2002. Synchronous neuronal activity is a signal for axonal sprouting after cortical lesions in the adult. *J. Neurosci.* 22, 6062–6070.
- Celik, A., 2016. Effect of imaging parameters on the accuracy of apparent diffusion coefficient and optimization strategies. *Diagnostic Interv. Radiol.* 22, 101–107.
- Colby, J.B., Soderberg, L., Lebel, C., Dinov, I.D., Thompson, P.M., Sowell, E.R., 2012. Along-tract statistics allow for enhanced tractography analysis. *Neuroimage* 59, 3227–3242.
- Corbetta, M., Shulman, G.L., 2011. Spatial Neglect and Attention Networks. *Annu. Rev. Neurosci.* 34, 569–599.
- Crofts, J.J., Higham, D.J., Bosnell, R., Jbabdi, S., Matthews, P.M., Behrens, T.E.J.,

- Johansen-Berg, H., 2011. Network analysis detects changes in the contralesional hemisphere following stroke. *Neuroimage* 54, 161–169.
- Cunningham, S.I., Tomasi, D., Volkow, N.D., 2017. Structural and functional connectivity of the precuneus and thalamus to the default mode network. *Hum. Brain Mapp.* 38, 938–956.
- Dacosta-Aguayo, R., Graña, M., Fernández-Andújar, M., López-Cancio, E., Cáceres, C., Bargalló, N., Barrios, M., Clemente, I., Monserrat, P.T., Sas, M.A., Dávalos, A., Auer, T., Mataró, M., 2014. Structural integrity of the contralesional hemisphere predicts cognitive impairment in ischemic stroke at three months. *PLoS One* 9, 1–11.
- Dai, P., Huang, H., Zhang, L., He, J., Zhao, X., Yang, F., Zhao, N., Yang, J., Ge, L., Lin, Y., Yu, H., Wang, J., 2017. A pilot study on transient ischemic stroke induced with endothelin-1 in the rhesus monkeys. *Sci. Rep.* 7, 45097.
- Damasio, A.R., Damasio, H., Chui, H.C., 1980. Neglect following damage to frontal lobe or basal ganglia. *Neuropsychologia* 18, 123–132.
- Damoiseaux, J.S., Greicius, M.D., 2009. Greater than the sum of its parts: A review of studies combining structural connectivity and resting-state functional connectivity. *Brain Struct. Funct.* 213, 525–533.
- Davis, S.W., Dennis, N.A., Buchler, N.G., White, L.E., Madden, D.J., Cabeza, R., 2009. Assessing the effects of age on long white matter tracts using diffusion tensor tractography. *Neuroimage* 46, 530–541.
- de Haan, B., Karnath, H.O., Driver, J., 2012. Mechanisms and anatomy of unilateral extinction after brain injury. *Neuropsychologia* 50, 1045–1053.
- de Haan, W., Mott, K., van Straaten, E.C.W., Scheltens, P., Stam, C.J., 2012. Activity Dependent Degeneration Explains Hub Vulnerability in Alzheimer’s Disease. *PLoS Comput. Biol.* 8.
- Deuel, R., Collins, R., 1983. Recovery from unilateral neglect. *Exp. Neurol.* 81, 733–748.
- Deuel, R.K., Farrar, C.A., 1993. Stimulus cancellation by macaques with unilateral frontal or parietal lesions. *Neuropsychologia* 31, 29–38.
- Di Pellegrino, G., Basso, G., Frassinetti, F., 1997. Spatial extinction on double asynchronous stimulation. *Neuropsychologia* 35, 1215–1223.
- Dijkhuizen, R.M., van der Marel, K., Otte, W.M., Hoff, E.I., van der Zijden, J.P., van der Toorn, A., van Meer, M.P.A., 2012. Functional MRI and Diffusion Tensor Imaging of Brain Reorganization After Experimental Stroke. *Transl. Stroke Res.* 3, 36–43.
- Fornito, A., Zalesky, A., Breakspear, M., 2015. The connectomics of brain disorders. *Nat. Rev. Neurosci.* 16, 159–172.
- Galantucci, S., Tartaglia, M.C., Wilson, S.M., Henry, M.L., Filippi, M., Agosta, F., Dronkers, N.F., Henry, R.G., Ogar, J.M., Miller, B.L., Gorno-Tempini, M.L., 2011.

- White matter damage in primary progressive aphasia: A diffusion tensor tractography study. *Brain* 134, 3011–3029.
- Ge, H., Yin, X., Xu, J., Tang, Y., Han, Y., Xu, W., Pang, Z., Meng, H., Liu, S., 2013. Fiber pathways of attention subnetworks revealed with tract-based spatial statistics (TBSS) and probabilistic tractography. *PLoS One* 8, 1–7.
- Gilbert, K.M., Gati, J.S., Barker, K., Everling, S., Menon, R.S., 2016. Optimized parallel transmit and receive radiofrequency coil for ultrahigh-field MRI of monkeys. *Neuroimage* 125, 153–161.
- Gonzalez, C.L.R., Kolb, B., 2003. A comparison of different models of stroke on behaviour and brain morphology. *Eur. J. Neurosci.* 18, 1950–1962.
- Gray, D.T., Umapathy, L., Burke, S.N., Trouard, T.P., Barnes, C.A., 2018. Tract-Specific White Matter Correlates of Age-Related Reward Devaluation Deficits in Macaque Monkeys. *J. Neuroimaging Psychiatry Neurol.* 03, 13–26.
- Grayson, D.S., Bliss-Moreau, E., Bennett, J., Lavenex, P., Amaral, D.G., 2017. Neural Reorganization Due to Neonatal Amygdala Lesions in the Rhesus Monkey: Changes in Morphology and Network Structure. *Cereb. Cortex* 27, 3240–3253.
- Gregersen, R., Christensen, T., Lehrmann, E., Diemer, N.H., Finsen, B., 2001. Focal cerebral ischemia induces increased myelin basic protein and growth-associated protein-43 gene transcription in peri-infarct areas in the rat brain. *Exp. Brain Res.* 138, 384–392.
- Greicius, M.D., Supekar, K., Menon, V., Dougherty, R.F., 2009. Resting-state functional connectivity reflects structural connectivity in the default mode network. *Cereb. Cortex* 19, 72–78.
- Hagmann, P., Cammoun, L., Gigandet, X., Meuli, R., Honey, C.J., Van Welden, J., Sporns, O., 2008. Mapping the structural core of human cerebral cortex. *PLoS Biol.* 6, 1479–1493.
- He, B.J., Snyder, A.Z., Vincent, J.L., Epstein, A., Shulman, G.L., Corbetta, M., 2007. Breakdown of functional connectivity in frontoparietal networks underlies behavioral deficits in spatial neglect. *Neuron* 53, 905–18.
- Heilman, K.M., Van Den Abell, T., 1980. Right hemisphere dominance for attention: the mechanism underlying hemispheric asymmetries of inattention (neglect). *Neurology* 30, 327–330.
- Herbert, W.J., Powell, K., Buford, J.A., 2015. Evidence for a role of the reticulospinal system in recovery of skilled reaching after cortical stroke: initial results from a model of ischemic cortical injury. *Exp. Brain Res.* 233, 3231–3251.
- Hofer, S., Frahm, J., 2008. In Vivo Mapping of Fiber Pathways in the Rhesus Monkey Brain. *Open Med. Imaging J.* 2, 32–41.
- Hofer, S., Merboldt, K.D., Tammer, R., Frahm, J., 2008. Rhesus monkey and human share a similar topography of the corpus callosum as revealed by diffusion tensor

- mri in vivo. *Cereb. Cortex* 18, 1079–1084.
- Honey, C.J., Sporns, O., Cammoun, L., Gigandet, X., Thiran, J.P., Meuli, R., Hagmann, P., 2009. Predicting human resting-state functional connectivity from structural connectivity. *Proc. Natl. Acad. Sci. U. S. A.* 106, 2035–2040.
- Hori, Y., Schaeffer, D.J., Gilbert, K.M., Hayrynen, L.K., Cléry, J.C., Gati, J.S., Menon, R.S., Everling, S., 2020. Comparison of resting-state functional connectivity in marmosets with tracer-based cellular connectivity. *Neuroimage* 204.
- Hutchison, R.M., Gallivan, J.P., Culham, J.C., Gati, J.S., Menon, R.S., Everling, S., 2012. Functional connectivity of the frontal eye fields in humans and macaque monkeys investigated with resting-state fMRI. *J. Neurophysiol.* 107, 2463–74.
- Ishiguro, H., Inuzuka, T., Fujita, N., Sato, S., Nakano, R., Tamura, A., Kirino, T., Miyatake, T., 1993. Expression of the large myelin-associated glycoprotein isoform in rat oligodendrocytes around cerebral infarcts. *Mol. Chem. Neuropathol.* 20, 173–179.
- Jenkinson, M., Bannister, P., Brady, M., Smith, S., 2002. Improved optimization for the robust and accurate linear registration and motion correction of brain images. *Neuroimage* 17, 825–841.
- Johnston, K., Lomber, S.G., Everling, S., 2016. Unilateral Deactivation of Macaque Dorsolateral Prefrontal Cortex Induces Biases in Stimulus Selection. *J. Neurophysiol.* 115, 1468–1476.
- Jones, D.K., Knösche, T.R., Turner, R., 2013. White matter integrity, fiber count, and other fallacies: The do's and don'ts of diffusion MRI. *Neuroimage*.
- Jones, T.A., Schallert, T., 1992. Overgrowth and pruning of dendrites in adult rats recovering from neocortical damage. *Brain Res.* 581, 156–160.
- Koch, M.A., Norris, D.G., Hund-Georgiadis, M., 2002. An investigation of functional and anatomical connectivity using magnetic resonance imaging. *Neuroimage* 16, 241–250.
- Latto, R., Cowey, A., 1971. Visual field defects after frontal eye field lesions in monkeys. *Brain Res.* 30, 1–24.
- Latzman, R.D., Tagliabata, J.P., Hopkins, W.D., 2015. Delay of gratification is associated with white matter connectivity in the dorsal prefrontal cortex: A diffusion tensor imaging study in chimpanzees (*Pan troglodytes*). *Proc. R. Soc. B Biol. Sci.* 282.
- Lewis, J.W., Van Essen, D.C., 2000. Corticocortical connections of visual, sensorimotor, and multimodal processing areas in the parietal lobe of the macaque monkey. *J. Comp. Neurol.* 428, 112–137.
- Li, K., Malhotra, P.A., 2015. Spatial neglect. *Pract. Neurol.* 15, 333–339.
- Liepert, J., Storch, P., Fritsch, A., Weiller, C., 2000. Motor cortex disinhibition in acute

- stroke. *Clin. Neurophysiol.* 111, 671–676.
- Lin, Y.C., Daducci, A., Meskaldji, D.E., Thiran, J.P., Michel, P., Meuli, R., Krueger, G., Menegaz, G., Granziera, C., 2015. Quantitative analysis of myelin and axonal remodeling in the uninjured motor network after stroke. *Brain Connect.* 5, 401–412.
- Lindenberg, R., Zhu, L.L., Rüber, T., Schlaug, G., 2012. Predicting functional motor potential in chronic stroke patients using diffusion tensor imaging. *Hum. Brain Mapp.* 33, 1040–1051.
- Liu, G., Dang, C., Chen, X., Xing, S., Dani, K., Xie, C., Peng, K., Zhang, Jingna, Li, J., Zhang, Jian, Chen, L., Pei, Z., Zeng, J., 2015. Structural remodeling of white matter in the contralesional hemisphere is correlated with early motor recovery in patients with subcortical infarction. *Restor. Neurol. Neurosci.* 33, 309–319.
- Liu, Y., D’Arceuil, H.E., Westmoreland, S., He, J., Duggan, M., Gonzalez, R.G., Pryor, J., De Crespigny, A.J., 2007. Serial diffusion tensor MRI after transient and permanent cerebral ischemia in nonhuman primates. *Stroke* 38, 138–145.
- Liu, Z., Li, Y., Zhang, X., Savant-Bhonsale, S., Chopp, M., 2008. Contralesional axonal remodeling of the corticospinal system in adult rats after stroke and bone marrow stromal cell treatment. *Stroke* 39, 2571–2577.
- Lunven, M., Bartolomeo, P., 2017. Attention and spatial cognition: Neural and anatomical substrates of visual neglect. *Ann. Phys. Rehabil. Med.* 60, 124–129.
- Lunven, M., De Schotten, M.T., Bourlon, C., Duret, C., Migliaccio, R., Rode, G., Bartolomeo, P., 2015. White matter lesional predictors of chronic visual neglect: A longitudinal study. *Brain* 138, 746–760.
- Lunven, M., Rode, G., Bourlon, C., Duret, C., Migliaccio, R., Chevillon, E., Thiebaut de Schotten, M., Bartolomeo, P., 2019. Anatomical predictors of successful prism adaptation in chronic visual neglect. *Cortex* 120, 629–641.
- Lynch, J.C., McLaren, J.A.Y.W., 1989. Deficits of Visual Attention and Saccadic Eye Movements After Lesions of Parietooccipital Cortex in Monkeys. *J. Neurophysiol.* 6, 74–90.
- Messé, A., Rudrauf, D., Benali, H., Marrelec, G., 2014. Relating Structure and Function in the Human Brain: Relative Contributions of Anatomy, Stationary Dynamics, and Non-stationarities. *PLoS Comput. Biol.* 10.
- Mesulam, M.-M., 1999. Spatial attention and neglect: parietal, frontal and cingulate contributions to the mental representation and attentional targeting of salient extrapersonal events. *Philos. Trans. R. Soc. Lond. B. Biol. Sci.* 354, 1325–1346.
- Mesulam, M. -Marchsel, 1981. A cortical network for directed attention and unilateral neglect. *Ann. Neurol.*
- Moseley, M., Wendland, M., Kucharczyk, J., 1991. Magnetic resonance imaging of diffusion and perfusion. *Top. Magn. Reson. Imaging* 3, 50–67.

- Moseley, M.E., Cohen, Y., Kucharczyk, J., Mintorovitch, J., Asgari, H.S., Wendland, M.F., Tsuruda, J., Norman, D., 1990. Diffusion-weighted MR imaging of anisotropic water diffusion in cat central nervous system. *Radiology* 176, 439–445.
- Murata, Y., Higo, N., 2016. Development and Characterization of a Macaque Model of Focal Internal Capsular Infarcts. *PLoS One* 11, e0154752.
- Murphy, T.H., Corbett, D., 2009. Plasticity during stroke recovery: from synapse to behaviour. *Nat. Rev. Neurosci.* 10, 861–872.
- Napiersalski, J.A., Butler, A.K., Chesselet, M.F., 1996. Anatomical and functional evidence for lesion-specific sprouting of corticostriatal input in the adult rat. *J. Comp. Neurol.* 373, 484–497.
- O'Reilly, J.X., Croxson, P.L., Jbabdi, S., Sallet, J., Noonan, M.P., Mars, R.B., Browning, P.G.F., Wilson, C.R.E., Mitchell, A.S., Miller, K.L., Rushworth, M.F.S., Baxter, M.G., 2013. Causal effect of disconnection lesions on interhemispheric functional connectivity in rhesus monkeys. *Proc. Natl. Acad. Sci. U. S. A.* 110, 13982–7.
- Paxinos, G., Huang, X., Toga, A., 2000. *The Rhesus Monkey Brain in Stereotaxic Coordinates*. Academic Press.
- Petrides, M., Pandya, D.N., 1984. Projections to the frontal cortex from the posterior parietal region in the rhesus monkey. *J. Comp. Neurol.* 116, 105–116.
- Pierpaoli, C., Barnett, A., Pajevic, S., Chen, R., Penix, L.R., Virta, A., Basser, P., 2001. Water diffusion changes in wallerian degeneration and their dependence on white matter architecture. *Neuroimage* 13, 1174–1185.
- Provenzale, J.M., Taylor, B.A., Wilde, E.A., Boss, M., Schneider, W., 2018. Analysis of variability of fractional anisotropy values at 3T using a novel diffusion tensor imaging phantom. *Neuroradiol. J.* 31, 581–586.
- Ramsey, L.E., Siegel, J.S., Baldassarre, A., Metcalf, N. V., Zinn, K., Shulman, G.L., Corbetta, M., 2016. Normalization of network connectivity in hemispatial neglect recovery. *Ann. Neurol.* 80, 127–141.
- Reitmeir, R., Kilic, E., Kilic, Ü., Bacigaluppi, M., Elali, A., Salani, G., Pluchino, S., Gassmann, M., Hermann, D.M., 2011. Post-acute delivery of erythropoietin induces stroke recovery by promoting perilesional tissue remodelling and contralesional pyramidal tract plasticity. *Brain* 134, 84–99.
- Rizzolatti, G., Matelli, M., Pavesi, G., 1983. Deficits in attention and movement following the removal of postarcuate (area 6) and prearcuate (area 8) cortex in macaque monkeys. *Brain* 106, 655–673.
- Ross, D.T., Ebner, F.F., 1990. Thalamic retrograde degeneration following cortical injury: An excitotoxic process? *Neuroscience* 35, 525–550.
- Saj, A., Cojan, Y., Vocat, R., Luaute, J., Vuilleumier, P., 2013. Prism adaptation enhances activity of intact fronto-parietal areas in both hemispheres in neglect patients. *Cortex.* 49, 107–119.

- Saleem, K.S., Logothetis, N.K., 2006. A combined MRI and histology atlas of the rhesus monkey brain in stereotaxic coordinates.
- Saxena, S., Caroni, P., 2011. Selective Neuronal Vulnerability in Neurodegenerative Diseases: From Stressor Thresholds to Degeneration. *Neuron* 71, 35–48.
- Schaechter, J.D., Fricker, Z.P., Perdue, K.L., Helmer, K.G., Vangel, M.G., Greve, D.N., Makris, N., 2009. Microstructural status of ipsilesional and contralesional corticospinal tract correlates with motor skill in chronic stroke patients. *Hum. Brain Mapp.* 30, 3461–3474.
- Schaeffer, D.J., Adam, R., Gilbert, K.M., Gati, J.S., Li, A.X., Menon, R.S., Everling, S., 2017. Diffusion weighted tractography in the common marmoset monkey at 9.4 T. *J. Neurophysiol.* 118, 1344–1354.
- Schiller, P.H., Chou, I., 1998. The effects of frontal eye field and dorsomedial frontal cortex lesions on visually guided eye movements. *Nat. Neurosci.* 1, 248–253.
- Schmahmann, J.D., Pandya, D.N., Wang, R., Dai, G., D’Arceuil, H.E., De Crespigny, A.J., Wedeen, V.J., 2007. Association fibre pathways of the brain: Parallel observations from diffusion spectrum imaging and autoradiography. *Brain* 130, 630–653.
- Shen, K., Hutchison, R.M., Bezgin, G., Everling, S., McIntosh, A.R., 2015. Network Structure Shapes Spontaneous Functional Connectivity Dynamics. *J. Neurosci.* 35, 5579–5588.
- Sotak, C.H., 2002. The role of diffusion tensor imaging in the evaluation of ischemic brain - A review. *NMR Biomed.* 15, 561–569.
- Stroemer, R.P., Kent, T.A., Hulsebosch, C.E., 1995. Neocortical neural sprouting, synaptogenesis, and behavioral recovery after neocortical infarction in rats. *Stroke* 26, 2135–2144.
- Tanaka, K., Nogawa, S., Suzuki, S., Dembo, T., Kosakai, A., 2003. Upregulation of oligodendrocyte progenitor cells associated with restoration of mature oligodendrocytes and myelination in peri-infarct area in the rat brain. *Brain Res.* 989, 172–179.
- Tehovnik, E.J., Sommer, M. a., Chou, I.H., Slocum, W.M., Schiller, P.H., 2000. Eye fields in the frontal lobes of primates. *Brain Res. Rev.* 32, 413–448.
- Teo, L., Bourne, J., 2014. A Reproducible and Translatable Model of Focal Ischemia in the Visual Cortex of Infant and Adult Marmoset Monkeys. *Brain Pathol.* 24, 459–474.
- Thiebaut de Schotten, M., Dell’Acqua, F., Valabregue, R., Catani, M., 2012. Monkey to human comparative anatomy of the frontal lobe association tracts. *Cortex* 48, 82–96.
- Thiel, A., Radlinska, B.A., Paquette, C., Sidel, M., Soucy, J.P., Schirmacher, R., Minuk, J., 2010. The temporal dynamics of poststroke neuroinflammation: A longitudinal diffusion tensor imaging-guided PET study with ¹¹C-PK11195 in acute subcortical

- stroke. *J. Nucl. Med.* 51, 1404–1412.
- Thimm, M., Fink, G.R., Sturm, W., 2008. Neural correlates of recovery from acute hemispatial neglect. *Restor Neurol Neurosci* 26, 481–492.
- Thomalla, G., Glauche, V., Koch, M.A., Beaulieu, C., Weiller, C., Röther, J., 2004. Diffusion tensor imaging detects early Wallerian degeneration of the pyramidal tract after ischemic stroke. *Neuroimage* 22, 1767–1774.
- Thomas, B., Eyssen, M., Peeters, R., Molenaers, G., Van Hecke, P., De Cock, P., Sunaert, S., 2005. Quantitative diffusion tensor imaging in cerebral palsy due to periventricular white matter injury. *Brain* 128, 2562–2577.
- Thomsen, C., Henriksen, O., Ring, P., 1987. In vivo measurement of water self diffusion in the human brain by magnetic resonance imaging. *Acta radiol.* 28, 353–361.
- Tyszka, M.J., Kennedy, D.P., Adolphs, R., Paul, L.K., 2011. Intact bilateral resting-state networks in the absence of the corpus callosum. *J. Neurosci.* 31, 15154–15162.
- Uddin, L.Q., 2013. Complex relationships between structural and functional brain connectivity. *Trends Cogn. Sci.* 17, 600–602.
- Uddin, L.Q., Mooshagian, E., Zaidel, E., Scheres, A., Margulies, D.S., Kelly, A.M.C., Shehzad, Z., Adelstein, J.S., Castellanos, F.X., Biswal, B.B., Milham, M.P., 2008. Residual functional connectivity in the split-brain revealed with resting-state functional MRI. *Neuroreport* 19, 703–709.
- Umarova, R.M., Beume, L., Reisert, M., Kaller, C.P., Klöppel, S., Mader, I., Glauche, V., Kiselev, V.G., Catani, M., Weiller, C., 2017. Distinct white matter alterations following severe stroke. *Neurology* 88, 1546–1555.
- Umarova, R.M., Nitschke, K., Kaller, C.P., Klöppel, S., Beume, L., Mader, I., Martin, M., Hennig, J., Weiller, C., 2016. Predictors and signatures of recovery from neglect in acute stroke. *Ann. Neurol.* 79, 673–686.
- Umarova, R.M., Reisert, M., Beier, T.U., Kiselev, V.G., Klöppel, S., Kaller, C.P., Glauche, V., Mader, I., Beume, L., Hennig, J., Weiller, C., 2014. Attention-network specific alterations of structural connectivity in the undamaged white matter in acute neglect. *Hum. Brain Mapp.* 35, 4678–4692.
- Umarova, R.M., Saur, D., Kaller, C.P., Vry, M.S., Glauche, V., Mader, I., Hennig, J.J., Weiller, C., 2011. Acute visual neglect and extinction: Distinct functional state of the visuospatial attention system. *Brain* 134, 3310–3325.
- van der Zijden, J.P., van der Toorn, A., van der Marel, K., Dijkhuizen, R.M., 2008. Longitudinal in vivo MRI of alterations in perilesional tissue after transient ischemic stroke in rats. *Exp. Neurol.* 212, 207–212.
- Wang, Y., Liu, G., Hong, D., Chen, F., Ji, X., Cao, G., 2016. White matter injury in ischemic stroke. *Prog. Neurobiol.* 141, 45–60.
- Wardak, C., Ibos, G., Duhamel, J.-R.R., Olivier, E., 2006. Contribution of the monkey

- frontal eye field to covert visual attention. *J. Neurosci.* 26, 4228–4235.
- Wardak, C., Olivier, E., Duhamel, J.-R., 2002. Saccadic target selection deficits after lateral intraparietal area inactivation in monkeys. *J. Neurosci.* 22, 9877–84.
- Wardak, C., Olivier, E., Duhamel, J.R., 2011. The relationship between spatial attention and saccades in the frontoparietal network of the monkey. *Eur. J. Neurosci.* 33, 1973–1981.
- Wardak, C., Olivier, E., Duhamel, J.R., 2004. A Deficit in covert attention after parietal cortex inactivation in the monkey. *Neuron* 42, 501–508.
- Wasserman, J.K., Schlichter, L.C., 2008. White matter injury in young and aged rats after intracerebral hemorrhage. *Exp. Neurol.* 214, 266–275.
- Werring, D.J., Toosy, A.T., Clark, C.A., Parker, G.J.M., Barker, G.J., Miller, D.H., Thompson, A.J., 2000. Diffusion tensor imaging can detect and quantify corticospinal tract degeneration after stroke. *J. Neurol. Neurosurg. Psychiatry* 69, 269–272.
- Wesbey, G.E., Moseley, M.E., Ehman, R.L., 1984. Translational molecular self-diffusion in magnetic resonance imaging: II. Measurement of the self-diffusion coefficient. *Invest. Radiol.*
- Wilke, M., Kagan, I., Andersen, R., 2012. Functional imaging reveals rapid reorganization of cortical activity after parietal inactivation in monkeys. *Proc. Natl. Acad. Sci.* 109, 8274–8279.
- Zhang, J., Zhang, Y., Xing, S., Liang, Z., Zeng, J., 2012. Secondary neurodegeneration in remote regions after focal cerebral infarction: A new target for stroke management? *Stroke* 43, 1700–1705.

CHAPTER 5

5. General discussion

5.1. Summary of main findings

Visual neglect and extinction are commonly observed after unilateral damage to the frontoparietal network (Corbetta and Shulman, 2011; Li and Malhotra, 2015). These visuospatial impairments typically manifest as reduced detection, discrimination, or selection of visual stimuli within the contralesional hemifield, especially in the presence of a competing stimulus in ipsilesional hemifield. Visual neglect and extinction reflect the breakdown of visual attention to contralesional space which recovers gradually over time. Thus, these disorders represent valuable models for studying brain networks that control shifts of gaze and attention and how those networks reorganize to compensate for loss of function. Here, we described the saccade target selection behaviour for visual stimuli in either hemifield before and after unilateral caudal PFC lesions in macaque monkeys. The main objective of this thesis was to examine the functional and structural alterations in the frontoparietal network following the lesions and how those changes relate with the recovery of contralesional target selection. In general, we found that reduced saccade selection of contralesional visual stimuli was not purely due to impaired oculomotor processing within the contralesional hemifield and that behavioural recovery was associated with different patterns of functional and structural alterations based on lesion size. Two findings from resting-state fMRI in Chapter 3 were common in all four monkeys: (1) compared to pre-lesion, the contralesional DLPFC showed a greater degree of functional connectivity with the frontoparietal network after the lesion and (2)

behavioural improvement correlated with increasing functional connectivity between contralesional DLPFC and ipsilesional PPC. Overall, the results of this thesis support the view that both the ipsilesional and contralesional frontoparietal networks play a compensatory role after unilateral PFC lesions to support the recovery of visuospatial deficits within the contralesional hemifield. The main findings from each chapter are reviewed below.

5.1.1. Recovery of lateralized visuospatial impairment after endothelin-1-induced lesions in the caudal lateral PFC

We have characterized a macaque model of focal cerebral ischemia to induce lateralized attentional deficits using the vasoconstrictor endothelin-1 in the caudal lateral PFC. Endothelin-1 has been previously used to develop nonhuman primate models of focal cerebral ischemia, specifically in the marmoset middle cerebral artery (Virley et al., 2004) and posterior cerebral artery (Teo and Bourne, 2014) and in the rhesus macaque motor cortex (Dai et al., 2017; Herbert et al., 2015) and posterior internal capsule (Murata and Higo, 2016). Teo and Bourne (2014) demonstrated that the post-ischemic pathophysiological processes from endothelin-1 are similar to the sequelae after ischemic strokes in humans (Teo and Bourne, 2014), while the other studies characterized the sensory/motor impairments and subsequent recovery (Dai et al., 2017; Herbert et al., 2015; Murata and Higo, 2016; Virley et al., 2004). We have added to this growing body of research on nonhuman primate models for ischemic stroke by showing that intracortical injections of endothelin-1 into the caudal PFC can produce long-lasting impairments of saccade target selection within the contralesional hemifield, resembling visual neglect and extinction in stroke patients. Injections of endothelin-1 directly into the cortical tissue of interest produce cellular sequelae similar to ischemic stroke and, unlike

occlusions of the middle cerebral artery, are less disabling to the animals, produce more controlled lesions in size and location, and allow for assessments of oculomotor behaviour (access to the middle cerebral artery requires eyeball enucleation). Altogether, this research project establishes an endothelin-1 macaque model that can be reproduced for future investigations into attentional disorders and potential avenues for rehabilitation.

In line with previous longitudinal reports on behaviour after permanent FEF lesions in monkeys (Rizzolatti et al., 1983; Schiller and Chou, 1998), we found that visuospatial deficits for a single stimulus in the contralesional hemifield largely recovered within 4 weeks post-lesion and that contralesional deficits during bilateral stimulus presentation recovered over 8-16 weeks. The pattern and time course of behavioural recovery that we found has also been documented in neglect patients, in which neglect and extinction co-occur in the acute stage and then dissociate in the chronic stage with recovery of neglect but lasting extinction (Bender and Furlow, 1945; Heilman et al., 2012, 1984; Milner and McIntosh, 2005; Ramsey et al., 2016; Robertson and Halligan, 1999).

Since the FEF plays a role in both covert shifts of visual attention and overt shifts of gaze, reduced saccade selection of a contralesional visual target after FEF lesions may have been due slower reaction times rather than impaired allocation of attention towards the contralesional hemifield. In Chapter 2, we showed that the spatially lateralized deficits in saccade target selection at the chronic stage were not explained by the mean or distribution of saccadic reaction times towards the contralesional hemifield. Schiller and Chou (2000) similarly reported that the degree of contralesional saccade choice deficits on the paired free-choice task were much larger than could be accounted for by differences between the mean left and right reaction times to single targets (Schiller and Chou, 2000). However, since the *mean* reaction time does not capture all of the

information present in reaction time distribution data (Ratcliff, 1979), we extended the work of Schiller and Chou (2000) by showing that reaction time *distributions* also could not predict free-choice task performance on a linear race model. In addition, we showed that reaction times on the paired target trials also did not account for the magnitude of the saccade choice bias. Overall, our results indicate that decreased saccade selection of contralesional targets after a caudal PFC lesion is not simply the result of impaired oculomotor programming but also reflects deficits in allocating attention toward the contralesional hemifield especially when bilateral stimuli compete for attention.

This dissociation between attentional and oculomotor impairment appears in contrast to Rizzolatti's premotor theory of attention, which proposes that covert shifts of attention arise from the same preparatory neural signals for generating saccades (Rizzolatti et al., 1987). If attentional selection relied on the same neural activity that coded for planning a saccade to that location, then we would have expected to see decreased contralesional saccade choice co-occur with impairments in saccade metrics in both severity and time course of recovery. Although visuospatial attention and oculomotor commands are closely linked in the FEF (Moore and Armstrong, 2003; Moore and Fallah, 2004), our results indicate that these two processes can diverge with contralesional selection deficits upon attentional competition potentially outlasting oculomotor impairment. Our findings are in line with electrophysiological and microstimulation studies which also challenge the premotor theory of attention by showing distinct neuronal populations in the FEF that signal the spatial locations which correspond to the locus of visual attention in the absence of overt eye movements (Juan et al., 2004; Sato and Schall, 2003; Thompson et al., 2005). The results from Chapter 2 show that in the early post-lesion stage, decreased selection of contralesional visual stimuli is coupled with slower saccadic reaction times to the contralesional hemifield. However, in the late post-lesion time points, we showed that

there was no delay in the onset of a saccade towards its selected target but that the target selection process was still affected when two bilateral stimuli competed for attention, with a lasting contralesional selection deficit.

One possibility is that this lasting selection bias was due to learned strategies throughout behavioural training. Since reward delivery on the free-choice task was not dependent on selecting the first-appearing target (i.e., monkeys could freely choose either stimulus as a saccade target), monkeys were always rewarded for selecting the ipsilesional stimulus on all free-choice paired stimulus trials, even if the contralesional stimulus appeared first. In the early days to weeks following the lesion, monkeys were severely impaired in detecting the contralesional stimulus and would instead select the ipsilesional stimulus at higher proportions. This in turn could have resulted in an incorrect assumption that reward delivery was contingent on selecting the ipsilesional stimulus or a learned behavioural strategy to always direct a saccade to the ipsilesional stimulus. However, the inclusion of single target ‘catch’ trials in an equal proportion to the free-choice paired stimulus trials in the task would have trained the monkeys to saccade towards the first stimulus that captures its attention since any given trial could have been a single target trial. Yet this alternative explanation is still possible since the strongest lasting selection bias was seen on the trials when both stimuli appeared simultaneously; the learned strategy could have been to select the ipsilesional stimulus when in doubt of which selection would deliver a reward.

5.1.2. Functional and structural alterations differ based on lesion size

We found that recovery of saccade target selection after smaller PFC lesions occurred in parallel with a normalization of network-wide functional connectivity towards pre-lesion baseline, whereas recovery after larger lesions occurred alongside increasing network-

wide functional connectivity. This lesion size-dependent pattern of functional reorganization is in line with previous studies of motor recovery in rodent models of stroke showing greater compensatory recruitment of distant brain areas after larger lesions to the premotor or primary motor cortex (Biernaskie et al., 2005; Frost, 2003; Touvykine et al., 2016). Moreover, when Biernaskie et al. (2005) temporarily inactivated the contralesional motor cortex in recovered rats with small or large motor cortex lesions, only those with large lesions showed a return of the initial motor deficits (Biernaskie et al., 2005). This suggested that motor recovery after smaller lesions did not rely on compensatory recruitment of distant/intact areas of the network to the same extent as recovery from large lesions.

Theoretical accounts have been proposed to explain the mechanisms underlying the effects of lesion size on neural plasticity during recovery of function. It has been suggested that functional recovery following small/incomplete lesions likely involves spared representations in adjacent perilesional cortex or transient recruitment of remote ipsilesional areas with similar function and connectivity as the lesion site (Biernaskie et al., 2005; Brown et al., 2009; Grafman, 2000; Nudo et al., 1996; Plow et al., 2015). Instead, larger lesions may completely impair functions normally carried out by the lesioned tissue and recovery of function may then depend on recruitment of bilateral areas distant to the lesion (Grafman, 2000; Liu and Rouiller, 1999; Plautz et al., 2003; Zeiler et al., 2013). Grafman (2000) proposed a conceptual framework for functional neuroplasticity to explain this divergent phenomenon in terms of the success of hemispheric transfer of function, such that larger lesions result in better transfer of function. Based on empirical studies, Grafman suggests that homologous areas in opposite hemispheres (e.g., area A and B) have a primary and secondary functional role, where the secondary function of area A is normally inhibited by its contralateral homolog

(area B) whose primary function is the normally dormant, secondary function of area A. The author then suggests that large/complete lesions of area B result in a complete transfer of function to area A in the contralateral hemisphere due to disinhibition. However, after a smaller lesion to area B, intact areas in the lesioned hemisphere may continue to inhibit area A and block the complete transfer of function.

Microstructural changes in frontoparietal white matter pathways also differed by lesion size. The major finding in Chapter 3 was that remote fiber tracts, namely the contralesional SLF and transcallosal PPC-PPC tracts, showed increased FA when behaviour had recovered after a small lesion, but that FA in those tracts had decreased after larger lesions compared to pre-lesion baseline. This result may be explained by potentially divergent patterns of structural plasticity that take place following lesions with differing extent of damage. Focal lesions disinhibit connected areas and may lead to large-scale depolarization of widespread, functionally related networks (Buchkremer-Ratzmann and Witte, 1997; Fornito et al., 2015; Liepert et al., 2000). In the case of small lesions, this hyperexcitability may induce *adaptive* structural plasticity in the form of axonal and dendritic growth of remote fibers, myelin remodeling, and synaptogenesis (Carmichael and Chesselet, 2002; Fornito et al., 2015; Gonzalez and Kolb, 2003; Jones and Schallert, 1992; Lin et al., 2015), which have been associated with improved motor function in a rodent model of stroke (Reitmeir et al., 2011). Since measures of FA from diffusion-weighted MRI are assumed to reflect axonal density and myelination (Beaulieu, 2002; Sotak, 2002), our finding that FA increased in the remote fiber tracts at the time of recovered behaviour after small lesions suggests that axonal sprouting in remote frontoparietal areas may reflect neural compensation. On the other hand, larger lesions with more widespread disinhibition may lead to excitotoxicity and excessive metabolic stress from persistent hyperactivation and likely result in increased degeneration of

remote white matter (Buchkremer-Ratzmann and Witte, 1997; de Haan et al., 2012; Fornito et al., 2015; Ross and Ebner, 1990; Saxena and Caroni, 2011). Differences in the extent of disinhibition and potential downstream excitotoxicity depending on lesion size may account for our finding that the FA in remote fiber tracts increased during recovery from small lesions, but that FA decreased after larger lesions.

One might wonder how decreased FA (i.e., ‘structural integrity’) of white matter pathways connecting frontoparietal areas in monkeys with large lesions appear in parallel with behavioural recovery and increased network functional connectivity. It is possible that behavioural compensation after larger PFC lesions may not be mediated by cortical frontoparietal connections, but instead may depend on a functionally-related third region/network (Damoiseaux and Greicius, 2009). Thalamic input to the frontoparietal network is one candidate source of compensatory signals relayed from subcortical areas. The superior colliculus sends indirect projections to the FEF in the caudal PFC via the mediodorsal nucleus of the thalamus (Barbas and Mesulam, 1981; Goldman-Rakic and Porrino, 1985; Kievit and Kuypers, 1977; Sommer and Wurtz, 2004) and to area LIP in the PPC via the lateral pulvinar (Asanuma et al., 1985; Baizer et al., 1993; Selemon and Goldman-Rakic, 1988). Moreover, these thalamic nuclei have been shown to play a role in visuospatial attention (Petersen et al., 1987; Schall, 2002; Sommer and Wurtz, 2004), which supports a potential role in the recovery of saccade target selection. In line with this possibility, studies have shown that thalamic input to distinct cortical areas can regulate the neural synchrony and functional connectivity between those cortical regions (Nakajima and Halassa, 2017; Saalman et al., 2012). Additionally, following extensive unilateral lesions in the macaque corticospinal tract, Zaaimi et al. (2012) showed that subcortical fiber tracts, but not the contralesional corticospinal tract, contributed to the recovery of motor function (Zaaimi et al., 2012). Future studies may consider testing the

role of thalamo-cortical connections in the recovery of function after large PFC lesions using neuroimaging techniques or inactivation methods.

It is important to note that we did not determine causality between the changes in network-wide functional/structural connectivity and behavioural performance. Thus, it is possible that the evolving pattern of functional reorganization and the diverging structural changes are an epiphenomenon of the lesion size alone and potentially unrelated to behavioural compensation. Instead, as I will discuss further in Section 5.1.3., increasing functional connectivity between contralesional DLPFC and ipsilesional PPC correlated with improved post-lesion behaviour in all monkeys and thus may have played a more important role in the recovery of function.

5.1.3. Functional role of the contralesional hemisphere in the recovery of lateralized target selection deficits

The results of this thesis contribute to the discussion of whether contralesional hemisphere involvement is beneficial or maladaptive to the recovery of function (Bütefisch et al., 2005; Ramsey et al., 2016; Rehme and Grefkes, 2013; Umarova et al., 2011; Wilke et al., 2012). Our findings support the idea that involvement of intact areas in both contralesional and ipsilesional frontoparietal networks are beneficial for post-lesion recovery. Across the four monkeys, we found that (1) contralesional DLPFC became functionally correlated with more areas of the frontoparietal network over the course of behavioural recovery and (2) that behavioural improvements were correlated with increasing functional connectivity between contralesional DLPFC and ipsilesional PPC (specifically, area PE in the superior parietal lobule).

The prominent functional involvement of the contralesional DLPFC instead of FEF was initially surprising given that the FEF is a major functional hub of the frontoparietal network (Vincent et al., 2007; Hutchison et al., 2011; Babapoor-Farrokhran et al., 2013) and we thus expected it to show a greater compensatory response. Although the DLPFC shares extensive structural connectivity with many frontoparietal areas (Miller and Cohen, 2001), functional connectivity between DLPFC- frontoparietal network is normally weaker than FEF-frontoparietal functional connectivity (Hutchison et al., 2012; Koval et al., 2014). In light of these differences, we speculate that since the FEF may already be optimally functionally correlated with the frontoparietal network, the functional connections between DLPFC and other frontoparietal areas have more dormant capacity for optimization to better exert compensatory changes in a lesioned animal model.

As reviewed in Chapter 1, the role of the undamaged contralesional hemisphere in the recovery of function has been considered detrimental to recovery by some (Kinsbourne, 1987; Ward et al., 2007), mostly in the motor domain, or instead has been shown to be related with improved visuospatial function (Thimm et al., 2008; Umarova et al., 2017, 2016, 2011; Wilke et al., 2012). The findings from Chapters 3 and 4 in this thesis contribute supporting evidence that involvement of the contralesional hemisphere is associated with behavioural recovery and thus may be valuable for post-lesion compensatory mechanisms.

5.2. Caveats and Limitations

Although macaque monkeys are advantageous over rodents for this research project due to a greater degree of similarity with humans in terms of their prefrontal cortex, eye

movements, and resting-state networks (Bell, Everling, & Munoz, 2000; Hutchison & Everling, 2012; Sallet et al., 2013), this animal model comes with its own limitations. For one, monkeys are a more costly lab animal, both financially and in terms of time spent, as it can take several months to a year to train naïve monkeys on behavioural tasks. Since this was a terminal study, we used a smaller sample size than what is traditionally used in rodent studies which prevented us from performing statistical analyses between subject groups (small vs large lesion). Although within-subject comparisons of brain and behaviour between pre- and post-lesion may be a more powerful approach than averaging out changes by group comparisons, having an additional control group with sham lesions would have been ideal for drawing more conclusive interpretation of results.

Although we aimed to induce saccadic behaviour that resembled visual neglect and extinction, there exist several key differences between this macaque model of focal cerebral ischemia and the clinical disorder of neglect/extinction commonly seen in stroke patients. As discussed in Chapter 1, ischemic stroke usually causes extensive and widespread brain damage such that patients presenting with neglect will typically also suffer from a variety of neurological impairment. This greater degree of brain damage and impairment in patient groups would no doubt result in differences in the patterns and time course of functional and structural network reorganization and their relation to recovery of function. In light of this, it may then be advantageous that animal models focus investigations on a single deficit and its recovery for targeted therapies. Second, the etiology of ischemic stroke in humans (e.g., atherosclerosis) may differentially affect the brain's ability to repair itself and compensate for lost function compared to models of experimentally induced ischemia. Lastly, the syndromes of neglect and extinction in patients are complex and often involve several different components which no doubt would have an impact on the function and structure of brain networks. Thus, while this

work may be limited in its direct clinical application, using a model of neglect and extinction was primarily of interest because it is invaluable in the study of brain reorganization in visuospatial attention networks.

A caveat of our behavioural assessment is that we may have missed other aspects of attentional or motor impairment by only testing performance on an oculomotor task. For instance, our paradigm measured overt shifts of attention by saccadic eye movements which overlooks deficits of covert visuospatial attention. Another possibility is that other measures of oculomotor performance (e.g., antisaccades, memory-guided saccades, visual search) may have offered better indices of impairment and recovery that correlated more consistently with functional/structural imaging across monkeys. Nevertheless, we opted to measure the visuospatial bias only on a free-choice saccade task for several reasons: (1) earlier work has shown substantial spatially lateralized deficits of saccade target selection on free-choice tasks after FEF lesions or DLPFC inactivation (Johnston et al., 2014; Koval et al., 2014; Schiller and Chou, 1998); (2) as mentioned earlier, it can take months to a years to train naïve monkeys on more difficult tasks and we did not want to risk training monkeys on difficult tasks that they likely would be unable to perform after the lesion; and (3) attempting to collect data from several tasks post-lesion would result in a less data points on each task and limit interpretation of behavioural findings.

While resting-state fMRI and diffusion-weighted MRI are valuable and non-invasive techniques that offer insight into whole-brain function and structure, these imaging approaches still have some shortcomings. Perhaps the most obvious is the lack of direct measures of neural activity or axon tract density and myelination. However, simultaneous fMRI and electrophysiological studies show that the BOLD signal is correlated with local field potentials (Logothetis, 2008, 2003; Logothetis et al., 2001), which reflects a component of neural activity. Diffusion tensor models of diffusion-weighted MRI is a

relatively newer approach with less well-defined parameters (Jones et al., 2013; Winston, 2012). For example, FA is frequently referred to as an index of ‘white matter integrity’, yet this is an overgeneralization since FA reflects various features of white matter (e.g., axon density and organization, axon diameter, myelination, membrane permeability) which limits DTI interpretability (Beaulieu, 2002; Jones et al., 2013).

Lastly, another potential limitation is that our imaging reports did not include subcortical areas, most importantly the superior colliculus which has been shown to play a role in saccade target selection (McPeck and Keller, 2004) and covert visuospatial attention (Krauzlis et al., 2013; Müller et al., 2005). BOLD signal in the superior colliculus is difficult to resolve due to its small size and location near major arteries and cerebrospinal fluid-filled spaces which confound its signal with physiological noise (Brooks et al., 2013; Linzenbold et al., 2011). While ultra-high field MR scanners (e.g., at 7-Tesla) offer higher spatial resolution necessary for imaging small structures, physiological noise increases with the square of the field strength which can drastically reduce signal-to-noise, especially in brainstem areas already affected by physiological noise (Parrish et al., 2000). Examination of the BOLD signal in the superior colliculus in our resting-state fMRI data set showed that the signal was indeed highly dominated by physiological noise (Beall and Lowe, 2007; Griffanti et al., 2017), and thus we opted to exclude further investigation.

5.3. Future directions

In addition to the improving on the limitations discussed above, there are many interesting avenues for future research that stem from this work. First, it will be important that future work determines the role of the DLPFC in the recovery of a saccade choice

bias after a PFC lesion in the opposite hemisphere. Reversible inactivation of the contralesional DLPFC using cooling loops or muscimol after behavioural recovery is complete may reveal a reinstatement of the initial visuospatial bias if that region is critically involved in the neural compensation. It would also be interesting to record the neural activity in possible compensatory areas to examine whether neurons in the contralesional hemisphere show greater ipsilaterally-tuned spatial representations over time to support recovery. Ipsilesional PPC and superior colliculus are also other areas of interest for inactivation and electrophysiological investigations. In addition, microstimulation of contralesional frontoparietal areas in post-lesion recovered monkeys and non-lesioned monkeys may provide more direct evidence on the role of contralesional activity in the recovery of function.

While we assume that increased resting-state functional connectivity implies functional recruitment of those areas for the recovery of function, this assumption might be addressed in future studies. Longitudinal task-based fMRI could expand on our results and test whether improved performance on the free-choice task after large PFC lesions is associated with greater task-related BOLD activation than after smaller lesions.

Finally, it is important to consider that the results in this thesis are based on data from male macaque monkeys. Murphy et al. (2008) found differences in the degree of variability of ischemic lesions between male and female rhesus macaques after occlusion of the middle cerebral artery (Murphy et al., 2008). While stroke incidence in women is lower than in men, this difference disappears with menopause which suggests a potential protective role for estrogen (Murphy et al., 2004). However, stroke in women is more severe and fatal than in men (Appelros et al., 2009). These sex differences in stroke severity and recovery are not well understood and warrant further research using male and female nonhuman primate models of stroke.

5.4. Concluding Remarks

Recovery after brain damage highlights the remarkable ability of the brain to repair itself and optimize functional and structural networks to compensate for lost function. The work in this thesis contributes to the research efforts aimed at uncovering the mechanisms underlying brain reorganization and recovery of function, specifically in the visuospatial attention domain. We described the target selection biases following prefrontal cortex lesions in a macaque model of focal cerebral ischemia and characterized the recovery of oculomotor and choice behaviour over time, establishing the contribution of attentional deficits in the model. The broad implication of this research is that involvement of both the contralesional and ipsilesional frontoparietal networks is associated with the recovery of contralesional target selection. Importantly, our findings provide evidence for greater functional recruitment of bilateral hemispheres during behavioural recovery after large lesions, whereas improved behaviour after smaller lesions was optimally supported by a normalization of the functional network connectivity. Differences in the structural alterations are also noteworthy; while the contralesional superior longitudinal fasciculus and transcallosal PPC tracts show adaptive changes in fractional anisotropy after recovery from small lesions, this potential compensatory response was not found after recovery from larger lesions. This research highlights the differences in the spatiotemporal patterns of post-stroke recovery based on the extent and location of brain damage. Looking forward, my hope is that future investigators will gain an understanding of the principles that guide altered patterns of brain reorganization following brain damage to then improve treatment and rehabilitation outcomes for patients living with the long-term effects of attentional impairment.

5.5. References

- Appelros, P., Stegmayr, B., Terent, A., 2009. Sex differences in stroke epidemiology: A systematic review. *Stroke* 40, 1082–1090.
- Asanuma, C., Andersen, R.A., Cowan, W.M., 1985. The thalamic relations of the caudal inferior parietal lobule and the lateral prefrontal cortex in monkeys: Divergent cortical projections from cell clusters in the medial pulvinar nucleus. *J. Comp. Neurol.* 241, 357–381.
- Babapoor-Farrokhran, S., Hutchison, R.M., Gati, J.S., Menon, R.S., Everling, S., 2013. Functional connectivity patterns of medial and lateral macaque frontal eye fields reveal distinct visuomotor networks. *J. Neurophysiol.* 109, 2560–70.
- Baizer, J.S., Robert, D., Ungerleider, L.G., 1993. Comparison of subcortical connections of inferior temporal and posterior parietal cortex in monkeys. *Vis. Neurosci.*
- Barbas, H., Mesulam, M. -M, 1981. Organization of afferent input to subdivisions of area 8 in the rhesus monkey. *J. Comp. Neurol.* 200, 407–431.
- Beall, E.B., Lowe, M.J., 2007. Isolating physiologic noise sources with independently determined spatial measures. *Neuroimage* 37, 1286–1300.
- Beaulieu, C., 2002. The basis of anisotropic water diffusion in the nervous system - A technical review. *NMR Biomed.* 15, 435–455.
- Bender, M.B., Furlow, L.T., 1945. Phenomenon of visual extinction in homonymous fields and psychologic principles involved. *Arch. Neurol. Psychiatry* 53, 29–33.
- Biernaskie, J., Szymanska, A., Windle, V., Corbett, D., 2005. Bi-hemispheric contribution to functional motor recovery of the affected forelimb following focal ischemic brain injury in rats. *Eur. J. Neurosci.* 21, 989–999.
- Brooks, J., Faull, O., Pattinson, K., Jenkinson, M., 2013. Physiological noise in brainstem fMRI. *Front. Hum. Neurosci.* 7, 623.
- Brown, C.E., Aminoltejari, K., Erb, H., Winship, I.R., Murphy, T.H., 2009. In Vivo Voltage-Sensitive Dye Imaging in Adult Mice Reveals That Somatosensory Maps Lost to Stroke Are Replaced over Weeks by New Structural and Functional Circuits with Prolonged Modes of Activation within Both the Peri-Infarct Zone and Distant Sites. *J. Neurosci.* 29, 1719–1734.
- Buchkremer-Ratzmann, I., Witte, O.W., 1997. Extended brain disinhibition following small photothrombotic lesions in rat frontal cortex. *Neuroreport* 8, 519–522.
- Bütefisch, C.M., Kleiser, R., Körber, B., Müller, K., Wittsack, H.J., Hömberg, V., Seitz, R.J., 2005. Recruitment of contralesional motor cortex in stroke patients with recovery of hand function. *Neurology* 64, 1067–1069.
- Carmichael, S.T., Chesselet, M.F., 2002. Synchronous neuronal activity is a signal for axonal sprouting after cortical lesions in the adult. *J. Neurosci.* 22, 6062–6070.

- Corbetta, M., Shulman, G.L., 2011. Spatial Neglect and Attention Networks. *Annu. Rev. Neurosci.* 34, 569–599.
- Dai, P., Huang, H., Zhang, L., He, J., Zhao, X., Yang, F., Zhao, N., Yang, J., Ge, L., Lin, Y., Yu, H., Wang, J., 2017. A pilot study on transient ischemic stroke induced with endothelin-1 in the rhesus monkeys. *Sci. Rep.* 7, 45097.
- Damoiseaux, J.S., Greicius, M.D., 2009. Greater than the sum of its parts: A review of studies combining structural connectivity and resting-state functional connectivity. *Brain Struct. Funct.* 213, 525–533.
- de Haan, W., Mott, K., van Straaten, E.C.W., Scheltens, P., Stam, C.J., 2012. Activity Dependent Degeneration Explains Hub Vulnerability in Alzheimer’s Disease. *PLoS Comput. Biol.* 8.
- Fornito, A., Zalesky, A., Breakspear, M., 2015. The connectomics of brain disorders. *Nat. Rev. Neurosci.* 16, 159–172.
- Frost, S.B., 2003. Reorganization of Remote Cortical Regions After Ischemic Brain Injury: A Potential Substrate for Stroke Recovery. *J. Neurophysiol.* 89, 3205–3214.
- Goldman-Rakic, P.S., Porrino, L.J., 1985. The primate mediodorsal (MD) nucleus and its projection to the frontal lobe. *J. Comp. Neurol.* 242, 535–560.
- Gonzalez, C.L.R., Kolb, B., 2003. A comparison of different models of stroke on behaviour and brain morphology. *Eur. J. Neurosci.* 18, 1950–1962.
- Grafman, J., 2000. Conceptualizing functional neuroplasticity. *J. Commun. Disord.* 33, 345–356.
- Griffanti, L., Douaud, G., Bijsterbosch, J., Evangelisti, S., Alfaro-Almagro, F., Glasser, M.F., Duff, E.P., Fitzgibbon, S., Westphal, R., Carone, D., Beckmann, C.F., Smith, S.M., 2017. Hand classification of fMRI ICA noise components. *Neuroimage* 154, 188–205.
- Heilman, K.M., Valenstein, E., Watson, R.T., 1984. Neglect and related disorders. *Semin. Neurol.* 4, 209–219.
- Heilman, K.M., Watson, R.T., Valenstein, E., 2012. Neglect and Related Disorders, in: Heilman, K.M., Valenstein, E. (Eds.), *Clinical Neuropsychology*. Oxford University Press, New York.
- Herbert, W.J., Powell, K., Buford, J.A., 2015. Evidence for a role of the reticulospinal system in recovery of skilled reaching after cortical stroke: initial results from a model of ischemic cortical injury. *Exp. Brain Res.* 233, 3231–3251.
- Hutchison, R.M., Gallivan, J.P., Culham, J.C., Gati, J.S., Menon, R.S., Everling, S., 2012. Functional connectivity of the frontal eye fields in humans and macaque monkeys investigated with resting-state fMRI. *J. Neurophysiol.* 107, 2463–74.
- Hutchison, R.M., Leung, L.S., Mirsattari, S.M., Gati, J.S., Menon, R.S., Everling, S., 2011. Resting-state networks in the macaque at 7T. *Neuroimage* 56, 1546–1555.

- Johnston, K., Koval, M.J., Lomber, S.G., Everling, S., 2014. Macaque dorsolateral prefrontal cortex does not suppress saccade-related activity in the superior colliculus. *Cereb. Cortex* 26, 12471–12478.
- Jones, D.K., Knösche, T.R., Turner, R., 2013. White matter integrity, fiber count, and other fallacies: The do's and don'ts of diffusion MRI. *Neuroimage*.
- Jones, T.A., Schallert, T., 1992. Overgrowth and pruning of dendrites in adult rats recovering from neocortical damage. *Brain Res.* 581, 156–160.
- Juan, C.H., Shorter-Jacobi, S.M., Schall, J.D., 2004. Dissociation of spatial attention and saccade preparation. *Proc. Natl. Acad. Sci. U. S. A.* 101, 15541–15544.
- Kievit, J., Kuypers, H.G.J.M., 1977. Organization of the thalamo-cortical connexions to the frontal lobe in the rhesus monkey. *Exp. Brain Res.* 29, 299–322.
- Kinsbourne, M., 1987. Mechanisms of unilateral neglect. *Neurophysiol. Neuropsychol. Asp. Spat. Negl.* 69–86.
- Koval, M.J., Hutchison, R.M., Lomber, S.G., Everling, S., 2014. Effects of unilateral deactivations of dorsolateral prefrontal cortex and anterior cingulate cortex on saccadic eye movements. *J. Neurophysiol.* 111, 787–803.
- Krauzlis, R.J., Lovejoy, L.P., Zénon, A., 2013. Superior Colliculus and Visual Spatial Attention. *Annu. Rev. Neurosci.* 36, 165–182.
- Li, K., Malhotra, P.A., 2015. Spatial neglect. *Pract. Neurol.* 15, 333–339.
- Liepert, J., Storch, P., Fritsch, A., Weiller, C., 2000. Motor cortex disinhibition in acute stroke. *Clin. Neurophysiol.* 111, 671–676.
- Lin, Y.C., Daducci, A., Meskaldji, D.E., Thiran, J.P., Michel, P., Meuli, R., Krueger, G., Menegaz, G., Granziera, C., 2015. Quantitative analysis of myelin and axonal remodeling in the uninjured motor network after stroke. *Brain Connect.* 5, 401–412.
- Linzenbold, W., Lindig, T., Himmelbach, M., 2011. Functional neuroimaging of the oculomotor brainstem network in humans. *Neuroimage* 57, 1116–23.
- Liu, Y., Rouiller, E.M., 1999. Mechanisms of recovery of dexterity following unilateral lesion of the sensorimotor cortex in adult monkeys. *Exp. Brain Res.* 128, 149–159.
- Logothetis, N.K., 2008. What we can do and what we cannot do with fMRI. *Nature* 453, 869–878.
- Logothetis, N.K., 2003. The underpinnings of the BOLD functional magnetic resonance imaging signal. *J. Neurosci.* 23, 3963–3971.
- Logothetis, N.K., Pauls, J., Augath, M., Trinath, T., Oeltermann, a, 2001. Neurophysiological investigation of the basis of the fMRI signal. *Nature* 412, 150–157.
- McPeck, R.M., Keller, E.L., 2004. Deficits in saccade target selection after inactivation of superior colliculus. *Nat. Neurosci.* 7, 757–63.

- Miller, E.E.K., Cohen, J.J.D., 2001. An integrative theory of prefrontal cortex function. *Annu. Rev. Neurosci.* 24, 167–202.
- Milner, A.D., Mcintosh, R.D., 2005. The neurological basis of visual neglect. *Curr. Opin. Neurol.* 18, 748–753.
- Moore, T., Armstrong, K.M., 2003. Selective gating of visual signals by microstimulation of frontal cortex. *Nature* 421, 370–373.
- Moore, T., Fallah, M., 2004. Microstimulation of the Frontal Eye Field and Its Effects on Covert Spatial Attention. *J. Neurophysiol.* 91, 152–162.
- Müller, J.R., Philiastides, M.G., Newsome, W.T., 2005. Microstimulation of the superior colliculus focuses attention without moving the eyes. *Proc. Natl. Acad. Sci. U. S. A.* 102, 524–529.
- Murata, Y., Higo, N., 2016. Development and Characterization of a Macaque Model of Focal Internal Capsular Infarcts. *PLoS One* 11, e0154752.
- Murphy, S.J., Kirsch, J.R., Zhang, W., Grafe, M.R., West, G.A., Del Zoppo, G.J., Traystman, R.J., Hurn, P.D., 2008. Can gender differences be evaluated in a rhesus macaque (*macaca mulatto*) model of focal cerebral ischemia? *Comp. Med.* 58, 588–596.
- Murphy, S.J., McCullough, L.D., Smith, J.M., 2004. Stroke in the female: role of biological sex and estrogen. *ILAR J.* 45, 147–159.
- Nakajima, M., Halassa, M.M., 2017. Thalamic control of functional cortical connectivity. *Curr. Opin. Neurobiol.* 44, 127–131.
- Nudo, R.J., Wise, B.M., SiFuentes, F., Milliken, G.W., 1996. Neural Substrates for the Effects of Rehabilitative Training on Motor Recovery After Ischemic Infarct. *Science* (80-.). 272, 1791–1794.
- Parrish, T.B., Gitelman, D.R., LaBar, K.S., Mesulam, M.M., 2000. Impact of signal-to-noise on functional MRI. *Magn. Reson. Med.* 44, 925–932.
- Petersen, S.E., Robinson, D.L., Morris, J.D., 1987. Contributions of the pulvinar to visual spatial attention. *Neuropsychologia* 25, 97–105.
- Plautz, E.J., Barbay, S., Frost, S.B., Friel, K.M., Dancause, N., Zoubina, E. V., Stowe, A.M., Quaney, B.M., Nudo, R.J., 2003. Post-infarct cortical plasticity and behavioral recovery using concurrent cortical stimulation and rehabilitative training: A feasibility study in primates. *Neurol. Res.* 25, 801–810.
- Plow, E.B., Cunningham, D., Varnerin, N., Machado, A., Clinic, C., Clinic, C., Clinic, C., 2015. Rethinking stimulation of brain in stroke rehabilitation: Why higher-motor areas might be better alternatives for patients with greater impairments. *Neuroscientist* 21, 225–240.
- Ramsey, L.E., Siegel, J.S., Baldassarre, A., Metcalf, N. V., Zinn, K., Shulman, G.L., Corbetta, M., 2016. Normalization of network connectivity in hemispatial neglect

- recovery. *Ann. Neurol.* 80, 127–141.
- Ratcliff, R., 1979. Group reaction time distributions and an analysis of distribution statistics. *Psychol. Bull.* 86, 446–461.
- Rehme, A.K., Grefkes, C., 2013. Cerebral network disorders after stroke: evidence from imaging-based connectivity analyses of active and resting brain states in humans. *J. Physiol.* 591, 17–31.
- Reitmeir, R., Kilic, E., Kilic, Ü., Bacigaluppi, M., Elali, A., Salani, G., Pluchino, S., Gassmann, M., Hermann, D.M., 2011. Post-acute delivery of erythropoietin induces stroke recovery by promoting perilesional tissue remodelling and contralesional pyramidal tract plasticity. *Brain* 134, 84–99.
- Rizzolatti, G., Matelli, M., Pavesi, G., 1983. Deficits in attention and movement following the removal of postarcuate (area 6) and prearcuate (area 8) cortex in macaque monkeys. *Brain* 106, 655–673.
- Rizzolatti, G., Riggio, L., Dascola, I., Umiltá, C., 1987. Reorienting attention across the horizontal and vertical meridians: Evidence in favor of a premotor theory of attention. *Neuropsychologia* 25, 31–40.
- Robertson, I.H., Halligan, P.W., 1999. Spatial neglect: A clinical handbook for diagnosis and treatment., *Spatial neglect: A clinical handbook for diagnosis and treatment., Brain damage, behaviour and cognition series.* Psychology Press/Taylor & Francis (UK), Hove, England.
- Ross, D.T., Ebner, F.F., 1990. Thalamic retrograde degeneration following cortical injury: An excitotoxic process? *Neuroscience* 35, 525–550.
- Saalman, Y.B., Pinsk, M.A., Wang, L., Li, X., Kastner, S., 2012. The Pulvinar Regulates Information Transmission Between Cortical Areas Based on Attention Demands. *Science* (80-.). 337, 753–756.
- Sato, T.R., Schall, J.D., 2003. Effects of stimulus-response compatibility on neural selection in frontal eye field. *Neuron* 38, 637–648.
- Saxena, S., Caroni, P., 2011. Selective Neuronal Vulnerability in Neurodegenerative Diseases: From Stressor Thresholds to Degeneration. *Neuron* 71, 35–48.
- Schall, J.D., 2002. The neural selection and control of saccades by the frontal eye field. *Philos. Trans. R. Soc. Lond. B. Biol. Sci.* 357, 1073–82.
- Schiller, P.H., Chou, I., 2000. The effects of anterior arcuate and dorsomedial frontal cortex lesions on visually guided eye movements: 2. Paired and multiple targets. *Vision Res.* 40, 1627–1638.
- Schiller, P.H., Chou, I., 1998. The effects of frontal eye field and dorsomedial frontal cortex lesions on visually guided eye movements. *Nat. Neurosci.* 1, 248–253.
- Selemon, L.D., Goldman-Rakic, P.S., 1988. Common cortical and subcortical targets of the dorsolateral prefrontal and posterior parietal cortices in the rhesus monkey:

- evidence for a distributed neural network subserving spatially guided behavior. *J. Neurosci.* 8, 4049–4068.
- Sommer, M.A., Wurtz, R.H., 2004. What the Brain Stem Tells the Frontal Cortex. I. Oculomotor Signals Sent from Superior Colliculus to Frontal Eye Field Via Mediodorsal Thalamus. *J. Neurophysiol.* 91, 1381–1402.
- Sotak, C.H., 2002. The role of diffusion tensor imaging in the evaluation of ischemic brain - A review. *NMR Biomed.* 15, 561–569.
- Teo, L., Bourne, J., 2014. A Reproducible and Translatable Model of Focal Ischemia in the Visual Cortex of Infant and Adult Marmoset Monkeys. *Brain Pathol.* 24, 459–474.
- Thimm, M., Fink, G.R., Sturm, W., 2008. Neural correlates of recovery from acute hemispatial neglect. *Restor Neurol Neurosci* 26, 481–492.
- Thompson, K.G., Biscoe, K.L., Sato, T.R., 2005. Neuronal basis of covert spatial attention in the frontal eye field. *J. Neurosci.* 25, 9479–9487.
- Touvykine, B., Mansoori, B.K., Jean-Charles, L., Deffeyes, J., Quessy, S., Dancause, N., 2016. The effect of lesion size on the organization of the ipsilesional and contralesional motor cortex. *Neurorehabil. Neural Repair* 30, 280–292.
- Umarova, R.M., Beume, L., Reiser, M., Kaller, C.P., Klöppel, S., Mader, I., Glauche, V., Kiselev, V.G., Catani, M., Weiller, C., 2017. Distinct white matter alterations following severe stroke. *Neurology* 88, 1546–1555.
- Umarova, R.M., Nitschke, K., Kaller, C.P., Klöppel, S., Beume, L., Mader, I., Martin, M., Hennig, J., Weiller, C., 2016. Predictors and signatures of recovery from neglect in acute stroke. *Ann. Neurol.* 79, 673–686.
- Umarova, R.M., Saur, D., Kaller, C.P., Vry, M.S., Glauche, V., Mader, I., Hennig, J.J., Weiller, C., 2011. Acute visual neglect and extinction: Distinct functional state of the visuospatial attention system. *Brain* 134, 3310–3325.
- Vincent, J.L., Patel, G.H., Fox, M.D., Snyder, A.Z., Baker, J.T., Van Essen, D.C., Zempel, J.M., Snyder, L.H., Corbetta, M., Raichle, M.E., 2007. Intrinsic functional architecture in the anaesthetized monkey brain. *Nature* 447, 83–86.
- Virley, D., Hadingham, S.J., Roberts, J.C., Farnfield, B., Elliott, H., Whelan, G., Golder, J., David, C., Parsons, A.A., Hunter, A.J., 2004. A New Primate Model of Focal Stroke: Endothelin-1-Induced Middle Cerebral Artery Occlusion and Reperfusion in the Common Marmoset. *J. Cereb. Blood Flow Metab.* 24, 24–41.
- Ward, N.S., Newton, J.M., Swayne, O.B.C., Lee, L., Frackowiak, R.S.J., Thompson, A.J., Greenwood, R.J., Rothwell, J.C., 2007. The relationship between brain activity and peak grip force is modulated by corticospinal system integrity after subcortical stroke. *Eur. J. Neurosci.* 25, 1865–1873.
- Wilke, M., Kagan, I., Andersen, R., 2012. Functional imaging reveals rapid reorganization of cortical activity after parietal inactivation in monkeys. *Proc. Natl.*

Acad. Sci. 109, 8274–8279.

Winston, G.P., 2012. The physical and biological basis of quantitative parameters derived from diffusion MRI. *Quant. Imaging Med. Surg.* 2, 254–25465.

Zaaimi, B., Edgley, S.A., Soteropoulos, D.S., Baker, S.N., 2012. Changes in descending motor pathway connectivity after corticospinal tract lesion in macaque monkey. *Brain* 135, 2277–2289.

Zeiler, S.R., Gibson, E.M., Hoesch, R.E., Li, M.Y., Worley, P.F., O'Brien, R.J., Krakauer, J.W., 2013. Medial Premotor Cortex Shows a Reduction in Inhibitory Markers and Mediates Recovery in a Mouse Model of Focal Stroke. *Stroke* 44, 483–489.

APPENDIX A: ETHICS APPROVAL



AUP Number: 2016-090

PI Name: Everling, Stefan

AUP Title: Role Of Frontal Cortex In Cognitive Control

Approval Date: 01/23/2017

Official Notice of Animal Use Subcommittee (AUS) Approval: Your new Animal Use Protocol (AUP) entitled "Role Of Frontal Cortex In Cognitive Control" has been APPROVED by the Animal Use Subcommittee of the University Council on Animal Care. This approval, although valid for four years, and is subject to annual Protocol Renewal.2016-090::1

1. This AUP number must be indicated when ordering animals for this project.
2. Animals for other projects may not be ordered under this AUP number.
3. Purchases of animals other than through this system must be cleared through the ACVS office. Health certificates will be required.

The holder of this Animal Use Protocol is responsible to ensure that all associated safety components (biosafety, radiation safety, general laboratory safety) comply with institutional safety standards and have received all necessary approvals. Please consult directly with your institutional safety officers.

Submitted by: Copeman, Laura
on behalf of the Animal Use Subcommittee
University Council on Animal Care

The University of Western Ontario
Animal Use Subcommittee / University Council on Animal Care
Health Sciences Centre, • London, Ontario • CANADA – N6A 5C1
PH: 519-661-2111 ext. 86768 • FL 519-661-2028
Email: auspc@uwo.ca • <http://www.uwo.ca/animal/website/>

CURRICULUM VITAE

Ramina Adam

Education

- 2014 – 2020 **Ph.D. Neuroscience**
 The University of Western Ontario
 Thesis: Functional and structural brain reorganization after a
 unilateral prefrontal cortex lesion in macaque monkeys
 Supervisor: Dr. Stefan Everling
- 2010 – 2014 **B.Sc. with Honors in Physiology and Psychology**
 The University of Western Ontario

Honors and Awards

- 2018 Queen Elizabeth II Graduate Scholarship in Science and Technology
 – Doctoral Award (\$15,000)
- 2018 Neuroscience Travel Award – Resting State and Brain Connectivity
 2018 Conference (\$500)
- 2017 Ontario Graduate Scholarship – Doctoral Award (\$15,000)
- 2017 Merit Abstract Award, Organization for Human Brain Mapping
 Conference (\$2,000 USD)
- 2017 Neuroscience Travel Award – Organization for Human Brain
 Mapping Conference (\$500)
- 2016 Queen Elizabeth II Graduate Scholarship in Science and Technology
 – Doctoral Award (\$15,000)
- 2016 Cobban Student Award in Heart and Stroke Research (\$1,500)
- 2016 Teaching Honour Roll Award of Excellence in Neuroscience
- 2015 Canada Graduate Scholarship – Master’s Program (CGSM),
 Canadian Institutes of Health Research (CIHR) (\$17,500)
- 2015 – 2018 Schulich Graduate Scholarship (\$2,000 per year)
- 2014 – 2019 Western Graduate Research Scholarship (\$2,333 per term)
- 2010 – 2014 Dean’s Honor List
- 2010 – 2014 Western Scholar Designation

2010 – 2014	Queen Elizabeth II Aiming for the Top Scholarship (\$1,922 per year)
2010	Western Scholarship of Excellence (\$2,000)

Teaching Experience

Feb 2019	Guest Lecture, <i>Hypothalamus and Motivated Behaviour</i> Neuroscience 2000: Introduction to Neuroscience The University of Western Ontario
Jan-Apr 2015	Teaching Assistant Neuroscience 2000: Introduction to Neuroscience The University of Western Ontario

Publications: Research Articles

- Adam, R.**, Johnston, K., Menon, R.S., Everling, S. (2020). Functional reorganization during the recovery of contralesional target selection deficits after prefrontal cortex lesions in macaque monkeys. *NeuroImage* 207, 116339.
- Adam, R.**, Johnston, K., Everling, S. (2019). Recovery of contralesional saccade choice and reaction time deficits after a unilateral endothelin-1-induced lesion in the macaque caudal prefrontal cortex. *Journal of Neurophysiology*, 122(2): 672-690.
- Schaeffer, D.J., **Adam, R.**, Gilbert, K.M., Gati, J.S., Li, A.X., Menon, R.S., Everling, S. (2017). Diffusion-weighted tractography in the common marmoset monkey at 9.4T. *Journal of Neurophysiology*, 118(2): 1344-1354.
- Vedagiri Sai, R., Singh, S.I., Qasem, F., Nguyen, D., Dhir, S., Marmai, K., **Adam, R.**, Jones, P.M. (2017). Onset of labour epidural analgesia with low-dose bupivacaine and different doses of fentanyl. *Anaesthesia*, 72(11): 1371-1378.

Publications: Commentaries

- Adam, R.**, Isabella, S., Chan, J.L. (2015). Insight into motor control and motor impairment from stroke and beta oscillations. *Journal of Neurophysiology*, 114(6): 3033-3035.

Submitted Manuscripts

- Adam, R.**, Schaeffer, D.J., Johnston, K., Menon, R.S., Everling, S. Structural alterations in cortical white matter tracts after prefrontal cortex lesions in macaques. *Submitted*. [preprint posted on bioRxiv]
- Greulich, S., **Adam, R.**, Everling, S., Scherberger, H. Where streams collide: dorso-medial and dorso-ventral stream in resting-state fMRI of macaques. *Submitted*.

Conference Presentations: Talks

- Adam, R.** & Everling, S. (2016). “Functional network changes during unilateral stroke recovery in nonhuman primates using resting-state fMRI”, 3rd Annual Retreat of the International Research Training Group (IRTG): ‘The Brain in Action’, Glashütten, Germany, July 2016.
- Adam, R.**, Johnston, K., Hutchison, R.M., & Everling, S. (2015). “Functional connectivity changes after a frontal cortex lesion in a nonhuman primate”, European Conference on Eye Movements, Vienna, Austria, August 2015.
- Adam, R.** & Everling, S. (2015). “Resting-state functional connectivity changes following an ischemic frontal cortex stroke in a macaque”, 2nd Annual Retreat of the International Research Training Group (IRTG): ‘The Brain in Action’, Ontario, Canada, June 2015.

Conference Presentations: Posters

- Adam, R.**, Johnston, K., Menon, R.S., & Everling, S. (2019). Functional connectivity changes during the recovery of a contralesional saccade choice deficit following a prefrontal cortex lesion in macaque monkeys. CIHR National Poster Competition – Canadian Student Health Research Forum, Winnipeg, Manitoba, Canada, June 2019. **Only top 5% of PhD students from each university were invited to attend.*
- Adam, R.**, Johnston, K., Menon, R.S., & Everling, S. (2018). Resting-state functional reorganization during recovery of a saccade choice bias following an experimental prefrontal cortex stroke in macaque monkeys. Resting State and Brain Connectivity, Montreal, QC, Canada, September 2018.
- Greulich, R.S., **Adam, R.**, Everling, S., & Scherberger, H. (2018). Where streams collide: Dorso-medial and dorso-ventral stream shown using resting-state fMRI in macaques. Federation of European Neuroscience Societies, Berlin, Germany, July 2018.
- Greulich, R.S., **Adam, R.**, Everling, S., & Scherberger, H. (2018). Dorso-medial and dorso-ventral stream shown using resting-state fMRI in macaques. Primate Neurobiology: Research, Methods, Ethics, Tübingen, Germany, March 2018.

- Greulich, R.S., **Adam, R.**, Everling, S., & Scherberger, H. (2017). Separate resting state networks for grasping and visually guided reaching in macaques. Society for Neuroscience, Washington, DC, USA, November 2017.
- Adam, R.**, Johnston, K., Schaeffer, D.J., Shen, K., & Everling, S. (2017). Neural compensation in the recovery of a saccade selection bias after unilateral stroke in macaques. Organization for Human Brain Mapping, Vancouver, BC, Canada, June 2017.
- Adam, R.**, Johnston, K., Schaeffer, D.J., Shen, K., & Everling, S. (2017). Neural compensation in the recovery of a saccade selection bias after unilateral stroke in macaques. Canadian Association for Neuroscience, Montreal, QC, Canada, May 2017.
- Schaeffer, D.J., **Adam, R.**, Gilbert, K.M., Gati, J.S., Li, A.X., Menon, R.S., & Everling, S. (2017). Diffusion weighted tractography in the common marmoset monkey at 9.4T. Canadian Association for Neuroscience, Montreal, QC, Canada, May 2017.
- Greulich, R.S., **Adam, R.**, Everling, S., & Scherberger, H. (2017). Exploring the macaque cortical grasp network with resting-state fMRI. 10th Annual Primate Neurobiology Meeting, Göttingen, Germany, March 2017.
- Adam, R.**, Johnston, K., Hutchison, R.M., & Everling, S. (2016). Graph theoretical analysis of functional network changes during recovery of saccade selection bias following stroke in nonhuman primates. Society for Neuroscience, San Diego, CA, USA, November 2016.
- Adam, R.**, Johnston, K., Hutchison, R.M., & Everling, S. (2016). Network-wide functional connectivity changes during unilateral frontal stroke recovery in nonhuman primates. Robarts Research Retreat, London, Canada, June 2016.
- Adam, R.**, Johnston, K., Hutchison, R.M., & Everling, S. (2016). Network-wide functional connectivity changes during unilateral frontal stroke recovery in nonhuman primates. 36th Annual Southern Ontario Neuroscience Association Conference, Waterloo, Canada, May 2016.
- Adam, R.**, Johnston, K., Hutchison, R.M., & Everling, S. (2015). Resting-state functional connectivity changes following an ischemic frontal cortex stroke in macaque monkeys. Society for Neuroscience, Chicago, IL, USA, October 2015.
- Adam, R.**, & Chan, J.L. (2014). Brain Busters: Neuromyths and Neuroscience in the Media. Brain Awareness Event at the Society for Neuroscience, Washington, DC, USA, November 2014.
- Nguyen, D., Sai, R., Jones, P., Marmai, K., Qasem, F., Dhir, S., **Adam, R.**, & Singh, I. (2014). Onset of labour epidural analgesia with varying doses of fentanyl. Canadian Anesthesiologists' Society Annual Meeting. Ottawa, Canada, June 2014.

Invited Panel Talks

- 2019 “Networks: Not Just for Brains – I Wish I Knew Panel Series”, Society of Neuroscience Graduate Students. This was an event for new graduate students about how to expand your academic network.
- 2019 “Science Communication”, London Health Research Day. Discussed the importance of communicating science responsibly as scientists.
- 2018 “Grad Expo – Q&A with Science Graduate Students”, Leadership and Academic Mentorship Program, Western University.
- 2017 “Navigating the Challenges of Graduate School for Women”, Teaching Support Centre, Western University.
- 2015 “Neuroscience Lecture Series: Recruitment Event”, Graduate Program in Neuroscience, Western University.

Academic Service

- 2018 – 2020 **Decanal Search Committee – Graduate Student Representative**, Schulich School of Medicine and Dentistry
- 2018 – 2019 **Supervision of Undergraduate Thesis Student**, 4th Year Honors Thesis, Project: Diffusion tractography in macaque monkeys
- 2016 – 2019 **Ad-hoc Reviewer**, Journal of Neurophysiology, Scientific Reports, Neuropsychologia, Cerebral Cortex, Human Brain Mapping
- 2017 – 2019 **Graduate Editor**, Western Undergraduate Psychology Journal
- 2019 **Research Poster Judge**, London Health Research Day, Robarts Research Day
- 2014 – 2015 **Neuroscience Councillor**, Society for Graduate Students
Represented the neuroscience graduate student body at council meetings

Volunteer & Science Outreach

- 2019 – *present* **Co-Founder & Editor-in-Chief – The Dorsal Column**
Student-led online and print publication for communicating neuroscience research to the wider community.
- 2016 – *present* **Volunteer, Arts & Crafts Group – Dale Brain Injury Services**
Lead arts and crafts sessions at a day program for individuals living with an acquired brain injury.

- 2015 – 2020 **Co-Founder & Co-Chair – Inspiring Diversity in STEM**
Biennial conference to promote equity, diversity, and inclusion in science, technology, engineering, and mathematics (STEM).
- Jan – May 2017 **Program Developer – Science Rendezvous**
Science Rendezvous is an annual nation-wide science festival meant to engage the local community.
- 2015 – 2016 **Radio Host & Social Media Manager– Gradcast Radio**
Interviewed graduate students from all faculties about their research for a lay audience on local radio. Created a social media presence for the radio show to increase public engagement and viewership.
- 2014 – 2016 **Graduate Liaison – Women in Science**
Provided mentorship and coordinated workshops and events with the undergraduate student group.